Decoding High Level Influences on Facial Expression Recognition

Vicky Samantha Adams

A thesis submitted in partial fulfilment of the requirements of the University of East Anglia for the degree of Doctor of Philosophy.

Research undertaken in the School of Psychology, University of East Anglia.

September 2018

Decoding High Level Influences on Facial Expression Recognition

Abstract

The present thesis explores the neural mechanisms underlying the recognition of emotion; the effect of high-level influences such as prior knowledge, task goals and the possible contribution of embodied simulation in facial expression recognition. The initial experiments (Chapters 2 & 3) investigate high-level processing that occurs when facial features are occluded in the recognition of facial expressions (visual route of recognition). This research examines the information about occluded facial features in early visual (V1-V3), face and emotion sensitive areas with fMRI, as well as the temporal dynamics of posterior brain regions in processing occluded facial features with EEG. MVPA reveals similar patterns of decoding across non-overlapping samples of face information, suggesting the involvement of contextual influences beyond low-level processing (Chapter 2), as well as reliable decoding of facial expression (happy, fear and disgust) in conditions missing feature information (Chapters 2 & 3). This decoding, found 50-700ms, has three decoding phases, which potentially reveal the presence of feedforward and feedback processes (Chapter 3). These chapters also investigate the influence of task constraints, finding decoding differences between implicit and explicit processing conditions. Overall, this research helps understand how the brain deals with occluded stimuli; in keeping with accounts implying the rich role for top-down influences, such as predictive coding. The following experiment (Chapter 4) investigates embodiment in emotion recognition with fMRI; exploring shared representation in the perception and production of facial expression. MVPA reveals reliable expression decoding in the premotor brain regions across perception and production, demonstrating representational overlap across the sensory perception and motor production of expression. This tentatively supports strongly embodied simulation-based (non-visual) theories. Collectively, the present research contributes to our knowledge of high-level influences in facial expression recognition, supporting the involvement of visual and non-visual routes to recognition, as well as providing further directions for future research.

Contents

List of Tables

List of Figures

Acknowledgements

First and foremost a massive thank you goes to my supervisor, Dr. Fraser Smith, for his continued support and guidance throughout my PhD. I am very grateful for the opportunities and experiences I have gained as a result of his expert knowledge and connections with other research institutions. Furthermore, I would like to thank Fraser for providing invaluable advice and feedback on my thesis. I would also like to thank my secondary supervisor, Dr. Andrew Bayliss, for his ongoing advice and encouragement during the course of my PhD. Andrew has supported me throughout my university experience, from undergraduate to PhD level, and I am extremely grateful for his constant understanding. Additionally I would like to extend my thanks to the School of Psychology for all their help and support, including the admin team, PhD students and staff, with a special mention to Louis Renault. It has been enjoyable working with such an excellent group of people.

I have also Kerri Bailey to thank for dedicating so much of her time collecting and analysing EEG data with me. We made an excellent team and it has been very enjoyable learning alongside you. Thanks also to Carolin, Carmen, Diana and Delia, I could not have asked for a better year group to share the PhD experience with. Huge thanks also goes to Ethan for our brain analysis days; we did a great job at keeping each other sane and had fun in the process! My gratitude also extends to the people working at Scannexus, in the Netherlands, and to Professor Lars Muckli, Dr. Lucy Petro and the PhD group at the University of Glasgow. I really appreciate everyone's willingness to help and their guidance through fMRI data collection and analysis. On top of this I am grateful for my friends and my brother, Charlie Worboys, willingly and patiently piloting my experiments, and the numerous students who signed up to take part in the studies.

An enormous thank you goes to my family and friends for listening to all the trials and tribulations of my PhD, providing lasting support and reassurances to my stresses and worries. I could not have done this without all of you! Mum, you always know what's best, thank you for believing in me; your love and encouragement has been integral to my success over the years. You always seem to know the right thing to say and give the best advice! Dad, thank you for taxi-ing me to and from airports for data collection / analysis trips as well as your constant support over the years. Last but not least, I want to thank Joe McGarry for relentlessly being there for me throughout it all; I love your eagerness to help and support me. Joe, both you and your parents have consistently made me realise that it is all going to work out and I will complete my thesis!

Author's Declaration

I declare that the work contained in this thesis has not been submitted for any other award and that it is all my own work. I also confirm that this work fully acknowledges opinions, ideas and contributions from the work of others.

Parts of this work has been presented at conferences:

Poster Presentations:

Adams, V., Petro, L., Muckli, L., & Smith, F.W. (2016). *Explicit and Implicit Decoding of Expression in V1 from Partial Face Stimuli.* Presented at the Organisation of Human Brain Mapping (OHBM), Geneva, Switzerland, June 2016.

Adams, V. & Smith, F.W. (2017). *Overlapping Networks in the Perception and Production of Facial Expressions; Embodiment in Emotion Recognition.* Presented at the Stop me if you think you've heard this one before: Novelty, Repetition and The Brain Conference, University of East Anglia, Norwich, UK, May 2017.

Any ethical clearance for the research presented in this thesis has been approved. Approval has been sought and granted by the School of Psychology Ethics Committee at the University of East Anglia.

Name: Vicky Adams

Signature: 

Date: 28/09/18

Word Count: 72,253

SECTION 1
–
Facial Expression Recognition

Chapter 1: Facial Expression Recognition

The visual recognition of emotion has been abundantly explored in previous literature due to the evolutionary and social importance of recognising emotion (Niedenthal, Krauth-Gruber, & Ric, 2006). Recognition activates basic fight or flight responses (approach or avoidance behaviours) and is key to successful social communication and relationships (Ekman, 1982). Research focuses on the six universal emotions identified by Ekman and Friesen (1975): fear, happiness, sadness, disgust, anger and surprise, with the understanding that complex emotional states can be obtained from subtle facial cues providing powerful nonverbal expressive displays (Peelen, Atkinson, & Vuilleumier, 2010). Successful decoding or recognition of a sender's expression is dependent on multiple aspects, including viewing distance (F. W. Smith & Schyns, 2009), presentation time (Balconi & Bortolotti, 2013), facial feature availability (Kotsia, Buciu, & Pitas, 2008), lighting (Bettadapura, 2012), context (Rousselet, Mace, & Fabre-Thorpe, 2004) and the emotional state of the observer (Niedenthal, Winkielman, Mondillon, & Vermeulen, 2009). The present research will continue to explore the visual recognition of emotion, with a particular focus on the high-level influences that occur under conditions of facial feature occlusion, and the possible contribution of embodied simulation in facial expression recognition.

To begin this research, it is important to define what a facial expression is. This definition is dependent on an individual's theory of emotion. This is because facial expressions can either be considered as universal, in line with earlier work advocating support for innate or evolutionary theories, or considered in terms of cultural differences, in line with social constructionism (Gendron & Barrett, 2009). With regards to evolutionary emotion theories, an expression is said to be an involuntary emotional response, functioning to increase our chances of survival; whereas in social constructionism theories, an expression is said to be voluntary, shaped by social communication and cultural display rules (Schmidt & Cohn, 2001; Adolphs 2002, E. Fox, 2008).

Evolutionary theories focus on the six universal emotions identified above (Ekman & Friesen, 1975). Evidence for these culturally ubiquitous facial expressions of emotion have been presented in research studying the isolated pre-literate western culture of New Guinea in 1971 (Ekman, 1994; Ekman & Friesen, 1971). This

cultural group was able to select a face expressing the appropriate emotional response to a story, in the absence of western media influences; showing that they could associate facial muscular patterns with a given emotion (Ekman & Friesen, 1971). On the other hand, social constructionist accounts categorise the experience of emotion using core shared affect (feeling of pleasantness or unpleasantness), with arousal, approach or reward systems (Lindquist et al., 2012; Wilson-Mendenhall, Barrett, & Barsalou, 2013). Evidence that the recognition of a sender's expression is dependent on a given situation, context and culture, is shown by western (U.S) and eastern (Japanese) cultures greater accuracy to recognise emotions expressed by members of their own culture (ethnic, national or regional group) (Dailey et al., 2010). This entrenched phenomena, known as in-group advantage, may explain the existence of recognition variability among cultures (Elfenbein & Ambady, 2002). Interestingly the recognition of happiness and anger were less affected by in-group advantage (Elfenbein & Ambady, 2002) and may be less culturally specific emotions.

Present work now widely advocates an interactionist perspective whereby both evolutionary and social elements of recognising expression are accepted (Elfenbein & Ambady, 2002). This is because there are universal emotions that seemingly share the same components, but there is also diversity across cultures (Elfenbein & Ambady, 2002). Nonetheless, it is important to note that there is also research in support of an embodied theory of emotion which considers sensorimotor brain activation and individual differences (Niedenthal, 2007).

1.1 Visual Recognition of Emotion

1.1.1 Visual Stream Model of Emotion Recognition.

The visual processing pathway is critical to expression recognition (Pessoa & Adolphs, 2010). This details the transfer of information from the retina to the lateral geniculate nucleus (LGN) and the primary visual cortex (V1), before information transfers to the extra-striate visual cortices (V2-V4) and inferior temporal areas (this information transfer is visually represented later as part of Figure 1.3). Research has shown that faces can be decoded around 70ms, suggesting the use of low-level image features when visual information first reaches the cortex (Cichy, Pantazis, & Oliva, 2014; Nemrodov, Niemeier, Mok, & Nestor, 2016), and the sensitivity to complex features and faces occurring further along the visual pathway (Pessoa & Adolphs, 2010). Simple feedforward computational models also account for the visual

recognition of expression (see Figure 1.1), these suggest that the categorisation of an expression occurs after a perceptual V1 level analysis and a gestalt inferior temporal (IT) level analysis has taken place (Dailey, Cottrell, Padgett, & Adolphs, 2002); this will be discussed further when considering bottom-up versus top-down processing of expression recognition.

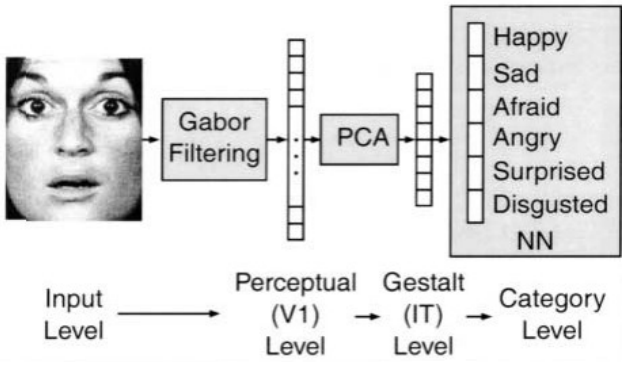

Figure 1.1. Diagram of a simple feedforward computational model that categorises facial expressions of emotion, from Dailey et al. (2002).

The advent of deep learning techniques and the use of deep neural networks for facial expression recognition have advanced computational modelling (Li & Deng, 2018). In deep learning models of facial expression recognition, there is a pre-processing step where facial information irrelevant to expression is normalised, as such faces are aligned and normalised for illumination, before deep models for feature learning, such as the convolutional neural network (CNN) or generative adversarial network (GAN), are applied for deep feature classification. These computational models are principally trained on large face and object recognition datasets and tested on small-scale expression recognition datasets; therefore, irrelevant facial information may be learnt, which could subsequently affect the networks ability to recognise facial expressions. Recently however large-scale datasets for facial expression have been created. It is important to note that both these deep neural networks and the simple feedforward computational models, described previously, may have difficulty processing occluded stimuli (Pepik, Benenson, Ritschel, & Schiele, 2015).

1.1.2 Face Models of Emotion Recognition.

Numerous cognitive models have been developed which separate components specialised for different aspects of facial processing (Bruce & Young, 1986; Haxby, Hoffman, & Gobbini, 2000). Bruce and Young (1986)'s model of face perception begins with the structural encoding of a face, before expression and other

aspects of the face are processed independently (Figure 1.2a). Whilst, the importance of the visual processing pathway to expression recognition has been specified, other brain regions have been identified as vitally important in the processing of faces. These are shown in a further model put forward by Haxby et al. (2000), who identified the inferior occipital gyrus (IOG), lateral fusiform gyrus (LFG) and the superior temporal sulcus (STS) as the three core face selective areas (see Figure 1.2b). Haxby et al. (2000) also detailed the function of these regions; notably separating the importance of the LFG in processing invariant aspects of faces, from the importance of the STS in processing changeable aspects of the face, involved in processing emotion (including static and dynamic facial features).

The existence of dedicated individual regions in the brain, separating facial identity from expression, is further suggested in the double dissociation found between the neurological disorder prosopagnosia (impairment to recognise faces) and prosopo-affective agnosia (inability to recognise expressions) (Calder & Young, 2005). Additionally research postulates the FG or Fusiform Face Area (FFA) as a domain-specific module activated during face perception or identity but not expression processing (Ghuman et al., 2014; Kanwisher, 2006; Li, Richardson, & Ghuman, 2018), which partially corresponds to the face-specific N170 component found in electroencephalogy (EEG) experiments (Bentin, Allison, Puce, Perez, & McCarthy, 1996; Itier, Alain, Sedore, & McIntosh, 2007; Yovel, 2016). On the other hand, the STS has been consistently implicated in expression processing (Engell & Haxby, 2007; Said, Moore, Engell, Todorov, & Haxby, 2010). The idea of domain-specificity in the brain with particular brain regions dedicated to aspects of cognition, has stemmed from evolutionary psychology (Cosmides & Tooby, 1994), the study of phrenology (Simpson, 2005) and cognitive psychology (Fodor, 1983). Whilst this research implicates dedicated neural substrates in the processing of facial perception, other research has shown the domain-specificity of the human primary motor cortex (Meier, Aflalo, Kastner, & Graziano, 2008) and five domain-specific areas of social cognition (Saxe, 2006).

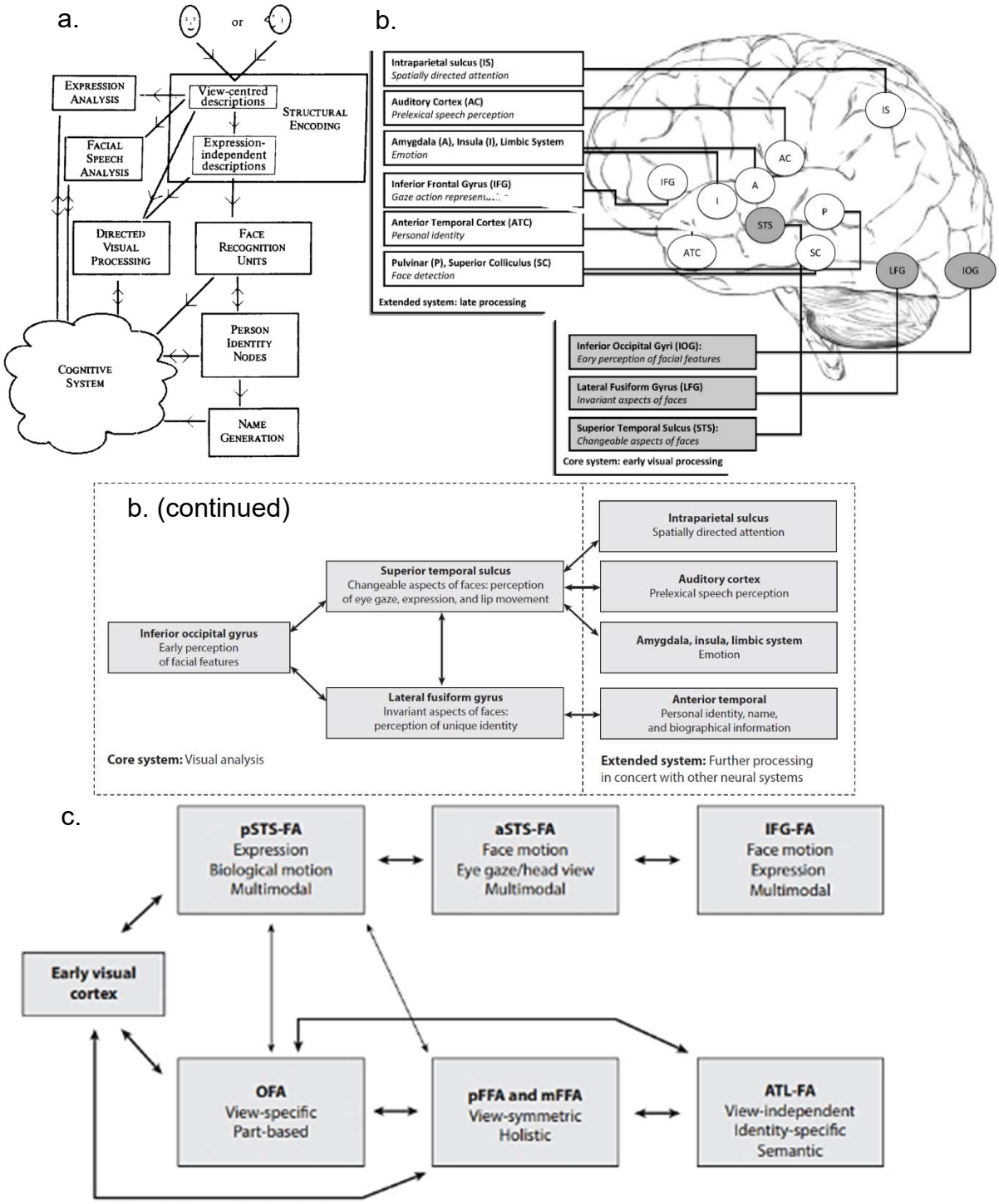

Figure 1.2. Face models of Emotion Recognition. a. Bruce and Young's (1986) model of face perception, expression analysis occurs after structural encoding. b. Haxby et al.'s (2000) hierarchical model of brain areas involved in processing faces (Apicella, Sicca, Federico, Campatelli, and Muratori, 2013). c. Duchaine and Yovel's (2015) revised neural framework for face processing revealing additional face-selective areas in anterior regions of the brain. This model shows a ventral face-processing pathway through the OFA, FFA and the Anterior Temporal Lobe (ATL), and a dorsal face-processing pathway, through the STS and the inferior frontal gyrus (IFG). -FA; face selective area. Model shows back connections/recurrent processing.

However, other research contradicts the finding of STS's independent involvement in processing changeable facial features and the segregation of identity and expression areas within the brain. This has been shown in adaptation studies finding the FFA (C. J. Fox, Moon, Iaria, & Barton, 2009; X. Xu & Biederman, 2010) and STS (C. J. Fox et al., 2009) sensitive to changes in both the perception of identity and expression. Furthermore, information about facial expressions has been represented in FG activation as opposed to the STS, within the same areas that represent identity (Li et al., 2018). Moreover Haxby et al. (2001) discredited evidence for domain specificity, finding representations between objects and faces to overlap in the ventral temporal cortex.

In light of new research and the contradictory results for domain specificity, findings for the roles and connections between face-selective areas were reviewed by Duchaine and Yovel (2015). These findings proposed several modifications and additions to Haxby's (2000) leading face model of emotion recognition (Duchaine & Yovel, 2015). Firstly, further evidence implicating the role of the FFA in the perception of changeable aspects of the face were discussed, and thus the role of this region in Haxby's (2000) version needed to be revised. Overall, the FFA is epitomised to have a general role in representing invariant facial structure information, such as identity, gender or age information, in addition to a contributing role in the recognition of facial expressions. Furthermore, Duchaine and Yovel (2015) identified three additional anterior face-selective areas besides the OFA, FFA and pSTS, namely the anterior temporal lobe (ATL), the anterior superior temporal sulcus (aSTS) and the inferior frontal gyrus (IFG), see Figure 1.2c. Duchaine and Yovel (2015) further showed that three of these regions, the pSTS, aSTS and IFG responded greater to dynamic face stimuli. Based on the new evidence they revised the three original core areas of Haxby's (2000) model and additional regions into a framework with a dorsal and ventral face-processing pathway. As such the areas that responded greater to dynamic face stimuli and gaze information were in the dorsal face processing pathway, driven by motion and form information, whereas the OFA, FFA and ATL comprised the ventral processing pathway, representing form information but also contributing to facial expression recognition. In the ventral route, the processing of structural information develops from processing faces in one particular view (view-specific), to processing across symmetrical viewpoints, and

finally to processing from any viewpoint (view-independent) that contains key featural information.

1.1.3 Using FMRI to Investigate the Regions Involved in Expression Recognition: Univariate or Multi-Voxel Pattern Analysis (MVPA).

Univariate fMRI analyses investigate the activation of regions in response to a specific stimulus, with activated voxels indicating their involvement (Mur, Bandettini, & Kriegeskorte, 2009). In univariate analyses, general linear models (GLM) are used to investigate activation between experimental conditions, both at a single-subject and group-level basis. It is important to note that these analyses lack sensitivity, as activation is spatially smoothed and averaged across voxels within a region of interest (ROI) (Haynes & Rees, 2006; Mur et al., 2009; Norman, Polyn, Detre, & Haxby, 2006). An abundance of fMRI (Functional Magnetic Resonance Imaging) studies use this analysis to investigate the regions involved in the perception and experience of emotion, however, studies are gradually applying MVPA to also investigate these regions. MVPA investigates the representational content of regions, allowing patterns of brain activation to be extracted and compared across stimuli or experimental conditions (Mur et al., 2009). Therefore, in this analysis, differences between conditions can be detected for the same ROI with fine-grained pattern information (Norman et al., 2006; Tong & Pratte, 2012). In MVPA, advanced pattern-classification algorithms are applied to fMRI data, these aim to decode information represented in an individual region of a participant's brain (Haynes, 2015; Mur et al., 2009; Norman et al., 2006). Thus, MVPA is a more sensitive measure than univariate analyses in recognising cognitive states and the organisation of these within the brain (Coutanche, Solomon, & Thompson-Schill, 2016; Norman et al., 2006). As a result of this, MVPA is the preferred choice of analysis in future fMRI studies investigating the regions involved in expression recognition.

1.1.3.1 FMRI studies investigating the regions involved in expression recognition.

Univariate fMRI (Functional Magnetic Resonance Imaging) research has focussed on investigating neural substrates dedicated to the perception and experience of an individual emotion (Lindquist, Wager, Kober, Bliss-Moreau, & Barrett, 2012). Findings from these univariate meta-analyses vary, with some suggesting the involvement of separate brain areas responsible for the experience of

discrete emotions (Phan, Wager, Taylor, & Liberzon, 2002), to others finding the perception and experience of emotion to activate areas across the brain (Fusar-Poli et al., 2009; Kober et al., 2008; Lindquist et al., 2012). Whilst the amygdala-fear hypothesis has been consistently supported, with the perception and experience of fear specifically linked to amygdala activity in 60% of studies (Murphy, Nimmo-Smith, & Lawrence, 2003; Phan et al., 2002); this finding is called into question with the processing of other emotions, including happiness, sadness, neutral, disgust and anger, which have been found to similarly activate the amygdala (Fusar-Poli et al., 2009; Murphy et al., 2003; van der Gaag, Minderaa, & Keysers, 2007). Thus, more recently the amygdala has been recognised as a centre for vigilance with face responsive neurons processing affective salient, uncertain, novel or unusual stimuli irrespective of valence (Fusar-Poli et al., 2009; Lindquist et al., 2012). Furthermore insular and basal ganglia activation has been consistently linked to the perception and experience of disgust, however increased activity also corresponds with experiencing anger, happiness or fear (Fusar-Poli et al., 2009; Lindquist et al., 2012; Phan et al., 2002; van der Gaag et al., 2007). Thus this region may correspond to valence and regulate approach or avoidance behaviour (Phan et al., 2002). Further hypotheses have linked activity in the lateral orbitofrontal cortex (OFC) to the experience and perception of anger, and activity in the Anterior Cingulate Cortex (ACC) to the perception and experience of sadness and happiness (Fusar-Poli et al., 2009; Lindquist et al., 2012).

Whilst correlations persist between certain brain areas and emotion categories, these may arise in the bias to report previously identified areas (Kober et al., 2008), thus overlooking the associated emotion labels is likely to yield new insights into the organisation of emotion in the brain (Kober et al., 2008). Therefore, Kober et al. (2008) undertook an inductive data-driven approach to which they located activated brain areas independent of basic emotion categories. They did this by identifying activated voxels in emotion perception and experience studies, and used a nonmetric dimensional scaling (NDMS) reduction technique and clustering to classify voxels into regions. This approach identified six functionally distributed networks in the brain for emotion (e.g. for visual processing, attention, regulation of emotion, motivation, selecting context appropriate actions, salience), with vast interconnections predominantly occurring between frontal and limbic areas (Kober et al., 2008). Connectivity may stem from posterior areas, such as the IOG, to the

prefrontal cortex (PFC), potentially bypassing limbic structures such as the amygdala (Dima, Stephan, Roiser, Friston, & Frangou, 2011). The PFC has been found to have an important role in the recognition of facial expressions (Dalgleish, 2004; Dima et al., 2011; Kober et al., 2008), in constructing knowledge of an emotion (Fusar-Poli et al., 2009).

Additionally a number of cortical and subcortical areas have been suggested in the emotional brain (Dalgleish, 2004; Kober et al., 2008); particularly the early role of occipital and temporal areas and the subsequent requirement of the amygdala to process emotional faces (Fusar-Poli et al., 2009). Moreover, a study by Saarimäki et al. (2015) found distinct neural signature patterns across the somatomotor and limbic regions for the experience of emotions, using Multi-Voxel Pattern Analysis (MVPA; an analysis technique that will be discussed further in the next paragraph). Alternatively an interplay between two neural systems: a ventral and dorsal stream have been suggested to identify, produce and regulate emotion (M. L. Phillips, Drevets, Rauch, & Lane, 2003). Furthermore, Haxby et al. (2000)'s identification of a core and extended system, and Pessoa and Adolphs (2010)'s multiple-waves model (see Figure 1.3), show additional support for a distributed network of brain regions involved in the processing of faces or emotions (Haxby & Gobbini, 2011). The distributed nature of activation may be a result of combining a variety of stimuli, measures, experimental tasks and different ways of transforming and pre-processing data (Lindquist et al., 2012).

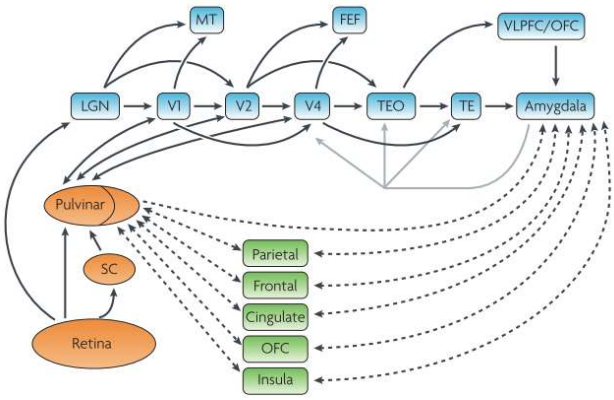

Figure 1.3. Diagram of the multiple-waves model of processing showing the involvement of a distributed network of brain areas in the recognition of emotion. TE and TEO, Inferior temporal area, from Pessoa and Adolphs (2010).

MVPA decoding studies have investigated selected regions involved in emotion perception, finding reliable decoding in the STS (Said et al., 2010), FFA (Harry, Williams, Davis, & Kim, 2013) and early visual cortex (Harry et al., 2013; Petro, Smith, Schyns, & Muckli, 2013). However, to allow comparisons to be made between regions, Wegrzyn et al. (2015) considered the seven brain regions involved in the core and extended face network, outlined in Haxby's model of face processing (Haxby & Gobbini, 2011). MVPA was implemented in seven regions of interest (ROI's, see Figure 1.4) to decode happiness, anger, fear and neutral expressions in a gender recognition task (Wegrzyn et al., 2015). They found decoding accuracies above chance in all ROI's, including the FG, STS and inferior occipital (IO) areas which form the core face network, as well as the anterior temporal (AT), insula (INS), intraparietal sulcus (IS), and the amygdala which form the extended face network (Wegrzyn et al., 2015). Highest decoding accuracy was present in the FG and STS, whereas decoding was lowest in the amygdala (Wegrzyn et al., 2015). Whilst these results show support for the regions conceptualised by Haxby et al. (2000), emotion recognition appears dependent on further overlapping and distributed neural mechanisms. The consistent finding of FFA or FG involvement in emotion (C. J. Fox et al., 2009; Fusar-Poli et al., 2009; Kawasaki et al., 2011) is surprising giving its initial conceptualisation of processing invariant facial features such as identity. Thus, the FFA may broadly be responsible for face processing (identity and expression) in which an individual has visual expertise (Tarr & Gauthier, 2000). However, the role of the FFA in the perception of changeable aspects of the face, or expression processing was later identified in the revised model of face processing by Duchaine and Yovel (2015), mentioned above. Furthermore, other literature suggests the role of the FFA in the processing of facial expression, as well as its role in processing structural identity information (Vuillemier, Armony, Driver, & Dolan, 2001; Ganel, Valyear, Goshen-Gottshein, & Goodale, 2005; Duchaine & Yovel, 2015). Vuillemier et al. (2001) found greater right fusiform and amygdala activation in response to fearful than neutral expressions, independent of attention; thereby concluding that the FFA may be receiving feedback related to an emotional response from the amygdala.

Furthermore, in Wegrzyn et al. (2015), the FG is not significantly different from decoding accuracy in the STS, but significantly higher than the amygdala, insula, intraparietal sulcus and the IOG. This is surprising given these other regions

are highly involved in processing emotion. However, this could be due to a number of reasons: the static face stimuli were not enough to elicit an arousal response, the difficulty of scanning limbic structures in fMRI or the absence of disgust stimuli (Wegrzyn et al., 2015). Critically, however, Wegrzyn et al. (2015) do not generalise across specific face identities or other non-overlapping representations in their MVPA, and thus do not necessarily tap into high-level representations to minimise the role of low-level features in decoding. Thus, their basic decoding analysis could be strongly influenced by low-level effects.

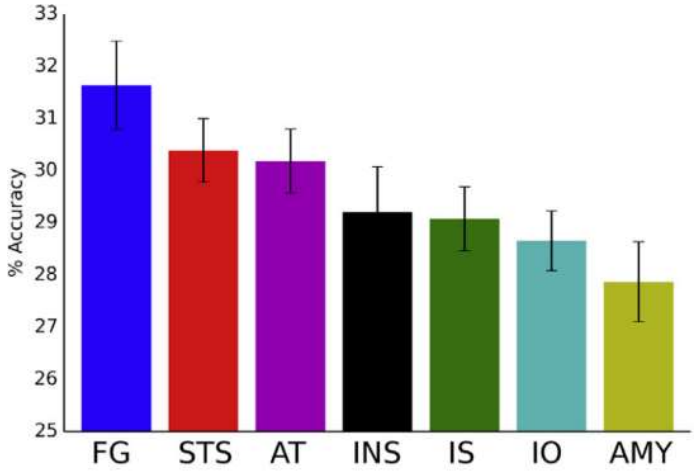

Figure 1.4. Mean accuracy for all seven ROI's selected in Wegrzyn et al. (2015), successful recognition in all brain areas is above chance (25%); FG, fusiform gyrus, STS, superior temporal sulcus; AT, anterior temporal; INS, insula; IS, intraparietal sulcus; IO, inferior occipital gyri; AMY, amygdala. Image from Wegrzyn et al. (2015).

Zhang et al. (2016) used a hierarchical classification analysis to investigate whether facial expressions (neutral, fear, angry and happiness) could be differentiated from other expressions in a number of face-selective regions. They found decoding present in the amygdala, primarily between fearful and non-fearful faces, and at a second-level classification between neutral and emotional faces (Zhang et al., 2016). Furthermore they found decoding in the posterior STS between neutral and emotional faces, and at the next level of analysis between happy versus fearful and angry faces, playing an additional role in discerning positive from negative emotions (Zhang et al., 2016). They did not find significant decoding within their other regions of interest (ROI's) including the OFA, FFA, aIT and V1; this may be due to using a slow event-related design because this is associated with lower statistical power and subject expectation and habituation, as a consequence of slow

and repeated stimuli presentations. Furthermore, the absence of this decoding may be due to the stringent permutation used to test for significance or generalising across identity (Zhang et al., 2016). However, it is important to highlight, unlike Wegrzyn et al. (2015), that this study, generalising across specific trained and then tested face identities in their MVPA analysis, is able to minimise the role of low-level features in decoding and consequently tap into high-level representations. This study also advocates evidence for the neural dissociation in expression and identity recognition, as decoding of identity was found in the FFA and aIT (Zhang et al., 2016).

Furthermore to augment the previous findings, a recent study, using all six basic emotions, found strong decoding accuracy in bilateral FFA, OFA and posterior rSTS; as well as in motion-selective areas: V5f/hMT+ and another posterior rSTS ROI (defined from a separate localiser but partially overlapping with the previous face-selective STS) (Liang et al., 2017). These findings support Wegrzyn et al. (2015) with significant decoding accuracy present in the FG and STS. Alongside these regions, finding significance in OFA (situated in or close to the inferior occipital gyrus) further supports the regions identified in Haxby's model of face processing (Haxby & Gobbini, 2011). However, it is important to note that this study, akin to Wegrzyn et al. (2015), only carried out basic decoding and did not generalise across specific face identities or representations in further MVPA cross-classification analyses. Therefore again, this study may not necessarily be tapping into high-level representations and could be strongly influenced by low-level effects.

1.1.4 Bottom-up Versus Top-down Models of the Visual System.

Computational models present a bottom-up feedforward approach to expression recognition, assuming that the visual cortex (V1) provides a direct representation of a presented visual signal (Kober et al., 2008; Murphy et al., 2003). This corresponds with standard models of V1 that establish the properties of V1's simple and complex cell responses (i.e. tuned for orientation, motion, colour and spatial frequency). Based on these assumptions, simple computational models (as aforementioned previously when detailing the visual stream model), have been developed to depict this feedforward network of expression recognition, representing some vital functions that occur within the visual system (Dailey et al., 2002). These neural network models are comprised of three processing layers (see Figure 1.1): the first layer, a perceptual analysis of V1, is carried out with the use of a Gabor filter to model the response properties of neurons in V1 (including edge detection), the

second layer provides a gestalt object representation in inferior temporal (IT) cortex, which is achieved with a dimensionality reduction method of principal component analysis (PCA), and lastly the third layer represents the categorisation of an expression.

Other computational bottom-up models decode facial expression anatomically with the classification of facial Action Units (AU's) (Tian, Kanade, & Cohn, 2011). Many systems of classifying these units have been developed, including the Facial Action Coding System (FACS) and Facial Animation Parameters (FAPs) (Bettadapura, 2012). Whilst FAC's is an approach requiring the identification of individual or sets of facial muscle movement involved in a given expression (Bettadapura, 2012; Ekman, 1982), FAPs is a system defining feature points (FPs) of an action, thus the degree of change such as subtleness or intensity of an expression is taken into consideration (Bettadapura, 2012; Igor & Robert, 2003).

These computational models are engineered to recognise emotion in clearly presented whole face stimuli, however, facial features are often occluded from view when interacting with individuals in the real world, and these models would not necessarily be able to process occlusion well. This is because bottom-up models do not generalise from whole objects and are unsuccessful in achieving human-level performance in partial object recognition (Tang et al., 2018). Additionally these models will have difficulty modelling contributions from recurrent connections (Tang et al., 2014). Furthermore, a large proportion of V1's function is unaccounted for, such that a representative sample of neurons have not been tested when ecologically complex stimuli are presented (Carandini et al., 2005; Olshausen & Field, 2005). Moreover, V1 is thought to contain feedback connections from a number of brain regions, including the amygdala, or more local connections from within the visual system (Olshausen & Field, 2005). Subsequently, there may be many top-down influences involved in the visual recognition of expression, and these may be especially relevant when processing conditions of uncertainty caused by partial occlusion (Greening, Mitchell, & Smith, 2018; Muckli, 2010; Muckli, Petro, & Smith, 2013).

The predictive coding framework offers an account into the mechanisms that take place within the visual system, including the role of top-down feedback processing to V1 (see Figure 2.11, Chapter 2) (Clark, 2013; Friston, 2005, 2008; Rao & Ballard, 1999). This framework details how predictions, concerning the current

sensory information in V1, originate in higher level areas of the cortex and are fed back to early visual regions, which in turn transmit error signals back with a computed difference between expected and observed information. Petro et al. (2013) tested the role of top-down feedback to V1 in face processing; demonstrating top-down modulation occurring in V1, where this region appeared to receive task dependent feedback from higher visual areas (Petro et al., 2013). Furthermore, research indicates the role of a bidirectional pathway; with V1 receiving feedforward information, as well as top-down or processed recurrent feedback from cortical (FFA, OFA) and subcortical brain areas (amygdala) (Bannert & Bartels, 2013; Petro et al., 2013). Other top-down models have been developed for the visual system, to account for the role of bottom-up and feedback processes in the brain, these include recurrent feedback models of object recognition (Tang et al., 2014; Tang et al., 2018; Wyatte, Curran, & O'Reilly, 2012), Bayesian and infomax accounts of processing (Lee & Mumford, 2003; W. A. Phillips, Kay, & Smyth, 1995), as well as a hierarchical neural network model (Heeger, 2017). Predictive coding and other top-down models of the visual system will be described in more detail in Chapter 2 (2.1.1.1).

Research has investigated the role of these top-down effects in conditions of occlusion; as these conditions offer a way to observe predictions regarding the visual context (Greening et al., 2018; F. W. Smith & Muckli, 2010). It is important to note that in predictive coding, occluded, as opposed to non-occluded stimuli, are suggested to create higher responses in sub-regions of V1, until continued processing acts to subdue uncertainty or error responses. Whilst other top-down models in comparison to predictive coding, suggest that occluded as opposed to non-occluded stimuli, create an overall decrease in response, which amplifies through processing (O'Reilly, Wyatte, Herd, Mingus, & Jilk, 2013; Wyatte et al., 2012). The contribution of cortical feedback processes in V1 is testable when taking advantage of V1's retinotopic organisation (Petro et al., 2013; F. W. Smith & Muckli, 2010). This is because mapping occluded parts of visual space and finding V1 sensitivity in an occluded area of a natural visual scene, devoid of feedforward input, suggests the involvement of contextual mechanisms (feedback and lateral connections) in early visual cortex (F. W. Smith & Muckli, 2010). These are most likely to be feedback effects as opposed to lateral connections, as the same paradigm investigating an occluded scene was applied in a study by Muckli et al. (2015), finding feedback in

superficial outer layers of V1 likely projecting from extra-striate visual, cortical and subcortical brain regions. Furthermore, research has begun to test the role of cortical feedback in perceiving facial expressions under occlusion; finding neural information in early visual cortex to generalise across independent visual face parts, such as faces depicting eyes only to the corresponding minus eyes stimuli (Greening et al., 2018). Comparing responses in the brain across non-overlapping visual face stimuli can tap into feedback processes, however, this study did not retinotopically map the visual cortex (using instead a group-level probabilistic V1 mask). This restricts the assumptions that can be made on the role of cortical feedback processing to V1.

Whilst research has studied the occlusion of objects and scenes, little research has examined the involvement of early visual cortex (V1-V3) in processing occluded facial features. As faces are such biologically salient signals (Pessoa & Adolphs, 2010), it is likely that facial occlusion may recruit greater use of top-down (or lateral interactions) to fill in missing feature information. Thus, it is pertinent for research to further understand what factors mediate or influence the recognition of emotional expression; the relatively unexplored top-down effects of context and prior experience in early brain areas (Petro et al., 2013).

1.1.5 Behavioural Studies Demonstrating the Optimal Conditions for Emotion Recognition.

The visual route to the recognition of emotion assumes that knowledge regarding a facial feature configuration is adequate for successful emotion recognition (Goldman & Sripada, 2005). Face perception typically relies on a holistic approach, whereby all facial features are taken into consideration to form the final percept (Bettadapura, 2012), thus, this plausibly suggests that the face as a whole will provide rich information vital for emotion recognition (Kanwisher & Yovel, 2009). To test the limits of the visual system, behavioural studies have researched the optimal conditions for accurate face recognition (Bettadapura, 2012). Many factors affect recognition such as occlusion, the difference between spontaneous “true” emotions and deliberate “posed” emotions and the faster detection of emotions in natural contexts (Cauchoix, Barragan-Jason, Serre, & Barbeau, 2014).

Studies demonstrate that expression recognition can occur when specific facial features or visual information from the face is occluded (M. L. Smith, Cottrell,

Gosselin, & Schyns, 2005). These studies are important for identifying which features for recognition are pertinent in everyday life (Bettadapura, 2012). Real-world occlusion is commonplace including instances of interacting with an individual whose hat, sunglasses, scarf, facial hair or hands may be covering up part of their face. Furthermore, emotion can still be recognised when facial features are presented blurred or scrambled (Bombari et al., 2013). Occlusion may also encompass situations where there is poor lighting and the only visible head orientation is non-frontal (Bettadapura, 2012). Observers seem well equipped to successfully recognise facial expressions under constrained viewing conditions (Calvo & Nummenmaa, 2015) and those presented in peripheral vision (Bayle, Schoendorff, Hénaff, & Krolak-Salmon, 2011; Calvo, Fernández-Martín, & Nummenmaa, 2014; F. W. Smith & Rossit, 2018).

The bubbles technique is commonly used, whereby Gaussian windows are randomly placed on face stimuli, to ascribe human's categorisation ability to specific visual information and reveal the information used in recognition (Gosselin & Schyns, 2001). Depending on the expression, the resulting classification images of the basic emotions implicated the eyes and mouth as the two central facial features (see Figure 1.5); with the mouth as the most important feature in happiness and disgust (with an additional focus for disgust recognition on wrinkles around the nose, mouth and eyes) and the eyes most important in fear (enlarged eye whites and raised eyebrows) and anger (with a further focus on a furrowed brow and lowered eyebrows) (F. W. Smith et al., 2008; M. L. Smith et al., 2005; M. L. Smith & Merlusca, 2014). Thus mouth occlusion would likely decrease the recognition of happiness and disgust, whereas eye occlusion would likely decrease the recognition of fear and anger (F. W. Smith & Schyns, 2009; M. L. Smith & Merlusca, 2014). However, strong evidence from 'Reading the Mind in the Eyes' task (RMET) for complex emotions (Baron-Cohen, 2004) and responsivity to eye-whites (Whalen et al., 2004), highlight the overarching importance of eye information in complex or secondary emotion recognition. However, Whalen et al. (2004) only presented participants with eye information, but not information from the mouth, to make their decisions on fear and happiness. It appears that the eyes and mouth are important facial features, but information from the eyes may be sufficient for recognition. Largely, results indicate a human's robust ability to recognise emotion even under conditions of uncertainty caused by partial occlusion.

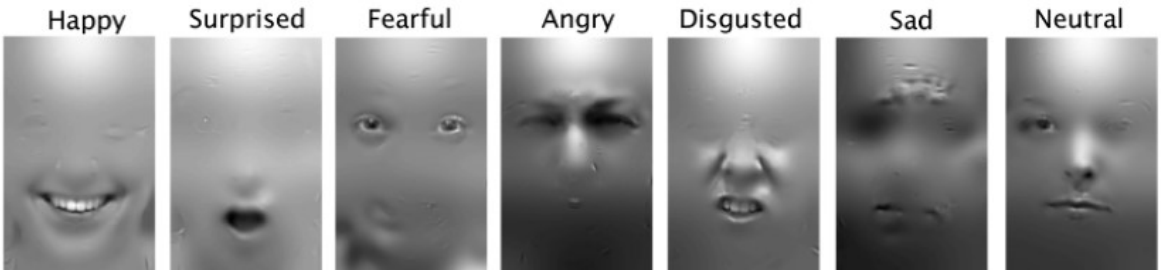

Figure 1.5. Diagnostic features necessary to categorise each of the basic emotions, adapted from M. L. Smith et al. (2005).

Further behavioural studies have investigated the ability to recognise different emotions, these show the ease at which humans recognise happiness and surprise over disgust, fear, anger and sadness (Du & Martinez, 2011; F. W. Smith & Schyns, 2009). Petro et al. (2013) also showed a faster reaction time in response to happy faces than fear or neutral. Many researchers turn to evolution to understand the differences amongst the emotions. It seems disadvantageous that humans poorly recognise fear and anger when these emotions signal threat and danger. However, it may be reasonable that sadness is poorly recognised as it has no survival advantage (F. W. Smith & Schyns, 2009). Finding surprise to be recognised well makes evolutionary sense as this signal is indicative of an unexpected event in an individual's environment that needs to be responded to (F. W. Smith & Schyns, 2009). Lastly the recognition of happiness can be explained in evolutionary terms with humans need for social contact and its role in society as an approach signal or through adaptation of a bared-tooth display hitherto used in fear (F. W. Smith & Schyns, 2009). Alternatively, the enhanced recognition may be due to the frequency that an emotion is viewed in an observers daily environment; when recording the frequency of seen expressions happiness and surprise were observed most (Calvo, Gutiérrez-García, Fernández-Martín, & Nummenmaa, 2014; Calvo & Nummenmaa, 2015). However, more simply, enhanced recognition may result from larger easily-identifiable facial shape deformations involving the mouth and eyebrows (Du & Martinez, 2011; Pardàs & Bonafonte, 2002; F. W. Smith & Schyns, 2009). Here I argue that the differences amongst the emotions can be explained in evolutionary terms, but evolution cannot provide a complete account as the emotions signalling threat and danger are not the most recognised. Therefore, I believe the frequency with which an expression is used and the presence of easily-identifiable features, such as the mouth, account for the differential ability to recognise emotions, particularly the increased ability to recognise happiness and surprise.

1.1.6 EEG Studies Demonstrating the Effect of Occlusion on the N170.

Even though research has demonstrated that expression recognition can occur when specific facial features are occluded (M. L. Smith et al., 2005), few studies have investigated how the N170 component may change as a result of partial face occlusion. The first studies to explore this investigated eye occlusion; they found a delayed N170 response to faces missing eye information (Eimer, 1998; Itier et al., 2007). This delay was approximately 10ms, with whole face processing (155-160ms), occurring significantly faster than processing faces missing eyes (155-170ms) (Itier et al., 2007). These studies, however, showed that faces missing eye information had no effect on the N170 amplitude (Eimer, 1998; Itier et al., 2007). Itier et al. (2007) also investigated the effect of only showing the eyes; this further delayed the N170 response (~175ms) and was again significantly different from the whole face condition. Conversely, the eyes prompted an earlier peak N170 (of ~10-15ms) in a more recent study that used the 'bubbles' technique to investigate which facial features had an effect on the N170 response (Rousselet, Ince, van Rijsbergen, & Schyns, 2014). This difference may result from the bubbles technique always comparing the same overall amount of information rather than comparing the eyes to a whole face stimulus. Furthermore, in both studies, they found that when the eyes were present the N170 was greater in amplitude (Itier et al., 2007) and this was particularly apparent for the left eye, activating the rN170 (Rousselet et al., 2014); this increase in amplitude to isolated eyes was also shown in an early study by Bentin et al. (1996). Overall, it seems apparent that the eyes are important to expression recognition, with their absence associated with delays in processing and their presence associated with a larger N170 response (Bentin et al., 1996; Itier et al., 2007).

Whilst the previous studies isolated individual facial features (Bentin et al., 1996; Eimer, 1998; Itier et al., 2007) or presented random samples of face information (Rousselet et al., 2014), a variant on this was conducted, whereby fixation was directed to the mouth, nose, right or left eye of a whole face (face offset, fixation remained central) (Neath-Tavares & Itier, 2016). This experiment additionally showed an increase in the N170 amplitude to the eyes, this eye-sensitivity did not vary across expression (happy, fear, neutral) (Neath-Tavares & Itier, 2016; Neath & Itier, 2015). The authors further state the surprising nature of this, as the eyes are more lateral and the N170 amplitude is known to decrease with

face eccentricity (Neath-Tavares & Itier, 2016). Additionally, this study found larger amplitudes around the P100 in occipital areas, when participants were directed to the mouth, (Neath-Tavares & Itier, 2016). Whilst this findings may, at 100ms, purely reflect the low-level visual properties of the mouth (its high contrast); it may be indicative of early top-down processing to this area that has previously been stated as important for expression recognition (F. W. Smith & Schyns, 2009).

1.2 Non-Visual Routes to Emotion Recognition

Currently only research detailing the visual routes to emotion recognition have been discussed; whilst the use of visual information is crucial, research has also suggested that individuals make use of sensorimotor simulation or embodiment for recognition (Wood, Rychlowska, Korb, & Niedenthal, 2016). Thus, these non-visual routes, implicating the critical involvement of sensorimotor simulation, are thought to be a top-down influence on recognition (Wood, Rychlowska, et al., 2016). A model developed by Wood, Rychlowska, et al. (2016), shows how simulation is fed back to a visual input, to enable the perception of a stimulus to be continuingly regulated. Thus the iterative loop between visual perception (visual routes of emotion recognition) and sensorimotor simulation (non-visual routes to recognition) suggests that both visual and sensorimotor pathways create sources of information in constructing a prediction of another's emotion (Wood, Rychlowska, et al., 2016). Furthermore, regions of the intraparietal sulcus (IPS), important for simulation, have been found to modulate higher-level and early visual regions, additionally showing support for the incorporation of both routes as being involved in the recognition of emotion (Iacoboni & Dapretto, 2006; K. N. Kay & Yeatman, 2017)

1.2.1 What is Embodiment?

Recent accounts ground emotion in modality-specific systems of introspection, perception and action (Niedenthal et al., 2009) with facial expression recognition being aided by simulation-like processes (Niedenthal et al., 2006). These simulation based accounts are known as the theories of embodied cognition or embodied simulation. The embodiment of emotion occurs when the processing of emotional information, including visual recognition, partly reactivates the neural substrates activated when the individual previously experienced that emotion (Niedenthal et al., 2009). Thus neural structures overlap in sensory, motor and affective systems when recognising a sender's facial expression and personally experiencing the same emotion (Niedenthal, 2007).

The notion of embodiment in facial expression research emerged from early research on the facial feedback hypothesis, which detailed how expression not only provides the outward manifestation of emotion, but can influence an observer's subjective state and the processing of information (Niedenthal et al., 2006). Further research has found that adopting a sender's expression produces the corresponding affective state in an observer (Niedenthal, 2007). This explains why smiles are viewed as contagious (Wild, Erb, Eyb, Bartels, & Grodd, 2003) and how feelings of fear and pain are shared (Bastiaansen, Thioux, & Keysers, 2009), as well as how an observer's preferences and behaviours are influenced (Niedenthal, 2007). The effects of embodiment, facial mimicry, and the phenomena of emotional contagion (Hatfield & Cacioppo, 1994) can influence recognition by intensifying emotions; promoting understanding and empathy between individuals (Niedenthal et al., 2006). Mimicry has been shown to play a fundamental role in processing a sender's expression (Niedenthal et al., 2009), with early research showing the strong nature to imitate yawning (Provine, 1986) and 12-21 day old infants propensity to imitate mouth opening and tongue protrusion (Meltzoff & Moore, 1977). However, embodiment theorists would argue that mimicry is not always necessary in the recognition of another's expression, suggesting that sensorimotor simulation can occur with or without the use of facial mimicry (Adolphs, 2002).

1.2.1.1 The importance of embodied simulation and mimicry.

Goldman and Sripada (2005) outline several models of embodiment including reverse simulation, the "as if" loop model of simulation and an unmediated resonance model. The reverse simulation model details the link between mimicry, experience and recognition of one's emotion (see Figure 1.6) (Goldman & Sripada, 2005). Classical studies have manipulated expression experimentally, by facilitating or inhibiting certain facial muscles, for example Strack, Martin, and Stepper (1988) asked participants to hold a pen between their front teeth to facilitate the muscles associated with smiling, but hold a pen between their lips to inhibit these muscles. Participants in the pen-in-teeth condition rated cartoons as more humorous (Strack et al., 1988). A further study fixed stickers to the inside of participant's eyebrows and instructed them to bring them together, this used muscles to contract the brow (Larsen, Kasimatis, & Frey, 2008). Consequently participants reported greater sadness to aversive photographs (Larsen et al., 2008). Furthermore, the application of a constrictive gel facemask was found to affect the ability to recognise

expressions but not non-face control stimuli (Wood, Lupyan, Sherrin, & Niedenthal, 2016). Overall, the manipulations of positive and negative affect, as well as the facemask expression manipulation technique, support the importance and specificity of mimicry in expression recognition (Wood, Lupyan, et al., 2016).

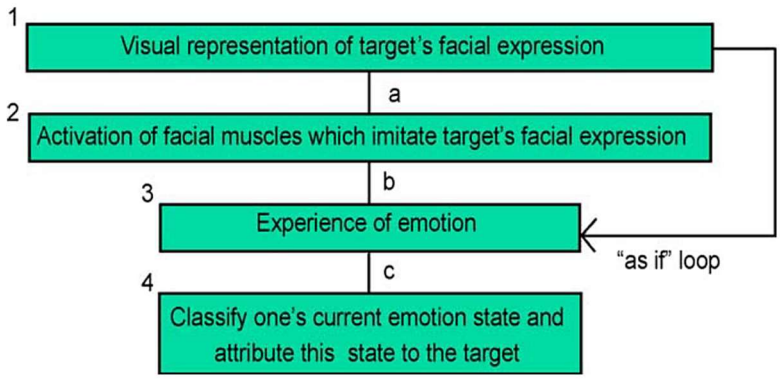

Figure 1.6. Reverse simulation model with the "as if" loop, from Goldman and Sripada (2005).

Niedenthal, Brauer, Halberstadt, and Innes-Ker (2001) showed individuals mimicking the first expression of a computerised morph movie to be faster at detecting a change in facial expression, than individuals who did not initially mimic the first expression. The experience of emotional state congruence with the first expression, portrays an ease and willingness to mimic the expression and detect an incongruent expression change as it occurs (Niedenthal et al., 2001). Conversely less shift in facial mimicry was required when experiencing incongruence (where the first expression was not mimicked) as the change becomes concurrent with a sender's own expression (Niedenthal et al., 2001). Comparatively an fMRI study by Wild et al. (2003) showed quicker responses to an expression that was congruent with the facial movement the participant was told to produce (e.g. participants were faster to respond to a smile if instructed to move the corners of their mouth upwards). Overall this research demonstrates the extent to which embodiment and convergence of facial movements can influence an observer's ability to experience, process and understand a sender's emotion (Niedenthal, 2007).

Studies have also investigated the embodiment of emotion concepts by asking participants to carry out property verification tasks, where they judge whether a word is associated with an emotion, or perceptual word tasks, where they judge a word as upper or lower case (Niedenthal et al., 2009). Furthermore embodiment was

tested directly with facial electromyography (EMG), these measurements were obtained by applying electrodes to four facial muscles (see Figure 1.7): the corrugator supercilii (strongly activated in response to anger to produce a frown), levator labii superioris (in response to disgust to produce a grimace), zygomaticus major and orbicularis oculi (activated in response to happiness to produce a smile) (Niedenthal et al., 2009). The emotion task revealed that words related to emotion significantly activated corresponding facial muscles, whereas no somatic or muscular responses were activated in the perceptual word task (Niedenthal et al., 2009). This provides observable evidence for simulation embodiment effects in relation to words that are judged as emotional (Niedenthal et al., 2009).

.

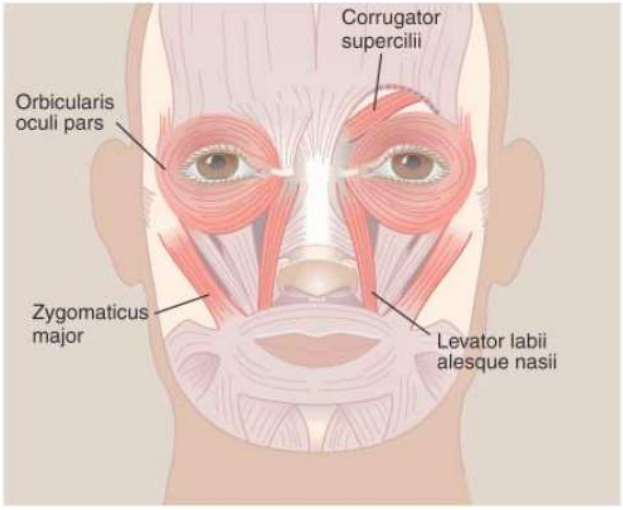

Figure 1.7. Diagram showing the muscles activated in response to facial expressions, measured using EMG, from Niedenthal (2007).

Studies have been carried out specifically investigating expression recognition with EMG. Using the biting pen manipulation, Oberman, Winkielman, and Ramachandran (2007) found this to significantly impair the recognition of happiness over disgust, fear and sadness, with happiness presumably the most affected due to its outward manifestation (requiring vast muscle activation) compared to the other emotions that are usually constrained and activated internally (Oberman et al., 2007). Although no facial muscles were inhibited, Kunecke, Hildebrandt, Recio, Sommer, and Wilhelm (2014), found mimicry to improve basic emotion recognition, showing increased corrugator activity when perceiving anger and sadness but decreased activity when perceiving happiness. Against expectations, zygomaticus activity was not found in response to happiness, although this may be due to artificial laboratory settings preventing the formation of a smile, and the high

variability of this muscle (Kunecke et al., 2014). Therefore, such disadvantages limit the application of EMG in studying the effects of embodied emotion. Greater control of upper and lower facial muscles is necessary to ascertain the effects of mimicry on recognition (Oberman et al., 2007).

A novel study investigated the effects of blocking facial mimicry on recognition with a sample of clinical patients (Neal & Chartrand, 2011). They tested recognition with the 'Reading the Mind in the Eyes' task, for subtle, non-prototypical emotions, likely to be encountered in everyday life. Patients were either undergoing Botox (treatment that paralyses facial muscles) or Restylane (dermal filler that does not modify muscles) injections for expression-related facial wrinkles (Neal & Chartrand, 2011). Patients receiving Botox experienced less muscular feedback and consequently were less accurate at perceiving positive and negative emotions, than patients receiving Restylane who showed typical task performance (Neal & Chartrand, 2011). Botox has also be shown to interact with depression; with paralysis of the corrugator muscle reducing depression (Finzi & Rosenthal, 2014; Wollmer et al., 2012) but paralysis of the zygomatic muscle increasing symptoms of depression (VanSwearingen as cited in Wood, Rychlowska, et al., 2016). It is noteworthy to highlight that although a significant difference was found between the Botox and Restylane group; those receiving Botox could nevertheless accurately recognise expressions. This finding suggests that mimicry is not vital for recognition as it can be achieved single-handedly through perceptual analysis, pattern matching or associated knowledge (Adolphs, 2002; Hess & Blairy, 2001). Overall, however, the results suggest that non-prototypical stimuli are more likely to engage mimicry and influence expression recognition (Hess & Blairy, 2001).

The clinical technique of facial muscle inhibition was valuable in strengthening previous research (Neal & Chartrand, 2011), as the preceding manipulation methods (e.g. biting a pen) recruit additional cognitive processing (Neal & Chartrand, 2011). Furthermore, most other studies only inhibit the mimicry of mouth movements (Niedenthal et al., 2009), but this study with clinical patients additionally blocked the use of the upper face and surrounding eye muscles; muscles pertinent in emotion recognition, particularly the recognition of fear (Whalen et al., 2004). Further research needs to address internally simulated aspects of emotion in brain regions, as opposed to just addressing the outward blocking of expressions (Oberman et al., 2007).

1.2.1.2 Is mimicry necessary for the recognition of facial expressions?

There are two main experimental techniques used to test whether mimicry is necessary for the recognition of facial expressions and these are expected to correspond to each other: facilitating or blocking certain facial muscles corresponding to specific expressions or testing the muscle activity corresponding to a specific expression with EMG. However, few studies using the first technique of faciliating or blocking expressions have directly tested expression recognition, instead showing mimicry to affect humour ratings (Strack et al., 1988), produce sadness (Larsen et al., 2008) and detect expression changes (Niedenthal et al., 2001; Wild et al., 2003). Manipulation studies that have directly tested expression recognition present conflicting findings; with the idea that mimicry may not be essential for recognition aforementioned in Neal and Chartrand (2011)'s Botox study, but the importance of mimicry in Wood, Lupyan, et al. (2016)'s constrictive gel facemask study (as preventing mimicry was shown to affect the recognition of sadness and anger). EMG studies have shown corresponding muscle activation to help detect emotive words (Niedenthal et al., 2009) and improve anger and sadness recognition (Kunecke et al., 2014). Further research combining facial blocking with EMG has found the inhibition of mimicry to impair expression recognition (Oberman et al., 2007). The previous EMG research suggests that mimicry is needed for recognition, and this corresponds with Lipps (1907) proposed three stage model detailing causal linear links between imitation, emotional contagion and recognition (Hess & Blairy, 2001). However, further EMG research has contradicted this claimed assumption, showing no benefit of mimicry on expression recognition (Blairy, Herrera, & Hess, 1999; Hess & Blairy, 2001).

Blairy et al. (1999) tested basic emotion recognition accuracy with varying physical intensities. They found no significant correlations between mimicry and recognition, and mimicry did not improve recognition through emotional contagion, when the participant reported a matched emotional state (Blairy et al., 1999). This contradicts Lipps model of recognition, as well as previous research showing that mimicry is needed in expression recognition (Oberman et al., 2007; Wood, Lupyan, et al., 2016); finding mimicry to lead to the perception of an easier task but not improve accuracy (Blairy et al., 1999). A follow-up study conducted by Hess and Blairy (2001) studied the application of mimicry when recognising non-prototypical dynamic expressions; as previous research has concentrated on the recognition of

basic strong prototypical emotions that may not require mimicry to recognise (Hess & Blairy, 2001). Again, however, no link was found between mimicry and recognition, and recognition was not mediated through emotional contagion (Hess & Blairy, 2001). Mimicry was measured through muscle activation and was apparent in all facial expressions (Hess & Blairy, 2001), however recordings from the zygomaticus were unusable, which is a significant muscle in facial expressiveness (Hess & Blairy, 2001). Furthermore counter to expectations lower levels of muscular activity (corrugator and orbicularis oculi) was related to greater recognition accuracy (Hess & Blairy, 2001). Thus, these findings present a chaotic picture, questioning why we use mimicry when viewing a sender's expression.

These contradictory findings can be explained with Goldman and Sripada (2005) "as if" loop model of simulation; this model suggests that successful expression recognition can occur without facial feedback (see Figure 1.6). Thus, this model purports the existence of a direct link between visual and somatosensory representations of what an expression would feel like (Goldman & de Vignemont, 2009; Goldman & Sripada, 2005). This embodied recognition model has close parallels with the Somatic Marker hypothesis (Damasio, 1996) as it additionally postulates an 'as if' body loop. This hypothesis was proposed following research into the role of the ventromedial PFC in responding to emotionally charged stimuli through bio-regulatory processes. The learnt associations between bio-regulatory 'marker' signals, or emotional state, and the correspondent factual knowledge of a complex situation were found to influence how an individual processes and responds to stimuli (Damasio, 1996). This theory suggests that emotions can be detected in specific brain areas and result from perceiving one's internal body states (ANS activation, skin conductance responses SCRs, biochemical or hormonal indicators). In other words, the brain can activate areas that would be associated with a change in bodily state or emotion even when these changes have not been overtly expressed (Damasio, 1996; E. Fox, 2008). Therefore, the "as if" model account is less affected by counter evidence as it shows how mimicry is not key for recognition (Goldman & de Vignemont, 2009; Goldman & Sripada, 2005). Furthermore, these inhibitory mechanisms may be in place to allow for expression perception without the development of mirror-touch synaesthesia (Case, Pineda, & Ramachandran, 2015).

There are strands of research that suggest a number of contextual and motivational moderators can suppress mimicry (Wood, Rychlowska, et al., 2016). In

regards to context, mimicry is more likely to occur in ambiguous situations, when an individual does not know what an expresser is feeling (Wood, Rychlowska, et al., 2016). However, motivation is also important, as mimicry is reliant on an individual's motivation to communicate and understand another's expression (Wood, Rychlowska, et al., 2016). An individual's motivation can differ depending on eye contact, gender, age, empathic ability, power status, social anxiety and their relationship with the expresser (Rychlowska, Zinner, Musca, & Niedenthal, 2012; Wood, Rychlowska, et al., 2016). An abundance of these factors have been considered in the context of Niedenthal, Mermillod, Maringer, and Hess (2010)'s Simulation of Smiles Model (SIMS). In particular, this model addressed how eye contact leads to greater mimicry, but it also highlights how mimicry can be suppressed due to societal or cultural factors, if a smile is perceived as too friendly or intimidating (Bastiaansen et al., 2009; Niedenthal et al., 2010). Research has also been carried out, purporting links between pacifier use in infancy with deficits in mimicry and emotional competence in young adolescent boys (Niedenthal et al., 2012) and further adults engaging in less facial mimicry when viewing babies with their mouths occluded (Rychlowska, Korb, et al., 2014). Preventing automatic mimicry and inhibiting embodiment during this important period in development is problematic for expression recognition. Furthermore, the relationship with the expresser is shown to affect embodiment as participants instructed to convey emotions (word concepts of joy or anger) to a close friend, engage in more facial activity and embodied simulation, than when they are conveying emotions to a superior (Niedenthal et al., 2009). Thus, it is clear that contextual factors can modulate these lower-level simulation processes, similar to effects seen in the visual recognition of emotion. Overall, due to the nature of task instructions and limited emotions tested, more research is needed to generalise findings (especially Niedenthal et al. (2009)'s research on emotive word concepts, as the processing of words would be very different to processes involved in the facial expression recognition) and elucidate the possible existence of individual differences in simulation and embodiment.

1.2.2 Brain regions involved in embodiment.

The aforementioned connectivity between perception and action, as well as the tendency for individuals to mimic and thus simulate a sender's state advocates the potential involvement of overlapping neural areas in a human mirror neuron

system (MNS) (Oberman et al., 2007). Mirror neurons (MNs) are neurons that fire when an individual perceives a sender's action and executes the same action (Iacoboni & Dapretto, 2006) and may be activated to support simulation. The MN system corresponds with Goldman and Sripada (2005)'s unmediated resonance model, which suggests that observing an emotive face directly produces sub-threshold brain activation in the correspondent motor substrate for that emotion. Whilst MNs are determined in frontoparietal areas in primate studies (di Pellegrino, Fadiga, Fogassi, Gallese, & Rizzolatti, 1992; Rizzolatti et al., 1988), evidence of equivalent regions in humans are less conclusive (van der Gaag et al., 2007). However, these regions are likely to be the intraparietal lobe (IPL), and the ventral premotor cortex (PMC) or the inferior frontal gyrus (IFG) (Niedenthal, 2007) (see Figure 1.8 for these regions on a human brain).

Neuroimaging and the fMRI analysis MVPA, has aided advancements in this field, revealing common crossmodal areas in the human brain that represent a stimulus in a similar way (Oosterhof, Wiggett, Diedrichsen, Tipper, & Downing, 2010). Common regions have also been found important in perceiving and producing the emotional meaning of voices (Adolphs, 2010; Aziz-Zadeh, Sheng, & Gheytanchi, 2010), social hand gestures (Montgomery & Haxby, 2008) and facial expressions (Heberlein & Atkinson, 2009; van der Gaag et al., 2007), showing the HMNS to contain distinct regions for different kinds of nonverbal communication.

Studies have shown the observation and execution of facial expressions to recruit common areas of the inferior frontal gyrus (IFG) and the posterior parietal cortex (see Figure 1.8) (Carr, Iacoboni, Dubeau, Mazziotta, & Lenzi, 2003; Hardwick, Caspers, Eickhoff, & Swinnen, 2017; Kircher et al., 2013; Montgomery & Haxby, 2008; van der Gaag et al., 2007). A further fMRI study discerned the relative activation of the frontal operculum (posterior IFG) in viewing faces as opposed to hand gestures in the MNS (Montgomery & Haxby, 2008). A double dissociation was found whereby gestures created greater parietal activation than faces (Montgomery & Haxby, 2008). However, the amalgamation of simulation within somatosensory, motor and subcortical brain areas has been implicated in expression (van der Gaag et al., 2007).

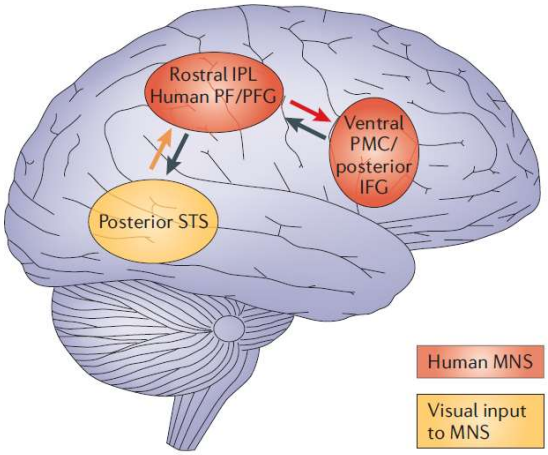

Figure 1.8. Human mirror neuron system for imitation, showing the implicated areas for the observation and execution of facial expressions: Premotor Cortex (PMC), Inferior frontal gyrus (IFG), Inferior Parietal Lobe (IPL) and Superior Temporal Sulcus (STS), from Iacoboni and Dapretto (2006).

1.2.2.1 Somatosensory and motor cortices.

Common activations in somatosensory and motor cortices have been found for action understanding, language and affective processing (Gazzola et al., 2012) and it is thought that the primary motor cortex and posteriorly bordered somatosensory cortex is important for embodiment (sensorimotor cortices). These areas comprise somatotopic body maps known as the sensory and motor homunculus, see Figure 1.9 (Meier et al., 2008). These maps are typically a reversed arrangement of the body; with the motor representation of the tongue located ventrally and the toes represented dorsally in the brain (Meier et al., 2008). Hand (or finger) movement and the face have a much larger brain representation than other body parts, due to the fine motoric abilities inherent in these areas (Meier et al., 2008).

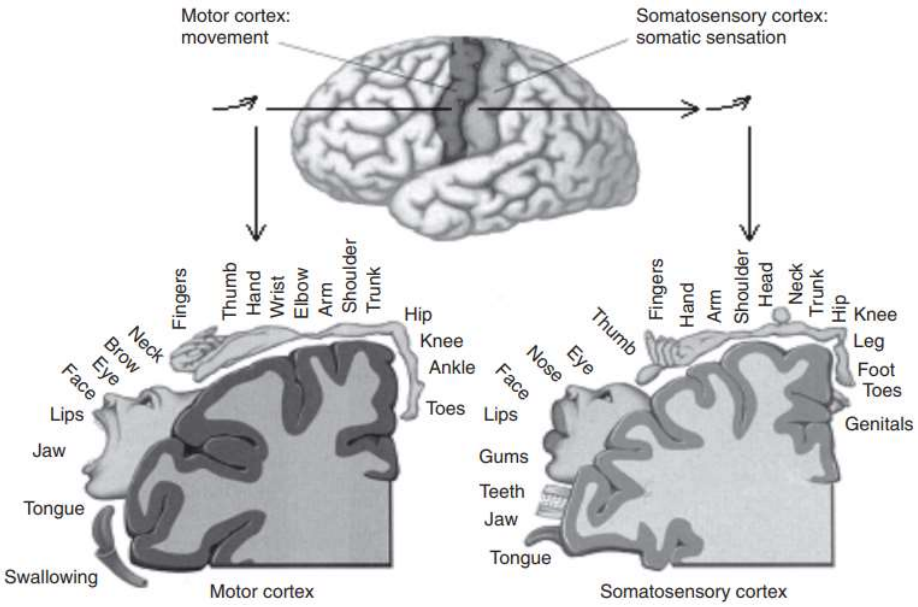

Figure 1.9. Somatotopic maps: the sensory and motor homunculus, from Ibric and Dragomirescu (2009).

Evidence from patients with focal brain lesions to their right somatosensory cortex show impairment in emotion recognition (Adolphs, Damasio, Tranel, Cooper, & Damasio, 2000), detailed further in Chapter 4 (4.1.2). Additionally, research investigating overlaps between the perception, imitation and production of facial expressions, have found activation in an abundance of motor, premotor and somatosensory regions: the primary motor cortex (Montgomery & Haxby, 2008), and the premotor cortices (Carr et al., 2003; Hardwick et al., 2017; Hennenlotter et al., 2005; Kircher et al., 2013; Leslie, Johnson-Frey, & Grafton, 2004; Montgomery & Haxby, 2008; van der Gaag et al., 2007), including the supplementary motor area (SMA) (Hardwick et al., 2017; Leslie et al., 2004) and pre-SMA (Hardwick et al., 2017; Kircher et al., 2013; van der Gaag et al., 2007), as well as the primary somatosensory cortex (Montgomery & Haxby, 2008; van der Gaag et al., 2007) and secondary somatosensory cortices (Hennenlotter et al., 2005; Leslie et al., 2004; van der Gaag et al., 2007). However, in Hardwick et al. (2017), no overlap was present in the primary motor cortex with activation only present in execution. The role this region plays in embodiment has been long debated; it is unclear whether it is important for observation, activated at a low-threshold, or whether it just reflects a motor-sensitive area (Hardwick et al., 2017).

Activation, occurring in the extended MNS for the perception, imitation and execution of expressions, is commonly found bilaterally in premotor regions (Carr et

al., 2003; Hardwick et al., 2017; Leslie et al., 2004; Montgomery & Haxby, 2008; van der Gaag et al., 2007). This activation was commonly stronger in the right hemisphere for perception but there were no differences between the hemispheres in imitation or production; this corresponds to theories of right hemispheric dominance in emotion processing (Hennenlotter et al., 2005; Leslie et al., 2004; Montgomery & Haxby, 2008). Moreover, studies that focussed exclusively on the perception and production of happiness versus neutral found overlaps in the right premotor cortex (PMD and PMV), see Figure 1.10 (Hennenlotter et al., 2005; Kircher et al., 2013). It is important to note that recent MVPA studies on shared brain networks in action have challenged the dominant role of the pre-motor cortex in the HMNS, suggesting that the pre-motor cortex is more concerned with observing one's own actions (Oosterhof, Tipper, & Downing, 2012, 2013). However, this research was based on hand actions and therefore cannot be generalised to all actions, including movements of the face.

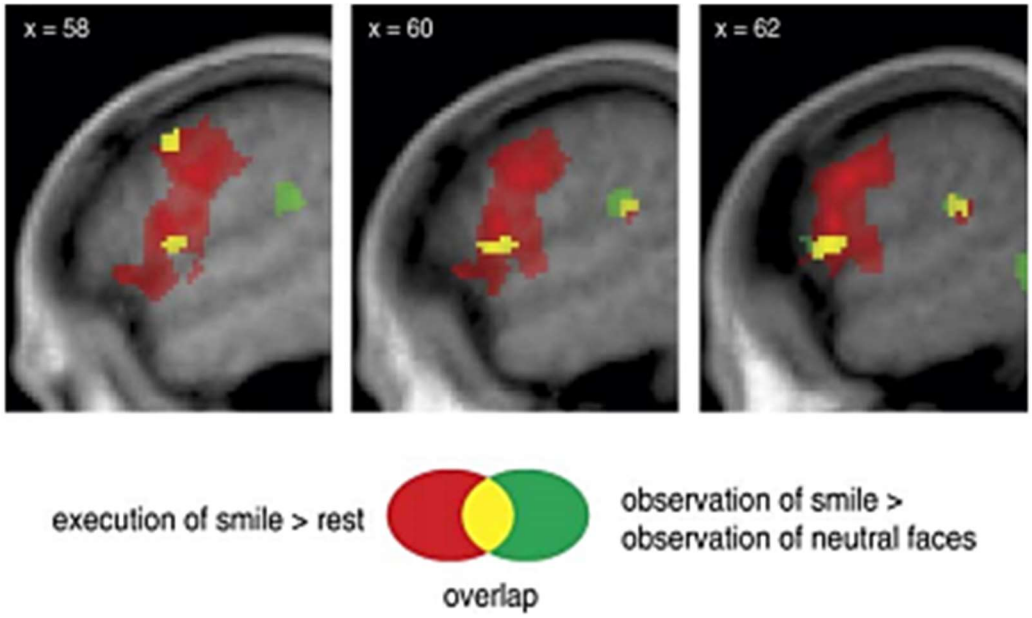

Figure 1.10. Brain activation for perceiving (green) and producing (red) happiness expressions; overlaps (yellow) present in the right PMD and PMV, as well as the right S2, adapted from Hennenlotter et al. (2005).

Recent studies have applied Transcranial Magnetic Stimulation (TMS) to create a momentary disruption to a specific area of cortex (Balconi & Bortolotti, 2013). Studies that have delivered TMS to the somatosensory cortex demonstrate the importance of this area in the expression recognition (Pitcher, Walsh, & Duchaine, 2011). Pitcher, Garrido, Walsh, and Duchaine (2008) targeted the right occipital face

area (OFA) and the right somatosensory cortex (SC), either administering no TMS (to the vertex) or high frequency TMS (to the OFA or SC) on the onset of a face, to compare performance across control and experimental conditions. Participants responded when a target face matched a previously presented face, either in terms of expression or identity (Pitcher et al., 2008). The disrupted brain areas independently compromised participants' ability to discriminate the six basic expressions; with identity task performance left intact (Pitcher et al., 2008). Furthermore, suppression of the right SC and right pre-motor cortex (PMC) was found to impair the discrimination of auditory emotions but not identity, showing support for areas specific to the recognition of facial expressions (Banissy et al., 2010). Furthermore, disrupting the PMC with TMS demonstrates the role of the simulation process in recognising expressions at both short and long stimulus durations (Balconi & Bortolotti, 2013). This presents the idea that simulation occurs both in response to conscious and unconsciously perceived stimuli (Balconi & Bortolotti, 2013). Results showed the pre-motor cortex (PMC) important in recognising emotion, in particular with the increased reaction times (RTs) and false alarms when recognising anger or fear during inhibition (Balconi & Bortolotti, 2013). As the ventral PMC is part of the HMNS, Goldman and Sripada (2005)'s unmediated resonance model may be a particularly relevant in explaining how face-based emotion recognition is undertaken.

Further research has shown that disrupting specific brain areas with TMS impairs the recognition of certain emotions (Pourtois et al., 2004; Rochas et al., 2013). A study by Pourtois et al. (2004) found TMS to the right SC disrupted fear but not happiness, however, Pitcher et al. (2008) found no differences between recognising the basic emotions. This disparity may be accounted for by differences in TMS intensity as Pitcher et al. (2008) delivered 10Hz for 500ms, but Pourtois et al. (2004) single-pulse TMS did not exceed 0.3Hz of stimulation. The lower intensity potentially shows the importance of an internal somatic representation in the recognition of fear (Pourtois et al., 2004) as this emotion is disrupted earlier at greater ease. Rochas et al. (2013) found disrupting left pre-SMA activity to impair facial happiness recognition (FHR) and laughter but not fear or anger. This finding shows a common area for happiness. Due to the seemingly robust ability and specificity to recognise basic prototypical displays of happiness (F. W. Smith & Schyns, 2009); Niedenthal et al. (2010) developed the aforementioned Simulation of

Smiles Model (SIMS) to focus on the conditions that embodied simulation uses to judge the meaning between a variety of smiles (enjoyment, affiliation or dominance smiles).

Furthermore, an MVPA study has explored the role of the somatosensory cortex in subjective emotional experience (Kragel & LaBar, 2016); whilst this differs from the study of emotion recognition, it is important to consider. Kragel and LaBar (2016) presented participants with facial or vocal expressions before asking them to report how they felt. This experiment could have been appraised on the networks involved in expression perception, but due to the nature of the task (using an atypical visual matching task) the perception of stimuli could not be separated from experience. They found that the experience of emotion could be decoded from patterns of activation in the right primary somatosensory cortex. Furthermore, Kragel and LaBar (2016) carried out a preliminary analysis to investigate whether the experience of emotion differentially activated parts of the somatotopic body maps relevant to the features used in their recognition. As mouth regions represent a large area in the homunculus (Figure 1.9), they hypothesised that happiness and surprise (emotions using the mouth region for recognition) would have larger classification weights than fear and anger (which primarily rely on information from the eyes for recognition). They found two clusters in the right lateral postcentral gyrus that responded more to surprise and happy expressions, fitting in with previous work on somatotopic organisation.

Somatosensory sensitivity to emotional versus neutral expression processing has been shown in an EEG study, using tactile stimulation to understand visual and somatosensory processing in emotion recognition (Sel, Forster, & Calvo-Merino, 2014). This novel design found facial expressions to enhance early somatosensory activity independent of visual processing. The study concluded that recognition must involve an *Emotional Homunculus*; where the body is represented in somatosensory cortex (Sel et al., 2014). However, Pitcher et al. (2008) demonstrated the time course of visual (60-100ms) and somatosensory brain areas (100-170ms) in recognising expressions; showing that somatosensory activity does not occur independently of visual processing. Finding expression processing to be disrupted early at the OFA and later at the SC support hierarchical models of face processing from the visual processing pathway (Pessoa & Adolphs, 2010). However, this study also showed support for embodied accounts of expression recognition as TMS applied to the face

region, as opposed to the finger region of the somatosensory cortex impaired expression recognition (Pitcher et al., 2008).

Overall, studies inhibiting the somatosensory and premotor cortex areas are indicative of their importance on expression recognition, however, we presently cannot assume that mirror neurons exist in these areas (Pitcher et al., 2011). This is supported in embodied accounts describing the initial involvement of visual areas before the simulation of somatic and visceral areas accompanied with recognising an expression (Pitcher et al., 2008). The particular disruption of the right SC infers the role of this area in internally simulating an expression and later using this simulation to recognise a sender's facial expression (Pitcher et al., 2011).

1.2.2.2 Subcortical activations.

Other areas of the brain have been found to overlap in the perception, production and imitation of facial expression, including the amygdala (Carr et al., 2003; Kircher et al., 2013; van der Gaag et al., 2007), insula (Carr et al., 2003; Hennenlotter et al., 2005; Montgomery & Haxby, 2008; van der Gaag et al., 2007), cerebellum (Kircher et al., 2013; Leslie et al., 2004; van der Gaag et al., 2007) and hippocampus (van der Gaag et al., 2007). Surprisingly, van der Gaag et al. (2007), found the insula and frontal operculum to be more involved in the recognition of expression, with neutral expressions causing greater activation in the somatosensory cortex. The importance of the insula is highlighted with its connections to the somatosensory cortex, IFG and amygdala (Kircher et al., 2013). Lastly, Wicker et al. (2003) identified a common neural basis in the perception and feeling of disgust. This fMRI experiment showed areas of the anterior insula and ACC to activate when participants watched an individual on video exhibit a disgust expression and when they inhaled a disgusting odour (Wicker et al., 2003).

In summary, evidence of the embodied account is shown with emotion processing to partly reactivate the neural substrates involved when personally experiencing a correspondent emotion (Niedenthal, 2007). The embodied evidence argues for the importance of mimicry (Niedenthal et al., 2001; Wood, Lupyan, et al., 2016) but also demonstrates that it is not always necessary in expression recognition (Adolphs, 2002; Blairy et al., 1999; Hess & Blairy, 2001). Instead an individual can experience an emotion without overtly expressing it (Goldman & de Vignemont, 2009; Goldman & Sripada, 2005). Neuroimaging (fMRI) provides strong evidence for the embodied account of expression recognition, with the observation and

execution of facial expressions to recruit similar areas of the HMNS, as well as additional somatosensory, motor, premotor and subcortical brain areas (Hardwick et al., 2017; van der Gaag et al., 2007). Further TMS experiments (inhibiting the somatosensory and premotor cortex) implicate the embodied account of expression recognition (Balconi & Bortolotti, 2013; Banissy et al., 2010; Pitcher et al., 2008; Pitcher et al., 2011).

1.3 Overall Aims and Objectives of the Current Research

The literature in this chapter details the two main routes involved in the study of emotion recognition, as well as detailing research into its correspondent brain basis. The literature presents a complex picture with research often focussing on the visual or non-visual (simulation-based) route of recognition (Goldman & Sripada, 2005). The visual route to expression recognition implicates a distributed number of cortical and subcortical areas, including the STS, FG and amygdala, as well as early visual regions (Harry et al., 2013; Haxby et al., 2000; Liang et al., 2017; Petro et al., 2013; Said et al., 2010; Wegrzyn et al., 2015; Zhang et al., 2016), whereas, the non-visual embodiment approach frequently identified premotor, somatosensory and subcortical structures (Hardwick et al., 2017; van der Gaag et al., 2007).

For the first line of experiments (Chapters 2 & 3) in the current thesis, top-down influences to the visual system (in the visual route of recognition) are investigated. As aforementioned, standard bottom-up computational models do not account for occlusion (Tang et al., 2018), which in regards to expression recognition may be especially needed, as accessories, such as wearing a scarf or sunglasses, can conceal certain facial features from view. Top-down influences may therefore be particularly relevant for recognition under conditions of occlusion, to help fill in missing feature information (Greening et al., 2018; Muckli, 2010; Muckli et al., 2013). Furthermore, the contribution of bottom-up information cannot necessarily be separated from top-down influences in many of the current fMRI decoding studies, that highlight some of the key regions involved in the recognition of expression (Liang et al., 2017; Wegrzyn et al., 2015). However, Zhang et al. (2016) performed further cross-classification analyses with decoding across identity, to highlight some of the key regions involved in expression recognition. This tapped into higher level representations and enabled the role of low-level features in decoding to be minimised to a degree. Nonetheless, it is important to note this as a relatively weak

form of tapping into high-level representations and there are other ways to achieve this.

Thus, a paradigm similar to F. W. Smith and Muckli (2010) was used; such that the visual cortex was retinotopically mapped, and sensitivity within V1 was investigated to see whether top-down feedback (and possibly lateral) influences contribute to the perception of occluded facial expressions. Although Greening et al. (2018) only investigated expression recognition with an explicit task and did not map the visual cortex with retinotopy, they compared responses of non-overlapping visual face stimuli, which can purely tap into high-level processes in the brain. Therefore, the experiments in this thesis will use retinotopic mapping and compare responses to non-overlapping face stimuli across both an implicit and explicit task, to provide a novel way to investigate how contextual mechanisms (top-down feedback and lateral connections) contribute to the perception of occluded facial expressions. By comparing representations across non-overlapping stimuli, e.g. eye region to rest of face minus eyes, this study provides a stronger form of tapping into high-level representations, strongly minimising the role of low-level features in decoding. Certain accounts of visual system processing, such as predictive coding and recurrent feedback models of object completion, imply that similar representations may be present in each case due to feedback (or lateral connections) (Clark, 2013; O'Reilly et al., 2013; Rao & Ballard, 1999; Tang et al., 2014; Wyatte et al., 2012). However at present, more research is necessary to understand the visual processes involved in facial expression recognition, especially in how we predict hidden features of emotional faces (Greening et al., 2018).

The present research will primarily investigate the role of cortical processing in V1, due to the previous literature highlighting V1's involvement in higher-level processing (Petro et al., 2013; F. W. Smith & Muckli, 2010). However, it is also important to understand the sources of the feedback connections (Clark, 2013; Pessoa & Adolphs, 2010) and subsequent involvement of face and emotion sensitive areas (such as the FG and STS) in the processing of occluded facial features (Harry et al., 2013; Liang et al., 2017; Said et al., 2010; Wegrzyn et al., 2015; Zhang et al., 2016). The current research will also investigate the high-level influence of task context and how this influences the early sensory processing of expression, to gain a greater understanding of top-down effects in emotion recognition (Petro et al., 2013; M. L. Smith & Merlusca, 2014).

Both fMRI and EEG data were obtained and subsequently analysed with univariate and multivariate analyses in the first line of experiments (fMRI data presented in Chapter 2 and EEG data presented in Chapter 3). However, the research focus lies with the decoding technique of multivariate pattern analysis (MVPA) to understand how occluded objects are represented in different regions (fMRI) of the brain and different time-windows of the EEG response. Furthermore, MVPA is particularly pertinent for investigating occlusion, as univariate research looking at brain activations may show slight or no differences in brain regions between occluded and non-occluded stimuli (Wyatte, Jilk, & O'Reilly, 2014). As the present research is looking to investigate the role of processing differently occluded facial expressions within the same ROI, such as V1, and univariate analyses spatially smooth and average activated voxels in an experimental condition within a ROI, differences in occlusion may likely go undetected using a univariate analysis (Haynes & Rees, 2006; Mur et al., 2009; Norman et al., 2006). In MVPA, patterns of brain activation can be detected in the same ROI and voxels are not spatially smoothed; consequently this analysis, which is highly sensitive in detecting fine-grained differences, is necessary to address the experimental aims and objectives of the current research. The collection of data from two neuroimaging approaches (fMRI and EEG) aim to provide a comprehensive picture of processing occluded facial features in the brain, as both high spatial and temporal information about brain activity is available (Cichy et al., 2014; Fusar-Poli et al., 2009; Sadeh, Podlipsky, Zhdanov, & Yovel, 2010). Thus, the experiments aim to understand how the brain compensates and feeds information back to account for missing feature information (Greening et al., 2018), as well as the temporal dynamics of this process.

At present MVPA research exploring the neural time-course of expression recognition under conditions of occlusion has not been undertaken, although research has shown that faces and expressions can be neurally decoded from EEG data (Cauchoix et al., 2014; Li et al., 2018). An investigation into timing information is pertinent to investigating the role of bottom-up versus top-down feedback mechanisms, as bottom-up processing is quicker and can take place before feedback has occurred (Tang et al., 2014). These studies will also help inform the theoretical accounts of visual processing, such as predictive coding (Clark, 2013; Friston, 2005, 2008; F. W. Smith & Muckli, 2010) and recurrent feedback models of object recognition (Tang et al., 2014; Tang et al., 2018; Wyatte et al., 2012; Wyatte et al.,

2014), to understand the mechanisms that take place in the visual system, including the role of top-down feedback processing of how the brain deals with occlusion. In the predictive coding account, the brain is assumed to the use context, experience and prior knowledge to make sense of visual input. To do this all areas of the brain continuously make predictions on expected visual information based on information from higher cortical areas, the resulting representations are compared with incoming sensory information (Clark, 2013; de Lange, Heilbron, & Kok, 2018). This account will be explained further in Chapter two (2.1.1.1.1). However, within this account it is implied that the processing of faces with missing feature information may occur later, as more feedback from higher cortical areas is necessary to predict occluded information.

The final experiment (Chapter 4) in the current thesis investigates the non-visual route of emotion recognition, as research on the embodied simulation account suggests that motor/premotor and somatosensory simulation of emotion contributes to the recognition of facial expressions (Goldman & Sripada, 2005; Niedenthal et al., 2009). Whilst neural networks have been identified in the brain for embodiment, the precise architecture of embodied cognition need refining in future work (Niedenthal, 2007). As a result, the present research investigates the neural mechanisms of embodiment, and tests the assumption that the same representations will be found across the sensory perception and motor production of expression. Again, fMRI data were obtained and subsequently analysed with univariate and multivariate analyses in the brain regions mentioned above (data presented in Chapter 4). Additionally, the present research focusses on MVPA, in an attempt to advocate a strongly embodied account of expression recognition, investigating representational overlap across perception and production of expression. This paradigm were designed to inform theories of embodied cognition or embodied simulation (Niedenthal, 2007; Niedenthal et al., 2006; Niedenthal et al., 2009), such as the reverse simulation model, the "as if" loop model of simulation and the unmediated resonance model (Damasio, 1996; Goldman & de Vignemont, 2009; Goldman & Sripada, 2005), described further in Chapter 4.

Thus, the proceeding chapters aim to investigate the involvement of both routes to the recognition of emotion, as it may be that one route cannot provide a full understanding of expression recognition (Wood, Rychlowska, et al., 2016). Both the visual and sensorimotor pathways are consistently found important in perceiving

expression (Wood, Rychlowska, et al., 2016), thus the focus of this thesis will be to investigate the role of implicated brain regions with MVPA. The overarching aim is to investigate the role of high-level influences, originating in both the visual (from occluded faces, task goals) and non-visual (embodiment) routes, on the neural processing of facial expressions.

SECTION 2
-
Experimental Chapters

Chapter 2: Early Visual (V1-V3), Face and Emotion Sensitive Areas Contain Information about Occluded Facial Features

2.1 Introduction

2.1.1 Visual processing.

Previous research has shown the substantial involvement of higher level processes in primary visual cortex (V1) (Petro et al., 2013; F. W. Smith & Muckli, 2010; Vetter, Smith, & Muckli, 2014). The presumption that V1 solely reflects retinal input has diminished, with evidence demonstrating the minor role of bottom-up or feedforward processing, and evidence of high-level effects to the visual cortex (Muckli, 2010; Muckli et al., 2015; F. W. Smith & Muckli, 2010). Research has shown that information from higher cortical areas is fed back to influence early visual regions (Muckli et al., 2015). It is particularly evident that feedback might play an even greater role in conditions of uncertainty; in highly ambiguous situations where objects are occluded (O'Reilly et al., 2013; F. W. Smith & Muckli, 2010; Tang et al., 2014; Tang et al., 2018; Wyatte et al., 2014).

Current research has begun to understand the role of cortical feedback in perceiving facial expressions under occlusion (Greening et al., 2018); as it is important to understand the involvement of early visual (V1-V3), face and emotion sensitive areas in processing occluded facial features. To study the involvement of feedback mechanisms beyond low-level processing, one method is to investigate whether representations of expression are similar across independent facial features, e.g. occluded eyes to eyes-only stimuli; occluded mouth to mouth-only stimuli (Greening et al., 2018; Petro et al., 2013). Similarity between these visual signals would be in keeping with accounts of visual processing, such as predictive coding, and recurrent feedback models of object recognition (F. W. Smith & Muckli, 2010; Tang et al., 2018; Wyatte et al., 2014). Accordingly, this chapter will extend upon the previous research helping to understand how the brain deals with occluded stimuli and whether high-level processing (spatial context and task goals) accounts for how humans recognise occluded facial expressions.

2.1.1.1 Accounts of visual processing.

2.1.1.1.1 Predictive coding.

Top-down processing or feedback may be explained by predictive coding (Clark, 2013; Friston, 2005, 2008). This account of visual processing details how

each visual region computes the difference between expected and observed incoming sensory information (Clark, 2013). As such, predictions originate in higher level areas of the cortex and are fed back to early visual regions, to predict the current information projected to V1; in turn early visual areas transmit error signals back to higher level regions with the computed difference between expected and observed information, see Figure 2.11 (Rao & Ballard, 1999; Wyatte et al., 2012). Thus, it is possible, that context, experience or prior expectations can affect the responses of neurons in V1 and subsequently the processing of information (Clark, 2013). Furthermore, research has shown the potential role of predictive coding when filling in missing information from occluded visual scenes (F. W. Smith & Muckli, 2010).

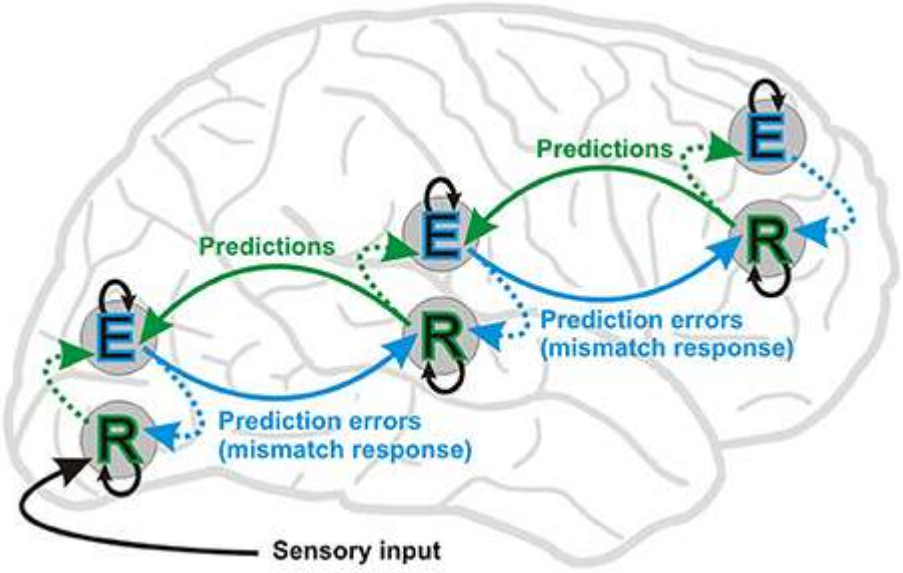

Figure 2.11. Model of predictive coding (Stefanics, Kremláček, & Czigler, 2014). E: Error; R: Representation.

2.1.1.1.2 Recurrent feedback models of object recognition.

The framework, derived from recurrent feedback models of object recognition, suggests the importance of recurrent feedback signals in hierarchically adjacent areas within the ventral visual stream (Tang et al., 2014; Tang et al., 2018; Wyatte et al., 2012). These signals are said to originate in extra-striate regions (high-level visual areas of V3, V4 and V5) to aid recognition in occluded situations immediately after the feedforward process (Wyatte et al., 2014). This local feedback has been receiving increasing attention, and differs from feedback that originates in frontal parietal areas: as it is rapid, automatic and excitatory (Wyatte et al., 2014). Recurrent feedback amplifies neurons in V1 that were weakened or prevented from

firing to start a complex filling-in process (Wyatte et al., 2012; Wyatte et al., 2014). Feedforward connections continue to the inferior temporal (IT) cortex and further excitatory reinforcement from the IT cortex can help strengthen V1 responses (Wyatte et al., 2012). Processes within the IT cortex could be enough to fully support object completion (Wyatte et al., 2014), however prefrontal areas may also be involved in this process, see Figure 2.12.

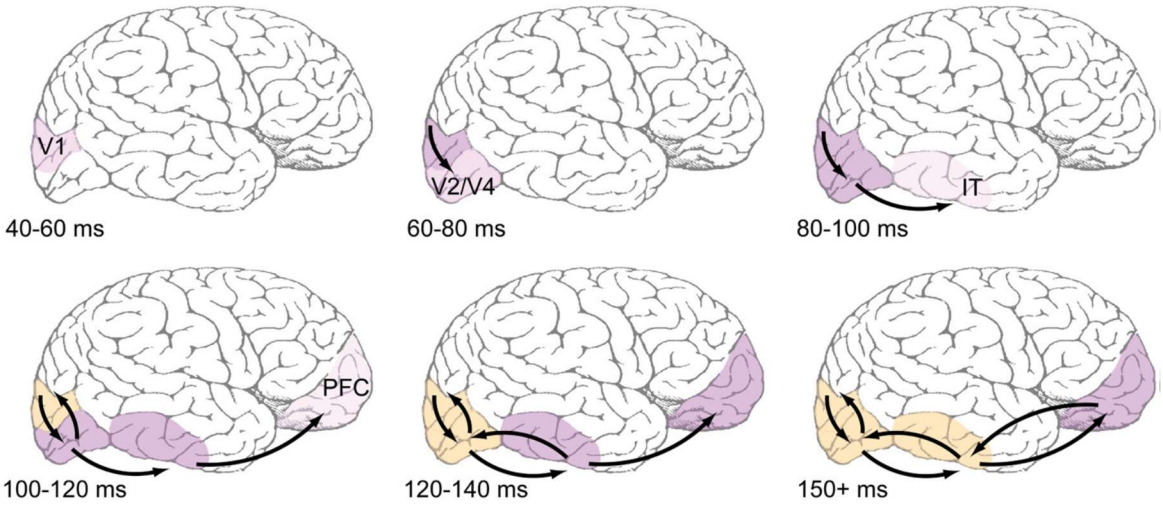

Figure 2.12. Feedforward and feedback connections in early visual processing (Wyatte et al., 2014). V1: Primary Visual Cortex; IT: Inferior Temporal; PFC: Prefrontal Cortex.

2.1.1.1.3 Other accounts of processing.

Alternative Bayesian accounts of processing suggest the existence of recurrent feedforward and feedback loops within the brain that concurrently assimilate bottom-up observations with top-down contextual priors to create probabilistic inferences (Kersten, Mamassian, & Yuille, 2004; Lee & Mumford, 2003; Yuille & Kersten, 2006). Coherent infomax accounts (W. A. Phillips, Clark, & Silverstein, 2015; W. A. Phillips et al., 1995) place greater weight on predictive and current relevance, seeking contextual guidance throughout processing and learning (J. W. Kay & Phillips, 2011).

These accounts are in keeping with the predictive coding and recurrent feedback models of object recognition. However, there is an important difference between the predictive coding and alternative accounts of processing, including recurrent feedback models of object recognition; whereby predictive coding requires inhibitory feedback, the other accounts advocate excitatory feedback. Thus with predictive coding, occlusion creates higher responses than non-occluded stimuli,

with processing over time acting to subdue response signals as error decreases. Whereas in the other accounts occlusion leads to an overall decrease in response, but processing over time amplifies the early visual response signals for degraded stimuli (J. W. Kay & Phillips, 2011; Lee & Mumford, 2003; Wyatte et al., 2012). Albeit this, all accounts portray vision and categorisation as extremely interactive and dynamic processes that are contingent on multiple brain areas within the visual stream (Wyatte et al., 2012). This is further supported with a recent hierarchical neural network model proposed by Heeger (2017), which details the relative contribution of a feedforward, feedback and prior drive in information processing. Overall, the processes detailed in these accounts need to be explored further in relation to understanding the mechanisms that aid the visual system, particularly the role of top-down feedback processing to V1 and how the brain deals with occluded face stimuli. Furthermore, these various possible top-down models help explain ambiguous information processing beyond the standard model of V1 (Tang et al., 2018).

2.1.1.2 How to study feedback?

2.1.1.2.1 Using retinotopy.

To underpin top-down processing, studies have tested the contribution of cortical feedback to ongoing processing in V1, and taken advantage of its retinotopic organisation (Petro et al., 2013; F. W. Smith & Muckli, 2010). A retinotopic localiser task is used to map positions in visual space, thus with visual space mapped, the sensitivity occurring in an occluded area of a visual scene can be investigated (F. W. Smith & Muckli, 2010). Sensitivity in such a region will suggest the involvement of contextual mechanisms (feedback and lateral connections) as the occluded area is devoid of feedforward input (F. W. Smith & Muckli, 2010). Only a few studies have investigated the role of top-down modulation in occluded visual space, but the use of multivariate pattern analysis (MVPA) has been insightful in understanding neural activity in early visual regions (Muckli et al., 2013). This is particularly apparent in the processing of occluded natural scenes; where MVPA was used to decode the scene shown to participants even when there was no visual scene information presented to specific sub regions of V1 (F. W. Smith & Muckli, 2010). This paradigm, developed by F. W. Smith and Muckli (2010), provides evidence that V1 can contain rich contextual information about the visual environment.

The former results investigate the feedback contribution within V1 when processing scenes, and it is only applicable to orthogonal tasks irrelevant to the context, such as a one-back task detecting a colour change (F. W. Smith & Muckli, 2010). It would be interesting to see whether this effect generalises across stimuli and tasks, especially to address the uncertainty around how early visual regions are involved in the recognition of occluded facial expressions. It is important to understand this, as real-world occlusion is commonplace in emotion recognition (Bettadapura, 2012) and it is unclear how humans have a robust ability to recognise expressions under conditions of occlusion (Kotsia et al., 2008; F. W. Smith et al., 2008; M. L. Smith et al., 2005).

Research by Greening et al. (2018) begins to address this gap in the literature, as to how context shapes the processing of expressions using non-orthogonal emotion categorisation tasks. However, this research did not specifically map V1 with retinotopy, instead mapping the cortex less effectively with a cytoarchitectonic map (Eickhoff et al., 2005). This map is sub-optimal because the same probabilistic V1 mask is applied to all participants, as opposed to retinotopic mapping that is based on each individual subject, defining spatially localised voxels from a constant fixation on different stimuli. Therefore caution is needed over the extent to which the results reflect early visual cortex and can account for individual differences (Greening et al., 2018). Nonetheless, they found neural information in early visual cortex to generalise across independent visual face parts, such as faces depicting eyes only to the corresponding minus eyes stimuli (Greening et al., 2018). This cross-classification MVPA analysis suggests the involvement of higher cortical regions and the potential role of cortical feedback in decoding occluded facial expressions. The following study will build on this research, using additional independent face parts and MVPA, to understand whether top-down processing accounts for how humans recognise occluded facial expressions. However, more generally this study will help to inform how V1 deals with occluded stimuli, adding to previous research studying occlusion (F. W. Smith & Muckli, 2010).

Overall, prior research has principally studied the occlusion of objects and scenes but not faces. However, more top-down or lateral interactions may be expected to fill in missing feature information when dealing with facial occlusion, as faces are such biologically salient signals (Pessoa & Adolphs, 2010). Research has begun to examine the visual processing involved in emotion recognition from

occluded eye stimuli (Greening et al., 2018). However, it is pertinent to further study how we compensate for missing facial feature information, and this research needs to be pursed in more depth, by examining the occlusion of additional facial features, such as the mouth.

2.1.1.2.2 Backwards masking.

Recurrent processing also becomes more important for recognition in highly ambiguous and occluded situations (O'Reilly et al., 2013; Tang et al., 2014). A number of studies have taken advantage of backwards masking to selectively disrupt feedback and disentangle feedforward from recurrent processing (Tang et al., 2018; Wyatte et al., 2012). A mask shown after stimulus presentation when recurrent processing begins, forces the brain to process the incoming mask stimuli and thus the only information recovered before mask encoding can be used in categorisation (Wyatte et al., 2012). These studies show decreased recognition ability for occluded stimuli with a mask than occluded stimuli with no mask; with greater levels of occlusion causing greater susceptibility to mask interference (Wyatte et al., 2012). Lamme and Roelfsema (2000) suggest that this impairment is due to the mismatch between mask responses propagating up through the ventral stream, when encoded responses regarding the initial stimulus are feeding information back through recurrent connections. Overall, backwards masking is an ingenious technique for investigating the visual processing involved in occluded object recognition.

2.1.1.3 Face and emotion selective areas.

Whilst it is pertinent to understand how we predict hidden features of emotional faces in the early visual cortex, it is crucial to understand the sources of the feedback connections (Clark, 2013; Pessoa & Adolphs, 2010). For this, it is important to reconsider the studies discussed in Chapter 1 (1.1.3), that research the brain regions involved in emotional face processing and the use of MVPA for decoding emotional expressions in these regions. This research showed high emotion decoding ability in the FG (Harry et al., 2013; Li et al., 2018; Liang et al., 2017; Wegrzyn et al., 2015) and the (p)STS (Liang et al., 2017; Said et al., 2010; Wegrzyn et al., 2015; Zhang et al., 2016). Further, decoding significance was found in the OFA (situated in or close to the IOG) (Liang et al., 2017; Wegrzyn et al., 2015) as well as the amygdala and insula (Wegrzyn et al., 2015). In these regions, decoding ability was reported less and was generally lower than the FG and STS (Wegrzyn et al., 2015; Zhang et al., 2016). It is important to note that these studies were not

explicitly studying feedback, they were investigating the relative importance of each region in expression recognition (Wegrzyn et al., 2015). However, Wegrzyn et al. (2015) state that if results were predominantly due to differences in low-level visual features, the highest decoding performance would have been expected in the occipital gyrus (Wegrzyn et al., 2015). The fact that decoding performance was highest in FG and STS advocates the role of higher level processing in emotion recognition.

Liang et al. (2017) also found strong decoding accuracy in motion-selective areas: V5f/hMT+. This was the first study to decode across multiple emotions using dynamic face stimuli, as well as dynamic stimuli with obscured eyes, and static stimuli to allow further comparisons; Said et al. (2010) used dynamic stimuli but only tested the STS. Counter to the previous results using static stimuli, this study found no decoding for static faces (Liang et al., 2017), it is not clear why, but it may result from using a six-way emotion classification. Furthermore this study found no decoding for obscured eye stimuli, even though behavioural recognition was the same for complete and obscured dynamic videos (Liang et al., 2017). The finding of no decoding in the brain for obscured eye stimuli is compatible with research showing the importance of the eye region in emotion recognition, and is especially relevant for the Eastern sample of participants collected, with this culture relying heavily on information from the eyes as opposed to the mouth (Jack, Blais, Scheepers, Schyns, & Caldara, 2009). Lastly, whilst this study is informative, an early visual ROI should have been investigated, to separate the decoding effects into high and low-level information.

To conclude, the idea that the early visual brain (or V1) uses cortical feedback to provide information to V1 about missing parts of a visual stimulus is relatively unexplored, especially in understanding how we process and compensate for missing facial information. To understand how high-level influences (spatial context and task goals) shape early visual processing warrants further investigation. Due to previous research highlighting V1's involvement in higher level processes to a surprising degree, this study places an emphasis on understanding the role of cortical processing in V1, however other regions will also be investigated. With a combination of fMRI, retinotopy and MVPA, this study will address the gaps in understanding how we process occluded facial expressions within the brain. It is clear that future research is needed to understand the relative contributions of

feedforward, recurrent and feedback connections within the brain and their time course (Wyatte et al., 2014) as there is currently considerable debate in the literature (O'Reilly et al., 2013). Furthermore, research looking at brain activations show slight or no differences in brain regions between occluded and non-occluded stimuli; thus more research using decoding or representational similarity analysis (RSA) techniques is needed to fully understand how occluded objects are represented in different brain regions (Wyatte et al., 2014).

2.1.1.4. Present study and hypotheses.

2.1.1.4.1 The involvement of early visual cortex.

As aforementioned, previous research has suggested that feedback to early visual cortex contains more than just low-level input information (F. W. Smith & Muckli, 2010). To test for feedback pathways that could modulate and in a way prepare the visual cortex with the correct contextual information, four differing partial face stimuli were created to present sub-samples of visual information.

H1: Similar brain representations will be revealed in V1 and EVC (V1-V3) when completely independent visual signals are presented (e.g. independent parts of a face: occluded eyes and eyes-only stimuli; occluded mouth and mouth-only stimuli) (see Figure 2.13).

This is important because if activity is similar between the independent signals, it will suggest an involvement of feedback mechanisms beyond low-level processing (Petro et al., 2013). This finding would be in keeping with accounts of feedback such as predictive coding models of early sensory processing, which propose to explain ambiguous information processing (F. W. Smith & Muckli, 2010). Furthermore this would be in line with recurrent feedback models of object recognition (Wyatte et al., 2014).

2.1.1.4.2 The involvement of face and emotion selective areas.

In the present study five other brain regions will be tested (as well as V1 and EVC), including the FG, STS, inferior occipital gyrus (IOG), amygdala (AMY) and insula (INS).

H2: Similar brain representations will be activated in face and emotion selective areas when completely independent visual signals or parts of a face are presented, akin to V1 and EVC.

2.1.1.4.3 The involvement of task.

In addition to above, the study will also investigate the sensitivity of task context (explicit vs implicit) when processing facial expressions, as only a small amount of research has studied how task context influences the early sensory processing of expression (Petro et al., 2013; M. L. Smith & Merlusca, 2014). As well as occlusion, task goals are high-level influences on visual processing. Petro et al. (2013) retinotopically mapped facial features (eyes and mouth) in regions of the primary visual cortex and show how task influences face category processing in specific sub-regions of V1. They found strong implicit task effects, whereby when participants were asked to judge expression (between happy and fearful faces) in the mapped eye region of the visual cortex, only gender information could be decoded, whereas gender could not be decoded in the gender task (Petro et al., 2013). Furthermore, when participants were asked to judge gender (male and female faces) in the mapped mouth region, their performance was higher (but not significantly so) when decoding emotion information (Petro et al., 2013). Overall, this study showed V1 to contain high-level information about facial expressions (Petro et al., 2013), but the implicit task effects were surprising. It is unclear why decoding would be better in implicit conditions, particularly in early visual cortex, so further studies are necessary. Most research has only studied implicit emotion recognition, by asking participants to carry out a one-back task (Harry et al., 2013), memory task (Said et al., 2010), colour change task (Zhang et al., 2016), or a gender recognition task (Wegrzyn et al., 2015). Whilst this research shows strong implicit performance of expression decoding, there is no direct comparison to explicit performance. One study has studied explicit emotion recognition without implicit task performance (Liang et al., 2017). Thus, it is imperative that this study investigates explicit and implicit task context, to provide a direct comparison between the two tasks.

H3: Emotion processing will be affected by its task context: whereby expression decoding will be stronger in the implicit task compared to the explicit task, for V1, EVC and the face and emotion selective areas.

2.2 Methods

2.2.1 Participants.

After piloting 22 participants (17 females, 5 males; aged 21-37) in a behavioural study aimed to inform about design and methodology, 15 participants (10 females, 5 male) took part in the functional imaging experiment, aged 19-35 years (M = 25, SD = 4). Due to excessive head motion in three participants, the final sample consisted of 12 participants (8 females, 4 males), aged 19-35 (M = 24.58, SD = 4.23). Participants were recruited via Scannexus (the company operating the scanning facilities at Maastricht Brain Imaging Centre) and paid for their participation. All were right-handed with normal or corrected to normal vision. Participants gave written, informed consent in accordance to approved ethics by the Psychology Research Ethics Committee at the University of East Anglia.

2.2.2 Stimuli.

Participants were presented with static grey-scale face images from the California Facial Expression of Emotions (CAFE) dataset, see Figure 2.13 or images at http://cseweb.ucsd.edu/~gary/ (Dailey, Cottrell, & Reilly, 2001). Six identities were chosen (3 males and 3 females) and based on the behavioural pilot study the following three emotions were used: disgust, fear and happiness. Non-overlapping samples of face information were created from these whole face (WF) stimuli producing four partial face (hereafter referred to as PF) conditions: eyes only (EO), rest of face minus eyes (Minus Eyes, ME), mouth only (MO) and rest of face minus mouth (Minus Mouth, MM) conditions, see Figure 2.13. The WF provided a control condition. The stimuli, totalling 90 different combinations from six identities, three emotions and five PF conditions, were presented at a visual angle height of 10° using Psychtoolbox 3 for Matlab (Brainard, 1997; Pelli, 1997). The size of the eye and mouth regions, as well as the occluded regions were a visual angle height of 3.1°, with a 1.4° visual angle difference between the eye and mouth region.

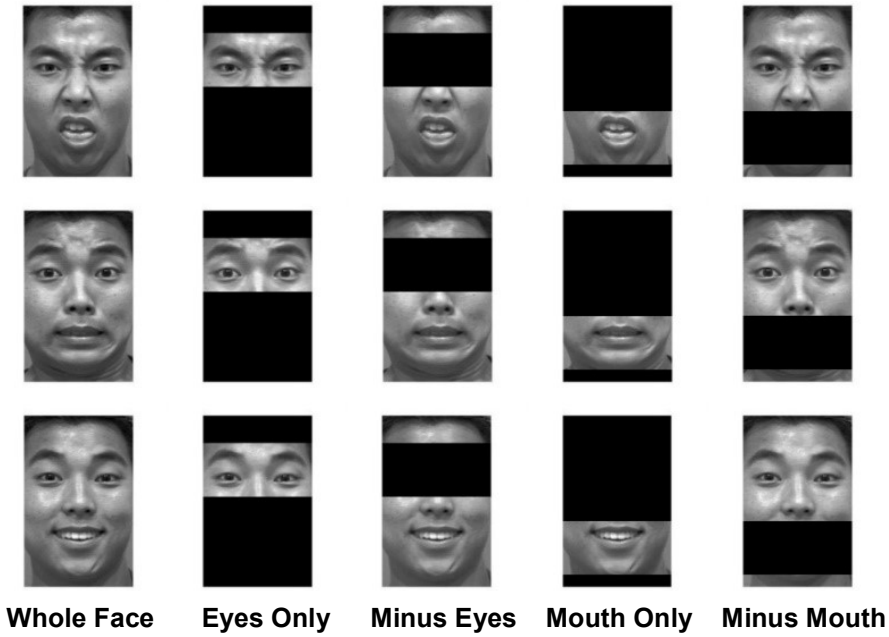

Figure 2.13. Example stimuli (15 conditions, one identity); disgust, fear and happiness (created using WF images from CAFE dataset).

2.2.3 Design and procedure.

Participants were presented with all PF stimuli (within-subjects) and asked to explicitly recognise facial expression or gender on different runs while in the fMRI scanner, see Figure 2.14. This rapid event related experiment consisted of eight experimental runs lasting 444 seconds (222 TR2 volumes). Four of the experimental runs entailed an explicit emotion recognition task, requiring participants to recognise expression in a three AFC (Alternative Forced Choice) task. In the remaining four runs participants completed an implicit task where they were asked to recognise gender, two AFC. Each run comprised 90 experimental four second trials (6 identities, 15 conditions: 3 emotions, 5 stimulus types: WF, EO, ME, MO, MM) and 15 null events, with each stimuli being presented for one second. There was also a 12 second fixation at the beginning and end of each run. Fixation was always on and participants were told to fixate throughout the run. Task order was blocked and counterbalanced among participants; whereby participants carried out the four runs of one task followed by the next. Participant responses were recorded with a button press; button order was also counterbalanced among subjects. Two participants only carried out three runs of expression.

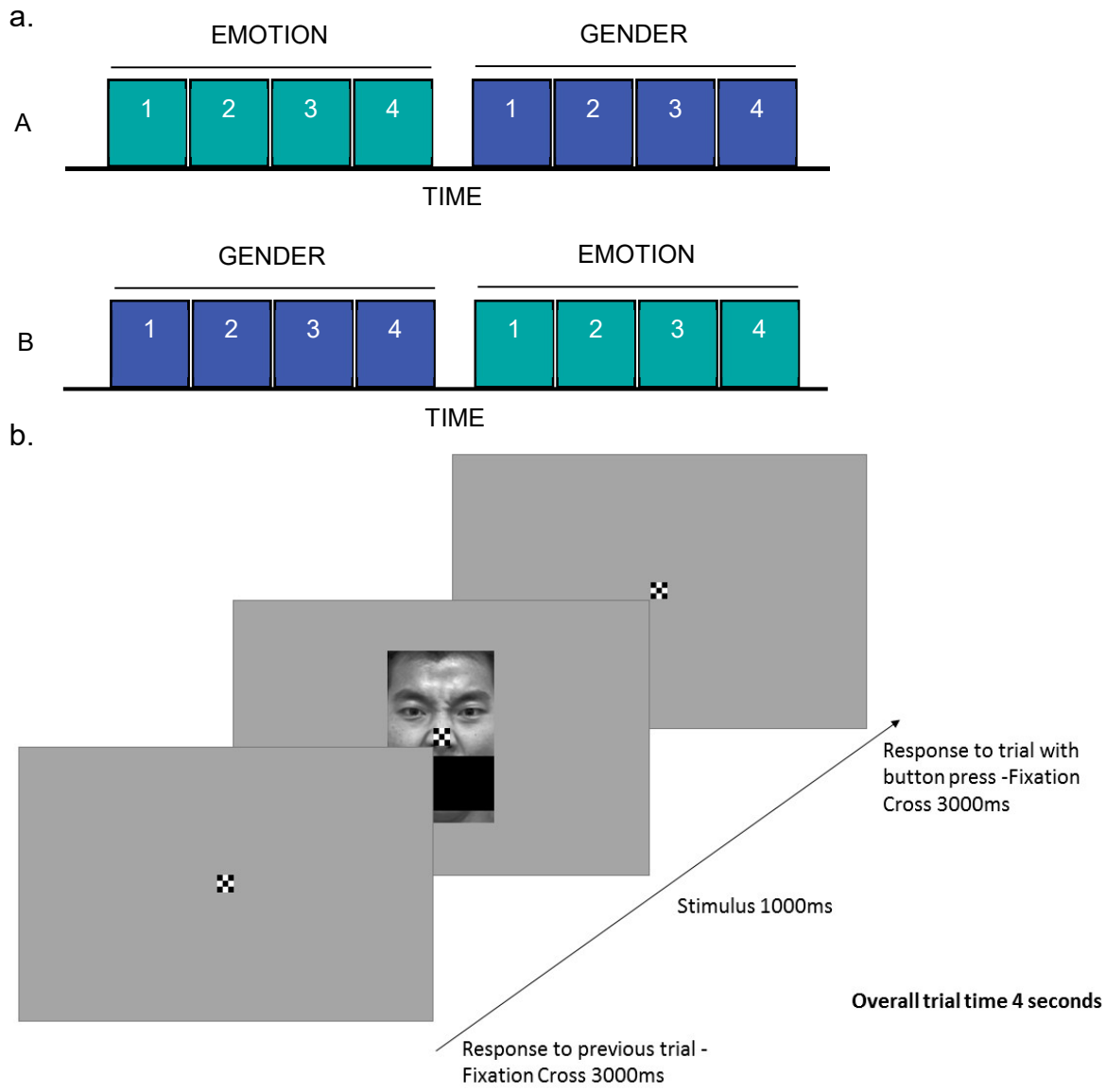

Figure 2.14. a. Experimental design, subjects either carried out four runs of the emotion task followed by four runs of the gender task (A), or subjects carried out four runs of the gender task followed by four runs of the emotion task (B); b. Sequence of stimulus presentation.

Following the experimental runs participants were asked to undertake a retinotopic mapping session lasting 664 seconds (Morgan, Petro, & Muckli, 2016; Muckli et al., 2015). In this task, participants were asked to fixate on a central blue dot in the middle of a flashing checkerboard. The checkerboard (9.34° visual angle) would rotate 10 times around their central fixation point. Participants were required to press their button when the fixation dot changed colour from blue to red (see Figure 2.15). The scanning session lasted a maximum of two hours, including time for set up (15 minutes), anatomy scans (10 minutes), retinotopic mapping to localise early visual regions (15 minutes) and the main experimental runs. Participants were

also shown the WF stimuli before entering the scanner to familiarise themselves with the stimuli. These stimuli were printed out for the participants and they were given a few minutes to look at the faces (please find stimulus sheets in Appendix A). The experimenter showed the participants which column of faces were displaying which emotion and where to find the male and female faces, but no specific training was given.

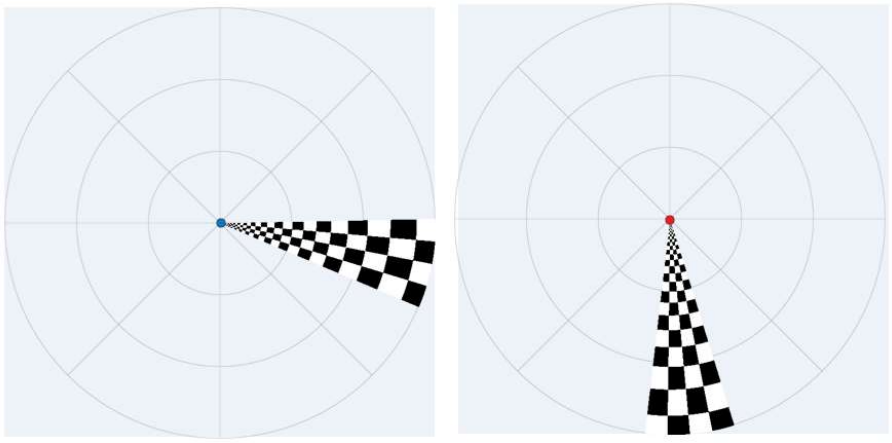

Figure 2.15. Retinotopy task; participants asked to fixate on the blue dot, see image to the left, and respond when the dot changed to red, see image on the right.

2.2.4 MRI data acquisition.

MRI data were collected with a 3T Siemens Prisma fit scanner with a 64 channel head coil and intergrated parallel imaging techniques (Scannexus, Brains Unlimited, Maastricht, Netherlands). Participants were positioned head first, supine in the scanner. For the main runs of the experiment and the retinotopic localiser task, blood oxygen level-dependent (BOLD) signals were recorded with a gradient echo-planar imaging sequence (TE = 30ms, TR = 2000ms, FOV = 200mm x 200mm, Flip angle = 77˚, matrix size 80x80 and slice thickness = 2.5mm (no gap) giving 2.5mm isotropic voxels). Data, collected from 35 oblique slices of the brain, was positioned over the visual cortex, temporal lobe and frontal cortex. High resolution anatomical scans were recorded in the same session (3DMPRAGE, 1 x 1 x 1mm^3 resolution).

2.2.5 MRI data processing.

BrainVoyager QX [version 2.8] (BrainInnovation, Maastricht, The Netherlands) was used for fMRI data analysis (Goebel, Esposito, & Formisano, 2006). Firstly, standard pre-processing steps were applied for each subject independently, these included slice scan time correction, 3D motion correction and temporal filtering. No spatial smoothing was carried out to maintain voxel

resolution. Anatomical and functional data was transformed into ACPC and Talairach space.

2.2.6 Retinotopic mapping.

Advanced segmentation methods were used to create high quality meshes of the visual cortex. This involved upsampling the $1mm^3$ anatomical scans to $0.5mm^3$, segmenting the white and grey matter, selecting the occipital lobe to be reconstructed and creating a map on the inflated cortex. This map was created using the phase-encoded retinotopic mapping data of the eight polar angle conditions and subsequently was used to define the early visual regions (Morgan et al., 2016) (see Figure 2.16). Linear cross correlation analysis was employed to correlate the maximally responsive V1 voxels with the number of lags per hemisphere (Goebel, Khorram-Sefat, Muckli, Hacker, & Singer, 1998).

Thus, the predicted hemodynamic signal time course was correlated for the first $1/8^{th}$ of stimulation cycle, corresponding to a 45° visual angle, and this reference function was shifted sequentially to match the recording time (4 seconds) for one volume (Muckli, Kohler, Kriegeskorte, & Singer, 2005; Muckli, Naumer, & Singer, 2009). Through selecting the lag values with the highest cross-classification voxels, the visual cortex was encoded by pseudo-colours (based on their intensities) (Muckli et al., 2005). These were then projected as surface patches (triangles) on each individuals reconstructed cortex; the boundaries of retinotopic cortical areas V1, V2, V3 were manually estimated on the corresponding inflated cortical surface (Muckli et al., 2005). The red, orange and yellow colours delineate boundaries of V1-V3 in the right upper hemisphere and left lower hemisphere; the blue and green colours delineate boundaries in the upper left hemisphere and lower right hemisphere, see Figure 2.16.

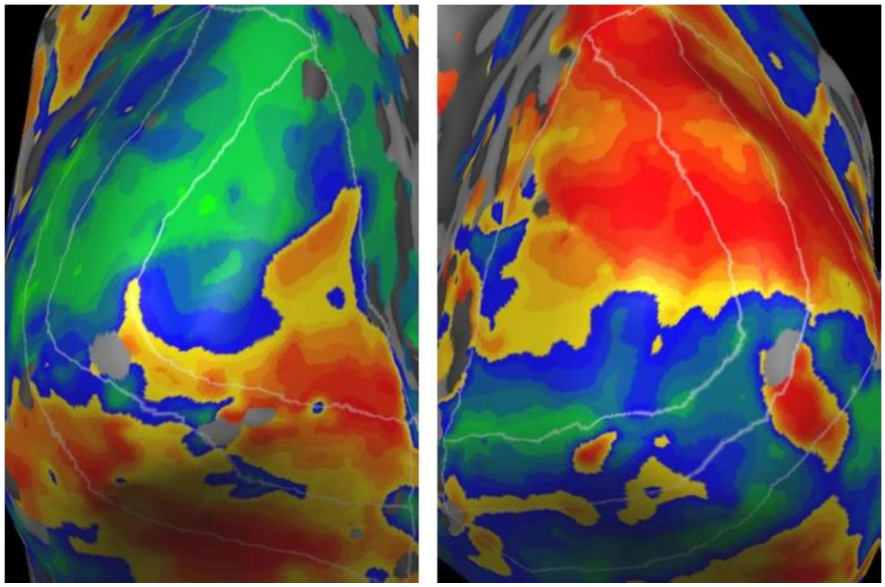

Figure 2.16. Example of retinotopic mapping; the borders between early visual regions are shown in white, V1-V3.

2.2.7 Analysis.

For the multivariate analyses, a GLM was applied to estimate response amplitudes independently for each voxel in each run on a single trial basis (5 PF conditions X 3 expressions X 6 identities, giving 90 predictors per run, plus confound). The resulting beta weights estimate peak activation for each single-trial, based on a standard 2γ model of hemodynamic response function (F. W. Smith & Muckli, 2010). These beta weight voxel estimates formed the input for the pattern classification analyses described below.

For univariate region of interest analysis of V1, a deconvolution analysis was necessary to accurately model the hemodynamic response function (HRF) in each condition. A general linear model (GLM) was performed with 10 predictors per condition (5 PF conditions X 3 emotions, totalling 150 predictors) to fully model the HRF per condition for each subject. The beta values for this analysis were extracted using a minimum threshold (approximately 6000 voxels for each participant) of significant voxels in V1. Time points three and four were extracted and averaged together to estimate peak activity of explicit and implicit expression perception; this gave the peak amplitude after stimulus for all subjects.

For the univariate whole brain random effects (RFX) analysis (WBA) (Appendix B), a deconvolution analysis was again necessary, however, unlike the

previous analyses, the data was spatially smoothed with a Gaussian Filter function of full width half maximum (FWHM) of 6mm. To identify active brain regions, corrected for multiple comparisons, a cluster threshold of 200 voxels (cluster level $p < .05$) was applied at t = 4.5 (corrected to voxel-wise $p < .001$) using the Cluster-level Statistical Threshold Estimator [Brain Voyager Qx Plug in]. Two analyses were carried out; the first analysis was a contrast between explicit and implicit expression recognition, whilst the second contrasted activated brain regions for WF against ME and MM.

2.2.8 Additional face and emotion related ROI's.

Five other ROIs were selected to investigate the potential role of several higher level visual or emotional areas to effects observed within retinotopically defined V1. These ROIs, consisting of the fusiform gyrus (FG), superior temporal sulcus (STS), inferior occipital gyrus (IOG), amygdala (AMY) and insula (INS), were defined from a meta-analysis in the NeuroSynth database (Yarkoni, Poldrack, Nichols, Van Essen, & Wager, 2011), see Table 2.1. These regions were chosen based on a previous study by Wegrzyn et al. (2015). Regions were generated from running a meta-analysis for a particular anatomical keyword (e.g. inferior occipital) using the reverse inference option and saving the generated statistical map (FDR corrected at q = .01) (Yarkoni et al., 2011). For comparability to Wegrzyn et al. (2015) a set of several voxel sizes in each ROI were defined (50, 100, 200, 400, 800) and the results were averaged across these voxel sizes.

Table 2.1.

Selected Reverse Inference Maps for ROI's downloaded from www.neurosynth.org on 27th July 2016. As of that date, the database consisted of 11406 studies. Peak voxel coordinates defined in Talairach space using BrainVoyager QX.

ROI	Neurosynth keyword	Number of studies	Peak voxel		
			x	*y*	*z*
Lateral fusiform gyrus	'fusiform gyrus'	475	-40	-50	-21
Superior temporal sulcus	'sts'	181	-58	-17	-6
Inferior occipital gyri	'inferior occipital'	81	47	-77	-12
Amygdala	'amygdala'	1245	-22	-4	-17
Insula	'insular cortex'	185	35	-8	9

2.2.9 Multivariate pattern classification analysis.

Classifiers were built independently for each ROI (including the retinotopically defined visual regions, and the higher order visual/emotional regions). Based on the retinotopy data, the 100 most visually sensitive voxels were extracted from V1, V2 and V3; as well as 1000 voxels from early visual cortex (EVC) as a whole for feature selection. Results from V2, V3 can be found in Appendix C. Furthermore, five different voxel sizes for each ROI defined from Neurosynth were extracted, including 50, 100, 200, 400 and 800 voxels (based on Wegreyzn et al's., 2015).

Pattern classifiers were trained to discriminate between the three expressions, independently for each PF condition and task, using a Linear Support Vector Machine (LIBSVM 3.12 toolbox, Chang & Lin, 2011). Accordingly, these classifiers were trained to learn the mapping between multivariate observations of brain activation and the expression condition presented, to test whether there was pattern information to discriminate between the emotions for each PF condition (in ROIs). The classifiers were trained with beta values from a set of single-trial brain activity patterns. These were tested on independent single trials (beta weights) for each stimulus condition in the independent set of test data. An n-fold leave-one-run-out

cross-validation approach was used to estimate performance, whereby the model was built from n – 1 runs and tested on the nth independent run (F. W. Smith & Goodale, 2015; F. W. Smith & Muckli, 2010). This procedure minimises the problem of overfitting data.

In further cross-classification analyses (hereafter referred to as XC) the classifier was trained to discriminate expression from one PF condition and tested on another, see Figure 2.17. This analysis was carried out on three pairs of conditions containing non-overlapping samples of face information: eye region and rest of face minus eye region (EO and ME), mouth region and rest of face minus mouth region (MO and MM) and, finally, the eye and mouth regions (EO and MO). In the final pair of conditions receptive cells in V1 are prevented from overlapping, as the typical maximum is 1˚ of receptive field size in the centre of V1 (up to eccentricities of 12˚) (A. T. Smith, Singh, Williams, & Greenlee, 2001) and there is a featural 1.4˚ angle separation between the stimuli in this study. Again an n-fold leave-one-run-out cross-validation approach was used. Performance for each direction of training and testing the classifier was computed and averaged (e.g. train eye region and test rest of face minus eyes, with train rest of face minus eyes and test eye region). Again, this data was trained on single-trial brain activity patterns and tested on single-trial brain activity patterns. For each ROI, a repeated measures ANOVA was conducted to investigate task and PF condition, or cross-classified PF pair, on decoding accuracy. The Greenhouse-Geisser correction was reported if sphericity was violated and the estimated epsilon was less than 0.75; the Huynh-Feldt correction was reported if the estimated epsilon was greater than 0.75, this correction was recommended by Girden (Field, 2009). For all analyses, decoding accuracy was reported for each PF condition using one-tailed one-sample t-test results with chance level at 33.3%. Significance levels are presented on graphs to $p < .05$ and $p < .01$.

The LIBSVM toolbox (version 3.12) was employed (Chang & Lin, 2011). Default parameters were used for the linear SVM with C = 1. Before inputting into the SVM, the training data was normalised to lie within -1 and 1, with the test data normalised using the relevant parameters from the training data (max, range) (Chang & Lin, 2011; F. W. Smith & Goodale, 2015; F. W. Smith & Muckli, 2010; Vetter et al., 2014).

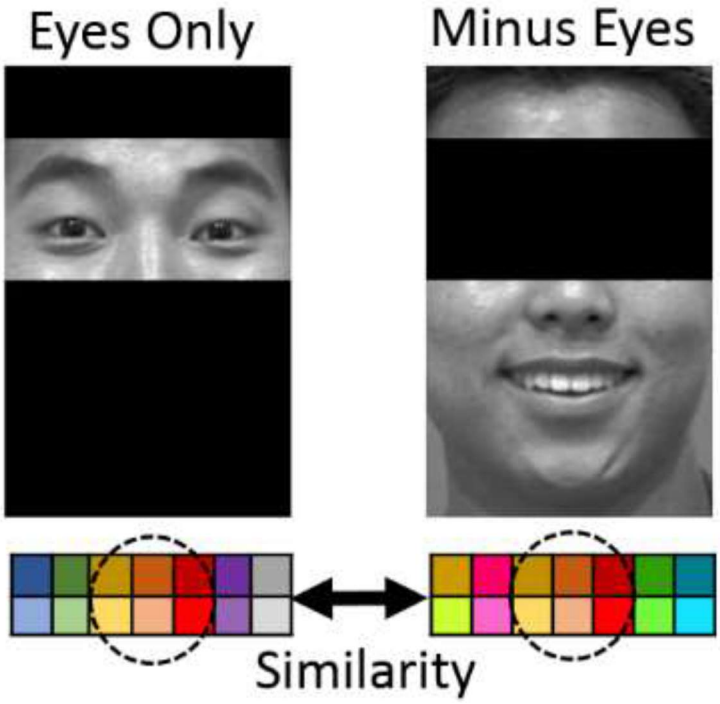

Figure 2.17. Example MVPA analysis; testing for pattern similarity in non-overlapping PF conditions, namely EO vs ME.

2.3 Results

2.3.1 Behavioural results.

Behavioural data revealed that participants, as expected, subjectively performed better at the gender task (M = 95.97%, SD = 5.94%) than the expression task (M = 82.42%, SD = 17.3%) across all PF conditions. With closer analysis of the PF conditions, see Table 2.2, it appears that participants performance was highest in the WF conditions, followed by MM and ME in the expression task (see Figure 2.18), and ME and MM in the gender task. Further, when comparing emotion recognition accuracy; happiness was subjectively the most recognisable emotion (M = 95.16%, SD = 7.08%), followed by disgust (M = 82.2%, SD = 13.96%) and then fear (M = 69.88, SD = 18.4%).

Table 2.2.

All to 2d.p in percentage. WF: whole face, EO: eyes only, ME: minus eyes, MO: mouth only, MM: minus mouth.

Task	WF	EO	ME	MO	MM
Expression	85.53 (SD = 15.42)	80.21 (SD = 15.93)	82.87 (SD = 18.9)	78.86 (SD = 21.39)	84.61 (SD = 13.85)
Gender	98.96 (SD = 1.97)	90.28 (SD = 9.55)	97.45 (SD = 2.83)	95.83 (SD = 4.41)	97.34 (SD = 3.52)

2.3.1.1 Emotion accuracy.

A two-way repeated measures ANOVA was employed to explore the effects of PF condition and emotion on accuracy. In the expression task, there was a significant main effect of PF condition on accuracy, $F(4, 44) = 4.851$, $p = .002$, $\eta_p^2 = .306$, as well as a significant main effect of emotion on accuracy, $F(2, 22) = 24.686$, $p < .001$, $\eta_p^2 = .692$. Collapsed across PF conditions, post-hoc pairwise comparisons with Bonferroni correction, showed accuracy rates for both disgust and fear statistically different from happiness ($p < .01$); with no significant accuracy difference between disgust and fear ($p = .062$). Furthermore, there was a significant interaction between PF condition and emotion, $F(3.270, 35.965) = 11.783$, $p < .001$, $\eta_p^2 = .517$ (greenhouse-geisser corrected).

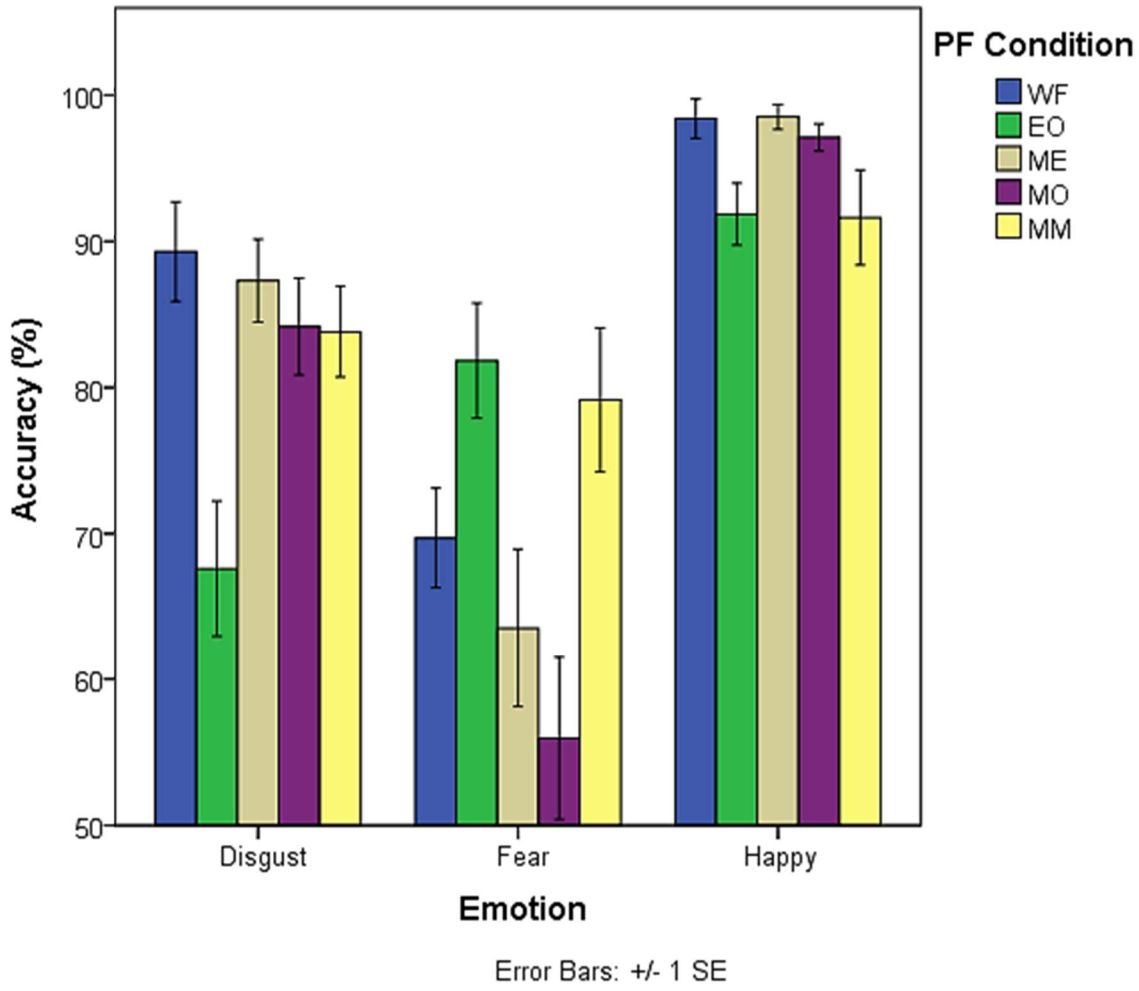

Figure 2.18. Overall recognition accuracy (%) in each PF condition for each emotion.

As a result of the significant interaction, a simple effects analysis was undertaken, whereby eight separate repeated measures ANOVA's were carried out. Firstly the effect of emotion at each PF condition was investigated by carrying out five ANOVAs (all five were significant at $p < .05$) and then the effect of PF condition for each emotion in turn was investigated by carrying out three separate ANOVAs (all three were significant at $p < .05$), these results can be found in Appendix D (Table D1 and Table D2). Additional post-hoc Bonferroni and paired sample t-tests were carried out to understand the differences between the conditions, see Figures 2.19 and 2.20.

A. WF

	Disgust	Fear	Happy
Disgust			
Fear			
Happy			

D. MO

	Disgust	Fear	Happy
Disgust			
Fear			
Happy			

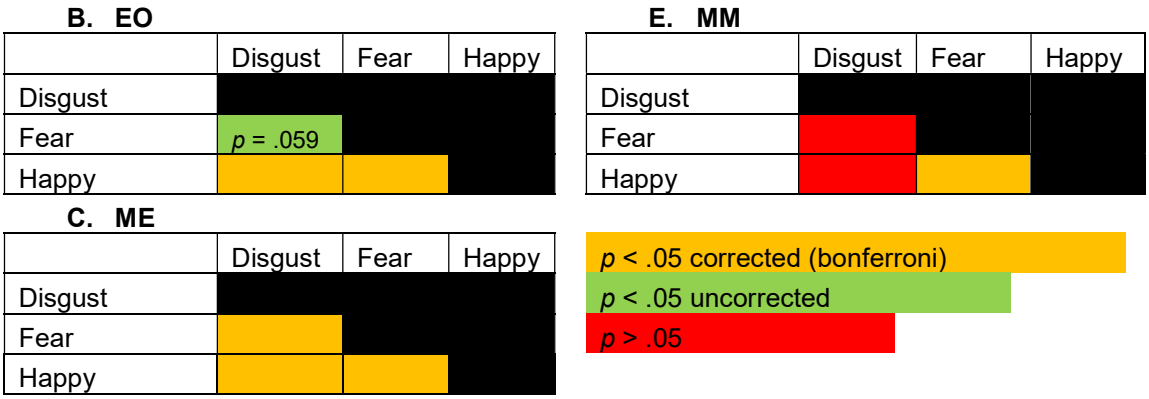

Figure 2.19. Paired sample t-test results comparing the differences between the emotions for each PF condition (see Table D3 in Appendix D for statistics).

Overall, these figures show that there were fewer differences between the emotions in the MM condition whereby participants showed similar accuracy across the three emotions (Figure 2.19 & 2.18). Participants showed greater differences in accuracy between all the emotions when there was mouth information present.

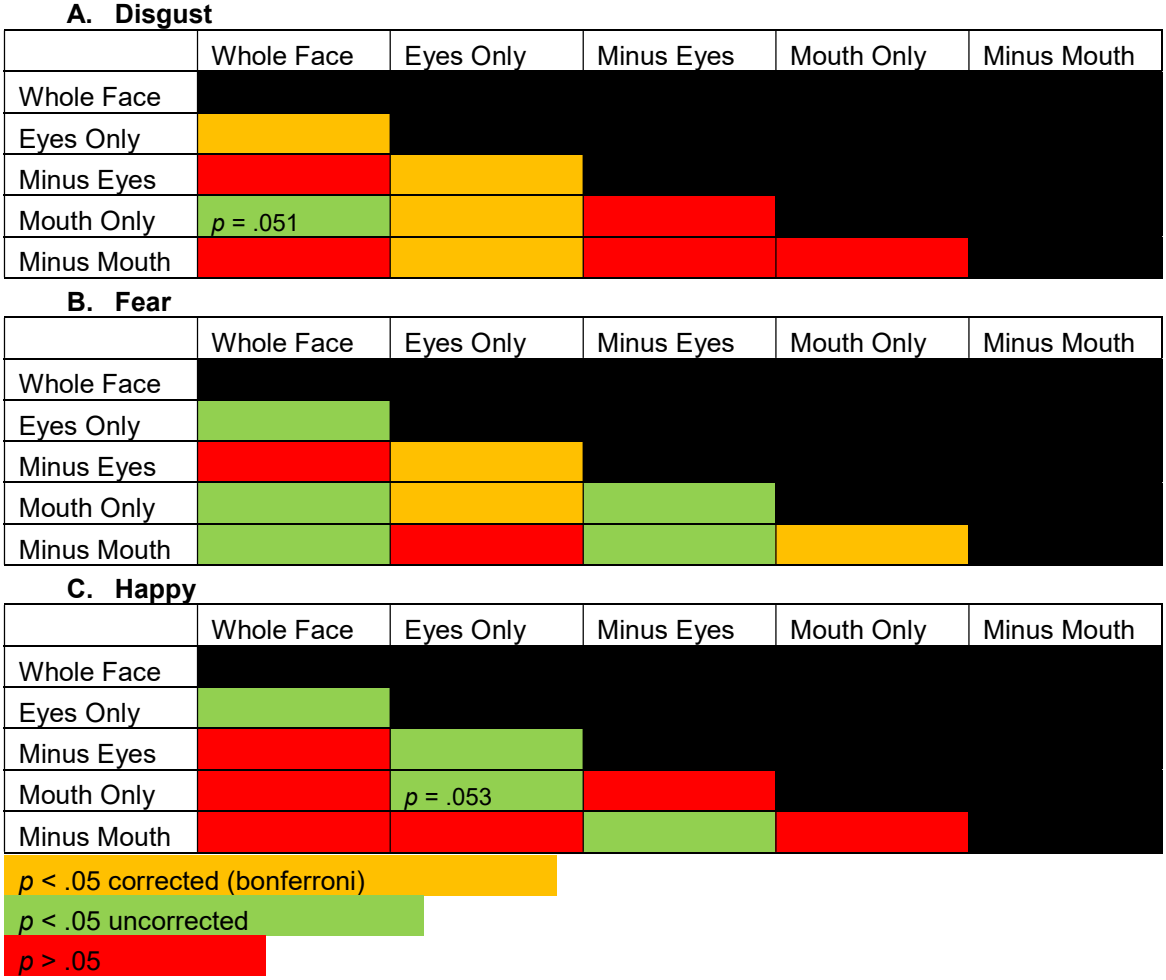

Figure 2.20. Paired sample t-test results comparing the differences between the PF conditions for each emotion (see Table D4 in Appendix D for statistics).

Results for disgust recognition (Figure 2.20A) show the EO condition significantly different from all other conditions; looking into the statistics of this the subjects are significantly worse at recognising disgust from purely eye information (M = 67.5% in comparison to the averaged mean of the other four PF condition = 85.9%). This is in line with previous findings showing humans reliance on information from the nose and mouth region to detect disgust (F. W. Smith & Schyns, 2009; M. L. Smith & Merlusca, 2014).

Similarly, results for fear recognition (Figure 2.20B) show the EO condition being statistically different from almost all other PF conditions. However, in comparison to disgust recognition this shows the importance of the eyes in recognising fear, with subjects performing significantly better ($p < .05$ Bonferroni corrected post-hoc pairwise comparison) in the EO condition (M = 81.6%) compared to the ME (M = 63.4%) and the MO condition (M = 55.9%). Fear recognition is the lowest in the MO condition, this is also significantly different from the MM condition. This supports literature detailing the importance of the eyes and "eye whites" in fear recognition (F. W. Smith & Schyns, 2009; M. L. Smith et al., 2005; M. L. Smith & Merlusca, 2014; Whalen et al., 2004). The finding of no difference in recognising fear in the MM and EO condition further supports this, as these conditions both contain information from the eyes.

The results for happy recognition suggest few differences in accuracy between the PF conditions (Figure 2.20C); participant's performance was similar when presented with a WF compared to ME and MO (Figure 2.18). Looking closer into the mean performance values, differences again arose in the EO (91.6%) and minus mouth (91.3%) conditions (with the M of other conditions – 97.6%), lending similarities to disgust recognition and in line with previous literature detailing the importance of the mouth in happiness recognition, subjects performed worse in these conditions (F. W. Smith & Schyns, 2009; M. L. Smith et al., 2005).

2.3.1.2 Gender accuracy.

A two-way repeated measures ANOVA was employed to explore the effects of PF condition and gender on accuracy in the gender task. In the gender task, there was a significant main effect of gender on accuracy, $F(1, 11) = 6.592$, $p = .026$, $\eta_p^2 = .375$, with participants significantly more accurate at recognising the male faces (M = 97.13%, SD = 3.23%) than the female faces (M = 94.81%, SD = 7.61%), see

Figure 2.21. In addition, there was a significant main effect of PF condition on accuracy, $F(2.081, 22.890) = 15.219$, $p < .001$, $\eta_p^2 = .580$ (greenhouse-geisser corrected). These effects are driven by the EO condition, as there were significant post-hoc pairwise comparisons, with Bonferroni correction, between the EO and WF condition ($p = .001$), EO and ME condition ($p = .012$) as well as the EO and MM condition ($p = .002$). Furthermore, there was a significant interaction between PF condition and gender, $F(1.765, 19.415) = 14.453$, $p < .001$, $\eta_p^2 = .568$ (greenhouse-geisser corrected).

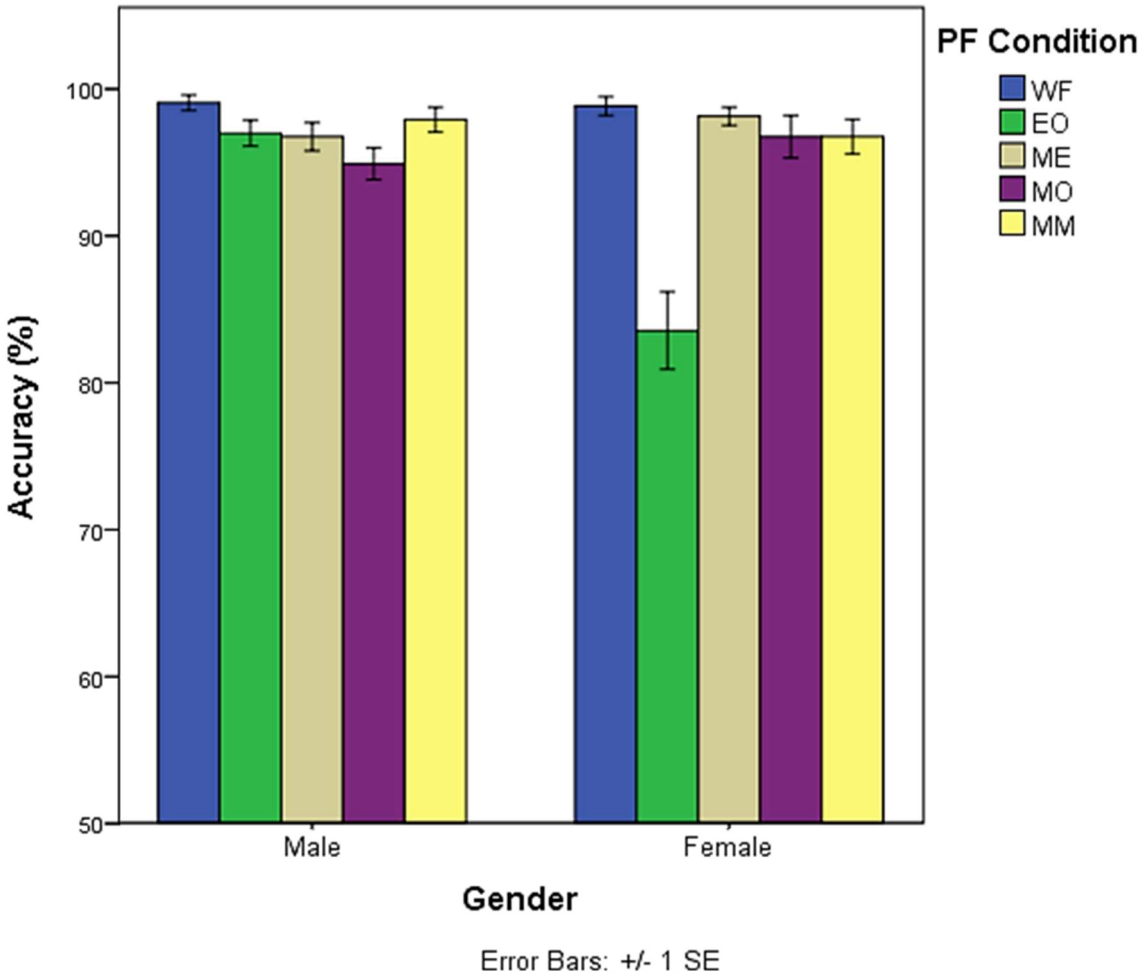

Figure 2.21. Showing overall recognition accuracy (%) in each PF condition between male and female stimuli.

Again, as a result of the significant interaction, a simple effects analysis was undertaken. ANOVAs testing the effect of gender for each PF condition only found significance in the EO condition ($F(1, 11) = 19.809$, $p = .001$, $\eta_p^2 = .643$). Testing the effect of PF condition on gender found significance for both male and female faces ($p < .01$); the simple effects ANOVA results can be found in Table D5 and

Table D6 (Appendix D). Further post-hoc tests and paired sample t-tests were carried out to establish the differences between the PF conditions for male and female faces, see Figure 2.22.

A. Male

	Whole Face	Eyes Only	Minus Eyes	Mouth Only	Minus Mouth
Whole Face					
Eyes Only					
Minus Eyes					
Mouth Only					
Minus Mouth					

B. Female

	Whole Face	Eyes Only	Minus Eyes	Mouth Only	Minus Mouth
Whole Face					
Eyes Only					
Minus Eyes					
Mouth Only					
Minus Mouth					

P < .05 corrected (bonferroni)
p < .05 uncorrected
p > .05

Figure 2.22. Paired sample t-test results comparing the differences between the PF conditions for male and female faces (see Table D7 in Appendix D for statistics: t-value, df and p-value).

These results suggest that it is harder to recognise male faces in ME or MO conditions compared to WF conditions, therefore indicative of using the eyes more to make a judgement on a male face (M. L. Smith, Gosselin, & Schyns, 2004). Generally recognising male faces is accurate across all PF conditions, whereas, when recognising female faces it seems that the EO condition is significantly different from all other conditions. It is unclear why it would be hard to recognise if a face is female from just seeing their eyes, but it is suggestive that to recognise a female either more mouth information or broader face information may be used.

2.3.2 Retinotopy.

The principal objective of this study was to investigate the decoding of expression across conditions with non-overlapping feature information in early visual regions (V1 and EVC); as such the main interest lies within the XC effects. However, to help understand these, the basic decoding results for each region will be presented first, followed by the XC results.

2.3.2.1 Basic decoding.

Results for decoding of expression in V1 and EVC are presented first; these are split by task for each PF condition. Explicit expression decoding refers to when a participant is performing the emotion recognition task and the classifier is decoding emotion in their brain, whereas implicit expression decoding refers to when a participant is asked to judge gender (between male and female faces) but the classifier is again decoding emotion in their brain.

2.3.2.1.1 Primary visual cortex (V1).

For decoding of expression, one sample t-tests showed explicit decoding in V1 significantly above chance in the WF ($t(11) = 1.823$, $p = .048$, $d = 0.526$ (medium effect-size)), ME ($t(11) = 1.847$, $p = .046$, $d = 0.533$ (medium effect-size)) and MO ($t(11) = 6.111$, $p < .001$, $d = 1.764$ (large effect-size)) conditions, see Figure 2.23. Implicit decoding of expression, in contrast, was subjectively higher and reliable in all PF conditions ($p < .01$) above chance; t-test results can be found in Table D8 (Appendix D). A repeated measures ANOVA showed a main effect of PF condition on decoding accuracy, $F(4, 44) = 4.308$, $p = .005$, $\eta_p^2 = .281$, as well as a significant main effect of task, $F(1, 11) = 34.507$, $p < .001$, $\eta_p^2 = .758$, with decoding accuracy significantly higher in the implicit task (M = 51%) compared to the explicit task (M = 37%). Additionally there was an interaction between PF condition and task on decoding accuracy, $F(4, 44) = 5.197$, $p = .002$, $\eta_p^2 = .321$.

As a result of the significant interaction, a separate ANOVA was carried out for each task. In the explicit task, a repeated measures ANOVA showed no significant main effect of PF condition, $F(4, 44) = .823$, $p = .518$, $\eta_p^2 = .070$, whereas in the implicit task there was a significant main effect of PF condition, $F(4, 44) = 8.545$, $p < .001$, $\eta_p^2 = .437$.

Post-hoc pairwise comparisons with Bonferroni correction show significant differences between WF and ME ($p = .033$), EO and ME ($p = .001$) as well as the ME and MO conditions ($p < .001$), such that decoding accuracy in the ME condition is significantly higher than WF, EO and MO. Furthermore, paired sample t-tests were carried out to explore the effect of task for each PF condition, apart from in the MO condition, there was a significant difference between the tasks in each PF condition ($p < .05$; t-test results can be found in Table D9, Appendix D).

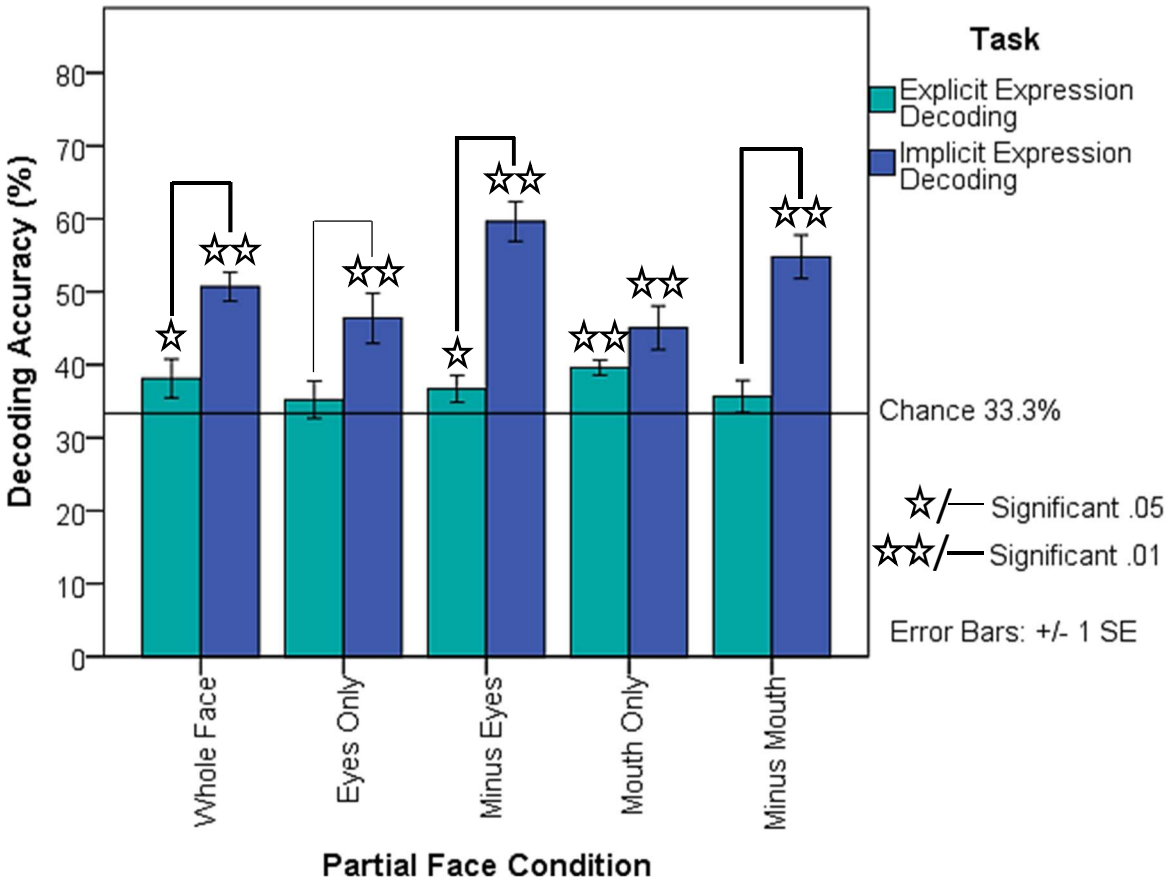

Figure 2.23. Explicit and implicit expression decoding accuracy of the PF conditions V1, significant results from one-sample t-tests represented with stars.

2.3.2.1.2 Early visual cortex.

For decoding expression from EVC (V1-V3), one sample t-tests show greater explicit decoding; with performance significantly above chance in the WF ($t(11) = 4.154$, $p < .001$, $d = 1.199$ (large effect-size)), MO ($t(11) = 6.351$, $p < .001$, $d = 1.833$ (large effect-size)) and MM conditions $t(11) = 2.449$, $p = .016$, $d = 0.707$ (medium effect-size)), see Figure 2.24. Analogous to V1, all implicit conditions were significantly above chance ($p < .001$); t-test results can be found in Table D10 (Appendix D). A repeated measures ANOVA showed a highly significant main effect of PF condition on decoding accuracy, $F(4, 44) = 6.985$, $p < .001$, $\eta_p^2 = .388$, with higher decoding accuracies in the ME and MM conditions demonstrated with significant post-hoc pairwise comparisons, with Bonferroni correction, between the EO and ME ($p = .008$), EO and MM ($p = .004$) and finally the MO and MM conditions ($p = .016$). There was also a highly significant main effect of task on decoding accuracy, $F(1, 11) = 149.739$, $p < .001$, $\eta_p^2 = .932$, with decoding accuracy significantly higher in the implicit (M = 66.5%) compared to the explicit task (M =

39.6%), as well as a significant interaction between PF condition and task, $F(4, 44) = 9.294$, $p < .001$, $\eta_p^2 = 458$. Further paired sample t-tests were carried out to explore the effect of task for each PF condition, these were all significant between the PF conditions ($p < .001$); t-test results can be found in Table D11 (Appendix D). As a result of the significant interaction, a separate ANOVA was carried out for each task. In the explicit task, a repeated measures ANOVA showed a non-significant main effect of PF condition, $F(4, 44) = 1.458$, $p = .231$, $\eta_p^2 = .117$. However, in the implicit task, a repeated measures ANOVA showed a significant main effect of PF condition, $F(4, 44) = 15.995$, $p < .001$, $\eta_p^2 = 593$. Post-hoc pairwise comparisons, with Bonferroni correction, show significant differences between WF and ME ($p = .009$), EO and ME ($p < .001$), EO and MM ($p = .002$), ME and MO ($p = .002$), as well as MO and MM ($p = .004$); highlighting that decoding accuracies are significantly higher in the ME and MM condition.

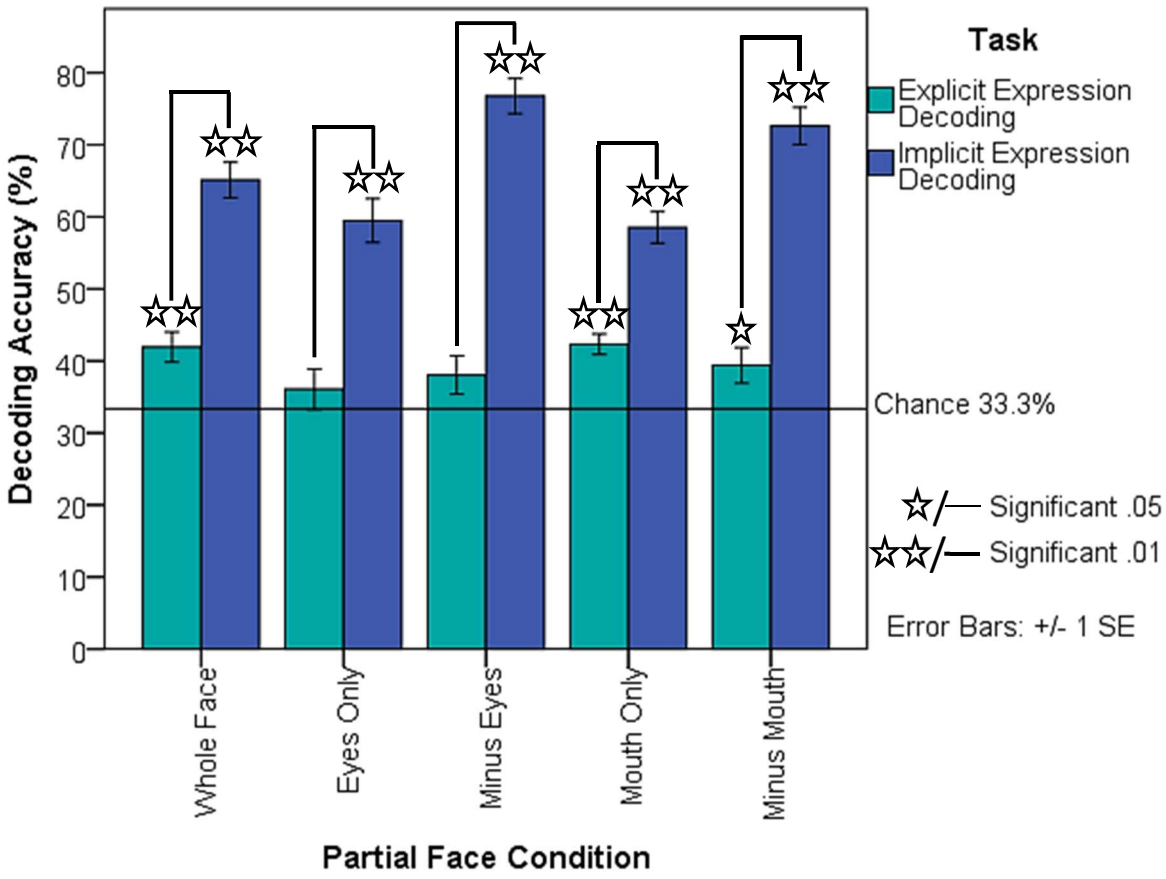

Figure 2.24. Explicit and implicit expression decoding accuracy of the PF conditions for 1000 voxels in EVC, significant results from one-sample t-tests represented with stars.

2.3.2.2 Cross classification (XC).

2.3.2.2.1 Primary visual cortex (V1).

One sample t-tests show implicit cross-decoding in V1 significantly above chance for the EO and ME ($t(11) = 5.033$, $p < .001$, $d = 1.453$ (large effect-size)) as well as the MO and MM pair ($t(11) = 6.031$, $p < .001$, $d = 1.741$ (large effect-size)), with explicit cross-decoding significantly above chance for the EO and MO pair ($t(11) = 2.107$, $p = .029$, $d = 0.608$ (medium effect-size)); see Figure 2.25 and other t-test results in Table D12 (Appendix D). A repeated measures ANOVA showed a significant main effect of task, $F(1, 11) = 8.03$, $p = .016$, $\eta_p^2 = .422$, and cross-classification pair, $F(2, 22) = 18.75$, $p < .001$, $\eta_p^2 = .630$, on decoding accuracy in V1, as well as a significant interaction, $F(2, 22) = 23.877$, $p < .001$, $\eta_p^2 = .685$. As a result of the significant interaction, a separate ANOVA for each task was carried out. In the explicit task, a repeated measures ANOVA showed no main effect of condition pair, $F(2, 22) = 1.270$, $p = .301$, $\eta_p^2 = .104$. However, in the implicit task there was a significant effect of condition pair, $F(2, 22) = 32.228$, $p < .001$, $\eta_p^2 = .746$, with all post-hoc pairwise comparisons, with Bonferroni correction, significant between the classification pairs ($p < .05$). Paired sample t-tests were carried out to explore the effect of task for each condition pair, these were all significant ($p < .01$; t-test results can be found in Table D13, Appendix D); with the implicit conditions significantly higher than the explicit conditions in the first two condition pairs (EO and ME; MO and MM), but significantly lower than the explicit condition in the last condition pair (EO and MO). To look into these findings further, confusion matrices can be found in Appendix E.

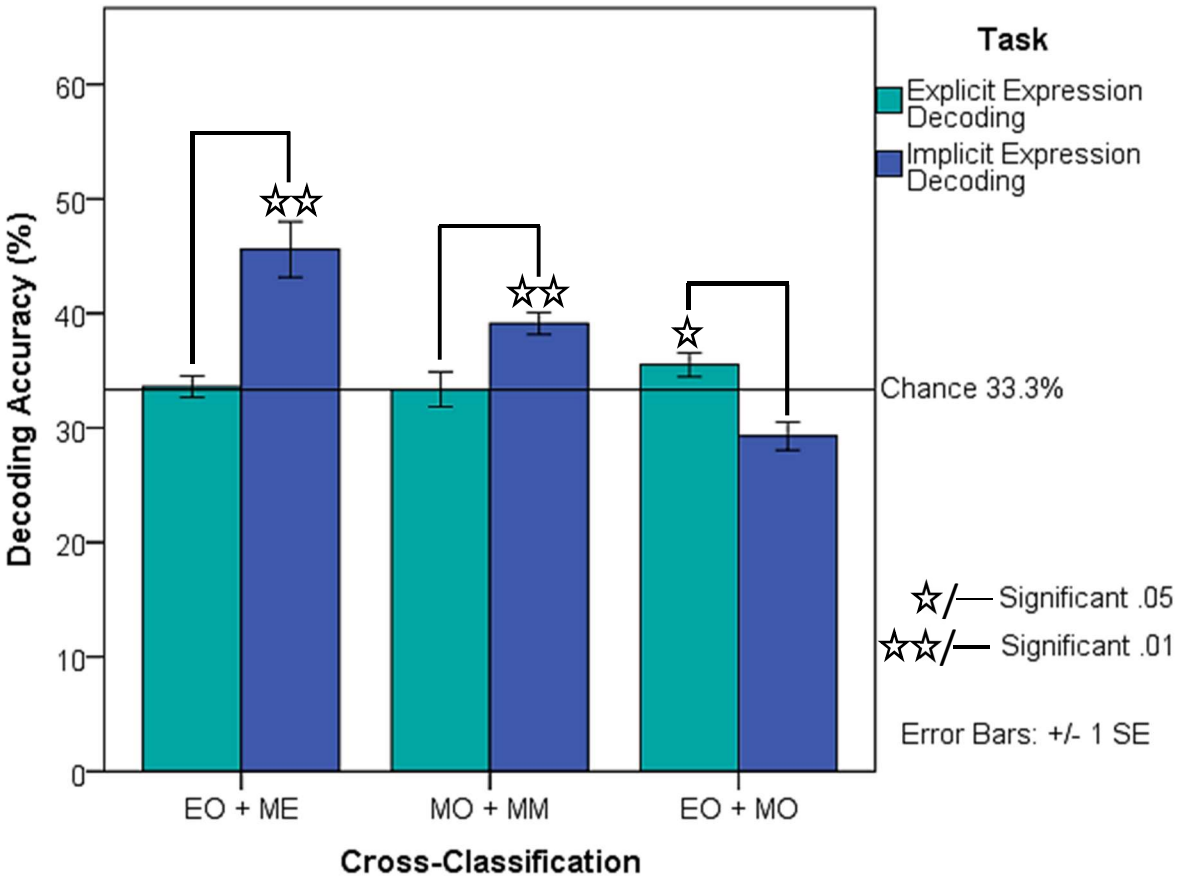

Figure 2.25. Explicit and implicit expression decoding accuracy of the condition pairs of PF conditions in V1. Results from one-sample t-tests included with stars representing significance.

2.3.2.2.2 Early visual cortex.

Akin to V1, one sample t-tests show implicit expression decoding significantly above chance for the EO and ME ($t(11) = 12.718$, $p < .001$, $d = 3.671$ (large effect-size)) as well as the MO and MM ($t(11) = 4.918$, $p < .001$, $d = 1.420$ (large effect-size)) condition pair, with explicit cross-decoding significant in the EO and MO pair ($t(11) = 5.065$, $p < .001$, $d = 1.462$ (large effect-size)). There is additional significance above chance in the explicit decoding of the MO and MM condition pair ($t(11) = 2.964$, $p = .006$, $d = 0.856$ (large effect-size)), see Figure 2.26 and other t-test results in Table D14 (Appendix D). Similar to V1, a repeated measures ANOVA showed a significant main effect of task ($F(1, 11) = 11.296$, $p = .006$, $\eta_p^2 = .507$) and cross-classification comparison ($F(2, 22) = 35.849$, $p < .001$, $\eta_p^2 = .765$) on decoding accuracy, as well as a significant interaction ($F(1.305, 14.358) = 87.945$, $p < .001$, $\eta_p^2 = .889$ (greenhouse-geisser corrected)). To explore the effect of task for each condition pair, paired sample t-tests were carried out, these

were significant at $p < .001$ in the EO and ME pair, as well as the EO and MO pair; with the implicit condition significantly higher than the explicit condition in EO and ME pair but significantly lower than the explicit condition in the EO and MO pair (see Table D15, Appendix D, for the t-test results). As a result of the significant interaction, a separate ANOVA for each task was carried out. In the explicit there was no main effect of condition pair, $F(2, 22) = 1.268$, $p = .301$, $\eta_p^2 = .103$; whereas there was a main effect of condition pair in the implicit task, $F(1.289, 14.183) = 90.080$, $p < .001$, $\eta_p^2 = .891$ (greenhouse-geisser corrected). Pairwise (Bonferroni corrected) comparisons between the condition pairs are all highly significant ($p < .001$), with decoding accuracies in the EO vs ME pair significantly higher than the other two condition pairs and the MO vs MM pair significantly higher than the EO vs MO pair.

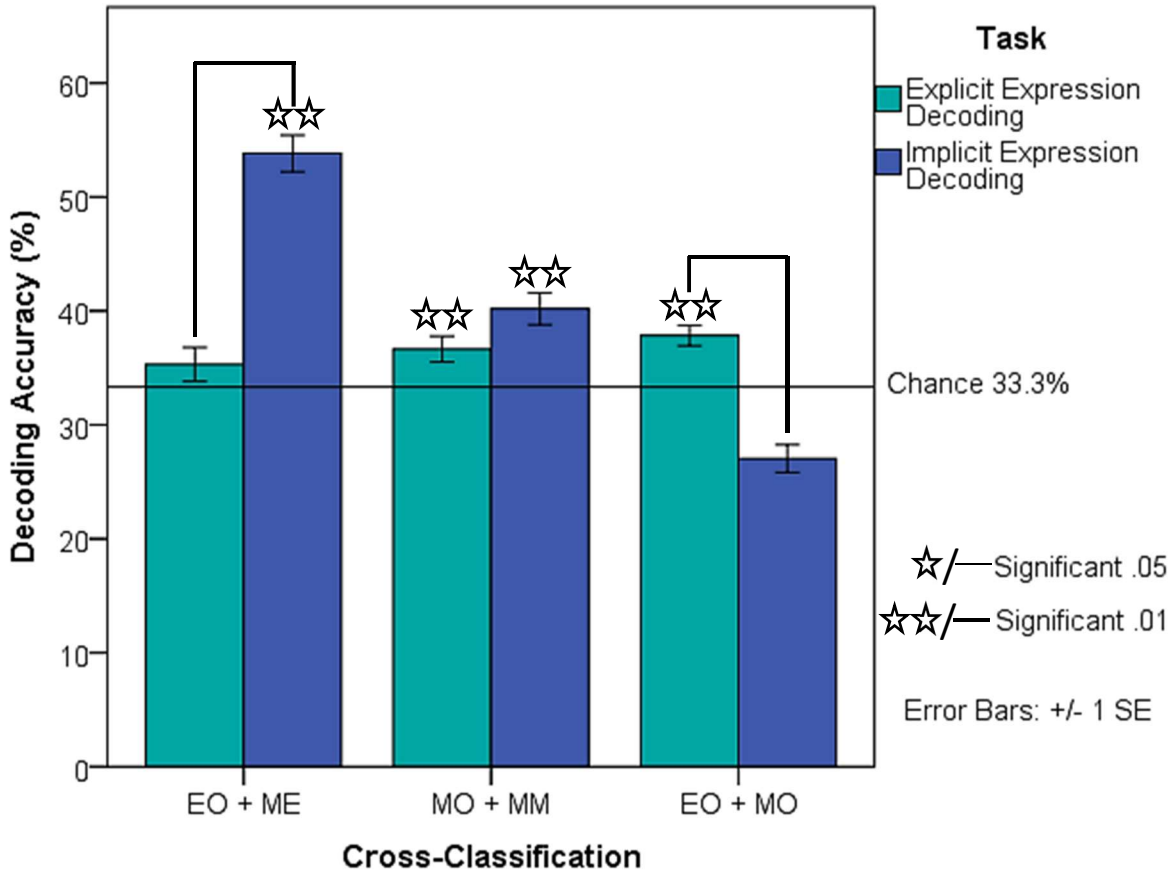

Figure 2.26. Explicit and implicit expression decoding accuracy of the condition pairs of PF conditions in EVC. Results from one-sample t-tests included with stars representing significance.

2.3.2.3 Permutation tests.

Permutation tests were performed to be sure that single-trial classification performance was around chance in the implicit conditions. These tests, using 1000 iterations per subject, randomised the relationship between stimulus labels and data, with the same cross-validation script and ROI's selected as the pattern classification analysis. Permutation analyses were performed in EVC (V1-V3) for basic and cross-decoding. Mean performance was, as expected, close to chance of 33%.

2.3.3 Additional face and emotion related ROI's.

2.3.3.1 Basic decoding.

A 2 (task) x 5 (ROI) x 5 (voxel size) x 5 (PF) repeated measures ANOVA was carried out (see full results write-up in Appendix F). ROI and voxel size were included in the analysis for comparability to Wegrzyn et al. (2015). Wegrzyn et al. (2015) found no interaction of ROI by voxel size and subsequently averaged across the voxel sizes. This method will also be applied in this study if no interactions are found. In respect to voxel size, there appears to be a trend between higher amounts of voxels and greater decoding (see Figure 2.27), however, there was no significance within pairwise comparisons and no significant interactions with voxel size; further analyses will thus average across this variable akin to Wegrzyn et al. (2015).

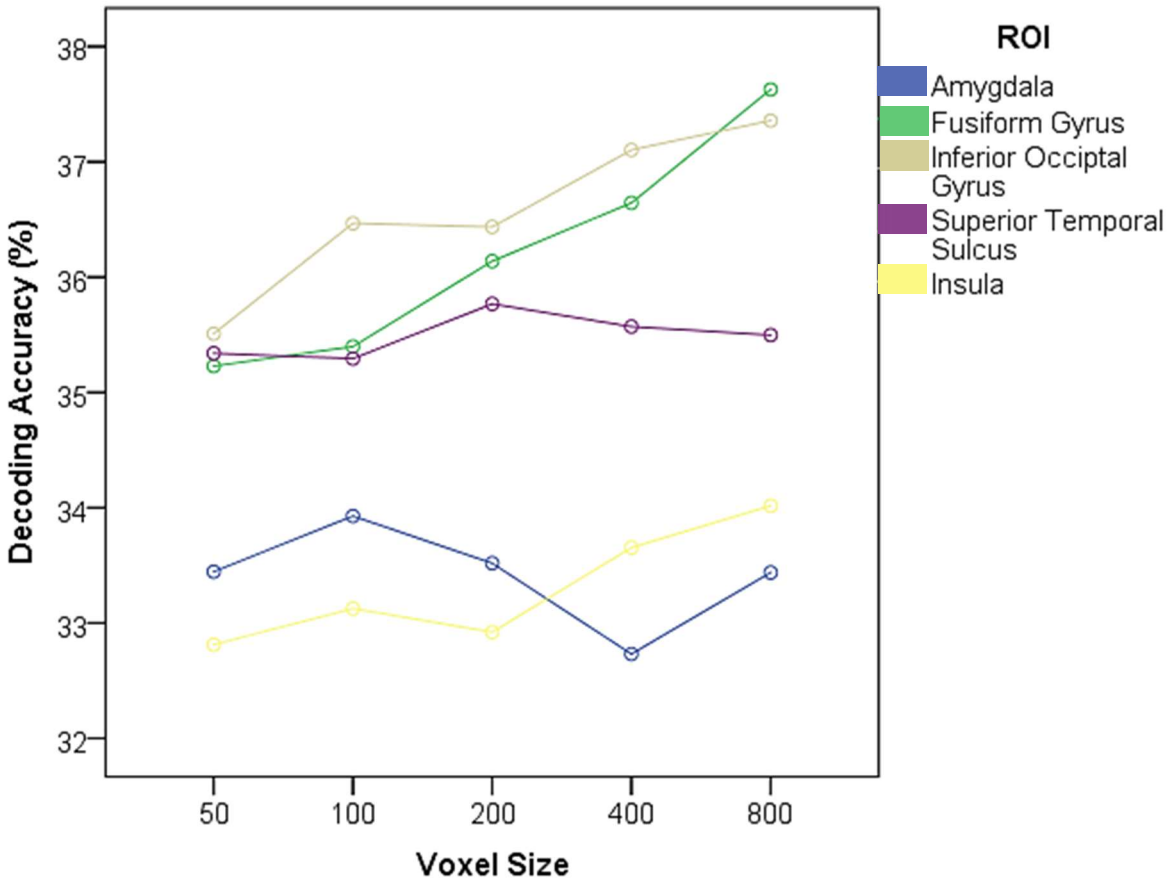

Figure 2.27. Showing decoding accuracy across voxel sizes for each ROI.

Similar to the retinotopy analysis, the five ROI's have been studied individually to investigate the effects of task and PF condition on decoding accuracy. Both basic and cross classification implicit and explicit expression decoding were investigated.

2.3.3.1.1 Fusiform gyrus (FG).

One-sample t-tests show implicit expression decoding in the FG significantly above chance in the WF ($t(59) = 2.584$, $p = .006$, $d = 0.334$ (small effect-size)), ME ($t(59) = 7.080$, $p < .001$, $d = 0.914$ (large effect-size)), MO ($t(59) = 3.125$, $p = .001$, $d = 0.403$ (small effect-size)) and MM conditions ($t(59) = 4.225$, $p < .001$, $d = 0.545$ (medium effect-size)), with explicit expression decoding significant above chance in the WF ($t(59) = 3.802$, $p < .001$, $d = 0.491$ (small effect-size)), EO ($t(59) = 2.279$, $p = .013$, $d = 0.294$ (small effect-size)), ME ($t(59) = 2.407$, $p = .001$, $d = 0.311$ (small effect-size)) and MO ($t(59) = 6.253$, $p < .001$, $d = 0.807$ (large effect-size)), see Figure 2.28 and Table D16 (Appendix D). A repeated measures ANOVA showed a non-significant main effect of task, $F(1, 59) = 1.735$, $p = .193$, $\eta_p^2 = .029$, but a

strong significant main effect of PF condition on decoding accuracy, $F(4, 236) = 3.942$, $p = .004$, $\eta_p^2 = .063$, as well as a significant interaction, $F(3.600, 221.388) = 4.565$, $p = .002$, $\eta_p^2 = .072$ (Huynh-Feldt correction).

As a result of the significant interaction, a separate one-way ANOVA, with PF condition as a factor, was carried out for each task. In the explicit task, there was a significant main effect of PF condition, $F(2, 236) = 3.376$, $p = .010$, $\eta_p^2 = .054$, with post-hoc Bonferroni corrected pairwise comparisons showing significance between the MO and MM condition ($p = .001$). There is also a significant main effect of PF condition in the implicit task, $F(4, 236) = 5.004$, $p = .001$, $\eta_p^2 = .078$, with post-hoc Bonferroni corrected pairwise comparisons showing significance between the EO and ME condition ($p = .001$). Paired sample t-tests were carried out to explore the effect of task for each PF condition, these found decoding accuracy between the tasks to be significantly different in the ME ($t(59) = -3.350$, $p = .001$, $d = -0.433$) and MM conditions ($t(59) = -3.185$, $p = .002$, $d = -0.411$), this mirrors the V1 effect (see other t-test results in Table D17, Appendix D).

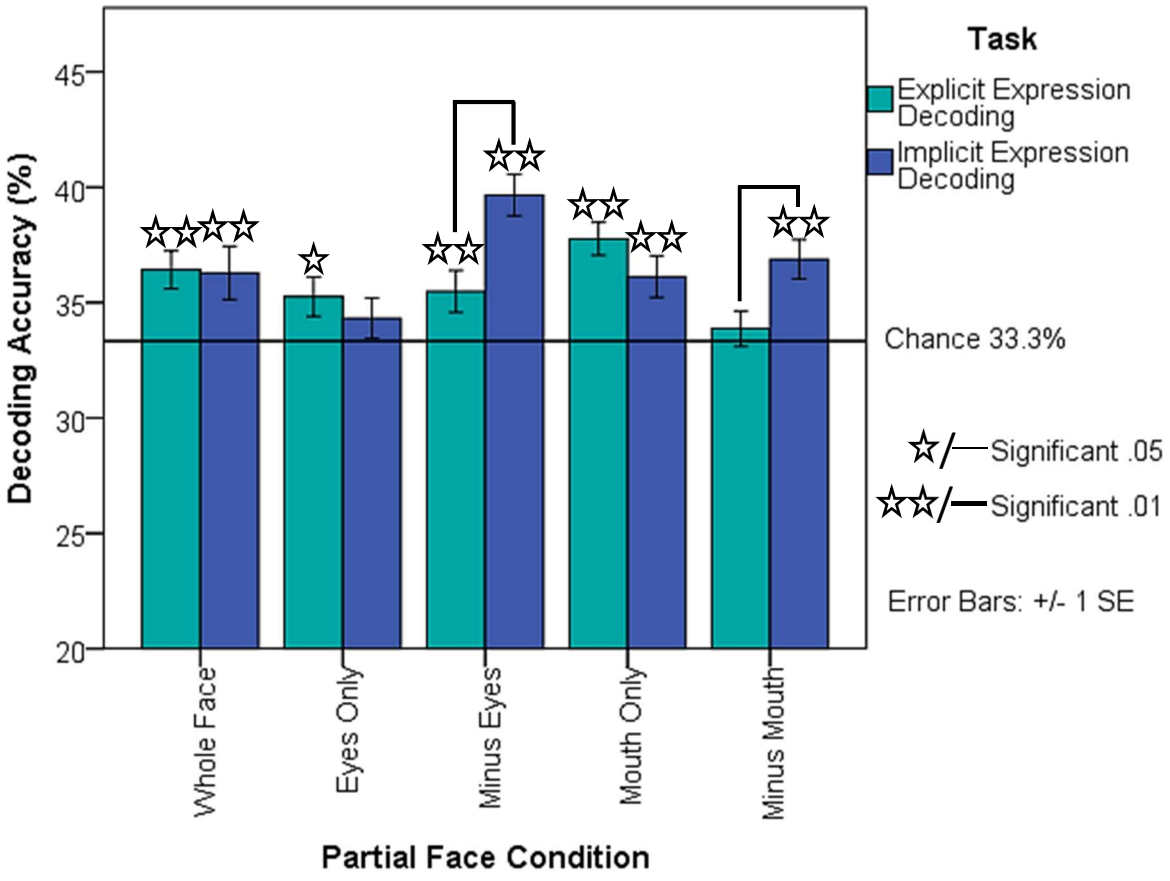

Figure 2.28. Explicit and implicit expression decoding accuracy of the PF conditions in the FG, significant results from one-sample t-tests represented with stars.

2.3.3.1.2 Superior temporal sulcus (STS).

One-sample t-tests show explicit expression decoding in the STS significantly above chance in the WF ($t(59) = 4.039$, $p < .001$, $d = 0.521$ (medium effect-size)), EO ($t(59) = 3.676$, $p < .001$, $d = 0.475$ (small effect-size)), ME ($t(59) = 5.598$, $p < .001$, $d = 0.723$ (medium effect-size)) and MO conditions ($t(59) = 5.792$, $p < .001$, $d = 0.748$ (medium effect size)), with implicit expression decoding significant in the MO condition ($t(59) = 2.872$, $p = .003$, $d = 0.371$ (small effect-size)), see Figure 2.29 and other t-test results in Table D18 (Appendix D). A repeated measures ANOVA showed a main effect of PF condition of decoding accuracy, $F(3.672, 216.674) = 3.411$, $p = .012$, $\eta_p^2 = .055$ (Huynh-Feldt correction), as well as a significant main effect of task, $F(1, 59) = 52.885$, $p < .001$, $\eta_p^2 = .473$, with decoding accuracy significantly higher in the explicit task (M = 37.3%) compared to the implicit task (M = 33.7%). There was also a near significant interaction between PF condition and task on decoding accuracy, $F(4, 236) = 2.344$, $p = .055$, $\eta_p^2 = .038$. As the interaction was near significance, further exploratory post-hoc Bonferroni corrected pairwise comparisons between task were carried out. Furthermore, exploratory paired sample t-tests showed a significant effect of task in all PF conditions ($p < .01$) except MM, see full results in Table D19 (Appendix D).

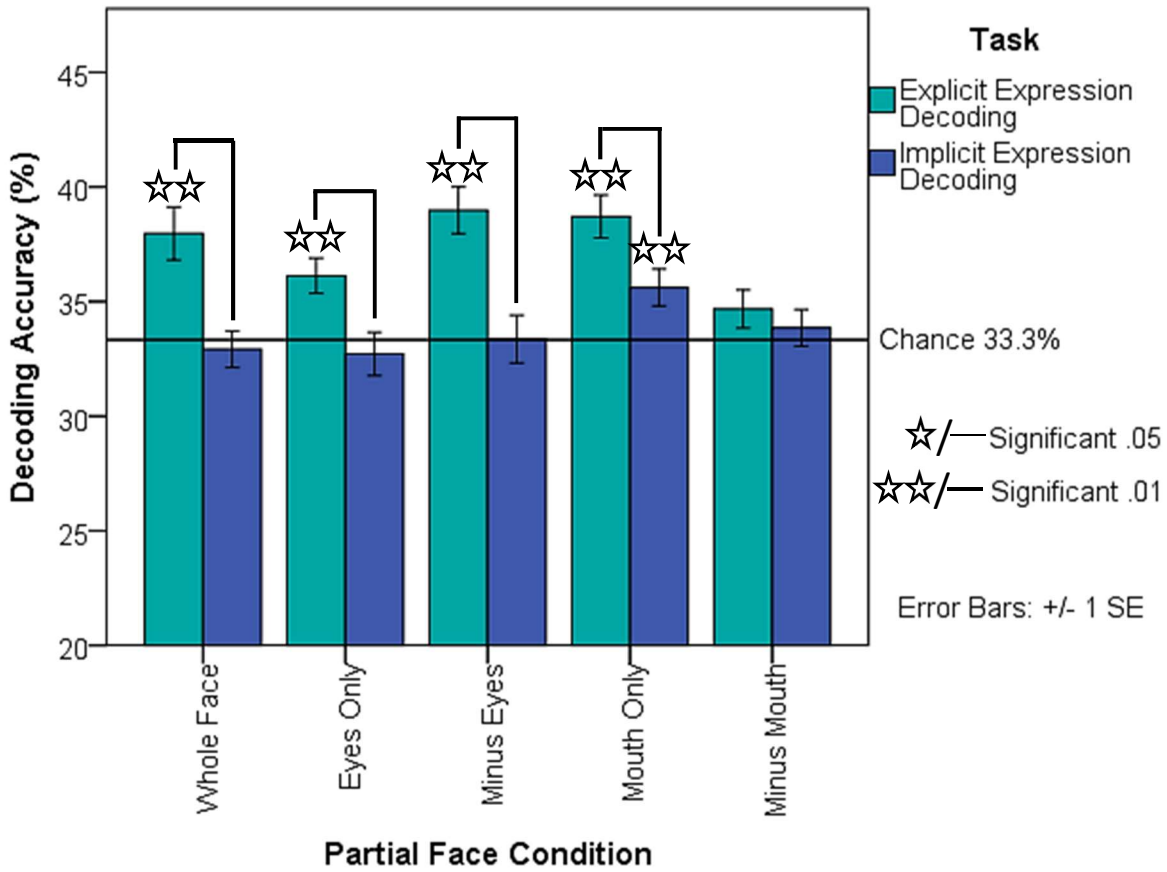

Figure 2.29. Explicit and implicit expression decoding accuracy of the PF conditions in STS, significant results from one-sample t-tests represented with stars.

2.3.3.1.3 Inferior occipital gyrus (IOG).

One-sample t-tests show explicit expression decoding in the IOG significantly above chance in the MO ($t(59) = 2.905$, $p = .003$, $d = 0.375$ (small effect-size)) and MM ($t(59) = 2.106$, $p = .020$, $d = 0.272$ (small effect-size)) conditions, with all implicit expression decoding conditions significantly above chance ($p < .01$), see Figure 2.30 and other t-test results in Table D20 (Appendix D). A repeated measures ANOVA showed a main effect of PF condition on decoding accuracy, $F(4, 236) = 7.557$, $p < .001$, $\eta_p^2 = .114$, as well as a significant main effect of task, $F(1, 59) = 33.967$, $p < .001$, $\eta_p^2 = .365$, with decoding accuracy significantly higher in the implicit task (M = 39%) compared to the explicit task (M = 34.1%). Additionally there was a significant interaction between PF condition and task on decoding accuracy, $F(3.728, 220.016) = 14.966$, $p < .001$, $\eta_p^2 = .202$ (Huynh-Feldt correction). Post-hoc pairwise comparisons, with Bonferroni correction, show significant differences between the WF and MM condition ($p = .028$), the EO and ME condition ($p = .001$) and finally the EO and MM condition ($p < .001$).

As a result of the significant interaction, one-way ANOVAs, with PF condition as a factor, were carried out for each task separately. In the explicit task, there was a significant main effect of PF condition, $F(4, 236) = 3.470$, $p = .009$, $\eta_p^2 = .056$, with post-hoc Bonferroni corrected pairwise comparisons showing decoding accuracy in the ME condition to be significantly lower than the MO condition ($p = .009$). In the implicit task, there was also a significant main effect of PF condition, $F(3.648, 215.225) = 16.721$, $p < .001$, $\eta_p^2 = .221$ (Huynh-Feldt correction), with post-hoc Bonferroni corrected pairwise comparisons showing decoding accuracy to be significantly higher in the ME condition compared to the WF ($p < .001$), EO ($p < .001$) and MO ($p < .001$) condition. As well as this, post-hoc Bonferroni corrected pairwise comparisons show decoding accuracy to be significantly higher in the MM condition compared to the EO ($p < .001$) and MO condition ($p = .003$). Paired sample t-tests were also carried out to explore the effect of task for each PF condition, apart from in the MO condition, decoding accuracy was significantly different in all other PF conditions ($p < .05$; t-test results can be found in Table D21, Appendix D).

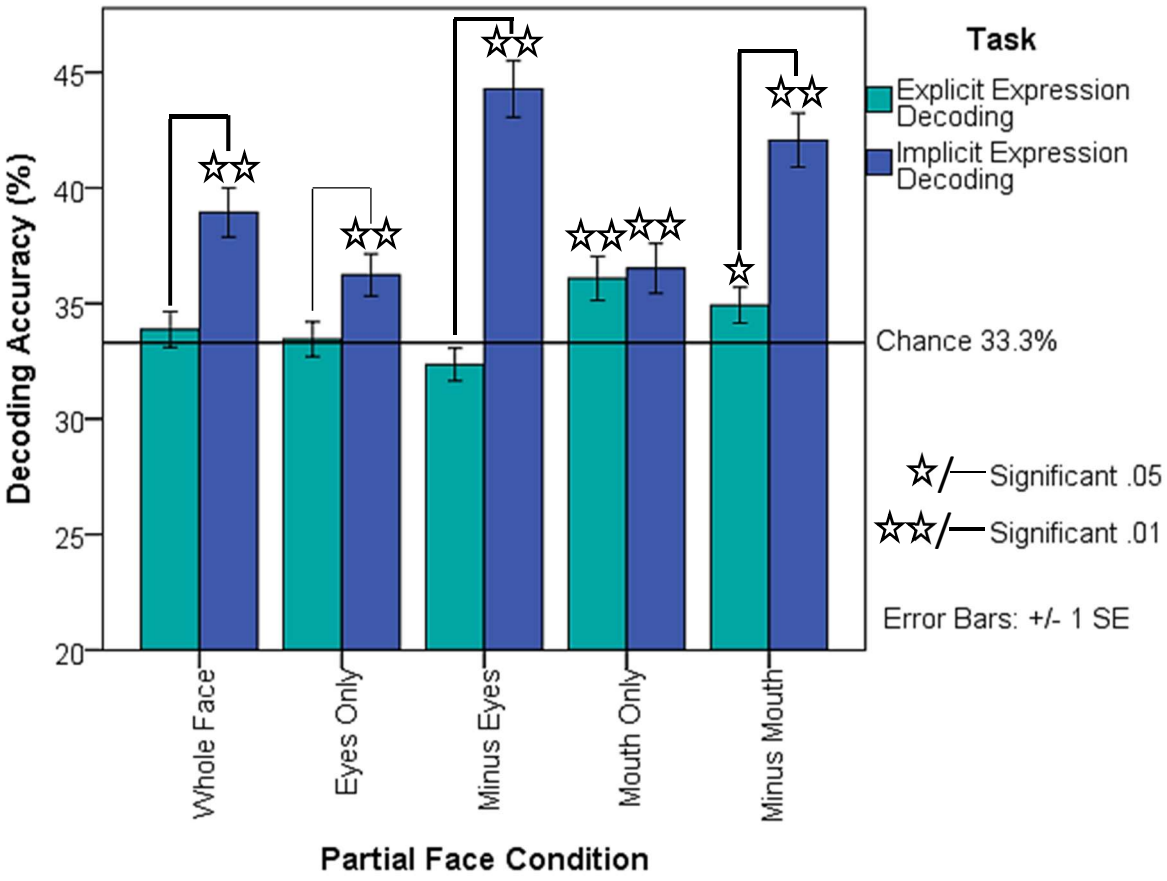

Figure 2.30. Explicit and implicit expression decoding accuracy of the PF conditions in the IOG, significant results from one-sample t-tests represented with stars.

2.3.3.1.4 Amygdala (AMY).

One-sample t-tests show implicit expression decoding in the amygdala only significantly above chance in the EO condition ($t(59) = 3.808$, $p < .001$, $d = 0.492$ (small effect-size)). In explicit expression decoding, the ME condition is significantly above chance ($t(59) = 2.356$, $p = .011$, $d = 0.304$ (small effect-size)), other t-test results can be found in Table D22 (Appendix D). A repeated measures ANOVA showed a non-significant main effect of task, $F(1, 59) = .033$, $p = .856$, $\eta_p^2 = .001$, but a strong significant main effect of PF condition on decoding accuracy, $F(4, 236) = 3.821$, $p = .005$, $\eta_p^2 = .061$, as well as a significant interaction $F(3.799, 224.129) = 4.900$, $p = .001$, $\eta_p^2 = .077$ (Huynh-Feldt correction).

As a result of the significant interaction, one-way ANOVAs, with PF condition as a factor, were carried out for each task. In the explicit task, there was no significant main effect of PF condition, $F(3.415, 201.492) = 2.040$, $p = .101$, $\eta_p^2 = .033$ (Huynh-Feldt correction). Whereas in the implicit task, there was a significant main effect of PF condition, $F(4, 236) = 6.921$, $p < .001$, $\eta_p^2 = .105$. Further, post-hoc pairwise comparisons, with Bonferroni correction, show a significant effect between WF and EO ($p = .013$), EO and ME ($p = .009$), and EO and MM conditions ($p < .001$). Paired sample t-tests were carried out to explore the effect of task for each PF condition, with significance in the EO ($t(59) = -2.886$, $p = .005$, $d = -0.373$) and ME condition ($t(59) = 2.383$, $p = .020$, $d = 0.308$), see Figure 2.31 and other t-test results in Table D23 (Appendix D). This potentially reveals a cross-over effect, with the presence of the eyes important for implicit tasks and their absence important for explicit tasks.

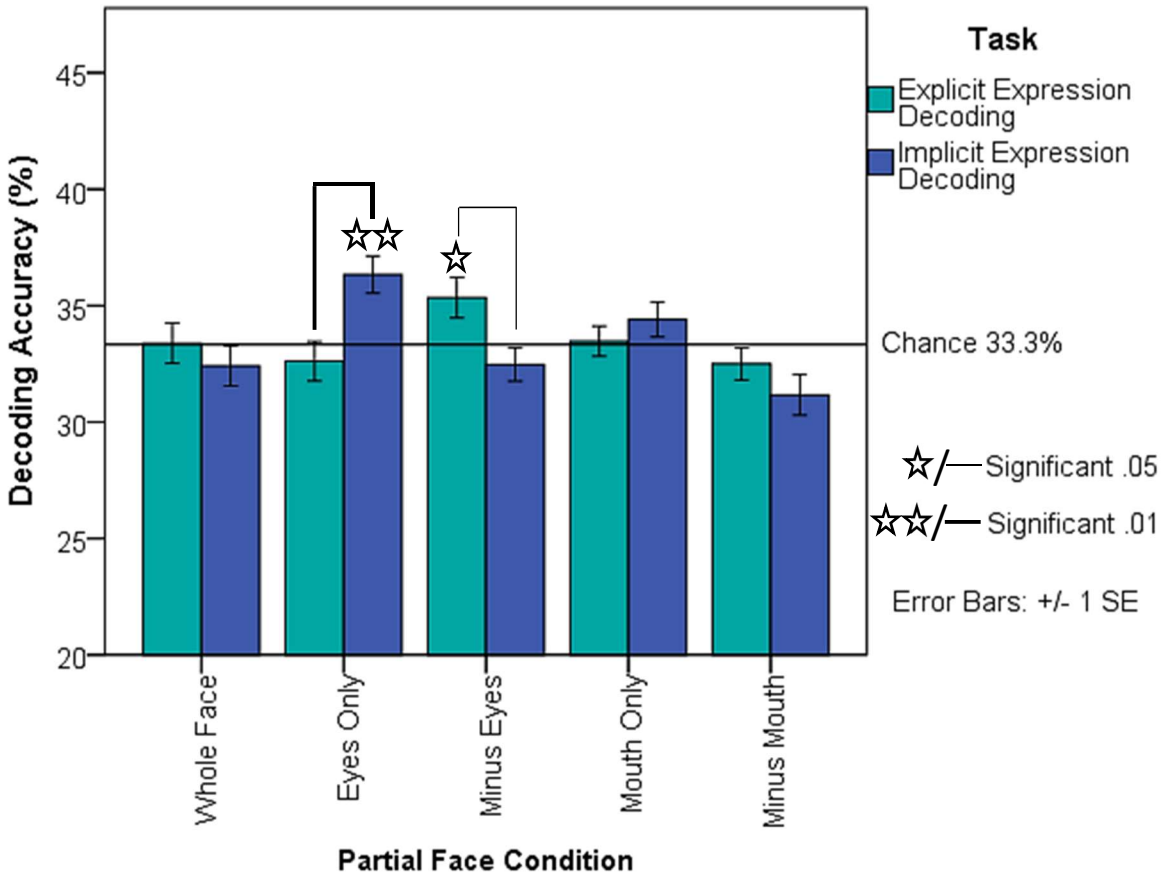

Figure 2.31. Explicit and implicit expression decoding accuracy of the PF conditions in the amygdala. Results from one-sample t-tests included with stars representing significance.

2.3.3.1.5 Insula (INS).

One-sample t-tests show explicit expression decoding in the insula significantly above chance in the ME ($t(59) = 3.163$, $p = .001$, $d = 0.408$ (small effect-size)) and MO condition ($t(59) = 3.706$, $p < .001$, $d = 0.478$ (small effect-size)), see Figure 2.32 and other t-test results in Table D24 (Appendix D). There was no implicit expression decoding significant above chance ($p > .05$). A repeated measures ANOVA showed a non-significant main effect of task, $F(1, 59) = 3.481$, $p = .067$, $\eta_p^2 = .056$, and PF condition on decoding accuracy, $F(3.653, 215.511) = 1.935$, $p = .112$, $\eta_p^2 = .032$ (Huynh-Feldt correction). However there was an interaction between task and PF, $F(4, 236) = 5.517$, $p < .001$, $\eta_p^2 = .086$. As a result of the significant interaction, a one-way ANOVA, with PF condition as a factor, was carried out for each task separately. In the explicit task, there is a significant main effect of PF condition, $F(3.758, 221.727) = 6.624$, $p < .001$, $\eta_p^2 = .101$ (Huynh-Feldt correction), with significant post-hoc Bonferroni corrected pairwise comparisons between EO and ME ($p = .047$), EO and MO ($p = .009$), ME and MM ($p = .002$) and

MO and MM (p = .001). There is a non-significant main effect of PF in the implicit task, $F(3.576, 210.961) = .354$, $p = .820$, $\eta_p^2 = .006$ (Huynh-Feldt correction). Paired sample t-tests were carried out to explore the effect of task for each PF condition, there was a significant difference in task for the ME ($t(59) = 2.583$, $p = .012$, $d = 0.333$), MO ($t(59) = 3.744$, $p < .001$, $d = 0.483$) and the MM ($t(59) = -2.085$, $p = .041$, $d = -0.269$) conditions, other t-test results can be found in Table D25 (Appendix D).

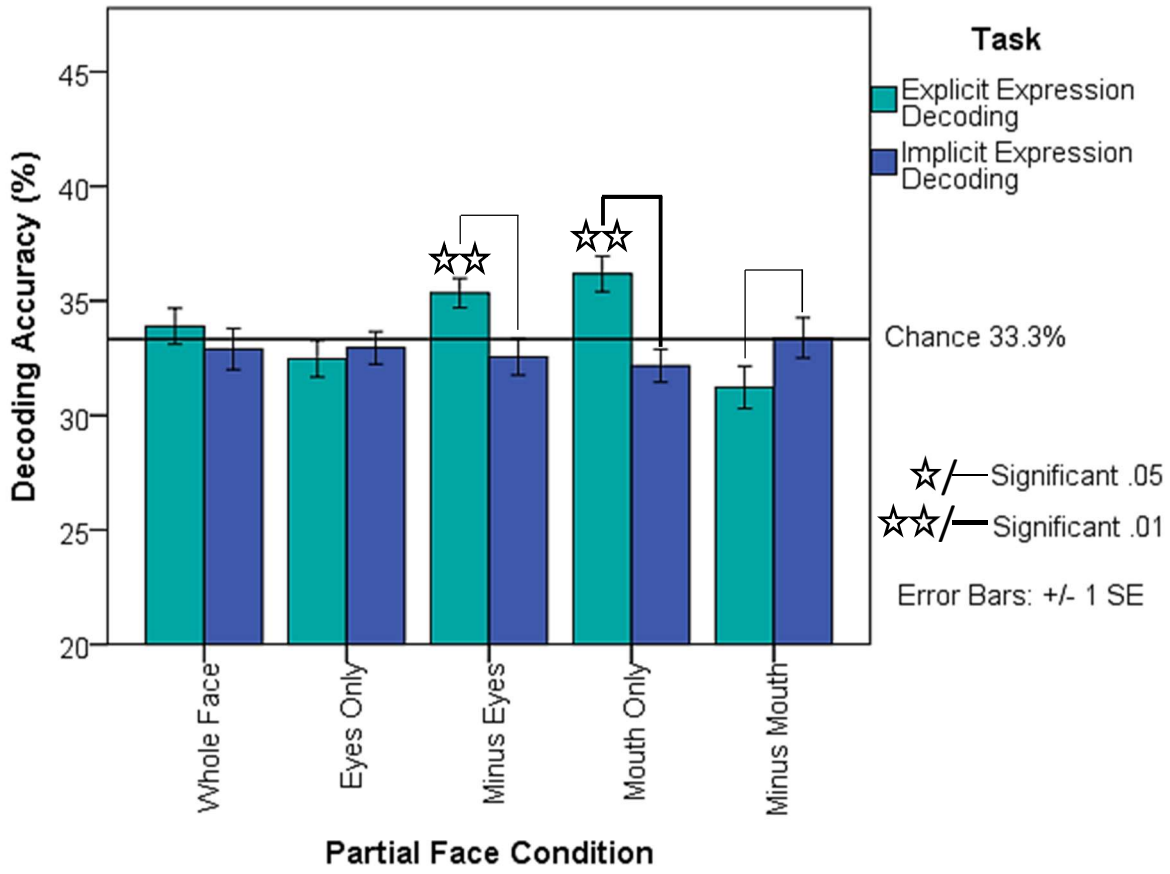

Figure 2.32. Explicit and implicit expression decoding accuracy of the PF conditions in the insula. Results from one-sample t-tests included with stars representing significance.

2.3.3.2 Cross classification (XC).

A 2 (task) x 5 (ROI) x 5 (voxel size) x 3 (condition pairs) repeated measures ANOVA was carried out. This showed no main effect of task, $F(1, 11) = .043$, $p = .839$, or ROI, $F(4, 44) = 2.119$, $p = .094$, or condition pair, $F(2, 22) = .045$, $p = .956$, but a significant main effect of voxel size, $F(4, 44) = 3.079$, $p = .025$, $\eta_p^2 = .219$. In respect to voxel size, there appears to be a trend between higher amounts of voxels and greater decoding, however, there was no significance in follow-up pairwise

comparisons and no significant interactions with voxel size; further analyses thus average across this variable akin to Wegrzyn et al. (2015).

Similar to the above, the five ROI's have been studied individually to investigate the effects of task and PF condition on decoding accuracy. Expression decoding was investigated, looking into the effects of implicit and explicit expression decoding. Paired sample t-tests for each ROI show no significant differences between the decoding accuracies of task across condition pairs.

2.3.3.2.1 Fusiform gyrus (FG).

One-sample t-tests show explicit expression decoding significantly above chance decoding accuracy in the EO and ME condition pair ($t(59) = 2.435$, $p = .009$, $d = 0.314$ (small effect-size)), and implicit expression decoding significantly above chance in the EO and ME condition pair ($t(59) = 2.731$, $p = .004$, $d = 0.353$ (small effect-size)), as well as the MO and MM condition pair ($t(59) = 2.456$, $p = .009$, $d = 0.317$ (small effect-size)), see Figure 2.33 and other t-test results in Table D26 (Appendix D). Further a repeated measures ANOVA was conducted to investigate task and condition pair on decoding accuracy in the FG; this showed a non-significant main effect of task, $F(1, 59) = .121$, $p = .729$, $\eta_p^2 = .002$, and condition pair on decoding accuracy, $F(2, 118) = 2.024$, $p = .137$, $\eta_p^2 = .033$, as well as a non-significant interaction, $F(2, 118) = 1.076$, $p = .344$, $\eta_p^2 = .018$.

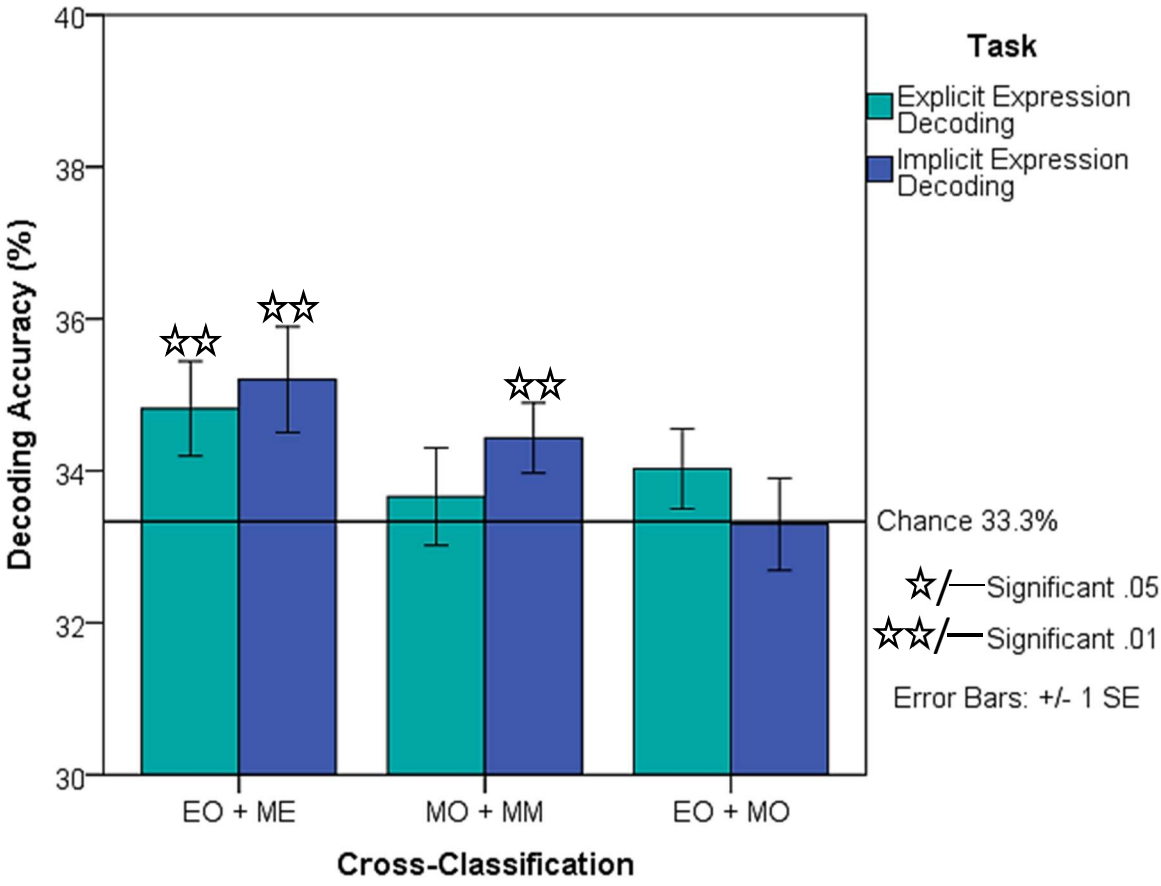

Figure 2.33. Explicit and implicit expression decoding accuracy of the condition pairs of PF conditions in the FG, significant results from one-sample t-tests represented with stars.

2.3.3.2.2 Superior temporal sulcus (STS).

One-sample t-tests show explicit expression decoding significantly above chance in the EO vs ME pair ($t(59) = 3.050$, $p = .002$, $d = 0.394$ (small effect-size)) and the EO vs MO pair ($t(59) = 4.837$, $p < .001$, $d = 0.625$ (medium effect-size)), these were also the condition pairs that were significantly above chance in the implicit expression decoding task ($t(59) = 2.234$, $p = .015$, $d = 0.288$ (small effect-size), $t(59) = 2.210$, $p = .016$, $d = 0.285$ (small effect-size) respectively), see Figure 2.34 and other t-test results in Table D27 (Appendix D). A repeated measures ANOVA was conducted to investigate task and condition pair on decoding accuracy in the STS. This showed a significant main effect of task, $F(1, 59) = 6.546$, $p = .013$, $\eta_p^2 = .100$, with decoding accuracy significantly higher in the explicit (M = 35.7%) compared to the implicit task (M = 34.4%). Furthermore, this showed a significant main effect of condition pair on decoding accuracy, $F(1.834, 108.212) = 5.591$, $p = .006$, $\eta_p^2 = .087$ (Huynh-Feldt correction), where post-hoc pairwise comparisons,

with Bonferroni correction, showed a significant difference between the lower decoding accuracies in the MO and MM condition pair compared with the higher decoding accuracies in the EO and MO condition pair (p = .016). However there was a non-significant interaction between task and condition pair on decoding accuracy, $F(2, 118) = .947$, p = .391, $\eta_p^2 = .016$.

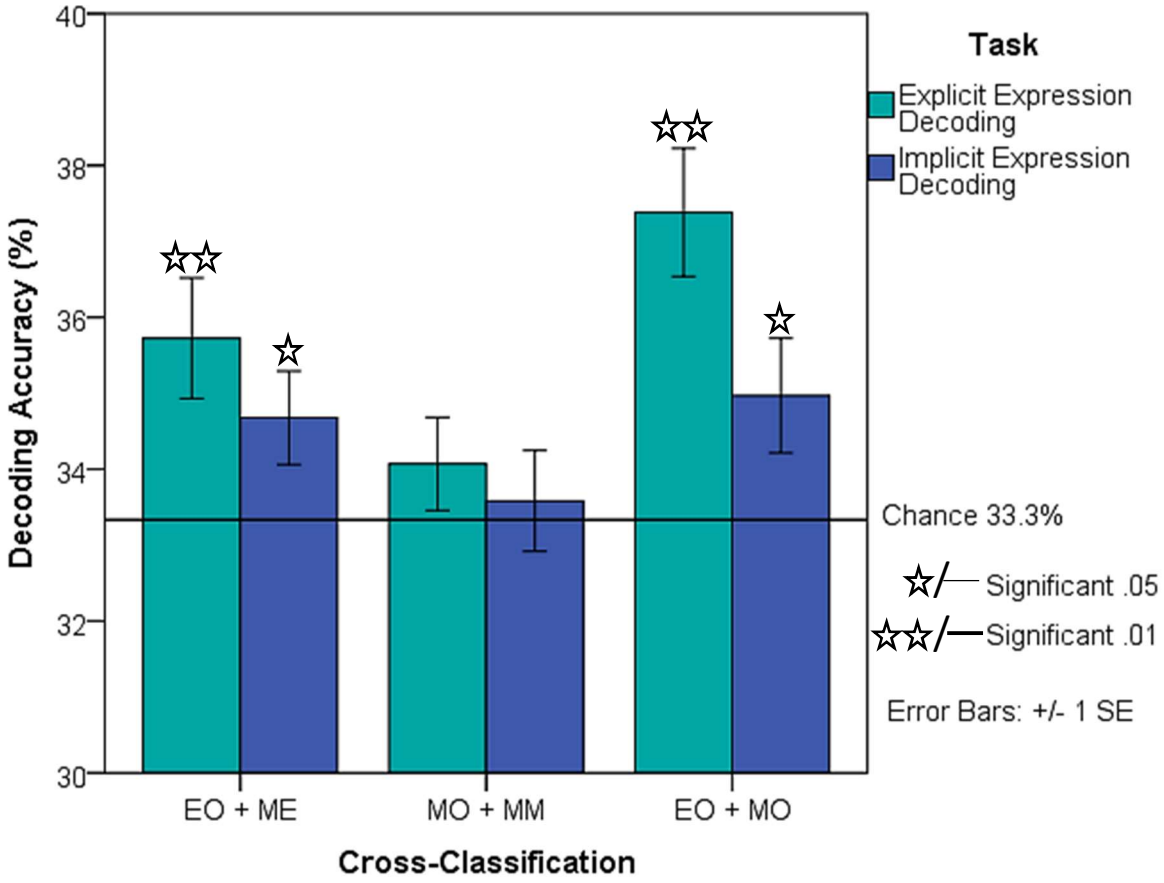

Figure 2.34. Explicit and implicit expression decoding accuracy of the condition pairs of PF conditions in the STS, significant results from one-sample t-tests represented with stars.

2.3.3.2.3 Inferior occipital gyrus (IOG).

One-sample t-tests show explicit expression decoding significant in the EO to MO condition ($t(59) = 2.432$, p = .009, d = 0.314 (small effect-size)), whereas in the implicit expression decoding conditions the EO to ME and MO to MM conditions were significant ($t(59) = 5.789$, $p < .001$, d = 0.747 (medium effect-size) and $t(59)$ = 5.650, $p < .001$, d = 0.729 (medium effect-size) respectively), see Figure 2.35 and other t-tests in Table D28 (Appendix D). A repeated measures ANOVA was conducted to investigate task and condition pair on decoding accuracy in the IOG. This showed a significant main effect of task, $F(1, 59) = 24.069$, $p < .001$, $\eta_p^2 = .290$

and cross-classification on decoding accuracy, $F(2, 118) = 3.511$, $p < .033$, $\eta_p^2 = .056$, as well as a significant interaction, $F(2, 118) = 18.087$, $p < .001$, $\eta_p^2 = .235$.

As a result of the significant interaction, separate one-way ANOVAs were carried out for each task. In the explicit task, a repeated measures ANOVA showed a significant main effect of condition pair, $F(2, 118) = 5.883$, $p = .004$, $\eta_p^2 = .091$, with post-hoc Bonferroni corrected pairwise comparisons significant between the EO vs ME and EO vs MO pair ($p = .002$). In the implicit task, there was a significant main effect of condition pair, $F(2, 118) = 17.100$, $p < .001$, $\eta_p^2 = .225$, with post-hoc Bonferroni corrected pairwise comparisons significant between the EO vs ME and EO vs MO pair, as well as the MO vs MM and EO vs MO pair (both $p < .001$). Further, a post-hoc Bonferroni corrected pairwise comparison between task shows decoding accuracy to be significantly higher ($p < .001$) in the implicit task (M = 36%) compared to the explicit task (M = 33.4%). Paired sample t-tests were carried out to explore the effect of task for each condition pair, these showed a significant main effect of task in the EO to ME pair ($t(59) = -6.598$, $p < .001$, $d = -0.852$) as well as the MO and MM pair ($t(59) = -3.666$, $p = .001$, $d = 0.473$), see Figure 2.35 and other t-tests in Table D29 (Appendix D).

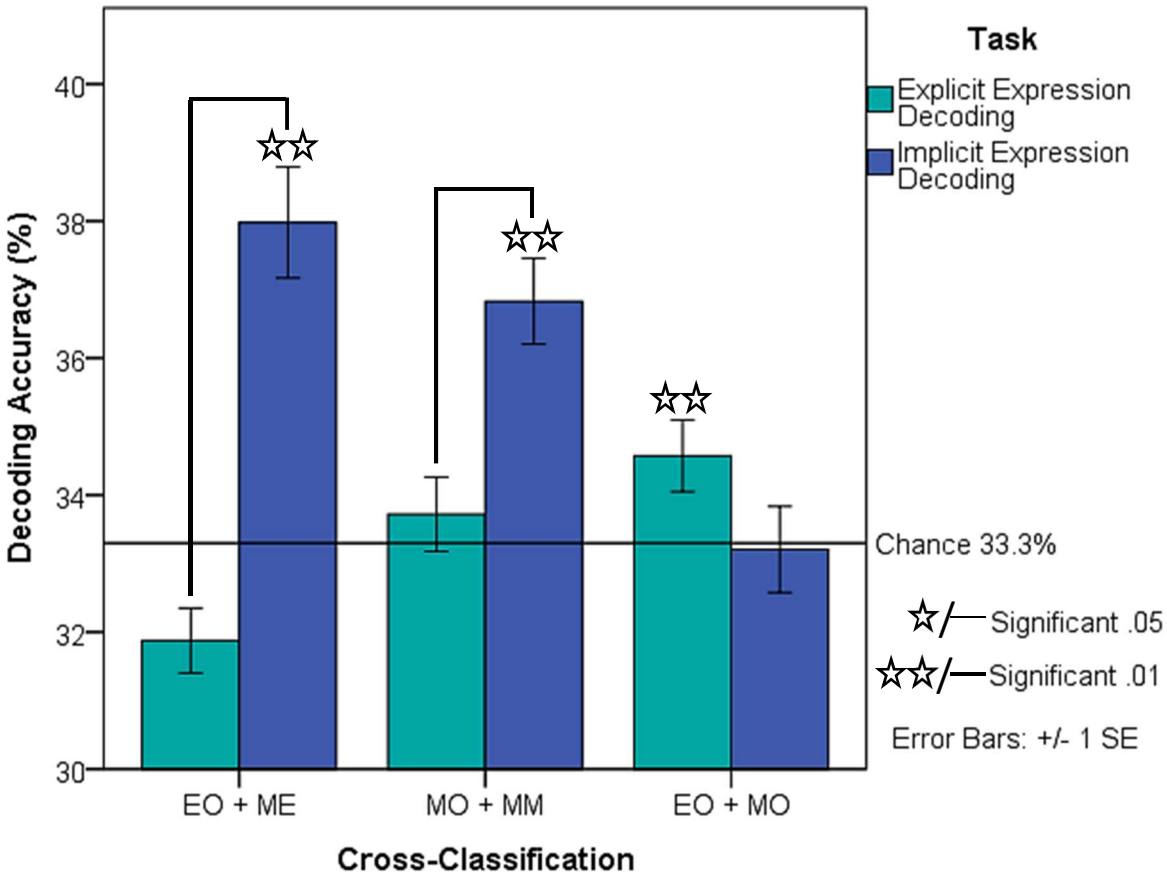

Figure 2.35. Explicit and implicit expression decoding accuracy of the condition pairs of PF conditions in the IOG. One-sample t-test results included with stars representing significance above chance.

2.3.3.2.4 Amygdala (AMY).

One-sample t-tests show explicit expression decoding significant in the EO to MO condition ($t(59) = 1.842$, $p = .035$, $d = 0.238$ (small effect-size)) but no significant PF conditions in implicit expression decoding ($p > .05$), see Figure 2.36 and all t-test results in Table D30 (Appendix D). A repeated measures ANOVA was conducted to investigate task and condition pair on decoding accuracy in the amygdala. This showed a non-significant main effect of task, $F(1, 59) = 1.701$, $p = .197$, $\eta_p^2 = .028$, and cross-classification on decoding accuracy, $F(2, 118) = .008$, $p = .992$, $\eta_p^2 < .001$, as well as a non-significant interaction, $F(1.826, 107.722) = 2.910$, $p = .064$, $\eta_p^2 = .047$ (Huynh-Feldt correction).

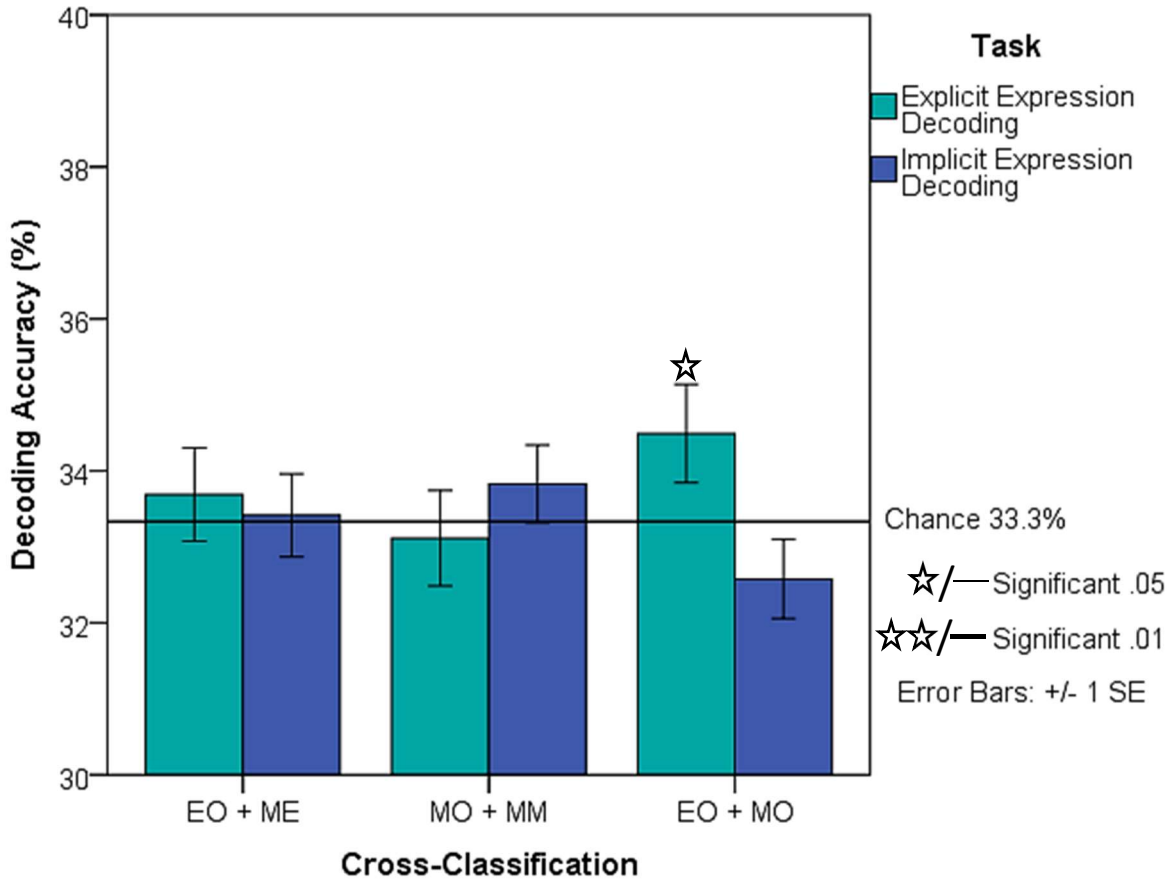

Figure 2.36. Explicit and implicit expression decoding accuracy of the cross classified pairs of PF conditions in the amygdala. One-sample t-test results included with stars representing significance above chance.

2.3.3.2.5 Insula (INS).

One-sample t-tests also show explicit expression decoding significant in the EO to MO condition ($t(59) = 1.952$, $p = .028$, $d = 0.252$ (small effect-size)) but no significant PF conditions in implicit expression decoding ($p > .05$), see Figure 2.37 and all t-test results in Table D31 (Appendix D). A repeated measures ANOVA was conducted to investigate task and condition pair in the insula. This showed a non-significant main effect of task, $F(1, 59) = 2.261$, $p = .138$, $\eta_p^2 = .037$ and cross-classification on decoding accuracy, $F(1.828, 107.873) = 1.850$, $p = .166$, $\eta_p^2 = .030$ (Huynh-Feldt correction), as well as a non-significant interaction, $F(2, 118) = .246$, $p = .782$, $\eta_p^2 = .004$.

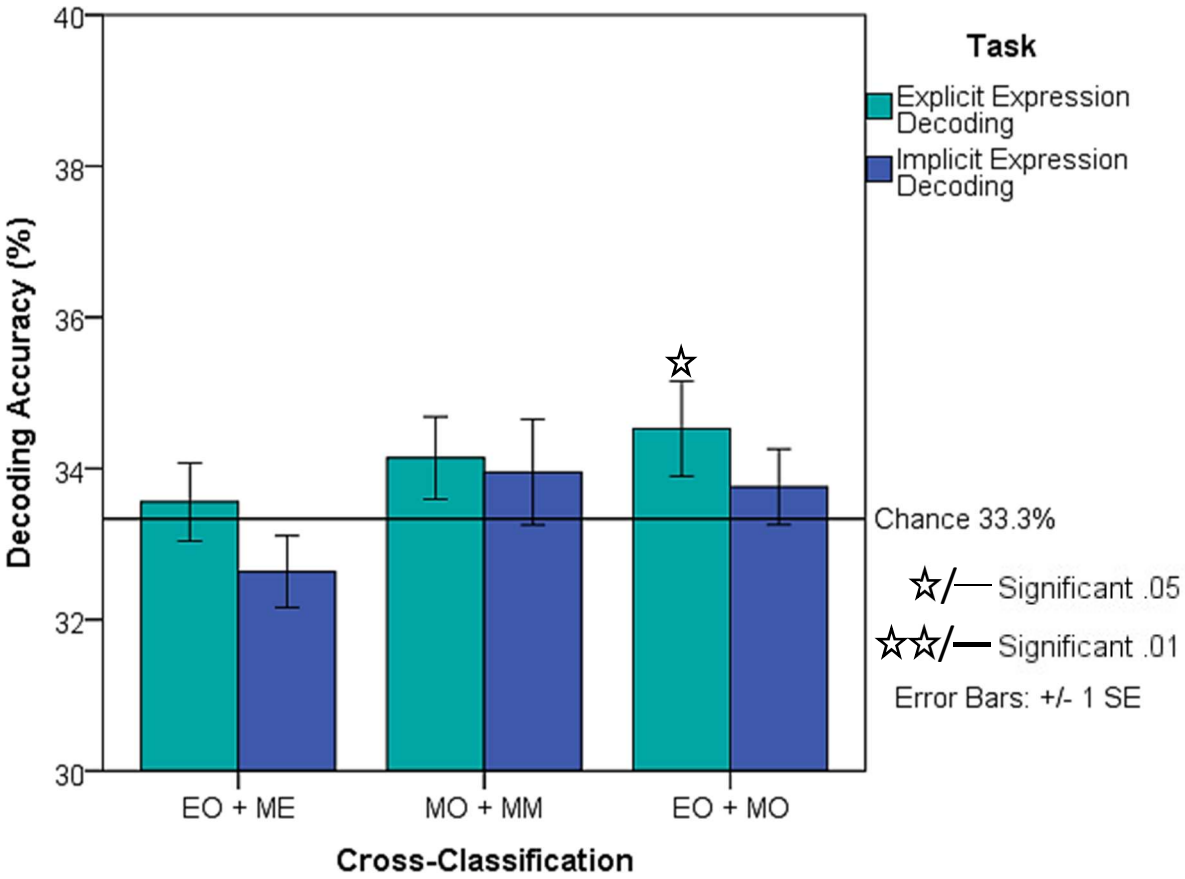

Figure 2.37. Explicit and implicit expression decoding accuracy of the cross classified pairs of PF conditions in the insula. One-sample t-test results included with stars representing significance above chance.

2.3.4 Univariate analysis in V1.

As a result of finding high-level effects within the expression decoding analyses of V1, a subsequent univariate analysis was carried out, to investigate whether similar effects are shown at a univariate level for V1. Thus, a deconvolution design was selected due to the use of a rapid-event related paradigm. A 2 (task) x 3 (emotion) x 5 (PF) repeated measures ANOVA was carried out. This showed no significant main effect of task, $F(1, 11) = 2.405$, $p = .149$, $\eta_p^2 = .179$, but a significant main effect of emotion, $F(2, 22) = 14.674$, $p < .001$, $\eta_p^2 = .572$ and PF condition, $F(4, 44) = 5.848$, $p = .001$, $\eta_p^2 = .347$. There was also a significant interaction between task and emotion, $F(2, 22) = 6.160$, $p = .008$, $\eta_p^2 = .359$. This interaction further suggests that a high-level effect is occurring in V1.

As a result of the significant interaction, a separate ANOVA was carried out for each task. In the explicit task, a repeated measures ANOVA showed a significant main effect of emotion, $F(2, 22) = 11.315$, $p < .001$, $\eta_p^2 = .507$ and PF condition,

$F(4, 44) = 4.456$, $p = .004$, $\eta_p^2 = .288$, but a non-significant interaction, $F(8, 88) = .885$, $p = .533$, $\eta_p^2 = .074$. Post-hoc pairwise comparisons, with Bonferroni correction, show significance between disgust and happy ($p = .023$) as well as fear and happy ($p = .008$), whereas there were no significant post-hoc pairwise comparisons between the PF conditions. In the implicit task there was also a significant main effect of emotion, $F(2, 22) = 8.107$, $p = .002$, $\eta_p^2 = .424$, and PF condition, $F(4, 44) = 2.647$, $p = .046$, $\eta_p^2 = .194$, as well as a non-significant interaction, $F(8, 88) = .899$, $p = .521$, $\eta_p^2 = .076$. Post-hoc pairwise comparisons, with Bonferroni correction, show significance between disgust and fear ($p = .008$), but again there were no significant post-hoc pairwise comparisons between the PF conditions, see Figure 2.38.

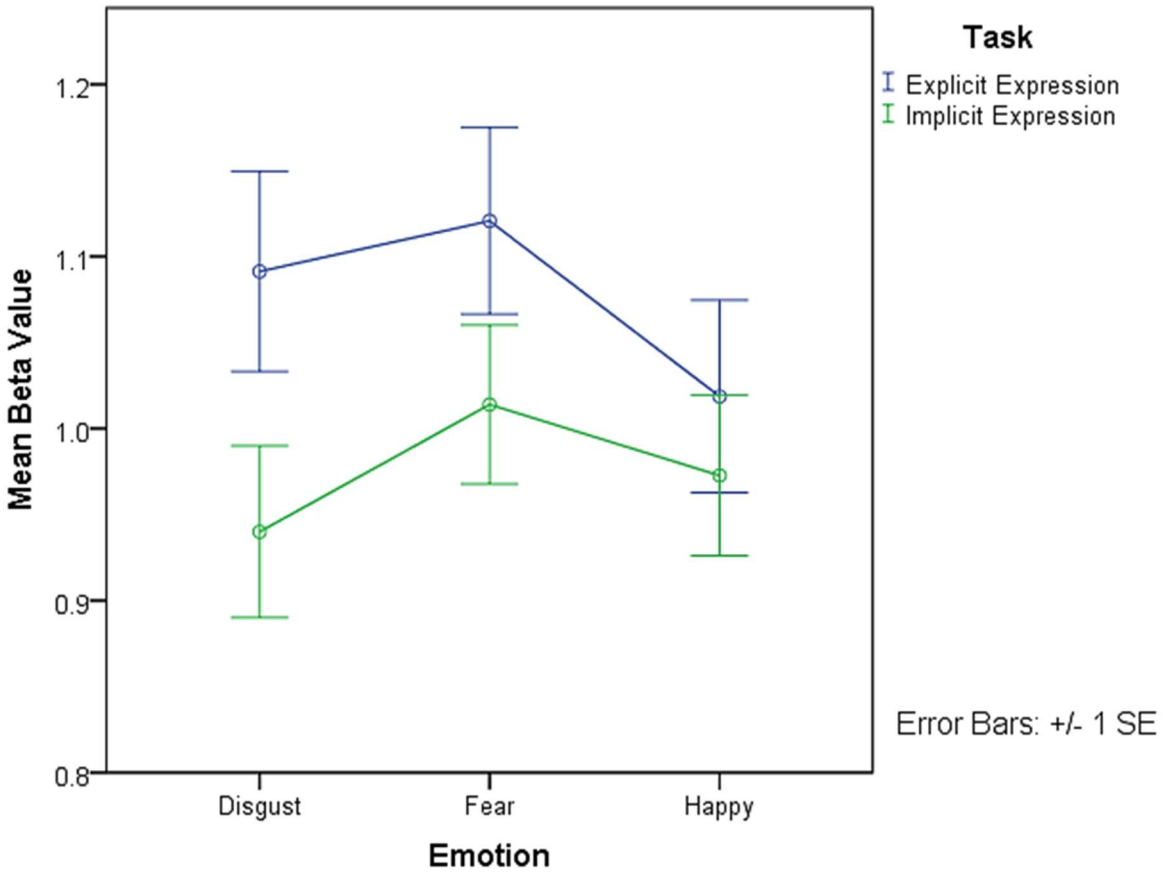

Figure 2.38. Mean beta weights of the task differences between the emotions.

Paired sample t-tests were carried out to explore the effect of task for each PF condition, the MM condition showed significance ($t(11) = 2.972$, $p = .013$), see Figure 2.39 and other t-test results in Table D32 (Appendix D). Thus there is a task effect when the mouth is absent.

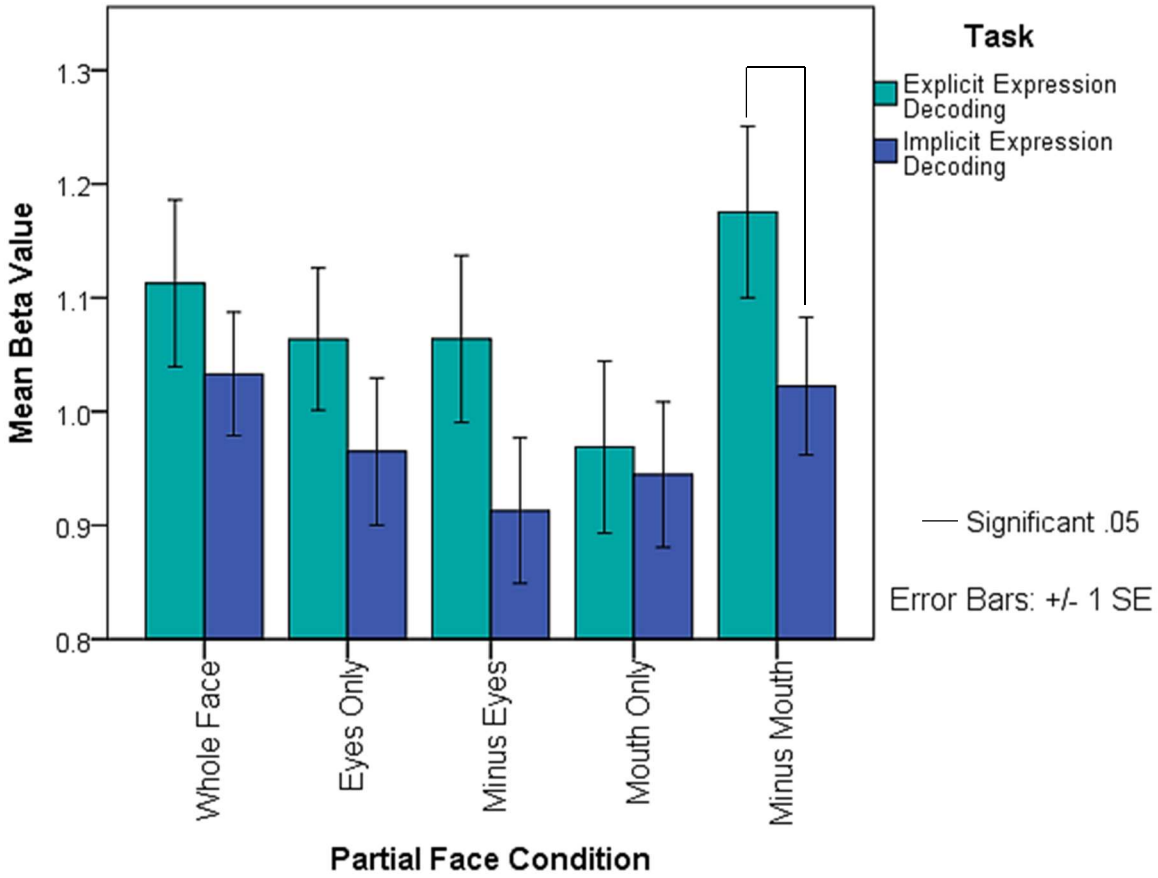

Figure 2.39. Univariate analysis showing the mean beta values for each PF condition as a function of task, explicit versus implicit expression perception. A paired samples t-test shows the tasks to be significantly different in the MM condition.

2.4 Discussion

This study principally set out to explore the decoding of expression across conditions with non-overlapping visual inputs in V1 and EVC, and investigate how task context may affect this. Therefore the cross-classification PF results will be outlined first, with reference to other brain analyses, where applicable, to help understand the effects. These results will be followed by the observed task effects in this study.

2.4.1 High-level information about facial expressions in V1 and EVC.

2.4.1.1 Cross-decoding shows high-level context effect.

The cross-decoding results are important to ascertain the role of contextual mechanisms (feedback and lateral connections) in early visual areas. As aforementioned, these results investigate whether there are similar brain representations across non-overlapping PF conditions. As there is no common visual information between the conditions, this provides a robust measure that purely taps into feedback and lateral connections in the brain (Greening et al., 2018). Therefore,

these results are important to ascertain how high-level information shapes early visual processing, and more specifically how feedback (and possible lateral connections) provide information about missing facial information potentially useful for expression recognition. XC analysis in V1 and EVC revealed implicit expression decoding across PF condition in two condition pairs, the EO to the ME, as well as the MO to the MM. The final condition pair, the EO to the MO, is decoded significantly in V1 and EVC for explicit expression decoding. The MO to the MM pair is also decoded significantly for explicit expression decoding in EVC. As similar brain representations were observed in V1 and EVC when completely independent parts of a face are presented, this supports the first hypothesis (H1) and suggests the involvement of contextual mechanisms beyond low-level processing (Petro et al., 2013). The presence of high-level information, accounting for how occluded and ambiguous stimuli are processed, is in line with predictive coding and recurrent feedback models of object completion (F. W. Smith & Muckli, 2010; Tang et al., 2014; Tang et al., 2018; Wyatte et al., 2014). Results showing EVC to contain information about missing facial features, is consistent with the idea that faces are such biologically salient signals (Pessoa & Adolphs, 2010); additionally the results extend previous research showing EVC to contain information about occluded natural scenes (F. W. Smith & Muckli, 2010).

2.4.1.2 Task effects.

Results show both whole and PF stimuli can be decoded in several regions in the brain, including early visual and face processing areas, during an explicit and implicit emotion recognition task. Results in V1 and EVC are similar, with extremely high classifier performance (decoding accuracy) discriminating between the emotions, across PF conditions in implicit expression decoding. This supports the last hypothesis (H3) that emotion processing in V1 will be affected by its task context, and more specifically will be stronger in the implicit compared to the explicit task. Past results have also shown these implicit task effects (Petro et al., 2013). Petro et al. (2013) additionally found implicit V1 task effects in the opposite direction (when participants were asked to judge expression, gender information could be decoded); this result can also be seen in the gender decoding results of this study, see Appendix G.

Classifier performance was higher than chance, and the WF condition, in the ME and MM implicit conditions where there is less information. In these conditions,

some important featural information for emotion recognition is missing, as such, in a purely feedforward model based on visual input, these conditions would likely be associated with lower brain signal. However, there is an implication that information is being fed back from higher brain regions to account for the missing visual input and predict the correct emotion. Kok, Failing, and de Lange (2014) showed that top-down or prior expectations of a visual stimulus can activate a reliable template of the expected stimuli in V1 to process omitted visual stimuli efficiently. It seems counterintuitive that the WF condition did not produce the highest decoding accuracy; however, Alink, Schwiedrzik, Kohler, Singer, and Muckli (2010) explain that predictive visual stimuli which resemble the natural world evoke smaller V1 responses, whilst unpredictable sensory inputs (missing facial features) require more activation of V1 and higher visual areas. This is further supported in the WBA for WF versus ME and MM stimuli, whereby these PF conditions corresponded with greater brain activation (see Appendix B for WBA). Additionally implicit task performance was higher in the XC pairs of EO to ME and MO to MM. The univariate analysis of V1 further shows the MM condition associated with greater brain activation, but it is important to note that there are no significant differences between this and the other PF conditions in this V1 analysis.

2.4.1.2.1 Task changes in basic decoding.

In the basic decoding results, there are changes between the tasks across the PF conditions; notably when decoding from 100 voxels in V1, significance is present across all conditions in the implicit task but not the explicit task. Decoding accuracies in explicit tasks are subjectively greater for conditions with mouth information present, whereby in implicit tasks high decoding accuracies are present for conditions where either mouth and/or eye information is present. This pattern change implies that differences do not simply arise as a result of accuracy. It may result from needing mouth information more in emotion recognition (explicit task) and both eye and mouth information in a gender task (implicit task); furthermore previous literature suggests that the eyes are used more to make a judgement on gender (M. L. Smith et al., 2004).

2.4.1.2.2 Task changes in XC.

In XC, the results for the EO to MO pair changes, with implicit task decoding performance being lower than explicit task performance in V1 and EVC. This was investigated further by running permutation tests and examining confusion matrices.

Permutation tests showed that classification performance was distributed around chance; hence, there was no bias in the classifier. The XC confusion matrices show happy and disgust to be systematically confused; whereby when the classifier was presented happy expressions, these were confused with disgust and when the classifier was shown disgust, the classifier thought the expression was happiness. However, this confusion does not explain the task difference between explicit and implicit task performance.

There are several possible reasons why implicit task performance could be lower for the EO to MO pair. Firstly, the EO and MO conditions contain the visual information central for expression recognition (F. W. Smith et al., 2008; M. L. Smith et al., 2005), unlike the other condition pairs that contain a stimulus with an occluded necessary feature. Thus, in the explicit case, a greater decoding accuracy may have been a result of participants attending to the central features given (eyes and mouth) to complete the task. This would potentially explain why there would be less confusion in classifier decoding. In the implicit task, decoding accuracies may have been lower as only one of the conditions (the EO) contains visual information central for gender recognition (M. L. Smith et al., 2004) where the eyes needed to be focused on. Ironically, a lack of attention to the mouth only stimuli may have resulted in confusions between expressions for recognition.

Secondly, asking the classifier to discriminate expressions from the EO to the MO partial face condition is the hardest test in the data, as there is a large space between the segments of feature information to fill. Furthermore, the missing information from the nose and centre of the face is important to visual scan paths of emotion recognition; as scanning the centre of the face allows the viewing of salient facial features (eyes, nose, mouth) (Horley, Williams, Gonsalvez, & Gordon, 2003; M. L. Smith & Merlusca, 2014). The absence of this feature information will predominantly affect disgust recognition. However, for this condition pair, where there is a 1.4° angle separation between the eye and mouth information, there was significance in the explicit task for V1 and EVC, giving credence to the influence of higher cortical feedback effects. Lateral interactions may be the main driver for filling in missing feature information in the previous two classifications, as in these cases there is no 1.4˚ separation in cells. As mentioned previously the maximum receptive field size in V1 is 1˚, up to eccentricities of 12˚, (A. T. Smith et al., 2001), thus the 1.4° separation prevents V1 cells from overlapping.

2.4.2 Decoding in face and emotion regions.

2.4.2.1 Comparison between the decoding results and previous research.

Results from the additional face processing ROI's vary, however, similar patterns of decoding were observed in the FG and IOG to that of V1 and EVC; finding high classifier performance across implicit conditions (apart from in the EO condition for FG), with highest decoding in ME and MM. The ability to decode emotions in the FG is supported by Harry et al. (2013), Li et al. (2018), Wegrzyn et al. (2015) and Liang et al. (2017), whilst decoding within the IOG was found previously in Liang et al. (2017) and Wegrzyn et al. (2015). However, whilst this study found high decoding in the ME condition, Liang et al. (2017) found no decoding for obscured eye stimuli (although behaviourally subjects could judge the correspondent expression on the face). It is worth noting that the results from Liang et al. (2017) are garnered from an explicit emotion recognition task, and the decoding results for the ME condition, in this study, are prevalent in the implicit emotion recognition task. Thus, task differences may be causing these differential effects in response to obscured eye stimuli, with implicit effects seen when attention is not explicitly directed to emotion in the eyes or face for recognition. The XC results were also similar to that of V1 and EVC, with significance above chance for implicit expression decoding in the EO to ME and the MO to MM condition pair; as well as significance in the IOG for the EO to MO condition pair in explicit expression decoding.

Furthermore high decoding was observed in the STS, but this showed opposite effects, with greater significance in the explicit task across PF conditions (excluding MM). The ability to decode emotions in STS is supported by Said et al. (2010), Wegrzyn et al. (2015), and Liang et al. (2017), with the pSTS found to decode between neutral and emotional as well as positive versus negative emotions in Zhang et al. (2016). In the XC analysis explicit decoding was also highest, but interestingly the implicit and explicit EO to MO condition pair was significant. Finding above chance significance is optimum in this pair and had not been reached in both tasks for other ROIs; this pair resembles pure feedback processes at work as the visual input is separated sufficiently to minimise lateral interaction effects. Thus, this suggests the presence of high-level representations in the STS; former XC research has also shown this with STS representations of emotion across different modalities such as facial expressions, vocal intonations and bodily movements

(Peelen et al., 2010). These supramodal emotion representations can generalise across the lighting and the positioning of facial expression stimuli (Skerry & Saxe, 2014). Similar high-level representations are also shown in a study where representations of identity generalise across face halves in the anterior temporal lobe (Anzellotti & Caramazza, 2016). This finding supports the current results of this study, showing the brains adept ability to generalise across non-overlapping facial features necessary for face recognition.

Significant decoding accuracies were observed for certain PF conditions in the amygdala and insula. Interesting the EO condition was significant in the amygdala for implicit expression decoding. This significance suggests the importance of the eyes in processing expression even if attention is not explicitly directed to emotion in the face for recognition. Furthermore, there was significance in the ME condition for explicit expression decoding. These significant results in the amygdala potentially reveal an exciting cross-over effect; with the absence of the eyes important for explicit tasks and the presence of the eyes important for implicit tasks. Furthermore, this corresponds to research showing the amygdala to be more responsive in an implicit task to larger as opposed to smaller eye whites (Whalen et al., 2004). In the insula there was significance in the explicit task for a couple of PF conditions, including the ME and MO conditions. Both these PF conditions are missing one of the important facial features in expression recognition. Significant decoding for the amygdala and insula was also found in Wegrzyn et al. (2015) as well as in Zhang et al. (2016) between fear and non-fear stimuli and between neutral and emotional stimuli. However, generally low decoding has been reported for the amygdala and insula throughout the previous literature; low decoding in the amygdala may result from the use of static stimuli or the low signal-to-noise ratio with this region difficult to scan with fMRI. Apart from the interesting effects described above, compared to the other face and emotion sensitive regions, decoding accuracies in the amygdala and insula were generally lower and there were subsequently weak cross decoding effects found.

Overall, the XC results reveal that the FG, IOG and STS were in line with the second hypothesis (H2) that similar brain representations will be activated when completely independent face parts are presented. However, against H2, weak XC significance was found in the amygdala and insula. In general, decoding accuracies are above chance in all the additional ROIs for some of the PF conditions. This is

supported in the univariate analyses that show greater brain activation in response to the ME and MM partial face conditions than the WF condition. This activation is distributed throughout the brain, including the FG, pSTS, middle occipital gyrus, and insula; potentially the recruitment of these additional face and emotion regions help process ambiguous facial information and feed information back to V1.

2.4.2.2 Task effects.

In support of H3 and past literature (Wegrzyn et al., 2015), high classifier performance was found in the IOG and FG for the implicit expression decoding task, whereby participants carry out a gender task but the classifier can decode the emotion shown. This suggests that implicitly the participant is attending to the emotion on the face. Furthermore, the univariate WBA (Appendix B) for explicit versus implicit processing is in line with the MVPA results: showing greater activation within the brain for implicit expression recognition. However, it is important to note that high classifier performance was found in the STS for the explicit expression decoding task and there were no task interactions in the amygdala and insula, these findings are against H3. The differences between implicit and explicit emotion processing will be addressed later to help explain these differing effects.

2.4.2.3 How do these results help explain the findings from V1 and EVC?

The results from the additional ROIs show promising trends regarding the higher cortical areas involvement in the feedback stream, adding greater weight that results are conforming with accounts of visual processing such as predictive coding, and explaining the significant findings in V1 and EVC. Whilst these results add to the body of research, and clearly show early visual and face-selective areas to contain information about occluded facial features, it is important to note some pitfalls to the experimental design. Notably, the regions of early visual cortex were individually defined for each participant, therefore the selection of voxels in the visual regions (V1 and EVC) was accurately represented. The other ROI's chosen in the ventral face processing stream were converted from an average brain mask in Neurosynth. Therefore sub-optimally, they are not based on each individual participant or a selected cluster of their activated voxels. Ideally, without scanning time constraints, localiser scans would have been carried out to define regions such as the STS and FG. However, whilst the primary focus of this study was to understand the contextual effects in early visual cortex, this was of less importance.

2.4.3 Can a low-level model explain the high-level effects in this data?

Whilst the strong cross-decoding results imply that they are not a result of low-level confounds in V1, further research using computational modelling (see Appendix H) was conducted within the laboratory (Maloret & Smith, 2017, Unpublished Raw Data). This aimed to investigate the extent to which expression recognition across the PF conditions relied on higher or lower-level processes. There were no significant differences between the PF conditions and WF condition in the standard model of V1, but significant differences between the PF conditions in the MVPA analysis (with better decoding in the ME and MM conditions than the WF condition). Furthermore, there were no significant differences between the condition pairs in the low-level model for cross-decoding, but differences in the MVPA analysis. These results support the idea that decoding performance in this study may be driven by top-down feedback processes in V1.

2.4.4 Implications for models of cortical feedback.

The various possible models of cortical feedback, outlined in the introduction of this chapter (2.1), could help explain the role of high-level effects in the processing of occluded facial expressions. In predictive coding, for instance, visual regions may be expecting whole face stimuli but when this stimulus is missing facial features and is therefore different from expectation, this may lead to an increased response to occlusion (Clark, 2013). Furthermore, in alternative Bayesian accounts of processing, early visual response signals would strengthen, following the formation of probabilistic inferences regarding the content of missing facial feature information, through concurrently assimilating bottom-up observations of occluded face stimuli with top-down contextual priors (Kersten et al., 2004; Lee & Mumford, 2003; Yuille & Kersten, 2006). Thus the heightened decoding found in the current cross-classification results for the early visual regions (V1-V3) provide support for these top-down models of visual processing.

The results could also be explained with a hierarchical neural network model (Heeger, 2017), whereby the neural responses and recognition of whole face stimuli are likely to depend on a feedforward bottom-up drive, but responses to partial face stimuli are likely to also depend on a feedback and prior drive. In these conditions top-down contextual knowledge and expectation is combined with the sensory input to predict the content of missing feature stimuli. Furthermore, the heightened decoding in the cross-classification results for the early visual regions as well as the

cross-classification results for the EO to ME pair in the fusiform gyrus, are in line with recurrent feedback models of object completion. This is because recurrent feedback signals to V1, sent immediately after the feedforward process, from extra-striate visual regions, followed by the inferior temporal cortex, would attempt to process occluded face stimuli (Wyatte et al., 2014). Overall, results are in keeping with various top-down models of visual processing and these models also help to explain how feedback or lateral connections may account for the present results.

2.4.5 Explicit and implicit emotion perception.

2.4.5.1 Why implicit decoding is higher?

2.4.5.1.1 Task difficulty?

The task effect, finding higher implicit than explicit expression decoding in V1, may to some extent be due to task difficulty, as there is an accuracy difference between the two tasks. This is shown in the behavioural results with lower accuracy in the emotion (3AFC) than the gender task (2AFC). However, results also show better implicit decoding of gender in V1 (when a participant is asked to judge emotion) (see Appendix G). Therefore, task difficulty does not seem to be driving the task effects in this research.

2.4.5.1.2 Default versus socially aware mode?

The high decoding rates in the implicit decoding expression task could reflect which mode of visual processing the brain is engaged in. Puce et al. (2015) identified two modes; one whereby a subject is not explicitly concentrating on or aware of the social meaning of a stimulus, namely default mode; or where a subject makes an overt social judgement, specifically social aware mode. It is worth noting that the brain can still be sensitive to potentially threatening stimuli in default mode whilst the brain is maximally primed to process stimuli optimally in social aware mode (Puce et al., 2015). In default mode, neural activation between conditions has been shown to differ depending on context or task influences; however, in socially aware mode, neural activations remain constant across conditions to process stimuli equally.

These modes could correspond to implicit and explicit decoding in this experiment, and could explain why decoding between the expression categories is found in the implicit but not in the explicit task. This is because the implicit task could be undertaken in default mode and as emotions are potentially threatening stimuli they are still attended to; but in the explicit task, the sensory systems could

be maximally primed to account for and recognise all emotions in the social aware mode. The default mode could also link to the key cross decoding findings where decoding accuracy is greater in the implicit task for a condition pair with an occluded feature necessary for expression recognition (ME and MM in the EO and ME, or MO and MM condition pair respectively). This is because these conditions are ambiguous and could contain potentially threatening stimuli that needs to be attended to. Furthermore, the default mode could also explain why decoding accuracy is low in the implicit task for the EO to MO condition pair, as this pair is less ambiguous containing visual information central for expression recognition (the eyes and the mouth) (F. W. Smith et al., 2008; M. L. Smith et al., 2005).

2.4.5.1.3 Differences between implicit and explicit emotion processing.

Following on from the previous argument regarding the engagement of a default brain mode in improving implicit expression decoding, the results reflect an enhancement of processing under conditions not explicitly directed to emotion in the face. This is not the only study to show implicit task effects, Petro et al. (2013) found implicit task effects when decoding emotion or gender in the visual cortex. In addition to this, explicit and implicit processing differences are present in other brain regions when processing emotions (Scheuerecker et al., 2007). An abundance of research has found increased brain signals in the amygdala and hippocampus for implicit compared to explicit processing; these regions, as well as a host of subcortical areas also respond faster under implicit conditions (Critchley et al., 2000; Gur et al., 2002; Hariri, Bookheimer, & Mazziotta, 2000; Scheuerecker et al., 2007). Nonetheless, these differences must be interpreted with caution as Habel et al. (2007) and Winston, Strange, O'Doherty, and Dolan (2002), found the amygdala and insula to activate similarly under implicit and explicit conditions. Winston et al., 2002, argued however, for a slight dissociation between the amygdala activating automatically (under implicit conditions) and the STS activating intentionally (under explicit conditions).

2.4.5.1.4 Biological Salience

Furthermore, the enhancement of processing under conditions where attention is not explicitly directed to emotion in the face tentatively suggests that as expressions are such biologically salient signals (Pessoa & Adolphs, 2010), feedback to V1 may be enhanced under these conditions. The rapid automatic activation of

subcortical pathways, when attention is not explicitly directed to an emotional task, further supports the biological significance of processing facial expressions.

2.5 Conclusion

Given evidence that primary visual cortex can contain and predict rich information about the visual environment, it was important to understand the involvement of retinotopically defined early visual regions in processing and compensating for missing facial information. In the present study, the influence of context on processing facial expressions of emotions in early visual and higher brain regions involved in face and emotion processing was investigated. Multivariate pattern analysis (MVPA) showed reliable decoding of facial expression (happy, fear and disgust) in V1, EVC, IOG, FG and STS across conditions with non-overlapping visual inputs. This study also found similar patterns of decoding across non-overlapping samples of face information, suggestive of the involvement of feedback mechanisms beyond low-level processing. This was particularly robust under implicit processing conditions. Overall, these results show that information about facial expression can be read out from early visual regions and demonstrate the strong involvement of contextual influences in early visual processing when devoid of overlapping feedforward information. Results are thus in keeping with top-down models of visual processing such as predictive coding (and other approaches such as recurrent feedback models of object completion, Heeger (2017)'s hierarchical neural network model and alternative Bayesian accounts of processing). This research has also helped to inform how V1 deals with occluded stimuli, adding to previous research studying occlusion.

Chapter 3: Temporal Dynamics Underlying Visual Perception of Occluded Faces

3.1. Introduction

3.1.1 Background.

Following up on the previous study and literature, this chapter provides a compliment to Chapter 2, where the same experimental paradigm and multi-variate pattern analyses (MVPA) are applied with electroencephalogy (EEG). Thus, in addition to understanding where the brain compensates and feeds information back to account for missing feature information (Greening et al., 2018), this experiment aims to understand the temporal dynamics of this process. The collection of fMRI and EEG data should provide a comprehensive picture of processing occluded facial features in the brain, as both high spatial and temporal information about brain activity will be available (Cichy et al., 2014; Fusar-Poli et al., 2009; Sadeh et al., 2010).

The use of EEG, can also add to the previous fMRI study, about the potential role of feedforward and feedback processes, see Figure 2.11 (Chapter 2). The findings from the fMRI study showed similar activity patterns in V1, EVC, IOG, FG and STS across conditions with non-overlapping visual inputs. An alternate way of looking at bottom-up versus feedback processing is by investigating time; this is because bottom-up processing is quicker and can take place before feedback has occurred (Tang et al., 2014; Tang et al., 2018). This is consistent with accounts of visual processing, such as predictive coding (Clark, 2013; Friston, 2005, 2008; F. W. Smith & Muckli, 2010) and recurrent feedback models of object recognition (O'Reilly et al., 2013; Tang et al., 2014; Tang et al., 2018; Wyatte et al., 2012; Wyatte et al., 2014). These theoretical accounts, outlined in Chapter 2 (2.1.1.1), address the ways the brain may process occlusion.

3.1.2 EEG and MVPA.

Current research has begun to apply MVPA to EEG data (for a review, see; Grootswagers, Wardle, & Carlson, 2017), and more specifically understanding when faces are detected and individuated (Cauchoix et al., 2014; Cichy et al., 2014; Ghuman et al., 2014; Kaneshiro, Perreau Guimaraes, Kim, Norcia, & Suppes, 2015; Li et al., 2018; Nemrodov et al., 2016). MVPA has numerous advantages, providing a data-driven EEG approach that is not restricted by its univariate counterpart

reliance on established event-related potentials (ERPs) (Cichy et al., 2014; Kaneshiro et al., 2015; Nemrodov et al., 2016). Essentially EEG face recognition research has focused on specific ERPs, however, these may overlook other components that have not been selected or have been lost in averaging electrodes (Das, Giesbrecht, & Eckstein, 2010; Ghuman et al., 2014; Nemrodov et al., 2016). Nemrodov et al. (2016) demonstrated this by carrying out univariate and whole-brain multivariate analyses in a face identity recognition study; whilst they found effects in traditional ERP components of individual face processing (P100, N170, N250), they also found early effects using MVPA from 63-96ms, as well as heightened effects for identity along the time interval (106-800ms).

A study, analysing whole-brain MEG (an alternative time-series neurophysiological measure to EEG) and fMRI data, found significant decoding between human / non-human faces at 70ms (Cichy et al., 2014). This time-point, within the significant interval for the study above, suggests that low-level feature processing may occur before the earliest recognised ERP component at 100ms. This time-point was followed by two significant peaks of activation at 127ms and 190ms (Cichy et al., 2014). Thus, MVPA can provide greater depth and precision into the time-course of face processing (Das et al., 2010). Furthermore, Cichy et al. (2014) investigated the correspondence between their MEG and fMRI data; showing early MEG responses to correlate more with V1 than the inferior temporal (IT) cortex at 79-102ms (with peak correspondence at 93ms), and later MEG responses to correlate more with IT activation than V1 at 152-303ms (peak at 284ms). The early activation corresponds with when visual information first reaches the cortex (Carlson, Tovar, Alink, & Kriegeskorte, 2013).

A whole-brain EEG study, using the same stimuli as the aforementioned MEG study (Cichy et al., 2014), found significantly stronger classifier decoding accuracy to faces than other animate (human body, animal body or face) or non-animate categories (fruit or vegetable, an inanimate object) in a six-class category-level decoding analysis (Kaneshiro et al., 2015). This decoding reached early significance at 48-128ms, before peak significance at 144-224ms, and additional above chance results between 336-464ms (Kaneshiro et al., 2015). Three significant decoding phases were also found in another EEG whole-brain MVPA study on face category detection: with an initial phase at 95-149ms (corresponding to the P100), followed by a plateau at 140-195ms (corresponding to the N170) and a later phase at

185-350ms (corresponding to the P300) associated with a significant increase in accuracy (Cauchoix et al., 2014).

In the initial decoding phase, Cauchoix et al. (2014) infer the involvement of feedforward processes from V1 to occipital-temporal areas; this is correlated with low-level stimulus properties. They surmise that the available face information hits maxima and stabilises in the following phase, as information is no longer feedforward but recurrently processed in posterior areas to the OFA via the FFA (Cauchoix et al., 2014). The third phase is thought to reflect a complete face representation which can be consciously accessed; at this point feedforward and feedback processes have occurred and activation is distributed in temporal, parietal and frontal brain regions (Cauchoix et al., 2014). The three decoding phases show resemblance with the three key univariate ERP components; with decoding analyses providing a richer account of visual information that can be read out from the brain (De Vos, Thorne, Yovel, & Debener, 2012).

Another study, using MVPA and intra-cranial EEG, positioned electrodes directly on the FFA, to investigate its responsivity to faces and further eye, mouth and configural face information (Ghuman et al., 2014). They found decoding in response to faces than other visual images (bodies, houses, hammers, shoes and phase-scrambled faces) at 50-75ms. Furthermore, they found face identity decoding, invariant of expression information, at 200-500ms (Ghuman et al., 2014). As they found this time window to also contain featural and configural face information, they suggest this information was used to help individuate faces (Ghuman et al., 2014). Ghuman et al. (2014) speculate that these two peaks of activation may reflect the involvement of a feedback loop, as the latter time window is consistent with timings for recurrent top-down and bottom-up interactions. Furthermore, intra-cranial EEG electrodes were placed on the FG in a recent study by Li et al. (2018) demonstrating two distinct stages of face processing: a rapid feedforward face-selective decoding stage around 180ms in posterior FG, and a later decoding of expression stage between 230ms-460ms in mid-fusiform regions. The later stage may resemble an integration of information, and consequently a possible backwards projection of top-down information.

Whilst MVPA has been used to explore the neural time-course of face detection and individuation across expression in the visual cortex (Nemrodov et al., 2016), these analyses have not explored the neural time-course of expression

recognition under conditions of occlusion. F. W. Smith and Smith (2016, June, OHBM Abstract) showed that it is possible to reliably decode expression using EEG, through investigating the representations of expression and identity. However, they did not study occlusion and studying this may elucidate the involvement of feedback in the brain beyond low-level processing. Thus, the present study will measure decoding accuracy to various partial face (PF) conditions, testing when the brain can decode the presented expression, to understand when feedforward and feedback processes are involved in the recognition of occluded faces. In the following sections, the current ERP research exploring the effects of occlusion and emotion will be detailed; whilst these do not use MVPA methods, this research is of relevance to understanding how and when the brain deals with occlusion and recognises an expression.

3.1.3 ERP research investigating occlusion.

An abundance of literature has focussed on the face-specific N170 component along the posterior, occipital-temporal brain (Bentin et al., 1996; Itier et al., 2007; Yovel, 2016), thought to reflect STS and FG (but not IOG) activation (Pitcher et al., 2011; Wronka & Walentowska, 2011). Furthermore research has investigated the recognition of occluded expressions (M. L. Smith et al., 2005). However, few studies have investigated how the N170 may change as a result of PF occlusion. Research that has investigated eye-occlusion has shown a delay (but no change in amplitude) in the N170 to faces missing eye information (Eimer, 1998; Itier et al., 2007), these delays are detailed in Chapter 1 (1.1.6). Conversely, research showed one or both eyes to prompt an earlier peak N170 (Rousselet et al., 2014), and a greater amplitude (Bentin et al., 1996; Itier et al., 2007; Neath-Tavares & Itier, 2016; Neath & Itier, 2015). Evidently limiting analyses to ERP components could overlook finding this early latency eye-sensitivity (Rousselet et al., 2014).

Research has also shown larger amplitudes to the nose and mouth at 150-200ms (occipitally) and 200-250ms (occipital-lateral) when participants fixation was directed to these features of a whole face (face offset, fixation remained central) (Neath-Tavares & Itier, 2016). Whilst this is not directly investigating occlusion, its methodology bears resemblance to an occlusion study, as the rest of the face is not openly in vision. Additionally, this study found larger amplitudes around the P100, in occipital areas, when participants were directed to the mouth (Neath-Tavares & Itier, 2016). Whilst this may purely reflect low-level visual properties; as

aforementioned in Chapter 1 (1.1.6), it may be indicative of early top-down processing to an area that has previously been stated important for expression recognition (Jack et al., 2009; F. W. Smith & Schyns, 2009).

Based on these studies, there is an expectation to see amplitude and timing differences between PF stimuli used in the present study; as such an isolated mouth may have some effects on the strength of processing emotion, with these affects distributed along the time-course, both before and after the N170 (Neath-Tavares & Itier, 2016). Furthermore, from the importance of processing eye information, isolated eyes are more likely to create stronger amplitudes around the N170 (Itier & Batty, 2009; Nemrodov, Anderson, Preston, & Itier, 2014). Overall, the occlusion of these features is likely to have an effect on the latency of the responses, with occlusion causing a delay in processing (Eimer, 1998; Itier et al., 2007). It is also important to note, that amplitudes are likely to be more pronounced for partial stimuli after 300ms as the P300 ERP responds to salient and unexpected stimuli (Hajcak, MacNamara, & Olvet, 2010). A detailed exploration into the efficacy and time-course of processing occluded stimuli will follow.

Using Gaussian bubbles, an intra-cranial electrode study, investigated the effects of occlusion among several whole and partial objects (including animals, faces and vehicles) in the visual ventral stream (Tang et al., 2014). They found similar object preferences, amplitude and waveform responses amongst electrodes (around the IOG and FG) when participants were presented with whole and highly occluded images (where only 9-25% of the object areas were visible) (Tang et al., 2014). However, responses to partial stimuli occurred ~100ms later; these delays were higher in the ventral stream (FG, ITG) (Tang et al., 2014). Tang et al. (2014) infer the involvement of top-down recurrent processing and reason against a feedforward model, as there are no latency delays in early visual areas. If delays were present in early visual regions these could potentially be caused by partial images propagating through the ventral stream at a slower rate (Tang et al., 2014).

Overall, a pattern of similar or stronger amplitude seems to be emerging among studies, depending on whether features are respectively occluded or isolated. A pattern of delayed latency also seems to be emerging for occluded and isolated stimuli, apart from finding an earlier peak for the isolated eyes in Rousselet et al. (2014). This discrepancy could result from comparing different but equals samples of face information, rather than comparing to a whole face stimulus, which is the

case for the other studies. To summarise, the research outlined, whilst important, does not fully consider emotion differences. These are important as Leppänen, Hietanen, and Koskinen (2008) found no N170 when recognising fear with an occluded eye region; thus the N170 is likely bound to which diagnostic emotion features, for fear the eyes, need to be encoded for recognition (Schyns, Petro, & Smith, 2007, 2009). Schyns et al. (2007) and Schyns et al. (2009) detailed how information for expression recognition focusses on the eyes, before attention moves towards the mouth for processing the whole face; thus emotions that require diagnostic eye information generate an earlier N170 than those that require mouth information.

3.1.4 ERP research investigating differences between emotions.

There is mixed evidence for differentiation amongst the N170 in processing separate emotions; some research has found differences in processing emotions (Batty & Taylor, 2003; Blau, Maurer, Tottenham, & McCandliss, 2007; Calvo & Nummenmaa, 2015; Hinojosa, Mercado, & Carretié, 2015; Neath-Tavares & Itier, 2016) where other research has not (Eimer & Holmes, 2002, 2007; Eimer, Holmes, & McGlone, 2003; Herrmann et al., 2002; Rossion, 2014).

The differences appear in emotional valence with positive emotions eliciting a significantly earlier ERP response (Batty & Taylor, 2003) but negative emotions, particularly fear, eliciting an increased N170 amplitude (Batty & Taylor, 2003; Blau et al., 2007; Calvo & Nummenmaa, 2015; Hinojosa et al., 2015; Turano et al., 2017). However, some studies show the N170 to be unaffected by expression; this is not surprising as the activation of the N170 is generally thought to reflect face perception (Eimer & Holmes, 2002, 2007; Eimer et al., 2003; Rossion, 2014). These results do not explain why differences have been shown in the literature, but the conflicting findings could result from task differences.

3.1.5 ERP research investigating task.

The differentiation of ERP response between emotions could be explained by task as the studies that find emotion differences in the previous section use implicit tasks (Batty & Taylor, 2003; Blau et al., 2007; Hinojosa et al., 2015; Neath-Tavares & Itier, 2016). These implicit task effects are reminiscent with research investigating how task context influences the processing of expression in fMRI experiments (Critchley et al., 2000; Hariri et al., 2000; Petro et al., 2013; Scheuerecker et al., 2007), and with findings from Chapter 2. To recap, findings from Chapter 2 (2.3)

showed higher classifier performance in the implicit expression decoding task (for V1, EVC and IOG compared to the explicit task), where participants carried out a gender task but the classifier was decoding emotion. However, there was high classifier performance in the explicit expression decoding task for the STS. This research also showed stronger brain activation for the implicit WBA in the rIOG, SFG, anterior cingulate, precuneus, lMFG, lIPL and lS2.

EEG studies also highlight the importance of attending to emotional stimuli in implicit conditions (Neath-Tavares & Itier, 2016; M. L. Smith, 2011). This is revealed in research showing: significant emotion differences in an implicit unaware condition (whereby a face is immediately masked with a scrambled image) (M. L. Smith, 2011) and an emotion irrelevant oddball task (Neath-Tavares & Itier, 2016). In implicit unaware conditions a significantly enhanced frontal positivity (M. L. Smith, 2011) and N170 (Neath-Tavares & Itier, 2016) have been reported in response to fear (vs neutral and happiness) recognition. Only a general increased N170 to emotional vs neutral expression has been reported in explicit aware conditions (Neath-Tavares & Itier, 2016; M. L. Smith, 2011). An ensuing meta-analysis and review propose a greater N170 amplitude to emotional than neutral expression in both implicit and explicit tasks (Hinojosa et al., 2015; Turano et al., 2017). However, they further state that effect sizes are larger in implicit tasks and thus, automatic processes are important for perception (Hinojosa et al., 2015). These findings suggest that processing occurs under conditions not explicitly directed to emotion in the face, and may result from expressions being biologically important to process (Pessoa & Adolphs, 2010).

However, Wronka and Walentowska (2011) found the N170 to be insensitive during an implicit (gender) task, proposing that expression effects involve voluntary, top-down modulation (FFA, STS) to differentiate expressions (Winston et al., 2002). In addition, an implicit perceptually demanding lines task in the presence of emotional faces also acted to eliminate any expression effects (Eimer et al., 2003). Furthermore, no differences in the N170 were reported between an expression and gender recognition task; in both tasks the N170 was sensitive to the eyes (Schyns, Jentzsch, Johnson, Schweinberger, & Gosselin, 2003; M. L. Smith et al., 2004).

Further task differences have been found in later ERPs to expression; with increases in P300 and late positive potential (LPP) when participants attend to emotional (counting surprised faces) rather than gender attributes (counting males /

females) of a face (Hajcak et al., 2010; Krolak-Salmon, Fischer, Vighetto, & Mauguière, 2001). More specifically, during an explicit expression task, ERPs to emotional vs neutral faces were observed between 250-550ms and expression differences emerged between 550-750ms (with happiness and fear significantly different from disgust) (Krolak-Salmon et al., 2001). These late ERPs have also been shown where participants carried out expression and gender recognition tasks; the P300 was sensitive when attending to the features relevant for task completion, such as when using the eyes diagnostically in a gender task and the mouth in an expression task (M. L. Smith et al., 2004). It is also important to note that a stronger P300 response has been shown when a participant detects a target stimulus in an oddball task (Picton, 1992), this may reflect a feedback effect to help the participant process the information.

3.1.6 Present study and hypotheses.

To conclude, this study will utilise EEG and MVPA to investigate the neural time-course of expression processing under conditions of face occlusion. This timing information is pertinent to understanding when the brain processes or compensates for ambiguous occluded information and the role of bottom-up vs top-down mechanisms. Prior MVPA research suggests that faces and expressions can be neurally decoded from EEG data (Cauchoix et al., 2014; F. W. Smith & Smith, 2016, June, OHBM Abstract) but research has not explored the time-course of expression recognition under conditions of occlusion.

H1: Successful decoding across non-overlapping visual inputs (e.g. independent parts of a face: occluded eyes and eyes-only stimuli; occluded mouth and mouth-only stimuli) will occur at a later time relative to whole face decoding, after feedback from higher cortical areas has filled in missing feature information.

H2: Emotion processing will be affected by task context: whereby expression decoding will be stronger in the implicit task compared to the explicit task.

3.2 Study 1

3.2.1 Methods.

3.2.1.1 Participants.

A total of 16 participants (8 females, 8 males) took part in this experiment, aged 20-36 years (M = 25.31, *SD* = 3.77). Participants were recruited via the University of East Anglia's (UEA) paid participant panel and advertisements around the university (they were paid for their participation). All participants had normal or corrected to normal vision. Participants gave written, informed consent in accordance to approved ethics by the Psychology Research Ethics Committee at the University of East Anglia.

3.2.1.2 Stimuli.

This study used the same stimuli from the CAFE dataset as the aforementioned fMRI experiment: six identities, created into five PF conditions (see Chapter 2, Figure 2.13), displaying three emotions (disgust, fear and happiness). The stimuli, totalling 90 different combinations were presented on a white background at a visual height of 10˚ using E-Prime 2.0 Software.

3.2.1.2.1 Materials.

Both the Empathy Quotient (EQ) (Baron-Cohen & Wheelwright, 2004) and The Toronto Alexithymia Scale (TAS) (Bagby, Parker, & Taylor, 1994) were used, for further details on these measures and the distribution of participant scores, see Appendix I.

3.2.1.3 Design and procedure.

Participants were presented with all the PF stimuli (within-subjects) and asked to explicitly recognise facial expression or gender depending on the task, while a 64-channel EEG cap measured their brain activation. In the explicit emotion task, participants were required to recognise expression in a three AFC task; in the implicit task they were asked to recognise gender (two AFC). Both tasks consisted of 540 trials with six repetitions of the 90 stimuli: 15 conditions (five PF conditions: WF, EO, ME, MO, MM; three emotions) and six identities. Each task began with six practice trials and took approximately 22 minutes to complete, with a break every 45 trials. Participants were asked to sit in a chin rest to minimise head movement. Each trial consisted of a fixation period (500ms) followed by a face (1000ms) and a variable delay period between 800ms and 1200ms before the next trial (see Figure 3.40). Participants were asked to respond after the stimulus was displayed and up to

the presentation of the next stimulus. Task order was blocked and counterbalanced among participants; whereby participants carried out one task followed by the other. Participant responses were recorded with a keyboard response of 1, 2 and 3 or 1 and 2; button order was also counterbalanced among subjects. The experiment lasted a maximum of three hours, including time for set up, the main experimental runs, cap removal and hair washing, as well as filling in the questionnaires and debrief. Participants were shown the WF stimuli before the experiment to familiarise themselves with the stimuli (see Appendix A for stimulus sheets).

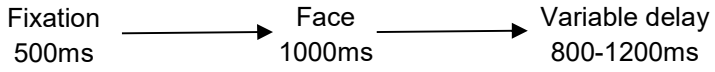

Figure 3.40. Sequence of stimulus presentation.

3.2.1.4 EEG acquisition.

The EEG was recorded with Brain Vision Recorder using an active 63-channel electrode system (ActiCAP, Brain Products GmbH) mounted to a nylon EEG cap. Electrodes were placed equidistantly according to the 10-10 system. The electrode FCz served as the reference, and the AFz as ground (see Figure 3.41). The electrooculography (EOG) channel was recorded using electrode FT9 (see Figure 3.41), this was positioned below the left eye to record vertical eye movements and eye blinks. Signals were continuously acquired at a sampling rate of 1000hz using a BrainAmp amplifier (Brain Products). The impedance was kept below 50kΩ.

3.2.1.5 EEG data pre-processing for MVPA.

For the MVPA analysis, the EEG data was pre-processed using EEGLAB (Delorme & Makeig, 2004) on Matlab R2014a. Firstly the data was high and low-pass filtered between 0.01 and 35hz. Epochs were then generated for each stimulus presentation: 200ms prior to stimulus, to provide a pre-stimulus baseline, and lasted a total of 800ms (600ms post-stimulus onset). Whilst standard pre-processing steps would reject noisy trials and epochs; for this analysis no artefact correction was applied and all trials and epochs were included in the analysis, with the intention to increase power with more trials. Furthermore, this step was less crucial for MVPA analysis as classifiers can learn to subdue noise and overlook bad channels during training (Grootswagers et al., 2017); artefact corrected results can however be found in Appendix J. Following epoch generation the eye channel was rejected and further

bad channels were interpolated. All epochs were included in the ERP analysis and data were re-referenced to an average of all electrodes excluding the eye channel.

3.2.1.6 Multi-variate pattern analysis.

MVPA was conducted on single-trial EEG signal using a linear support vector machine (LIBSVM 3.20 toolbox, Chang & Lin, 2011). Pattern classifiers were trained to discriminate between the three expressions, independently for each PF condition and task. Accordingly these classifiers were trained to decode the expression presented in single trials from 15 time windows of the EEG signal across 19 posterior visual electrodes (O1, O2, Oz, PO7, PO8, PO9, PO10, PO4, PO3, POz, P7, P8, P5, P6, P3, P4, P1, P2 and Pz), to test at each time window whether there was information to discriminate between the emotions for each PF condition. A k-fold cross validation approach was used to estimate performance, whereby the model was built from k – 1 subsamples (70% of trials) and tested on the remaining independent k subsample (30% of trials). This was carried out on ten randomly partitioned training test set iterations. An overlapping time bin approach was used to reduce data dimensionality from multiple time points (800) (Kaneshiro et al., 2015) and clearly reveal the temporal aspects of information processing in the brain, as such time bins commenced at -200ms, with a length of 100ms, shifting in 50ms steps; for example -200ms to -100ms, -150ms to -50ms, 250ms to 350ms, up until 450ms to 550ms and 500ms to 600ms (Hausfeld, De Martino, Bonte, & Formisano, 2012).

For the analyses, decoding accuracy was reported for each PF condition in 15 time steps of an 800 time point window (-200 to 600ms) using one-tailed one sample t-test results, with chance level of 33.3%. Significance levels are presented on graphs with $p < .05$ displayed with an 'X' and $p < .05$ (FDR corrected) displayed with a '*'. Unfortunately, as the basic decoding results were poor (see MVPA results, 3.3.2.2); the planned cross-classification analyses were not run.

3.2.1.7 Univariate EEG pre-processing and analysis.

Offline analyses were conducted using the following MatLab toolboxes: EEGLAB (Delorme & Makeig, 2004) and ERPLAB (Lopez-Calderon & Luck, 2014), toolboxes run with Matlab R2014a (The Mathworks, Inc., Natick, MA, USA). The recordings were high and low pass filtered at 0.01 and 35Hz, respectively, before epochs were created. Epochs were generated every 1s: 200ms prior to stimulus, to provide a pre-stimulus baseline, and lasted a total of 800ms, 600ms post-

stimulus onset. All epochs were included in the ERP analysis. Before data were re-referenced to an average of all electrodes, an automated artefact reduction technique was carried out to reject the trials consisting of an abrupt change in voltage (the eye channel was rejected entirely). The voltage threshold was set to 100uV in this step function technique (Luck, 2005). Furthermore, if the rejection rate was high (above 12%), bad channels affecting the dataset were manually interpolated.

The following occipito-temporal-parietal ERP's or ROIs were selected: the P100 (O1, O2) at 80-120ms (Jacques & Rossion, 2006; M. Xu, Lauwereyns, & Iramina, 2012), the lN170 (P7, PO7) and rN170 (P8, PO8) at 140-190ms (Jacques & Rossion, 2006; M. L. Smith, 2011; M. Xu et al., 2012), as well as the P300 (Pz, POz, PO3, PO4) at 300-500ms (Hajcak et al., 2010; Luck, 2014), see Figure 3.41. The chosen electrodes and time windows were based on the ERP data; from the individual electrode plots with high amplitudes and scalp maps. Furthermore, this was also based on previous literature consistently using these electrodes and time windows. The P100 and P300 were selected to analyse earlier versus higher-level processing in the brain (Cauchoix et al., 2014), whilst also aiming to correspond to the fMRI study; the P100 closest to reflecting early visual processing, including potentially feedback, and the P300 reflecting higher visual processing (Cichy et al., 2014).

For each ROI, a repeated measures ANOVA was conducted to investigate task, emotion and PF condition on accuracy.

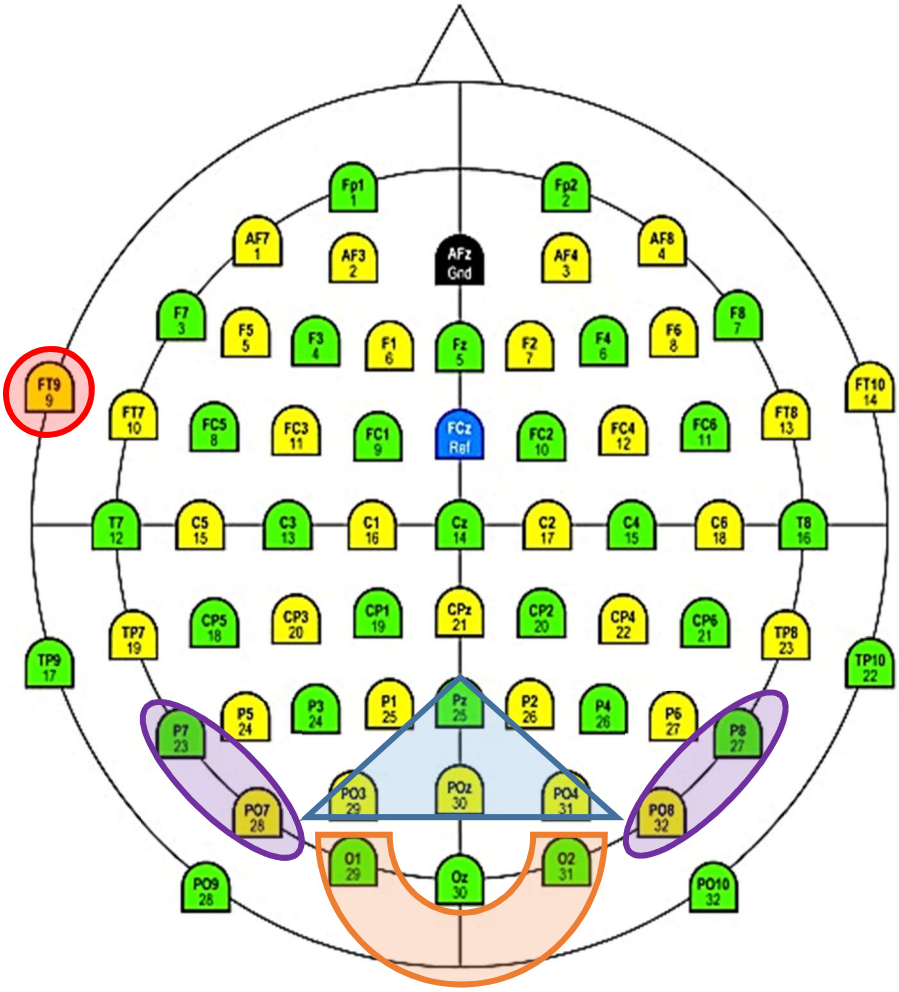

Figure 3.41. ROIs displayed on EEG electrode map (www.fieldtriptoolbox.org/_media/template/acticap-64-channel-standard-2_original.jpg). ROIs include the P100 (O1, O2) highlighted in orange, the lN170 (P7, PO7) and rN170 (P8, PO8) highlighted in purple, as well as the P300 (Pz, POz, PO3, PO4) highlighted in blue. The EOG eye channel is highlighted in red; ground and reference electrodes also displayed.

3.2.2 Results.

3.2.2.1 Behavioural results.

Due to excessive eye blinks in one participant and another reporting left-handedness during the experiment, the final analysed sample consisted of 14 participants (8 females, 6 males), aged 20-28 (M = 24.64, SD = 2.65).

Akin to the fMRI experiment, behavioural data revealed that participants, as expected, subjectively performed better at the gender (M = 95.93%, SD = 4.15%) than the expression task (M = 85.37%, SD = 9.63%) across all PF conditions. Performance was highest in the WF conditions, followed by the MO and ME in the expression task, and ME and MO in the gender task (Table 3.3). Comparing emotion recognition accuracy; happiness was subjectively the most recognisable emotion (M

= 94.21, SD = 7.16), followed by disgust (M = 83.25, SD = 11.28) and fear (M = 78.65, SD = 12.75), further akin to the fMRI experiment.

Table 3.3.

All to 2 d.p in percentage. WF: whole face, EO: eyes only, ME: minus eyes, MO: mouth only, MM: minus mouth.

Task	WF	EO	ME	MO	MM
Expression	89.09 (SD = 7.71)	83.73 (SD = 11.18)	84.33 (SD = 9.56)	87.24 (SD = 11.39)	82.47 (SD = 7.44)
Gender	98.15 (SD = 1.54)	88.96 (SD = 6.16)	96.69 (SD = 2.92)	96.16 (SD = 2.90)	94.71 (SD = 3.15)

3.2.2.1.1 Emotion accuracy.

A two-way repeated measures ANOVA was employed to explore the effects of PF condition and emotion on accuracy in the expression task. There was a significant main effect of PF condition, $F(4, 52) = 8.565$, $p < .001$, $\eta_p^2 = .397$ and emotion on accuracy, $F(2, 26) = 19.136$, $p < .001$, $\eta_p^2 = .595$. Collapsed across PF conditions, post-hoc pairwise comparisons with Bonferroni correction, showed accuracy rates for both disgust and fear statistically different from happiness ($p < .01$), with happiness being the most recognisable emotion; accuracy differences between disgust and fear were not statistically significant ($p = .535$), see Figure 3.42. Furthermore there was a significant interaction between PF condition and emotion, $F(8, 104) = 13.995$, $p < .001$, $\eta_p^2 = .518$ (greenhouse-geisser corrected).

As a result of the significant interaction, a simple effects analysis was undertaken; whereby eight separate repeated measures ANOVA's were carried out. Firstly the effect of emotion at each PF condition was investigated by carrying out five ANOVAs (all five were significant at $p < .05$) and then the effect of PF condition for each emotion in turn was investigated by carrying out three separate ANOVAs (all three were significant at $p < .05$), these results can be found in Appendix D (Table D33 and Table D34). Additional post-hoc Bonferroni and paired sample t-tests were carried out to understand the differences between the conditions, see Figures 3.43 and 3.44.

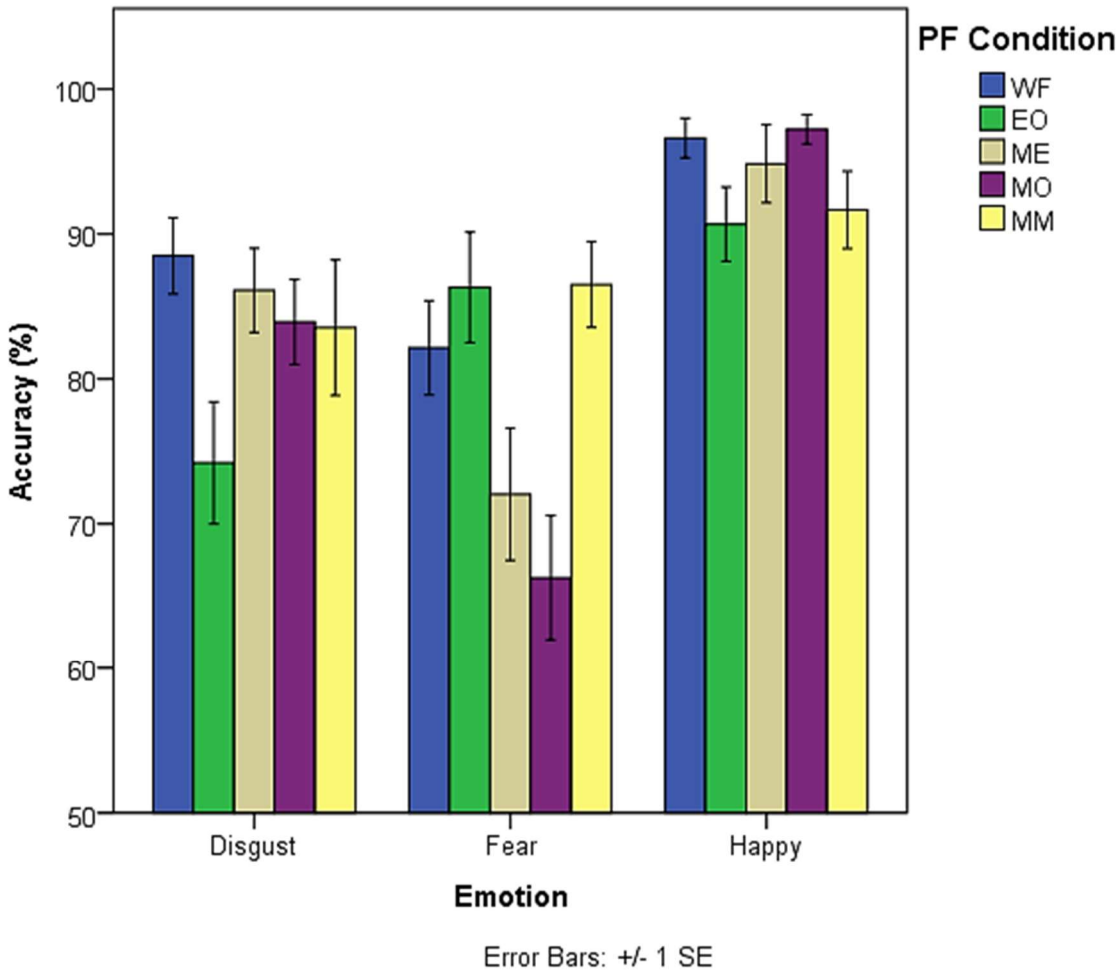

Figure 3.42. Overall recognition accuracy (%) in each PF condition for each emotion.

Overall, there were greater accuracy differences between the emotions in the MO condition (Figure 3.43). In disgust there were differences between the EO and other PF conditions, reflecting the poor performance for EO (Figure 3.44 & 3.42). In fear there were differences within the MO and ME in comparison to the other PF conditions, reflecting the poorer performance in these PF stimuli missing eye information (Figure 3.44 & 3.42). Furthermore, in happiness there were more differences within the EO and MM in comparison to the other PF conditions, reflecting poorer performance in these PF stimuli missing mouth information (Figure 3.44 & 3.42). These results support the importance of the nose and mouth in disgust, the eyes in fear and the mouth in happiness recognition (F. W. Smith & Schyns, 2009; M. L. Smith et al., 2005).

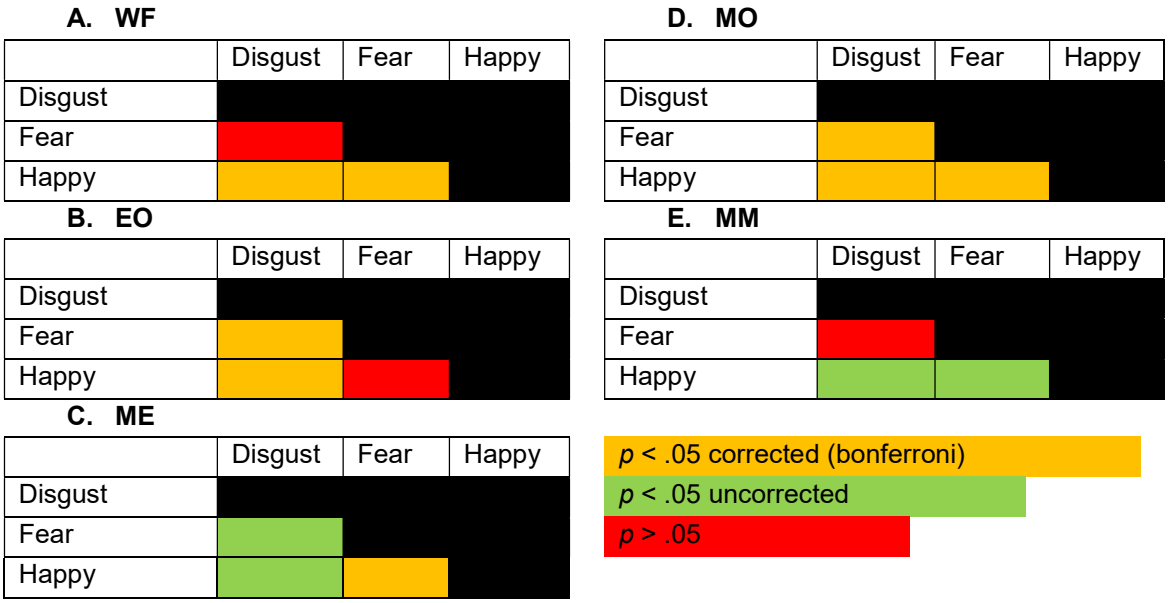

Figure 3.43. Paired sample t-test results comparing the differences between the emotions for each PF condition (see Table D35 in Appendix D for statistics: t-value, df and p-value).

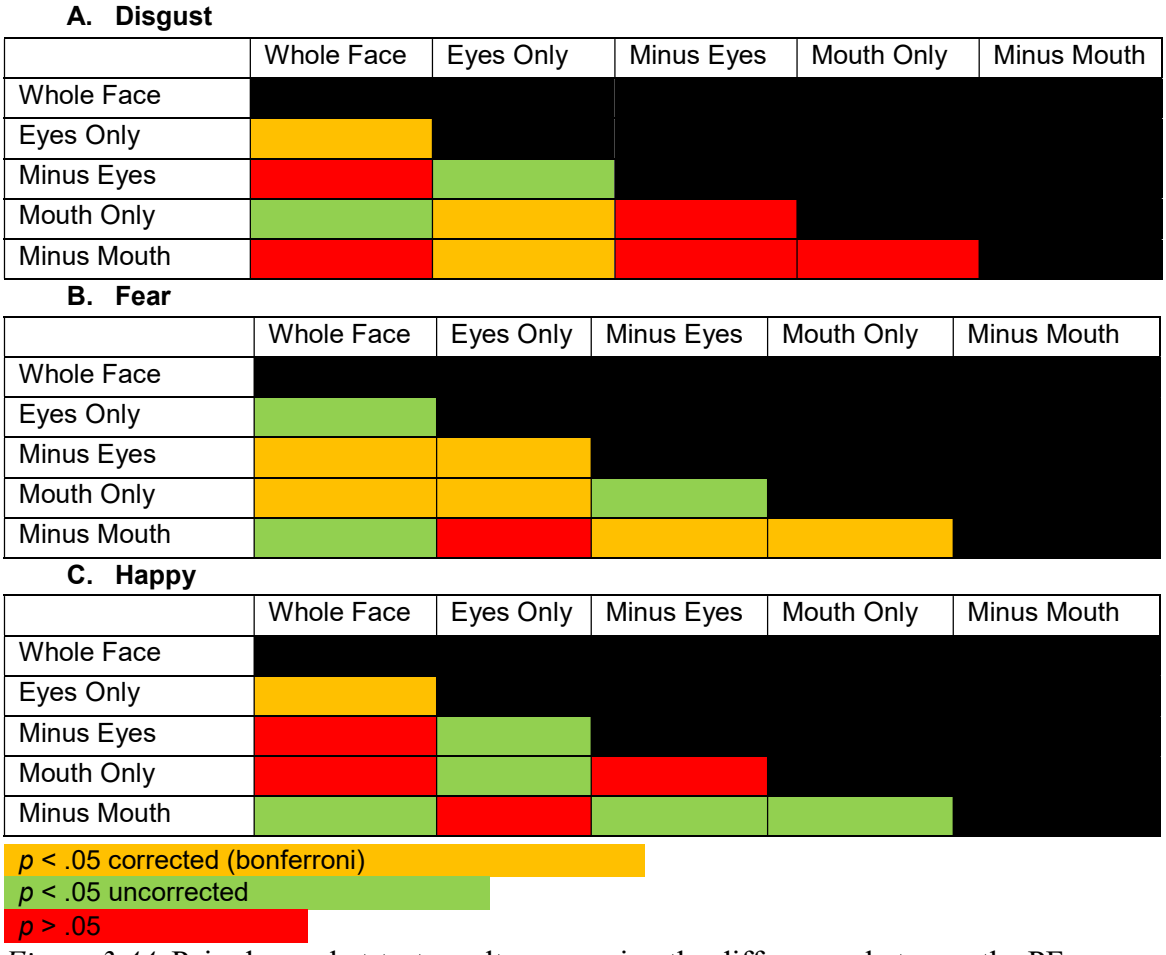

Figure 3.44. Paired sample t-test results comparing the differences between the PF conditions for each emotion (see Table D36 in Appendix D for statistics: t-value, df and p-value).

3.2.2.1.2 Gender accuracy.

A two-way repeated measures ANOVA was employed to explore the effects of PF condition and gender on accuracy (Figure 3.45). There was a significant main effect of PF condition, $F(2.141, 27.831) = 24.396$, $p < .001$, $\eta_p^2 = .652$ (greenhouse-geisser corrected), but no significant main effect of gender, $F(1, 13) = 4.02$, $p = .066$, $\eta_p^2 = .236$. However, there was a significant interaction between PF condition and gender on accuracy, $F(2.212, 28.752) = 13.379$, $p < .001$, $\eta_p^2 = .507$ (greenhouse-geisser corrected).

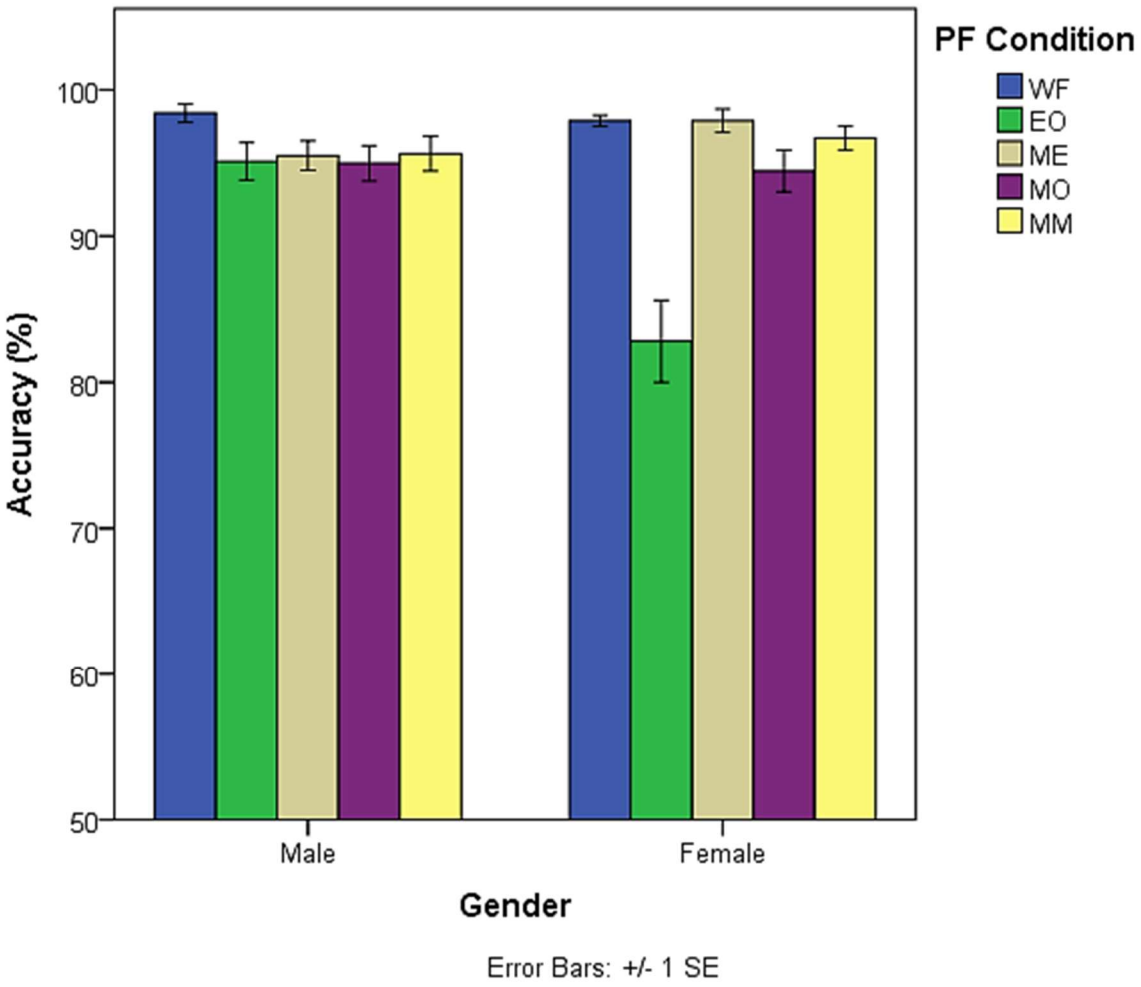

Figure 3.45. Overall recognition accuracy (%) in each PF condition between male and female stimuli.

Again, as a result of the significant interaction, a simple effects analysis was undertaken. ANOVAs testing the effect of gender at each PF condition found significance in the EO ($F(1, 13) = 18.539$, $p = .001$, $\eta_p^2 = .588$) and ME ($F(1, 13) = 6.707$, $p = .022$, $\eta_p^2 = .340$) condition. Testing the effect of PF condition on gender found significance for both male and female faces ($p < .05$); the simple effects

ANOVA results can be found in Table D37 and Table D38 (Appendix D). Additional post-hoc Bonferroni and paired sample t-tests were carried out to understand the differences between the conditions, see Figure 3.46.

The differences seen in the male faces between the WF and PF conditions, suggest that it is easier to recognise WF male stimuli (see also Figure 3.45). Nonetheless, the recognition of male faces is accurate across all PF conditions. However, the significant differences seen in the females faces between the EO and other PF conditions, suggest that it is hard to recognise female faces from the EO condition. This finding was also present in the aforementioned fMRI study and it is unclear why it would be hard to recognise a female face from just seeing their eyes.

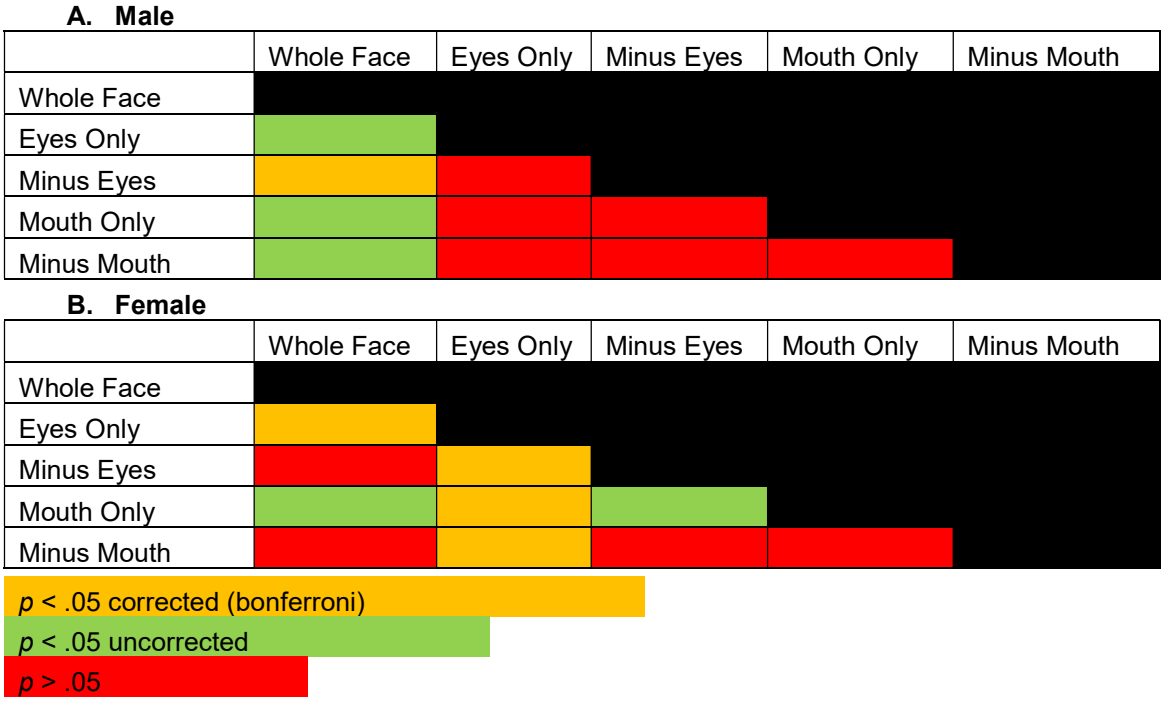

Figure 3.46. Paired sample t-test results comparing the differences between the PF conditions for male and female faces (see Table D39 in Appendix D for statistics: t-value, df and p-value).

An ANOVA (akin to the emotion task) exploring the effect of PF and emotion on accuracy was also conducted (see Appendix K). Furthermore, ANOVAs exploring the effect of PF and emotion on reaction time for both the emotion and gender task were conducted (see Appendix L).

3.2.2.2 MVPA results.

The main goal of this study was to provide an additional way of looking at bottom-up versus feedback processing, to the previous fMRI experiment (Chapter 2), by investigating the neural time-course of cross-decoding expression (under conditions of occlusion) in posterior visual electrodes. These electrodes were studied as a comparison to the fMRI experiment, which principally investigated early visual regions, as well as a host of posterior face and emotion selective areas. The central hypothesis is to investigate the decoding of expression across conditions with non-overlapping visual inputs, with the expectation that decoding across non-overlapping visual inputs will occur at a later time point, after feedback has filled in missing information. As such the main interest lies within the XC effects, however, as aforementioned, the basic decoding results were poor and the planned cross-classification analyses were not run. Nonetheless, the basic decoding results are presented next.

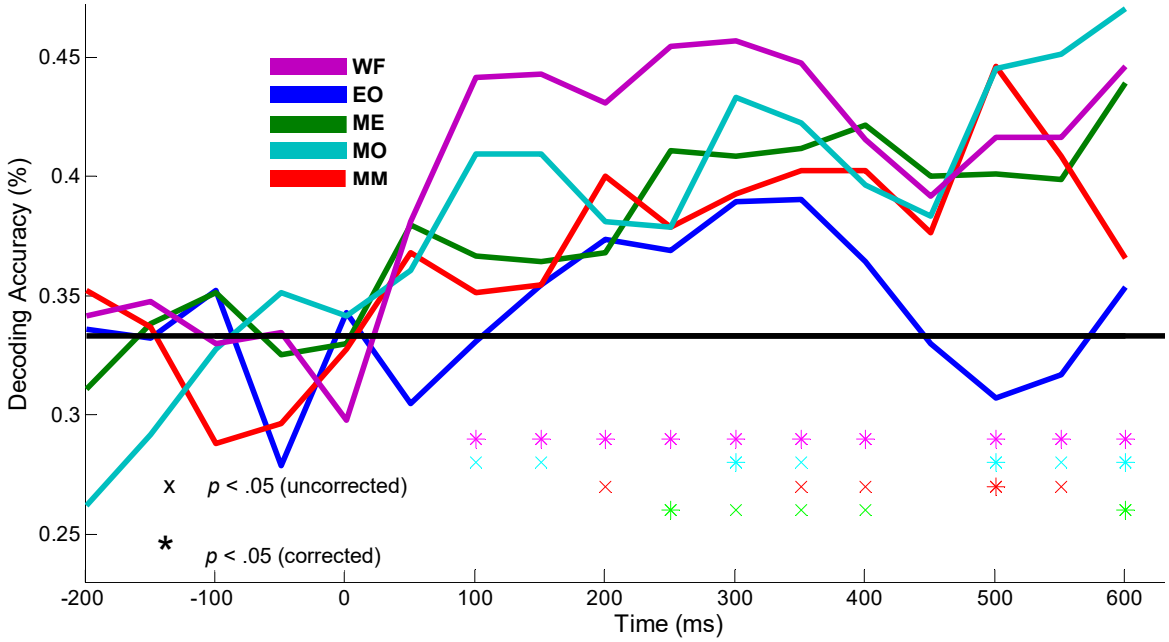

Figure 3.47. Decoding Expression, Expression Task.

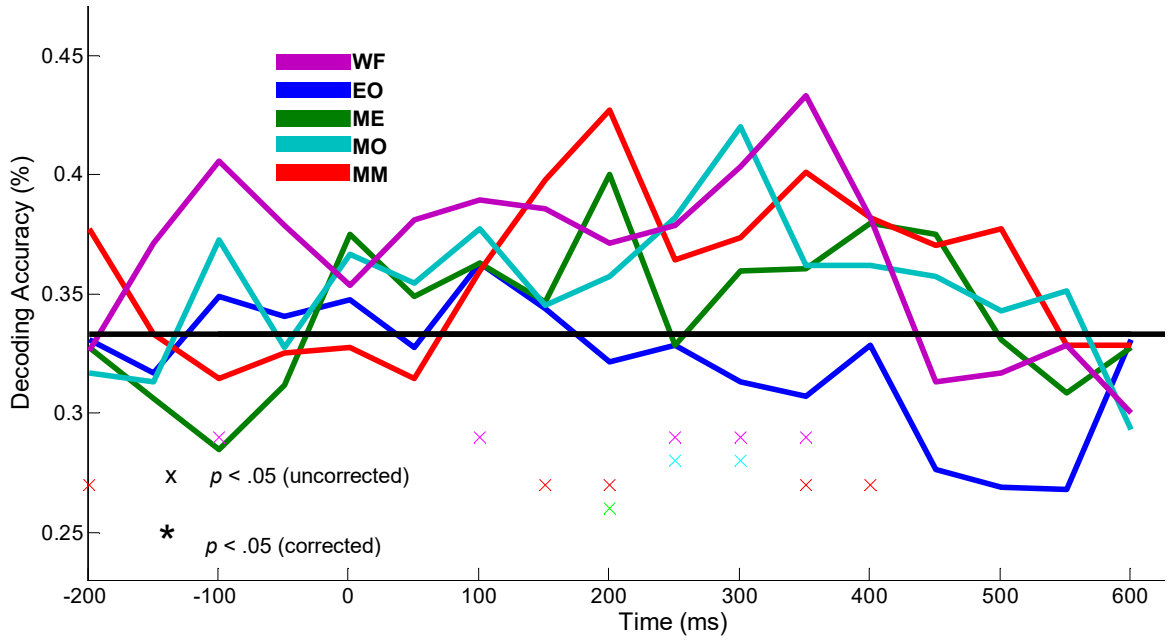

Figure 3.48. Decoding Expression, Gender Task.

As expected, significant ($p < .05$) FDR effects are greatest in the WF condition, with medium to large effect-sizes, for 100-500ms in the explicit task; demonstrating very early decoding accuracy for expression in the WF condition. Significant FDR effects are also present in the explicit task (Figure 3.47) for the ME condition at 250-350ms, $t(13) = 3.506$, $p = .002$, $d = 0.94$ (large effect-size), and similarly, in the MO condition at 300-400ms, $t(13) = 2.851$, $p = .007$, $d = 0.76$ (medium effect-size). These two conditions have mouth information present and thus it seems that the mouth is more informative; corroborating with Neath-Tavares and Itier (2016) and other research demonstrating the importance of the mouth in early expression recognition (Jack et al., 2009; F. W. Smith & Schyns, 2009). Furthermore the MM condition was not FDR significant around this time point.

Significant FDR effects with medium to large effect-sizes are also present for the explicit task post 500ms, in the WF (500-700ms), ME (600-700ms), MO (500-600ms and 600-700ms) and MM conditions (500-600ms). This could reflect attention to the explicit task, allowing continued processing of the emotion (similar to the P300 ERP), but it may just reflect the participants response as they are required to make a three-way choice as opposed to a binary choice in the implicit task. Surprisingly, considering the importance of the eyes in processing faces and more specifically emotions (Baron-Cohen, 2004; F. W. Smith et al., 2008; M. L.

Smith et al., 2005; Whalen et al., 2004), decoding accuracy in the EO condition was not significant anywhere in the time-course.

Given that behavioural accuracy is good in the implicit task, it is surprising that there are no significant FDR decoding effects present (Figure 3.48). Although there are trends in expression decoding accuracy in the WF (100-200ms and 250-450ms), ME (200-300ms), MO (250-400ms) and MM conditions (150-300 and 350ms-500ms) associated with medium effect-sizes. It may be that more robust decoding in the explicit compared to the implicit task (seen in terms of more significant time points overall), maps onto the STS results found in the preceding fMRI chapter, where explicit decoding of expression was stronger than implicit decoding of expression. Strangely there are also trends for expression decoding in the baseline for the WF condition between -100 to 0ms and the MM condition between -200 to -100ms.

Whilst the basic decoding MVPA analysis has provided some interesting results, this study, as abovementioned, did not have enough significant conditions to reliably run the planned cross-classification analyses and answer the key hypothesis. Statistical power may be a potential factor causing this; to increase this, a bigger sample size (closer to 30 or more participants) and/or the inclusion of more trials or fewer conditions would have been beneficial. Thus, these results must be classed as exploratory, and therefore the time-course of processing and potential feedforward and feedback affects cannot be ascertained reliably from the present data. In order to relate the current studies to the past ERP face perception research outlined in the introduction (see 3.1) (Batty & Taylor, 2003; Eimer, 1998; Hinojosa et al., 2015; Itier et al., 2007; Neath-Tavares & Itier, 2016), a univariate ERP analysis was carried out on the data.

3.2.2.3 Univariate results.

3.2.2.3.1 rN170.

A repeated measures ANOVA was employed to explore the effects of task (2), emotion (3) and PF condition (5) on the mean amplitude in the rN170 time window (140-190ms). There was a non-significant main effect of task, $F(1, 13) = .090$, $p = .769$, $\eta_p^2 = .007$, and emotion on the mean amplitude, $F(2, 26) = 1.939$, $p = .164$, $\eta_p^2 = .130$. However, there was a significant main effect of PF condition, $F(4, 52) = 15.088$, $p < .001$, $\eta_p^2 = .537$, where amplitudes were greatest for the ME (M =

-8.51) followed by the MO (M = -8.17), EO (M = -8.03), MM (M = -7.07) and WF condition (M = -5.82) (Figure 3.49). Post-hoc pairwise comparisons, with Bonferroni correction, show significant differences between the WF and EO (p = .023), WF and ME (p < .001), WF and MO (p < .001), WF and MM (p = .045), ME and MM (p = .003), as well as the MO and MM conditions (p = .025) as decoding accuracy in the WF and MM was significantly lower than other PF conditions. Furthermore there was a significant interaction between emotion and PF condition, $F(8, 104) = 3.896$, p < .001, η_p^2 = .231 (Figure 3.50).

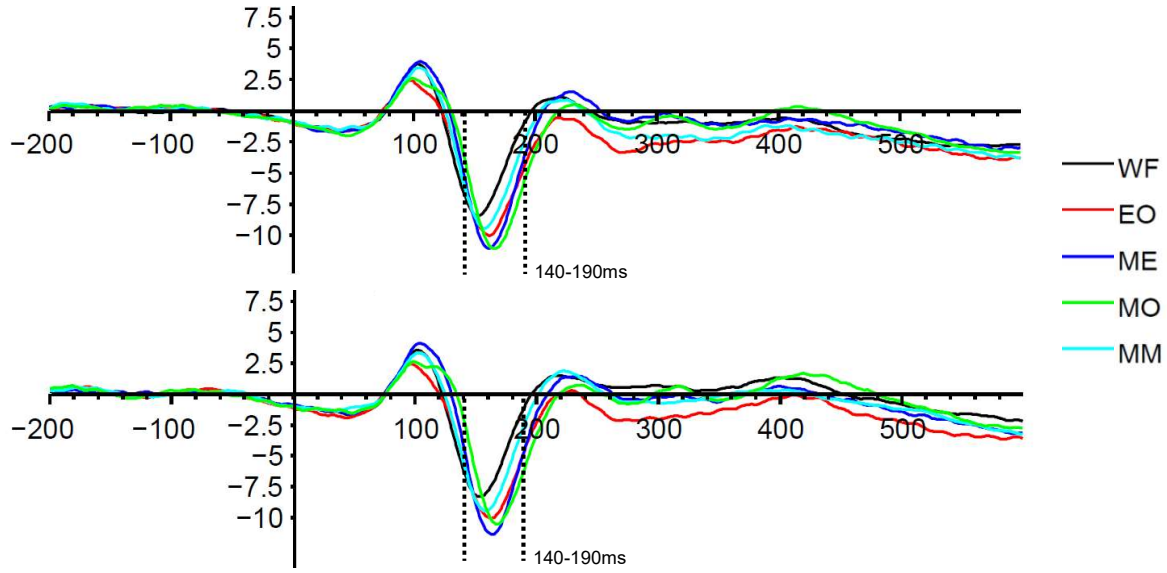

Figure 3.49. rN170 (PO8, P8) grand average ERP (μV) split by PF condition in the emotion task (top), gender task (bottom). Time window (140-190ms) used for analysis marked with dash lines. Negative voltage plotted down.

To explore this interaction a simple effects analysis was conducted, where, as above, eight separate repeated measures ANOVAs were carried out (these analyses were collapsed across task). Firstly, the effect of emotion at each PF condition was investigated by carrying out five ANOVAs (the WF, EO and MO were significant at p < .05), and then the effect of PF condition for each emotion in turn was investigated by carrying out three separate ANOVAs (all three were significant at p < .05), the simple effects ANOVA results can be found in Table D40 and Table D41 (Appendix D). Additional post-hoc Bonferroni and paired sample t-tests were carried out to understand the differences between the conditions, see Figures 3.51 and 3.52.

These additional post-hoc tests show differences between disgust and happiness in the WF condition (Figure 3.51), with amplitudes weaker in happiness than disgust (Figure 3.50). This corresponds with the emotion behavioural results of

this study, as well as previous research showing happiness to be recognised with ease; thus less amplitude may occur with easier recognition (F. W. Smith & Schyns, 2009). These tests also show fear and happiness to be significantly different in the MO condition (Figure 3.51); the stronger amplitude to happiness (Figure 3.50) corresponds with research demonstrating the importance of the mouth (F. W. Smith & Schyns, 2009). These findings suggest that higher amplitudes occur when the task is easier, for example features most important for recognition are present, but higher amplitudes may also imply that greater processing is needed for recognition. The latter explanation is more probable when behavioural results between the PF condition and emotion can justify that the effects are not a result of task difficulty, however, the behavioural emotion results show the MO condition associated with significantly stronger accuracy in happiness than fear.

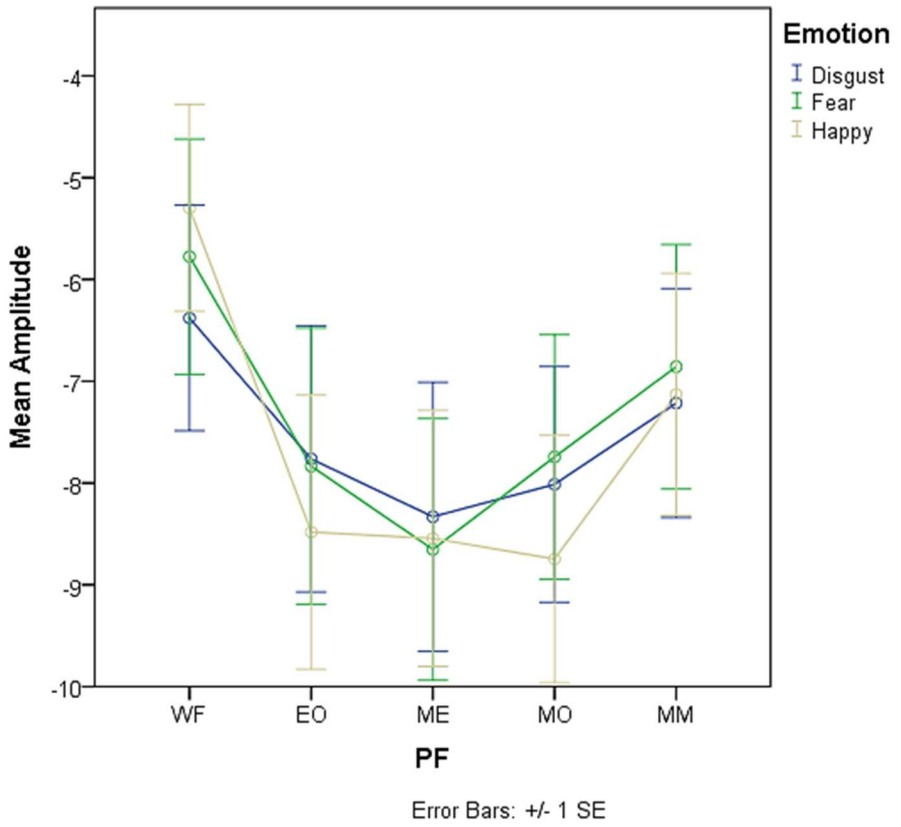

Figure 3.50. Mean amplitude of the rN170 for each emotion and PF, collapsed across task.

There is greater significance in fear and happiness recognition for the WF comparisons (Figure 3.52); this corresponds to lower amplitudes in the WF compared to the PF conditions (Figure 3.50). Thus, it seems the rN170 responds to process occlusion; however, it may simply be a result of task difficulty with the

partial stimuli being harder to recognise. Furthermore, there are differences between the ME and MM conditions in fear and happiness, with stronger amplitudes in the ME compared to the MM conditions (Figure 3.50). There is a significant accuracy difference in the behavioural emotion results for fear, with significantly lower accuracy in the ME compared to the MM. As this is the inverse to the difference found in the ERP results, the higher amplitude may reflect where feedback is needed to help fill in missing important information. Behavioural results for happiness recognition show no difference between the ME and MM conditions, thus finding stronger amplitudes to the ME in happiness also suggests that greater processing is needed to account for key features missing. This seemingly contradicts most research showing the importance of the mouth in happiness (F. W. Smith & Schyns, 2009), but the importance of eye information in happiness recognition has also been found (M. L. Smith et al., 2005). Whilst the amplitude for the ME is strong in happiness, the difference between the EO and MM and between the MO and MM reflects equally strong amplitudes to other PF conditions (Figure 3.50).

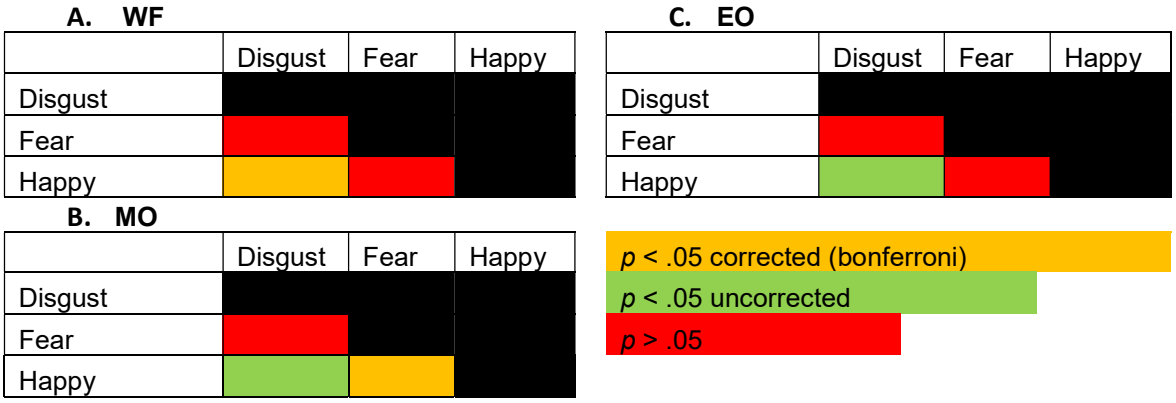

Figure 3.51. Paired sample t-test results comparing the differences between the emotions for the significant PF conditions (see Table D42 in Appendix D for statistics: t-value, df and p-value).

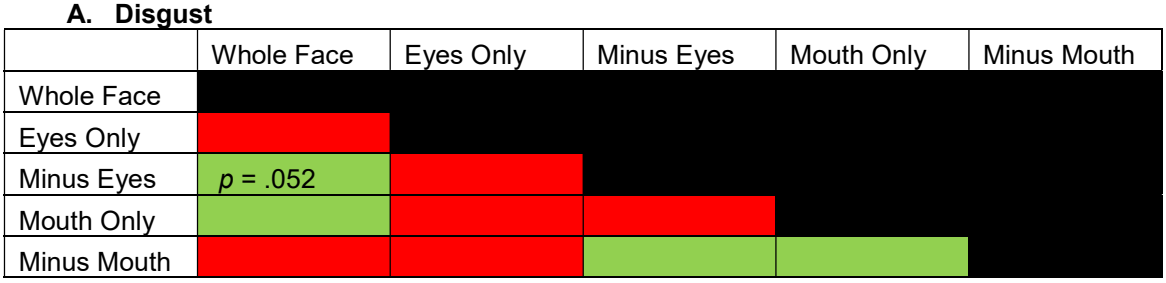

B. Fear

	Whole Face	Eyes Only	Minus Eyes	Mouth Only	Minus Mouth
Whole Face					
Eyes Only					
Minus Eyes					
Mouth Only					
Minus Mouth					

C. Happy

	Whole Face	Eyes Only	Minus Eyes	Mouth Only	Minus Mouth
Whole Face					
Eyes Only					
Minus Eyes					
Mouth Only					
Minus Mouth					

$p < .05$ corrected (bonferroni)
$p < .05$ uncorrected
$p > .05$

Figure 3.52. Paired sample t-test results comparing the differences between the PF conditions for each emotion (see Table D43 in Appendix D for statistics: t-value, df and p-value).

3.2.2.3.2 lN170.

A repeated measures ANOVA was employed to explore the effects of task, emotion and PF condition on the mean amplitude in the lN170 time window (140-190ms). There was a non-significant main effect of task, $F(1, 13) = .103$, $p = .753$, $\eta_p^2 = .008$ and emotion on the mean amplitude, $F(2, 26) = .924$, $p = .410$, $\eta_p^2 = .066$. However, there was a significant main effect of PF condition, $F(2.253, 29.286) = 3.531$, $p = .037$, $\eta_p^2 = .214$ (greenhouse-geisser corrected), where amplitudes were greatest for the MO (M = -4.13), followed by the ME (M = -4.07), MM (M = -3.01), WF (-2.79) and EO condition (-2.6) (Figure 3.53). However, post-hoc pairwise comparisons, with Bonferroni correction, show no significance between the PF conditions. Furthermore, there were no significant interactions within the ANOVA.

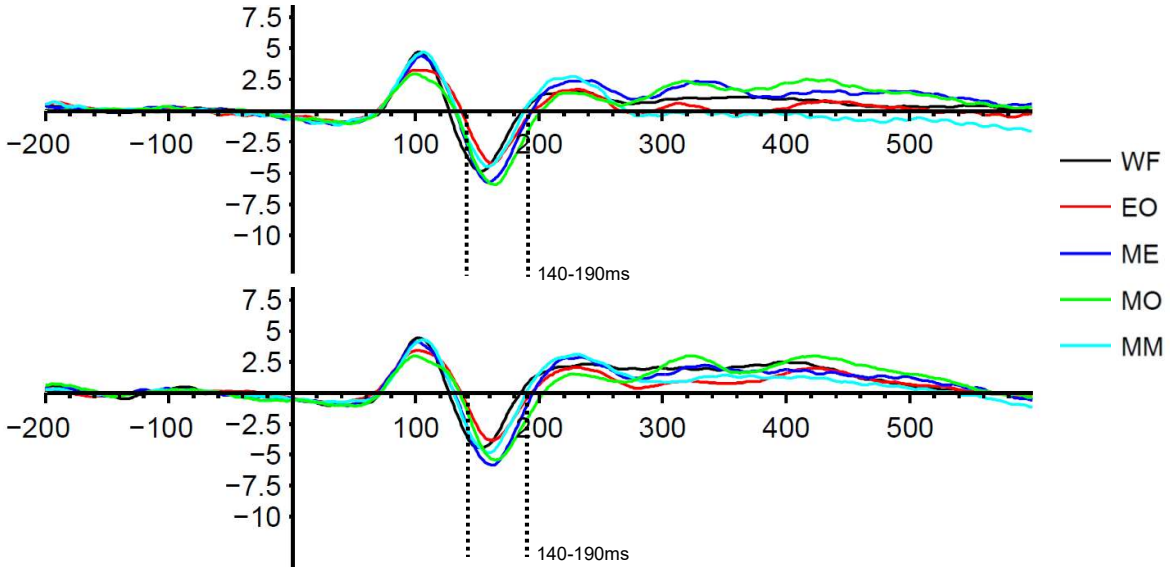

Figure 3.53. lN170 (PO7, P7) grand average ERP (μV) split by PF condition in the emotion task (top) and gender task (bottom). Time window (140-190ms) used for analysis marked with dash lines. Negative voltage plotted down.

3.2.2.3.3 P100.

A repeated measures ANOVA was employed to explore the effects of task, emotion and PF condition on the mean amplitude in the P100 time window (80-120ms). There was a non-significant main effect of task, $F(1, 13) = .230$, $p = .639$, $\eta_p^2 = .017$, but a significant main effect of emotion on the mean amplitude, $F(2, 26) = 4.776$, $p = .017$, $\eta_p^2 = .269$, whereby amplitudes were greatest for disgust (M = 5.67), followed by fear (M = 5.55) and happiness (M = 5.32). Post-hoc pairwise comparisons, with Bonferroni correction, show a significant difference between disgust and happiness ($p = .05$). There was also a significant main effect of PF condition, $F(2.173, 28.249) = 3.298$, $p = .048$, $\eta_p^2 = .202$ (greenhouse-geisser corrected), where amplitudes were greatest for the ME (M = 5.97), followed by the MM (M = 5.86), WF (M = 5.51), EO (M = 5.38) and MO condition (M = 4.84) (Figure 3.54). Post-hoc pairwise comparisons, with Bonferroni correction, show a significant difference between the ME and MO condition ($p = .016$). There were no significant interactions within the ANOVA.

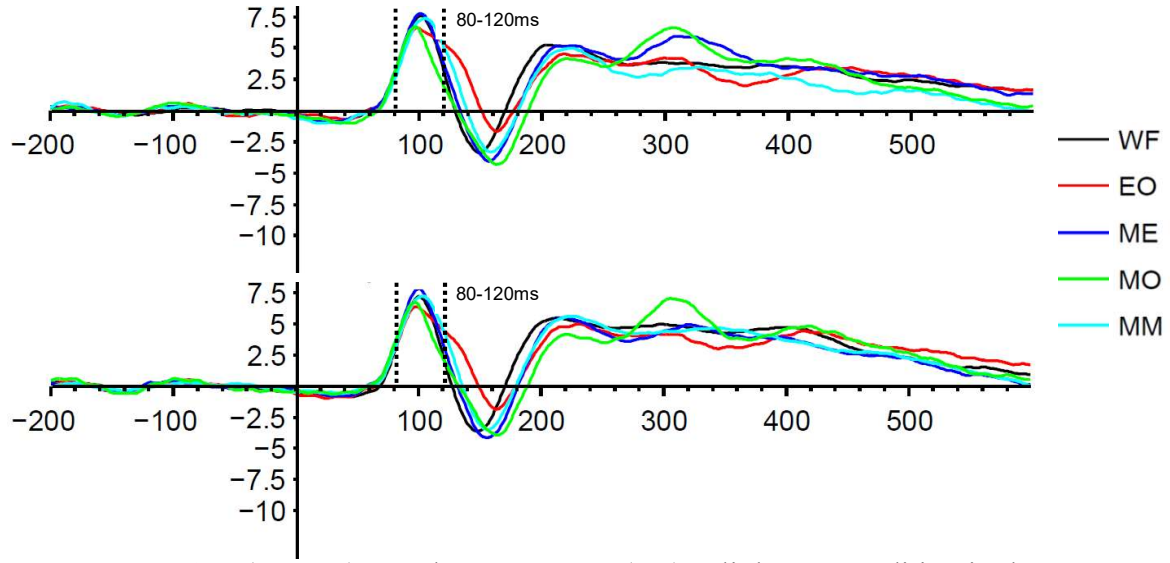

Figure 3.54. P100 (O1, O2) grand average ERP (μV) split by PF condition in the emotion task (up) and gender task (bottom). Time window (80-120ms) used for analysis marked with dash lines. Positive voltage plotted up.

3.2.2.3.4 P300.

A repeated measures ANOVA was employed to explore the effects of task, emotion and PF condition on the mean amplitude in the P300 time window (300-500ms). There was a non-significant main effect of task, $F(1, 13) = 1.915$, $p = .190$, $\eta_p^2 = .128$, but a significant main effect of emotion on the mean amplitude, $F(2, 26) = 5.271$, $p = .012$, $\eta_p^2 = .288$, whereby amplitudes were greatest for fear (M = 6.43), followed by disgust (M = 6.1) and happiness (M = 5.99). Post-hoc pairwise comparisons, with Bonferroni correction, show a significant difference between disgust and fear ($p = .015$), as well as between fear and happy ($p = .043$). There was also a significant main effect of PF condition, $F(4, 52) = 4.156$, $p = .005$, $\eta_p^2 = .242$, where amplitudes were greatest for the MO (M = 6.85), followed by the ME (M = 6.48), WF (M = 6.34), EO (M = 5.61) and MM condition (M = 5.58) (Figure 3.55). Post-hoc pairwise comparisons, with Bonferroni correction, show a significant difference between the MO and MM condition ($p = .023$). Furthermore, there was a significant interaction between task, emotion and PF condition, $F(8, 104) = 2.514$, $p = .015$, $\eta_p^2 = .162$.

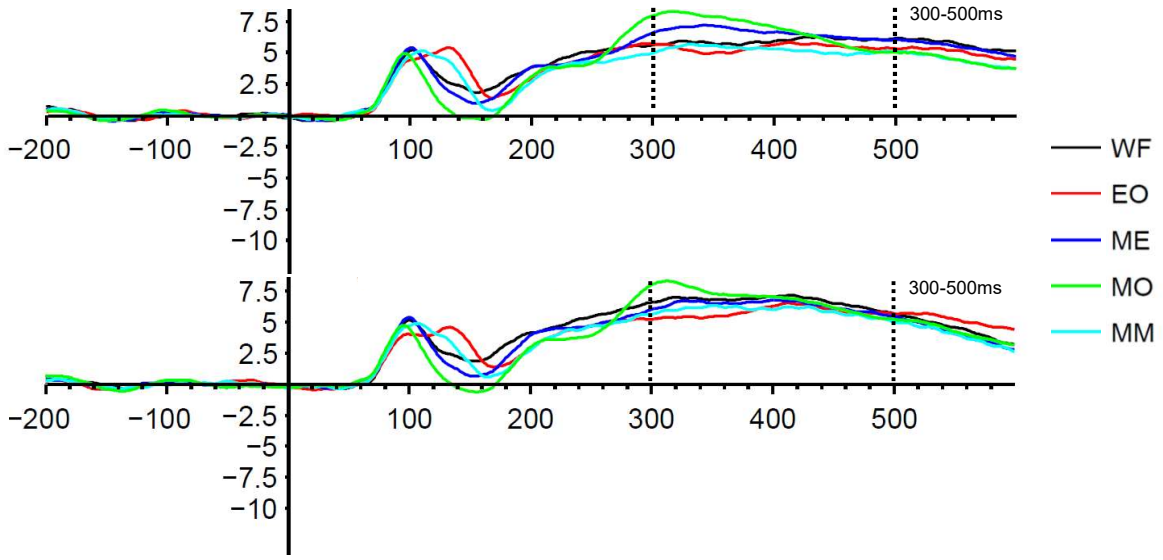

Figure 3.55. P300 (Pz, PO3, POz, PO4) grand average ERP (μV) split by PF condition in the emotion task (top) and gender task (bottom). Time window (300-500ms) used for analysis marked with dash lines. Positive voltage plotted up.

To explore this interaction, further two-way ANOVAs were carried out, where the interaction between emotion and PF was tested on the basis of task. Firstly a repeated measures ANOVA was carried out on the emotion task. This showed a significant main effect of emotion, $F(2, 26) = 5.092$, $p = .014$, $\eta_p^2 = .281$, whereby amplitudes were greatest for fear (M = 6.361), followed by disgust (M = 5.98) and happiness (M = 5.65), and also a significant main effect of PF condition, $F(4, 52) = 5.029$, $p = .002$, $\eta_p^2 = .279$ (greenhouse-geisser corrected) where the amplitudes were greatest for the MO (M = 6.82), followed by the ME (M = 6.59), WF (M = 5.95), EO (M = 5.4) and MM condition (M = 5.22). Post-hoc pairwise comparisons, with Bonferroni correction, show significant differences between fear and happiness ($p = .020$) and between the MO and EO ($p = .032$), as well as the MO and MM conditions ($p = .006$) respectively. There was no significant interactions within this ANOVA, $F(8, 104) = 1.590$, $p = .137$, $\eta_p^2 = .109$. Results from the gender task found no significant main effect of emotion, $F(2, 26) = 1.745$, $p = .194$, $\eta_p^2 = .118$, or PF on mean amplitude, $F(4, 52) = 2.332$, $p = .068$, $\eta_p^2 = .152$, but a significant interaction between emotion and PF condition, $F(8, 104) = 2.392$, $p = .021$, $\eta_p^2 = .155$ (Figure 3.56).

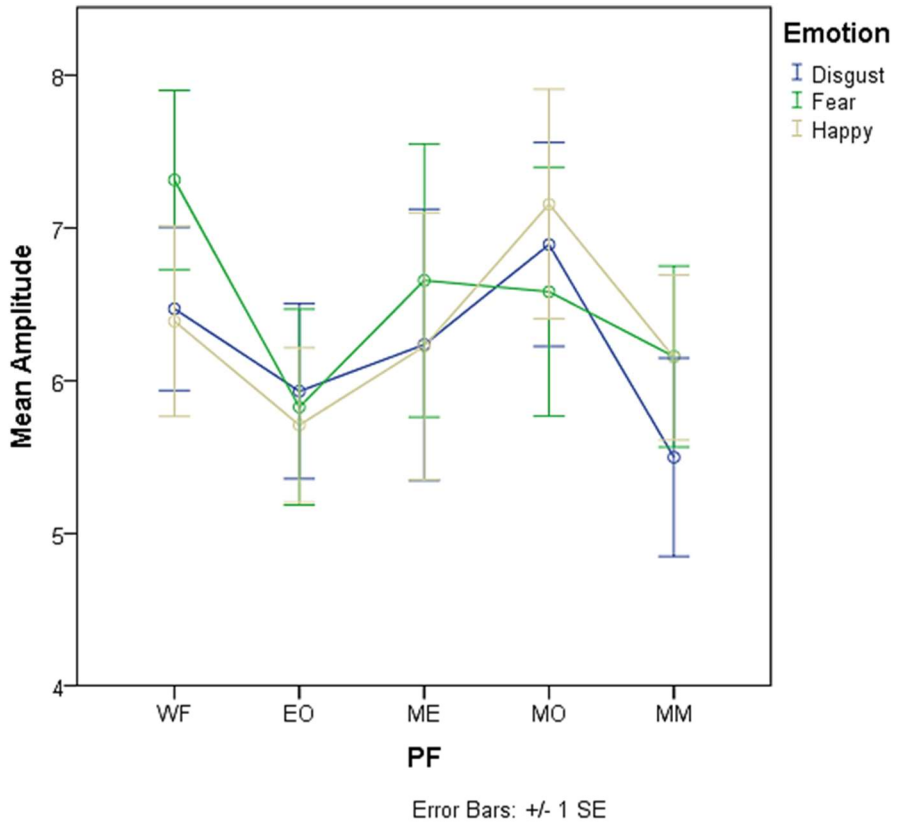

Figure 3.56. Mean amplitude of the P300 response for each emotion and PF in the gender task.

As a result of the significant interaction within the gender task, a simple effects analysis was conducted. Firstly, the effect of emotion at each PF condition was investigated by carrying out five ANOVAs (the WF condition was significant at p = .01), and then the effect of PF condition for each emotion in turn was investigated by carrying out three separate ANOVAs (disgust and fear were significant at p = .04), see simple effects ANOVA results in Table D44 and Table D45 (Appendix D). Additional post-hoc Bonferroni and paired sample t-tests were carried out, see Figures 3.57 and 3.58.

Post-hoc tests revealed differences in the WF condition between fear and happy, as well as fear and disgust (Figure 3.57), with fear causing the strongest amplitude (Figure 3.56). This difference is unlikely to be a result of task difficulty as there was no differences between these conditions in the behavioural gender results (Appendix K), thus the higher signal may be a result of greater processing needed for fear recognition. There is additional significance in disgust between MO and MM, with the MO causing the strongest amplitude (Figure 3.58). This difference is also not seen (uncorrected) in the behavioural gender results for disgust, thus finding

disgust recognition associated with a stronger amplitude in the MO condition implies that features missing for recognition (nose information) have resulted in a bigger ERP response (F. W. Smith & Schyns, 2009). Furthermore, there is significance in fear with a stronger amplitude for the WF than EO and MM. In the gender behavioural results recognition in the WF condition is significantly higher than the EO condition as well as the MM condition (uncorrected). Thus the findings may simply reflect the amount of activity that is generated with whole faces important for recognition. It is also interesting to note that amplitudes were greater, but not significantly so, in the gender task across the emotions and most PF conditions.

A. WF

	Disgust	Fear	Happy
Disgust			
Fear	p = .024		
Happy			

p < .05 corrected (bonferroni)
p < .05 uncorrected
p > .05

Figure 3.57. Paired sample t-test results comparing the differences between the emotions for the significant WF condition (see Table D46 in Appendix D for statistics: t-value, df and p-value).

A. Disgust

	Whole Face	Eyes Only	Minus Eyes	Mouth Only	Minus Mouth
Whole Face					
Eyes Only					
Minus Eyes					
Mouth Only					
Minus Mouth				p = .05	

B. Fear

	Whole Face	Eyes Only	Minus Eyes	Mouth Only	Minus Mouth
Whole Face					
Eyes Only					
Minus Eyes					
Mouth Only					
Minus Mouth					

p < .05 corrected (bonferroni)
p < .05 uncorrected
p > .05

Figure 3.58. Paired sample t-test results comparing the differences between the PF conditions for the significant emotions (see Table D47 in Appendix D for statistics: t-value, df and p-value).

3.3 Study 2

3.3.1 Methods.

3.3.1.1 Participants.

A total of 20 participants (10 females, 10 males) took part in this experiment, aged 18-35 years (M = 23.8, SD = 4.25). Akin to study one, participants were recruited via the paid participant panel and advertisements. All participants were right-handed with normal or corrected to normal vision; they gave written, informed consent in accordance to approved ethics.

3.3.1.2 Stimuli.

Study one unfortunately had limited trials per condition for the nature of an EEG experiment. Therefore, this study was devised using two emotions: fear and happy; as fear concentrates on recognition from the eyes and happiness from the mouth. Thus, the stimuli, totalling 60 different combinations from six identities, five partial face conditions and two emotions, were presented on a grey background at a visual height of 10˚ using E-Prime 2.0 Software.

3.3.1.2.1 Materials.

Again, the Empathy Quotient (EQ) (Baron-Cohen & Wheelwright, 2004) and The Toronto Alexithymia Scale (TAS) (Bagby et al., 1994) were used, for further details on these measures and the distribution of participant scores, see Appendix I.

3.3.1.3 Design and procedure.

Akin to study 1, participants carried out an expression or gender recognition task on presented PF stimuli, whilst their brain activation was measured. In this study both the explicit emotion task and implicit gender task were two AFC; each task consisted of 600 trials, with 10 repetitions of 60 stimuli: 10 conditions (five PF conditions, two emotions), six identities. Each task began with practice trials and took approximately 25-30 minutes, with a break every 50 trials. Each trial consisted of a fixation period (500ms) followed by a face (500ms) and a variable delay period between 1100 and 1500ms before the next trial (see Figure 3.59). Again, sat in a chin rest, participants were asked to respond after the stimulus was displayed; and again, task order was counterbalanced and blocked. Fixation was always on and participants were told to fixate throughout the run. Responses were recorded with a counterbalanced keyboard response of 1 and 2. Participants also undertook an eye-tracking calibration test. Again, the experiment lasted a maximum of three hours and participants were shown the WF stimuli before the experiment commenced.

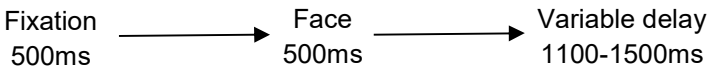

Figure 3.59. Sequence of stimulus presentation.

3.3.1.4 EEG acquisition.

The EEG was recorded with Brain Vision Recorder using the same active 63-channel electrode system (ActiCAP, Brain Products GmbH) as study one. Accordingly the same 10-10 electrode placement system and electrodes for ground, reference and EOG were used (refer to study 1 EEG acquisition). Furthermore, akin to study one, signals were continuously acquired at a sampling rate of 1000hz, with impedance kept below 50kΩ.

3.3.1.5 EEG Data pre-processing for MVPA.

The EEG data were pre-processed with the same steps as study one (refer to the previous pre-processing steps). However, as accuracy rates were higher in this study, only epochs containing correct responses (M = 88%, SD = 8.1%) were included, this ranged from 62% to 98%. Subsequently the number of correct trials per condition was reduced to the lowest number of correct trials in one of the conditions to reduce classification bias.

3.3.1.6 Multi-variate pattern analysis.

Again, MVPA was conducted on single-trial EEG signal using a linear SVM (LIBSVM 3.20 toolbox, Chang & Lin, 2011). In this study, pattern classifiers were trained to discriminate between the two expressions, independently for each PF condition and task. The classifiers were again trained to decode the expression presented in single trials from 15 time windows of the EEG signal across 19 posterior and visual electrodes using the same k-fold cross validation and overlapping time bin approach (refer to the MVPA analysis in study one). Akin to study one, decoding accuracy was reported for each PF condition in 15 time steps of an 800 time point window (-200 to 600ms) using one-tailed one sample t-test results, with chance level of 50%. Significance levels are presented on graphs with $p < .05$ displayed with an 'X' and $p < .05$ (FDR corrected) displayed with a '*'.

3.3.1.7 Univariate EEG pre-processing and analysis.

The same offline pre-processing and analysis steps were conducted to that of study one (see above); with the analysis carried out on the previously chosen ROIs

(Figure 3.41). However, in this study, instead of including all epochs in the analysis, only epochs containing correct responses were included.

3.3.2 Results

3.3.2.1 Behavioural results.

Unlike the fMRI experiment, behavioural data revealed that participants subjectively performed better in the expression (M = 88.88%, SD = 9.65%) than the gender task (M = 87.59%, SD = 8.51%) when averaged across all PF conditions. Performance was highest in the ME and MM, followed by the WF in the expression task and performance was highest in the WF for the gender task, closely followed by the ME, MO and MM conditions (Table 3.4). Comparing emotion recognition accuracy, participants were subjectively more accurate at recognising happiness (M = 89.9%, SD = 8.41%) than fear (M = 87.8%, SD = 10.25%).

Table 3.4.

All to 2d.p in percentage. WF: whole face, EO: eyes only, ME: minus eyes, MO: mouth only, MM: minus mouth.

Task	WF	EO	ME	MO	MM
Expression	90.33 (SD = 8.93)	83.58 (SD = 10.75)	91.58 (SD = 7.98)	87.54 (SD = 9.73)	91.38 (SD = 9.14)
Gender	90 (SD = 7.67)	82.78 (SD = 9.44)	88.97 (SD = 7.38)	88.17 (SD = 9.24)	88.1 (SD = 7.54)

3.3.2.1.1 Emotion accuracy.

A two-way repeated measures ANOVA was employed to explore the effects of PF condition and emotion on accuracy in the expression task. There was a significant main effect of PF condition, $F(2.460, 664.995) = 21.665$, $p < .001$, $\eta_p^2 = .533$ (greenhouse-geisser corrected), but no significant main effect of emotion on accuracy, $F(1, 19) = .483$, $p = .496$, $\eta_p^2 = .025$ (Figure 3.60). Furthermore there was a near significant interaction between PF and emotion, $F(2.961, 56.254) = 2.765$, $p = .051$, $\eta_p^2 = .127$ (greenhouse-geisser corrected).

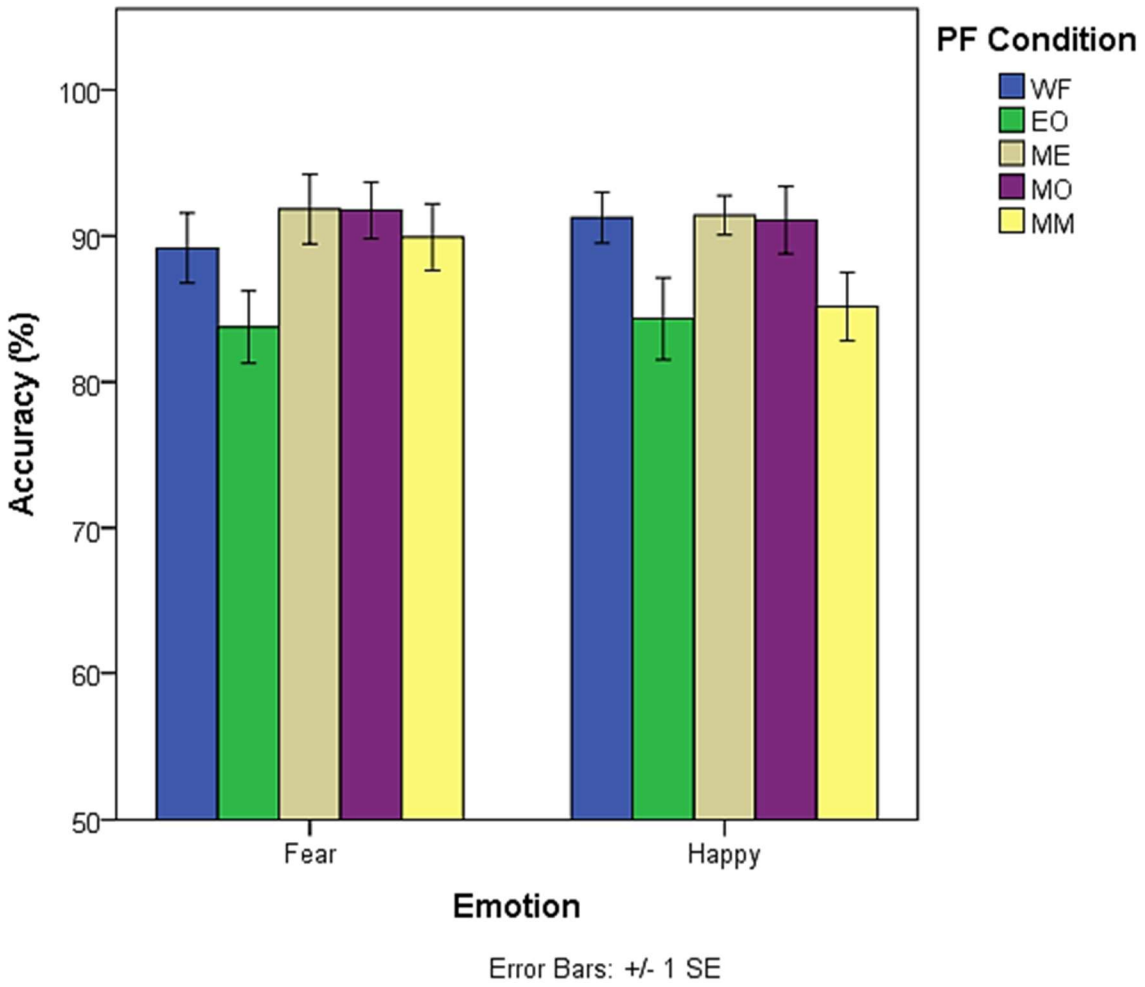

Figure 3.60. Overall recognition accuracy (%) in each PF condition for each emotion.

As it was a near significant interaction, a simple effects analysis was carried out to understand what effects were likely to be behind this. ANOVAs testing the effect of emotion at each PF condition found significance in the MM condition ($F(1, 19) = 8.855$, $p = .008$, $\eta_p^2 = .318$) with fear recognised more accurately than happiness. Testing the effect of PF condition for each emotion found significance for both happiness and fear ($p < .001$); the simple effects ANOVA results can be found in Table D48 and Table D49 (Appendix D). Additional post-hoc Bonferroni and paired sample t-tests were carried out to understand the differences between the conditions, see Figure 3.61.

A. Happy

	Whole Face	Eyes Only	Minus Eyes	Mouth Only	Minus Mouth
Whole Face					
Eyes Only					
Minus Eyes					
Mouth Only					
Minus Mouth					

B. Fear

	Whole Face	Eyes Only	Minus Eyes	Mouth Only	Minus Mouth
Whole Face					
Eyes Only					
Minus Eyes					
Mouth Only					
Minus Mouth					

$p < .05$ corrected (bonferroni)

$p < .05$ uncorrected

$p > .05$

Figure 3.61. Paired sample t-test results comparing the differences between the PF conditions for the significant emotions (see Table D50 in Appendix D for statistics: t-value, df and p-value).

In fear and happiness recognition there were significant differences between the EO and other PF conditions (apart from EO and MM in happiness), reflecting the poor performance for EO (Figure 3.60 & 3.61). There were also differences between the MM and most other PF conditions in happiness, also reflecting poor performance in this condition. Interestingly, these results show eye information in fear to be less important when asked to categorise between these two emotions, but still the mouth to be more important in happiness than fear recognition (F. W. Smith & Schyns, 2009; M. L. Smith et al., 2005).

3.3.2.1.2 Gender accuracy.

A two-way repeated measures ANOVA was employed to explore the effects of PF condition and gender on accuracy in the gender task. There was a significant main effect of PF condition, $F(4, 76) = 11.290$, $p < .001$, $\eta_p^2 = .393$ and gender on accuracy, $F(1, 19) = 5.424$, $p = .031$, $\eta_p^2 = .222$, with participants significantly more accurate at recognising the male faces (M = 89.23%) than the female faces (M = 85.96%) (Figure 3.62). There was also a significant interaction between PF and gender, $F(2.474, 47.002) = 11.791$, $p < .001$, $\eta_p^2 = .383$ (greenhouse-geisser corrected).

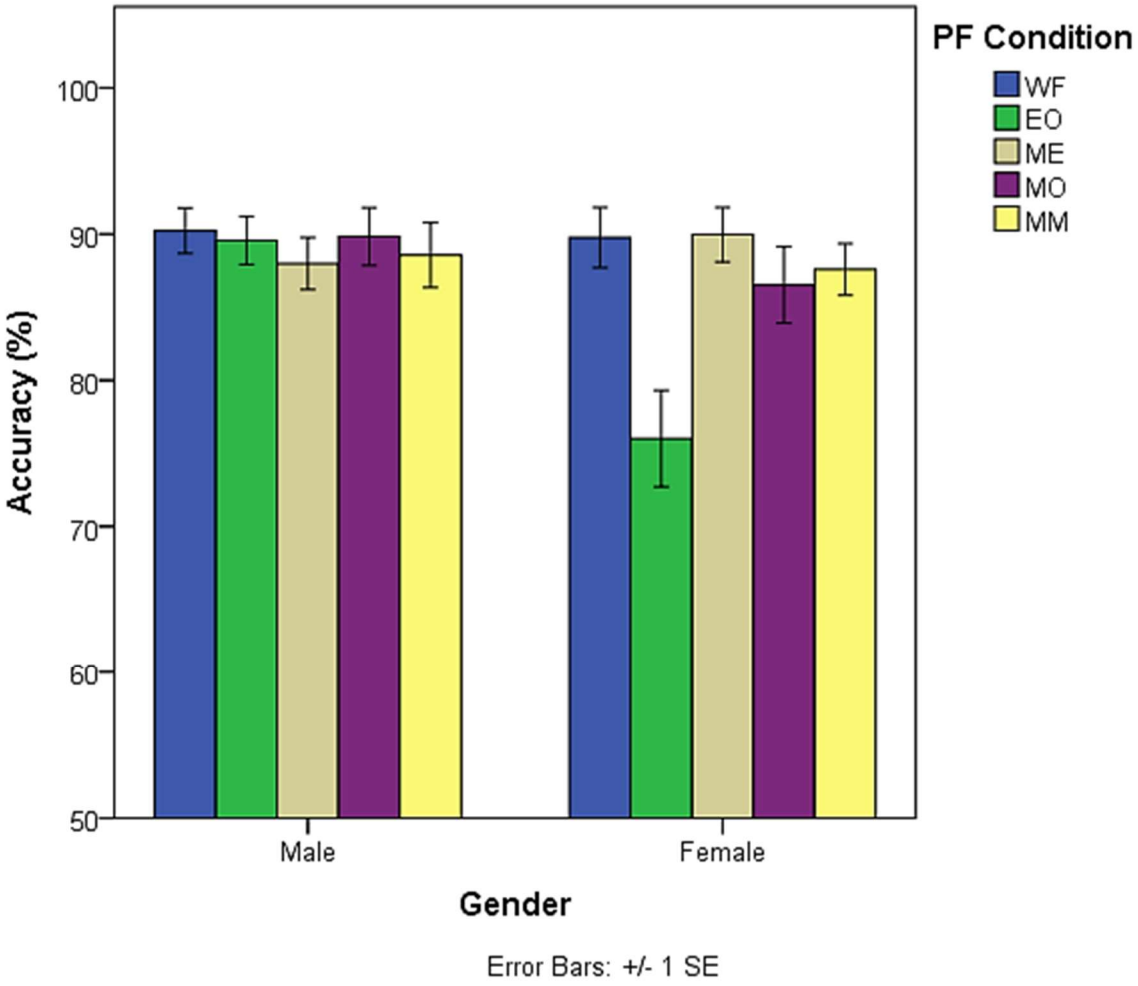

Figure 3.62. Overall recognition accuracy (%) in each PF condition between male and female stimuli.

Again, a simple effects analysis was undertaken. ANOVAs testing the effect of gender for each PF condition only found significance in the EO condition ($F(1, 19) = 19.919$, $p < .001$, $\eta_p^2 = .512$) with male faces being recognised better than female faces in this condition. Testing the effect of PF condition on gender found significance for the female faces only ($F(2.047, 38.893) = 17.034$, $p < .001$, $\eta_p^2 = .473$ (greenhouse-geisser corrected)); the simple effects ANOVA results can be found in Table D51 and Table D52 (Appendix D). Further post-hoc tests were carried out (Figure 3.63). These show greatest significance in the EO condition (Figure 3.63), where performance is worse (Figure 3.62). This finding was also present in the previous EEG study and in the fMRI results (Chapter 2), although it is unclear why this is.

A. Female

	Whole Face	Eyes Only	Minus Eyes	Mouth Only	Minus Mouth
Whole Face					
Eyes Only					
Minus Eyes					
Mouth Only					
Minus Mouth					

$p < .05$ corrected (bonferroni)
$p < .05$ uncorrected
$p > .05$

Figure 3.63. Paired samples t-test results for PF condition in female stimuli (see Table D53 in Appendix D for statistics: t-value, df and p-value).

An ANOVA (akin to the emotion task) exploring the effect of PF and emotion on accuracy was also conducted (see Appendix M). Furthermore, ANOVAs exploring the effect of PF and emotion on reaction time for both the emotion and gender task were conducted (see Appendix N).

3.3.2.2 MVPA results.

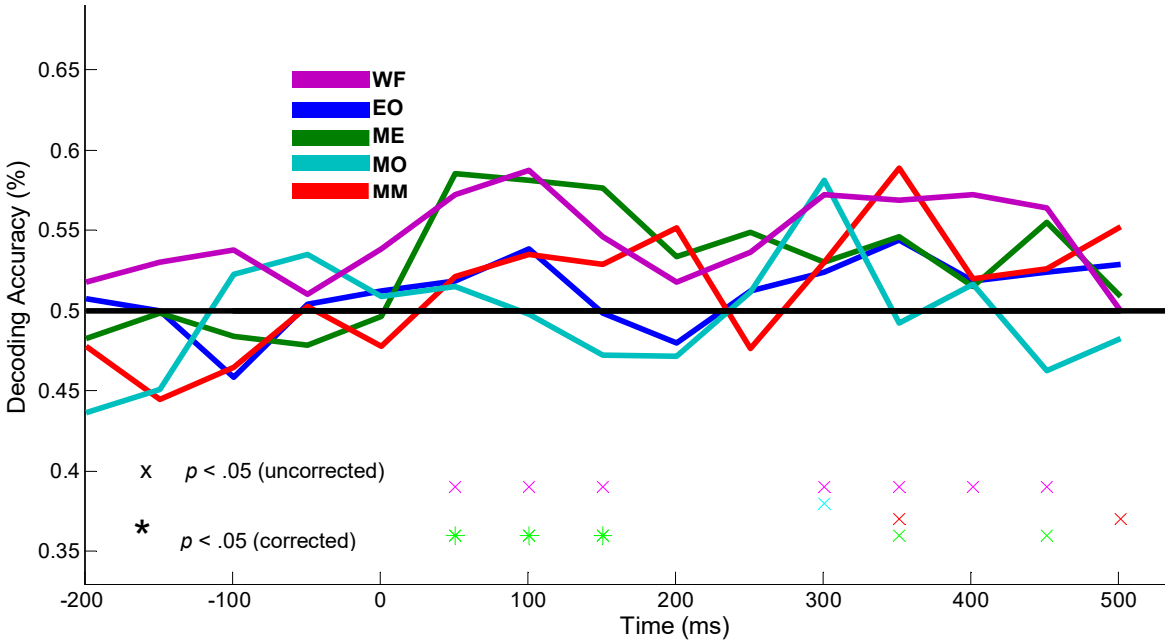

Figure 3.64. Decoding Expression, Expression Task.

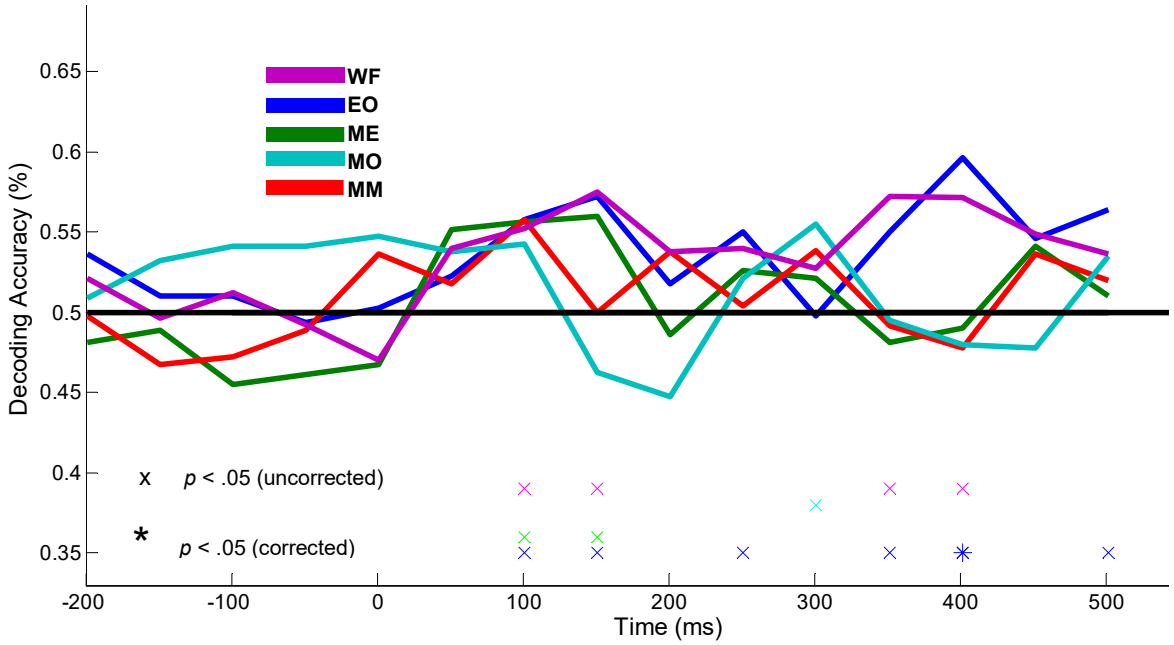

Figure 3.65. Decoding Expression Gender Task.

Significant ($p < .05$) FDR effects are greatest in the ME condition with medium effect-sizes for 50-250ms in the explicit task (Figure 3.64); demonstrating early decoding accuracy for expression in the ME condition. As this condition has mouth information present, it seems, akin to study 1, that the mouth is more informative; corroborating with Neath-Tavares and Itier (2016) and other research demonstrating the importance of the mouth in early expression recognition (Jack et al., 2009; F. W. Smith & Schyns, 2009). This early significance is also likely to reflect the N170 response and thus STS or FG activation and again matches up with finding explicit task decoding accuracy for the STS in the preceding fMRI experiment. In addition, there are trends with small to medium effect-sizes in the WF (50-250ms and 300-550ms), ME (350-450ms and 450-550ms) and MO condition (300-400ms). These trends also somewhat demonstrate the importance of the mouth in expression recognition, and this is further supported with finding no trends for the EO condition in the explicit task. This is surprising considering the importance of the eyes in processing faces and more specifically emotions (Baron-Cohen, 2004; F. W. Smith et al., 2008; M. L. Smith et al., 2005; Whalen et al., 2004), however, there is also a trend for the MM condition (350-450ms with a medium effect-size, and 500-600ms with a small effect-size).

Given that behavioural accuracy is good in the implicit task, it is surprising that there is only one significant ($p < .05$) FDR effect, and this is in the EO condition between 400 and 500ms (Figure 3.65), $t(19) = 3.176$, $p = .003$, $d = 0.71$ (medium

effect-size). There are trends with small to medium effect-sizes in expression decoding for the implicit task; with early decoding accuracy in the WF, EO and ME condition between 100 and 250ms, MO condition between 300 and 400ms, as well as later decoding trends in the WF condition between 350 and 500ms, and the EO condition between 250-350ms, 350-450ms and 500-600ms. These late decoding trends are likely to reflect when the brain has completed its representation of a face (Cauchoix et al., 2014). The suggestion of more robust decoding of expression in the explicit (Figure 3.64) compared to the implicit task (Figure 3.65), in terms of more significant time points overall, maps onto the STS fMRI results, as it is comparable to the results found for the STS, where explicit decoding of expression was stronger than implicit decoding of expression.

It is interesting to find the EO condition significant for the implicit task in this study; this is supportive of previous literature finding information from the eyes sufficient for expression discrimination (Itier et al., 2007). It is surprising that this did not show in the explicit task or in study 1. However, it was the implicit task in the previous literature where emotion differences were present, rather than in the explicit task (Neath-Tavares & Itier, 2016; M. L. Smith, 2011). Furthermore, the classifier in study 2 was decoding between two emotions: fear and happy; as a stronger difference tended to be found in implicit fear recognition (Neath-Tavares & Itier, 2016; M. L. Smith, 2011), generally garnered from eye information (F. W. Smith & Schyns, 2009; M. L. Smith et al., 2005), the extra emotion and subsequent conditions in study 1 may have concealed this result.

Whilst the basic decoding MVPA analysis has again provided some interesting results, this study, as aforementioned, does not have enough significant conditions to reliably run the planned cross-classification analyses. Again, statistical power may be a potential factor causing this. Thus, these results must, for a second time, be classed as exploratory; the time-course of processing and potential feedforward and feedback affects cannot be ascertained reliably from the present data. Again, in order to relate the current studies to the past ERP face perception research outlined in the introduction (Batty & Taylor, 2003; Eimer, 1998; Hinojosa et al., 2015; Itier et al., 2007; Neath-Tavares & Itier, 2016), an ERP analysis was carried out on the data.

3.3.2.3 Univariate results.

3.3.2.3.1 rN170.

A repeated measures ANOVA was employed to explore the effects of task (2), emotion (2) and PF condition (5) on the mean amplitude in the rN170 time window (140-190ms). There was a near significant main effect of task, $F(1, 19) = 4.303$, $p = .052$, $\eta_p^2 = .185$, with amplitudes greater in the gender (M = -6.06) than the emotion task (M = -5.47), but a non-significant main effect of emotion on the mean amplitude, $F(1, 19) = .274$, $p = .607$, $\eta_p^2 = .014$. However, there was a significant main effect of PF condition, $F(2.321, 44.092) = 3.932$, $p = .022$, $\eta_p^2 = .171$ (greenhouse-geisser corrected), where amplitudes were greatest in the ME (M = -6.66), followed by EO (M = -6.19), MO (M = -5.86), MM (M = -5.13) and WF condition (-5) (Figure 3.66). Post-hoc pairwise comparisons, with Bonferroni correction, show a significant difference between the ME and MM condition ($p = .001$). There were no significant interactions within the ANOVA.

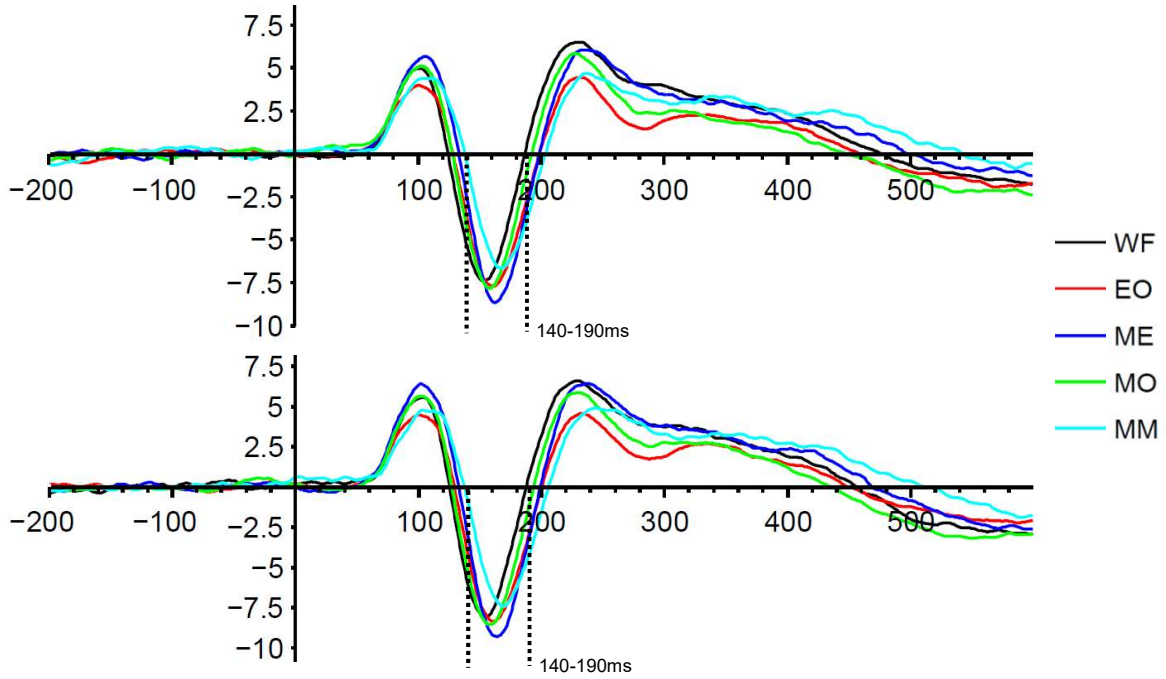

Figure 3.66. rN170 (PO8, P8) grand average ERP (µV) split by PF condition in the emotion task (top) and gender task (bottom). Time window (140-190ms) used for analysis marked with dash lines. Negative voltage plotted down.

3.3.2.3.2 lN170.

A repeated measures ANOVA was employed to explore the effects of task, emotion and PF condition on the mean amplitude in the lN170 time window (140-

190ms). There was a non-significant main effect of task, $F(1, 19) = 2.274$, $p = .148$, $\eta_p^2 = .107$ and emotion on the mean amplitude, $F(1, 19) = .570$, $p = .460$, $\eta_p^2 = .029$. However, there was a significant main effect of PF condition, $F(2.638, 50.117) = 4.311$, $p = .011$, $\eta_p^2 = .185$ (greenhouse-geisser corrected), where amplitudes were greater in the MO (M = -4.29), followed by the ME (M = -4.28), WF (M = -3.74), EO (M = -3.57) and MM condition (M = -2.57) (Figure 3.67). Post-hoc pairwise comparisons, with Bonferroni correction, show significant differences between the ME and MM ($p = .012$), as well as the MO and MM conditions ($p = .011$). There was also a significant interaction between emotion and PF condition, $F(4, 76) = 5.534$, $p = .002$, $\eta_p^2 = .226$, see Figure 3.68.

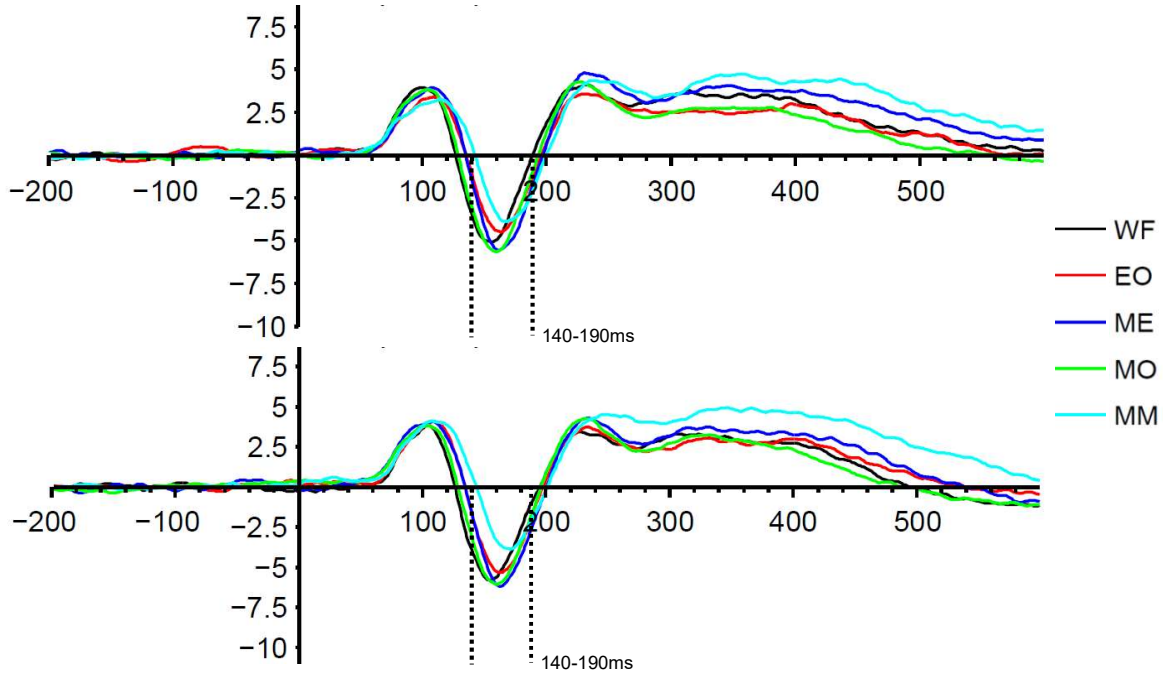

Figure 3.67. lN170 (PO7, P7) grand average ERP (μV) split by partial face condition in the emotion task (top) and gender task (bottom). Time window (140-190ms) used for analysis marked with dash lines. Negative voltage plotted down.

To explore this interaction a simple effects analysis was conducted, where, seven separate repeated measures ANOVAs were carried out (these analyses were collapsed across task). Firstly, the effect of emotion at each PF condition was investigated by carrying out five ANOVAs (the MM condition was significant at $p < .05$), and then the effect of PF condition for each emotion in turn was investigated by carrying out two separate ANOVAs (fear was significant at $p < .05$, happiness was near significance at $p = .055$); the simple effects ANOVA results can be found in

Table D54 and Table D55 (Appendix D). Additional post-hoc Bonferroni and paired sample t-tests were carried out (Figure 3.69), these included further exploratory tests for happiness as the ANOVA result was near significance.

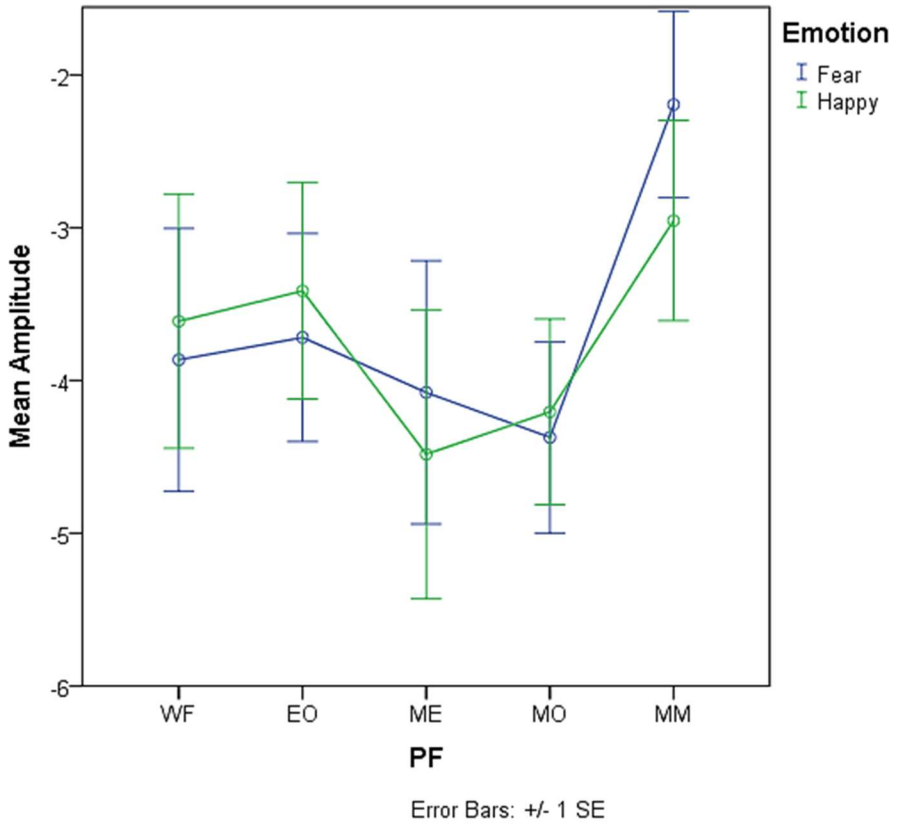

Figure 3.68. Mean amplitude of the lN170 for each emotion and PF, collapsed across task.

These tests revealed significance between the ME and MM for fear and happiness (Figure 3.69); as strong amplitudes are present in the ME and weak amplitudes are present in the MM condition (Figure 3.68). Finding fear associated with a stronger amplitude in the ME condition implies that occluding the features needed for fear recognition (the eyes) (Greening et al., 2018; F. W. Smith & Schyns, 2009; M. L. Smith et al., 2005) creates stronger amplitudes around the N170 ERP, potentially involved in feedback processes. This corresponds with the behavioural results showing no differences in accuracy between the ME and MM condition for fear. However, finding larger amplitudes in the ME condition for happiness supports the task difficulty explanation as behavioural emotion results show participants to be more accurate at recognising happiness from ME than MM stimuli; as the mouth is more important for task completion (F. W. Smith & Schyns, 2009).

A. Fear

	Whole Face	Eyes Only	Minus Eyes	Mouth Only	Minus Mouth
Whole Face					
Eyes Only					
Minus Eyes					
Mouth Only					
Minus Mouth					

B. Happy

	Whole Face	Eyes Only	Minus Eyes	Mouth Only	Minus Mouth
Whole Face					
Eyes Only					
Minus Eyes					
Mouth Only					
Minus Mouth					

$p < .05$ corrected (bonferroni)
$p < .05$ uncorrected
$p > .05$

Figure 3.69. Paired sample t-test results comparing the differences between the PF conditions for each emotion (see Table D56 in Appendix D for statistics: t-value, df and p-value).

3.3.2.3.3 P100.

A repeated measures ANOVA was employed to explore the effects of task, emotion and PF condition on the mean amplitude in the P100 time window (80-120ms). There was a non-significant main effect of task, $F(1, 19) = 1.422$, $p = .248$, $\eta_p^2 = .070$ and emotion on the mean amplitude, $F(1, 19) = .750$, $p = .397$, $\eta_p^2 = .038$. However, there was a significant main effect of PF condition, $F(2.506, 47.610) = 3.876$, $p = .020$, $\eta_p^2 = .169$ (greenhouse-geisser corrected), where amplitudes were greater in the ME (M = 5.518), followed by the MM (M = 4.78), MO (M = 4.4), WF (M = 4.05) and EO condition (M = 4.02) (Figure 3.70). Post-hoc pairwise comparisons, with Bonferroni correction, show a significant difference between the WF and ME condition ($p = .022$). There was also a significant interaction between emotion and PF condition, $F(4, 76) = 3.441$, $p = .012$, $\eta_p^2 = .153$, see Figure 3.71.

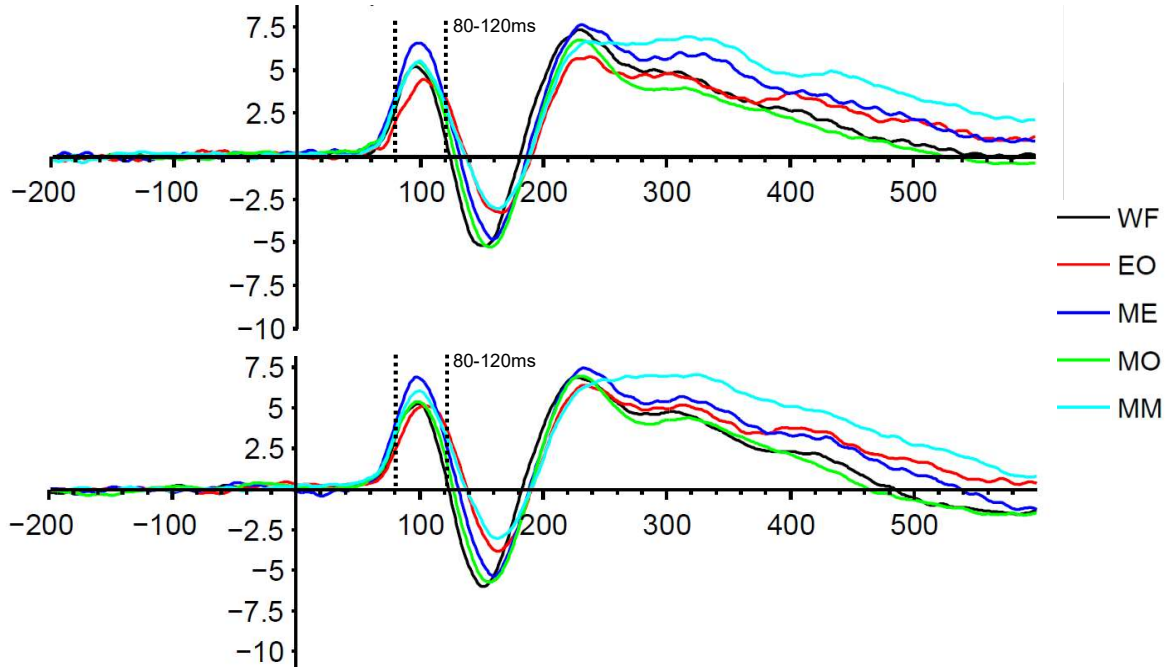

Figure 3.70. P100 (O1, O2) grand average ERP (μV) split by PF condition in the Emotion Task (top) and gender task (bottom). Time window (80-120ms) used for analysis marked with dash lines. Positive voltage plotted up.

To explore this interaction a simple effects analysis was conducted, where, seven separate repeated measures ANOVAs were carried out (these analyses were collapsed across task). Firstly, the effect of emotion at each PF condition was investigated by carrying out five ANOVAs (the EO, $F(1, 19) = 4.367$, $p = .05$, $\eta_p^2 = .187$, and MO condition were significant, $F(1, 19) = 4.532$, $p = .047$, $\eta_p^2 = .193$, as responses to happiness were greater than fear in these two conditions), and then the effect of PF condition for each emotion in turn was investigated by carrying out two separate ANOVAs (fear but not happiness was significant at $p < .05$); the simple effects ANOVA results can be found in Table D57 and Table D58 (Appendix D). Additional post-hoc Bonferroni and paired sample t-tests were carried out to understand the differences between the conditions in fear recognition, see Figure 3.72. These tests showed differences between the ME and all other PF conditions (Figure 3.72); with the P100 responding maximally to the ME condition in fear (Figure 3.71). Thus the heightened amplitude in the ME condition for fear may reflect early top-down processing to the eye region that is missing for recognition, or it may simply result from task difficulty.

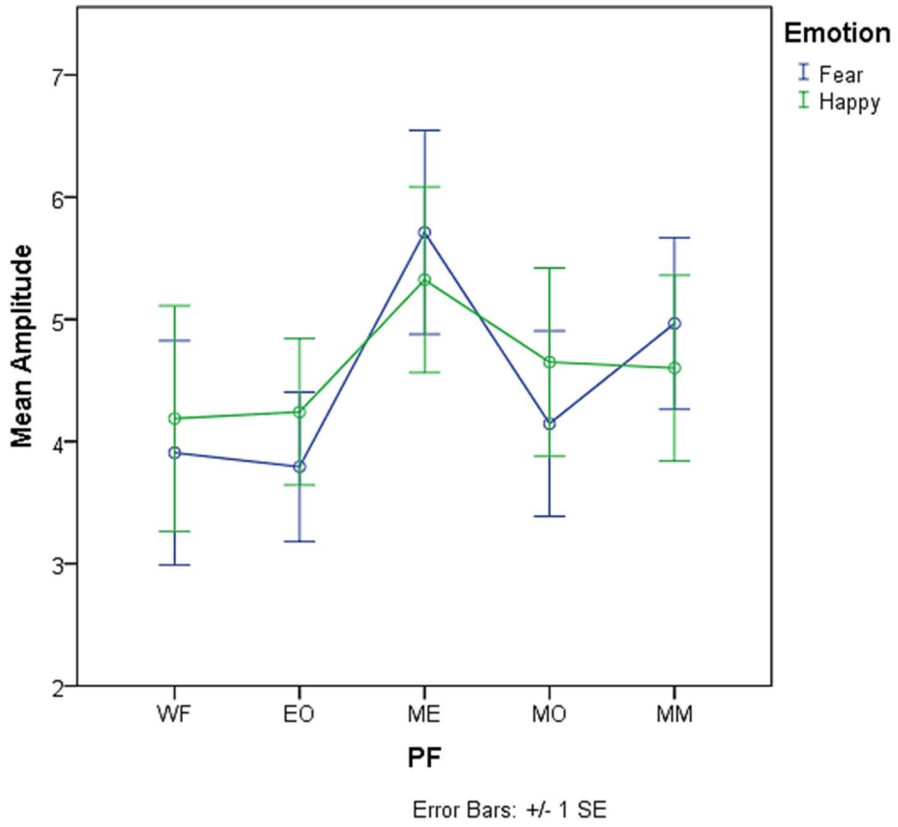

Figure 3.71. Mean amplitude of the P100 for each emotion and PF, collapsed across task.

A. Fear

	Whole Face	Eyes Only	Minus Eyes	Mouth Only	Minus Mouth
Whole Face					
Eyes Only					
Minus Eyes					
Mouth Only					
Minus Mouth					

$p < .05$ corrected (bonferroni)
$p < .05$ uncorrected
$p > .05$

Figure 3.72. Paired sample t-test results comparing the differences between the PF conditions for fear (see Table D59 in Appendix D for statistics: t-value, df and p-value).

3.3.2.3.4 P300.

A repeated measures ANOVA was employed to explore the effects of task, emotion and PF condition on the mean amplitude in the P300 time window (300-500ms). There was a non-significant main effect of task, $F(1, 19) = .484$, $p = .495$, $\eta_p^2 = .025$, but a significant main effect of emotion on the mean amplitude, $F(1, 19)$

= 9.274, p = .007, η_p^2 = .328, with greater amplitudes for fear (M = 5.92) than happy (M = 5.59). There was also a significant main effect of PF condition, F(2.414, 45.862) = 16.649, p < .001, η_p^2 = .467 (greenhouse-geisser corrected), where amplitudes were greater for the MM (M = 7.08), followed by the ME (M = 6.39), EO (M = 5.53), WF (M = 5.1) and MO condition (M = 4.68) (Figure 3.73). Post-hoc pairwise comparisons, with Bonferroni correction, show significant differences between the WF and ME (p = .013), WF and MM (p = .005), EO and MO (p = .003), EO and MM (p = .002), ME and MO (p < .001), as well as the MO and MM conditions (p < .001). There were no significant interactions within the ANOVA.

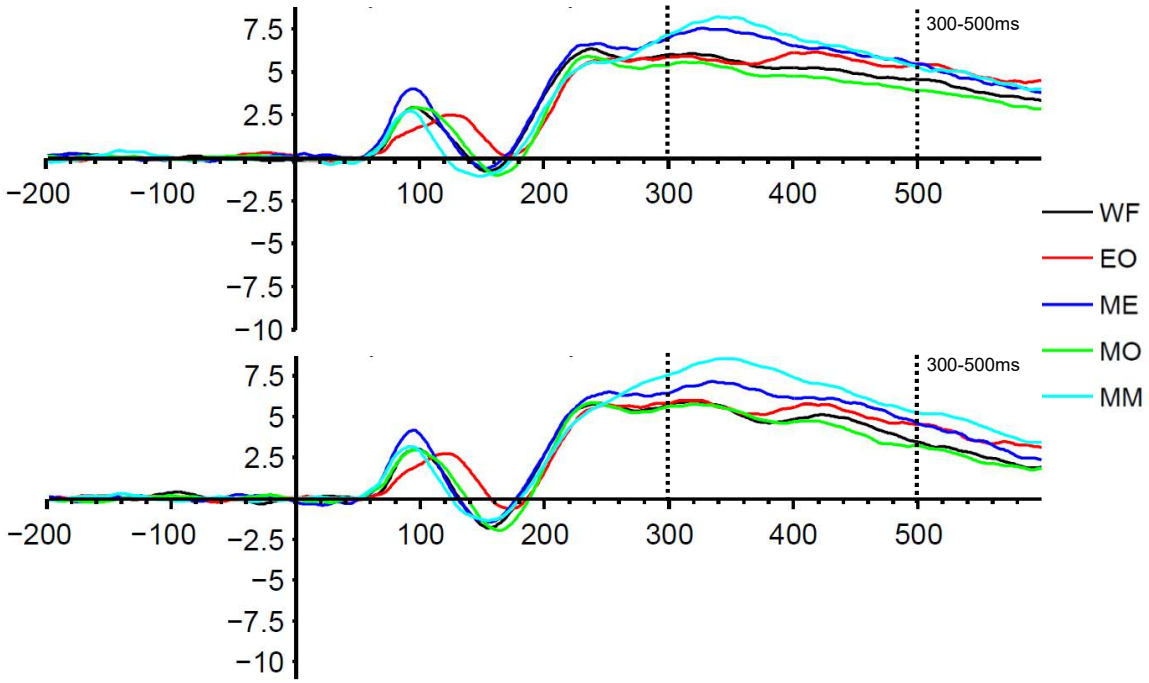

Figure 3.73. P300 (Pz, PO3, POz, PO4) grand average ERP (μV) split by partial face condition in the Emotion task (top) and gender task (bottom). Time window (300-500ms) used for analysis marked with dash lines. Positive voltage plotted up.

3.4 Discussion

This study, akin to the fMRI experiment, principally set out to explore the cross-decoding of expression across conditions with non-overlapping feature information and investigate how task context may affect this. Unfortunately, due to the limited significance found in the basic MVPA decoding, the cross-classification analyses to investigate H1 could not be carried out. Nevertheless, the basic decoding and ERP analyses provide insight into the temporal processing of occluded facial expressions and are fruitful to compare against the fMRI results.

3.4.1 MVPA results.

The basic MVPA decoding results showed that expression could be decoded from 50ms to 700ms post-stimulus onset, with variations across PF conditions. The heightened early significance, distributed across the time window, supports research demonstrating the sensitivity of multivariate approaches, in revealing effects that are overlooked by traditional ERP components (Ghuman et al., 2014; Nemrodov et al., 2016). It is surprising that expression can be decoded at 50-150ms in this study, but other research has found significance for identity or general face decoding as early as 50ms (Ghuman et al., 2014; Kaneshiro et al., 2015) or 70ms (Cichy et al., 2014; Nemrodov et al., 2016). These early time effects could reflect the processing of low-level stimulus features, or suggest the importance of processing faces due to their biological salience (Pessoa & Adolphs, 2010). However, it is not possible to ascertain whether the early time effects in this study (between 50 and 150ms) are or are not a result of low-level stimulus features. To clearly adjudicate this, these results need to be compared with behavioural studies or a low-level model.

For both studies, decoding was more robust (with more time points significant overall) in the explicit task where subjects were asked to recognise expression. Whilst this seems to contradict H2, and prior fMRI findings, that expression decoding will be stronger in the implicit task; it should be noted that this experiment, as opposed to the fMRI experiment, was more closely linked to decoding in the FG and STS than early visual areas of the brain. As such, the suggestion of stronger decoding in the explicit task corresponds with the high classifier performance found in the fMRI experiment for the STS (Chapter 2, 2.3.3.1.2). In the explicit task for study one, decoding accuracy was significant in the ME (250-350ms) and MO condition (300-400ms), with significance greatest in the ME condition (50-250ms) for study two. Both the ME and MO conditions show significant decoding accuracy in the fMRI experiment for the STS; and the MO condition was subjectively higher for explicit than implicit in the FG (but this was not significant). Thus these results further support the idea that this is more closely linked to decoding in the STS and FG. Furthermore, the MM condition was not significant in study two or in study one before 500ms. The MM condition was also not significant in the explicit task for the STS or FG in the fMRI experiment, suggesting further consistency between the two studies.

The finding of more robust decoding in the explicit task corroborates with research showing an attenuation of the N170 (thought to reflect FG or STS activation) during an implicit task involving gender categorisation (Wronka & Walentowska, 2011). Further research found greater P300 amplitudes (reflecting processing further down the ventral stream and around the STS) when participants were asked to attend to an explicit emotion task with features relevant for task completion, than to a gender task (Hajcak et al., 2010; Krolak-Salmon et al., 2001; M. L. Smith et al., 2004).

The MVPA results appear to reflect three decoding phases that also bear resemblance with face-selective ERP components (Cauchoix et al., 2014; Kaneshiro et al., 2015). It seems that there is an early decoding phase around 100ms that is indicative of feedforward processing (P100). This feedforward sweep is generally associated with the processing of low-level stimulus properties (Cauchoix et al., 2014), such as the high contrast of the mouth (Neath-Tavares & Itier, 2016). This supports the idea that responses to positive emotions are elicited earlier than negative emotions, as the mouth is most commonly used for happiness recognition (Batty & Taylor, 2003; Neath-Tavares & Itier, 2016). However, the early decoding of the mouth, only apparent in the explicit tasks (MO trend at 100-250ms in study one and the early ME significance in study two at 50-250ms), could also reflect essential rapid (top-down feedback) processing to an area important for expression recognition (Jack et al., 2009; F. W. Smith & Schyns, 2009). This is also supported by the P100 likely corresponding to V1 activation, thus whilst reflecting early visual processing, this area could also contain feedback effects (Cichy et al., 2014). There also seems to be a second decoding phase around 170ms (N170), likely to reflect recurrent processing of the stimulus, and a later phase post 300ms (P300).

This later phase would be indicative of feedback processes if amplitudes are greater for partial than WF stimuli. This is because unexpected partial stimuli are likely to be more difficult to process (Ghuman et al., 2014; Hajcak et al., 2010; Tang et al., 2014) with subjects needing to predict missing feature information (Greening et al., 2018) to make an accurate emotion or gender categorisation. Results suggest this in the explicit task with significance in study one at 300-400ms, 500-600ms and 600-700ms for the MO condition, additional significance at 500-600ms for the MM condition and at 600-700ms for the ME condition; as well as trends in expression decoding in study two for the MO (300-400ms), MM (350-450ms and 500-600ms)

and the ME condition (350-450ms and 450-550ms). However, the WF condition was also significant in study one at these times points, with additional respective trends in study two. Nonetheless, in the implicit task for study two, the EO could be decoded but the WF condition could not at 400-500ms, supporting the idea that later time points are involved in the processing of partial stimuli.

Finding significance in the EO condition for the implicit task in study two is interesting, suggesting the importance of the eyes in processing expression, particularly when attention is not explicitly directed for recognition. Significance in the EO condition was shown in the amygdala of the fMRI experiment for implicit expression decoding. This potentially reveals an exciting cross-over effect; with the absence of the eyes important for explicit tasks and the presence of the eyes important for implicit tasks. Whilst, the presence of the eyes was also important for implicit tasks in V1 and EVC, it is important to note that the absence of the eyes was more important for these regions in the implicit task.

In the explicit task the most consistent decoding occurred in response to the WF condition in study 1 and the ME condition in study 2. However, the ME condition seems particularly important in the explicit tasks of both studies, with significance in study 1 around 250-350ms and significance in study 2 around 50-250ms. In the implicit tasks, there were trends in decoding for all PF conditions except the EO condition in study 1 and the MM condition in study 2.

Based on previous literature, it is expected that the time of decoding would occur later for partial that whole face stimuli. This seems to apply in the explicit task for study 1, whereby significant decoding begins in the WF condition around 100ms and significant decoding in the PF conditions begins later around 250-350ms. This is in line with accounts of visual processing, such as predictive coding and recurrent feedback models of object recognition. However, it is important to note the potential confound of less information in the partial stimuli, which may instead be driving these delays in response. Moreover, partial stimuli cannot be compared with whole stimuli in the implicit task of study one as no conditions were significantly decoded. Further, results in the explicit task for study two only show significant decoding to occur in the ME condition, and results for the implicit task only show the EO significant at 400-500ms. Therefore, from the MVPA results, it is not possible to fully address whether decoding would occur later for partial than whole face stimuli.

Overall these were the first EEG experiments to examine the decoding of expression from PF stimuli and the MVPA analyses garnered some interesting results. It has shown that expression can be decoded from partial stimuli, and provides a complementary view to the ERP analysis, on the neural time-course of expression processing under conditions of occlusion (De Vos et al., 2012). Whilst the concern of insufficient trials (36 trials per condition in study one when split by both PF and emotion) was addressed by carrying out a second study with more trials and only two emotions; there were potentially still insufficient trials in study two (60 trials per condition) to yield enough basic decoding significance and reliably run the cross-classification analyses. Previous MVPA face decoding EEG and MEG studies have used a range of trials per condition, from 20-30 trials in Cichy et al. (2014), 72 trials in Kaneshiro et al. (2015), 270 trials in Cauchoix et al. (2014), to over 650 trials per condition in Nemrodov et al. (2016). Furthermore, the experiments in this chapter may have also tested insufficient participants and thus generally had insufficient power. This is a greater concern in experiment one, with only 14 participants used in the final analyses. Ideally a sample size close to 30 or above would have been collected. Although research has started to apply MVPA to EEG data, it has not examined the ideal number of trials or participants to use in these studies. It is clear that future MVPA research is needed to explore the neural processing of occluded facial expressions; with a simplified design consisting of more trials or fewer conditions, as well as a greater number of participants.

3.4.2 Univariate results.

In both experiments the ERP analysis showed PF condition and emotion to affect the mean amplitudes of the selected ERP components (the N170, P100 and P300). This was particularly evident bilaterally in the N170 (rN170 of study one, lN170 of study two), whereby amplitudes were greatest when the eyes were occluded (albeit the ME or the MO condition) and weakest when information from the eyes was available (MM). These findings are inconsistent with previous research finding occluded eyes to have no effect on the N170 (Eimer, 1998; Itier et al., 2007) and eyes only stimuli to increase the amplitude (Bentin et al., 1996; Itier & Batty, 2009; Nemrodov et al., 2014; Rousselet et al., 2014). This previous research was focussed on face detection and orientation or contrast judgement tasks; expression or gender recognition tasks were not used. However, studies using the bubbles technique has shown information from the eyes and mouth to be important (M. L.

Smith et al., 2005), and further the presence of the eyes to drive the N170 response, especially in fear (Schyns et al., 2007). Whilst the greatest amplitudes are to the ME condition in this study, the research does not dispute the eye-sensitivity of the N170. This is because the increased amplitude may reflect the occurrence of a prediction or an error signal in predictive coding, helping predict and fill in the important missing feature information; that they expect to make their emotion or gender judgement (Greening et al., 2018; Hajcak et al., 2010).

However, the nature of occlusion may be driving the differences in N170 effects for occluded eye stimuli. In this chapter's experiments, the occluded eyes are overlaid in black; whereas the previous research removed the eyes by blending it to the same colour of the face (Eimer, 1998; Itier et al., 2007). Johnson and Olshausen (2005) showed how the recognition of a partially occluded object is affected by removing information, as opposed to using an occluder. This recognition advantage of using an occluder is thought to occur as feature absence can be explained by amodal completion; visualising the continuation of an objects shape (Johnson & Olshausen, 2005). This amodal completion cannot occur when objects have been removed (Johnson & Olshausen, 2005). Therefore, finding an N170 effect in the chapter's experiments, as opposed to previous research, may be explained by an occluder promoting the use of amodal completion.

Similarly amplitudes were greatest when the eyes were occluded in the P100. This could reflect early top-down processing to the eyes, which have previously been stated as important for expression recognition, but it is likely to reflect feedforward processes as amplitudes for the occluded mouth are also high. Amplitude strength appears to be based on the amount of information; with more information associated with higher amplitudes and less information associated with lower amplitudes. This processing, based on visual input, reflects the involvement of early visual regions and subsequently strengthens the idea that these amplitudes are a reflection of feedforward processing (Cauchoix et al., 2014).

Amplitudes in the P300 were associated with the features relevant for task completion and also responded to unexpected stimuli (Hajcak et al., 2010; M. L. Smith et al., 2004). This was evidenced with greater amplitudes to an isolated mouth (compared to the minus mouth condition) when participants were to discriminate between disgust, fear and happiness, but greater amplitudes to an occluded mouth (compared to a whole face, eyes only or mouth only stimulus) when asked to

discriminate between fear and happy. An isolated mouth was found to impair disgust and fear recognition in the 3AFC task, with significant accuracy differences between all three emotions (disgust, M = 83.93%; fear, M = 66.27%; happy, M = 97.2%), this is because there is an absence of nose information for disgust recognition and eye information for fear, making the task harder and more unexpected. Categorising between fear and happy, on the other hand, can be achieved with the presence of mouth information. Thus, the high amplitude to an occluded mouth makes sense, as the features relevant for task completion are missing, and this is unexpected. In both cases, the bigger amplitude could be associated with where feedback is needed to help fill in important missing information, potentially reflecting P300 oddball effects (Picton, 1992) with an increased response to target stimuli necessary to make the correct categorisation, but more simply it could just be a result of task difficulty. Furthermore, akin to the N170 and P100, amplitudes were strong when the eyes were occluded in the P300. This may again reflect a feedback effect or top-down processing (Greening et al., 2018; Schyns et al., 2007; M. L. Smith et al., 2005), where the amplitude is associated with the requirement to fill in the important missing eye information, or again, it may be a reflection of task difficulty because information from the eyes is important for recognition.

There were subsequent interactions between PF condition and emotion; these interactions primarily occurred between the occluded eye condition and fear recognition. Whilst the rN170 in study one and lN170 of study two responded greater in the occluded eyes condition (compared to the occluded mouth condition), this was seen in both fear and happiness recognition. Previous literature found no differences in the N170 when recognising fearful faces with an occluded eye region (Leppänen et al., 2008). However finding greater amplitudes to fear supports a number of previous studies, including Batty and Taylor (2003), Blau et al. (2007), Calvo and Nummenmaa (2015) and Turano et al. (2017), suggesting a propensity to detect threat in the environment (Calvo & Nummenmaa, 2015). Turano et al. (2017) additionally found fear associated with a distinctive neural signature. Previous research has also shown increased N170 amplitudes in response to happiness (Hinojosa et al., 2015), which could be explained with the attentional salience of a smile (Calvo & Nummenmaa, 2015). Although there is an association between the importance of mouth information and the recognition of happiness, research carried out using the bubbles paradigm also showed the importance of eye information in

recognition (M. L. Smith et al., 2005). Moreover, the stronger amplitude observed in fear and happiness recognition in response to occluded eyes, could suggest that the brain is trying to fill in missing diagnostic information for successful recognition (Greening et al., 2018; Schyns et al., 2007, 2009). The amplitude was not stronger in the occluded eyes condition for disgust recognition; and furthermore, research using the bubbles paradigm does not show the eyes important for disgust (M. L. Smith et al., 2005). Thus, this may provide further support that emotion recognition firstly focusses on the eyes and the N170 only peaks in an attempt to fill in missing diagnostic information (Greening et al., 2018; Schyns et al., 2007, 2009). The behavioural results in this chapter (3.2.2.1 and 3.3.2.1) provide further supporting evidence that the increased ME amplitude for fear (in the rN170 study one and lN170 study two) reflects feedback, where the brain could be forming a prediction of the diagnostic facial feature. This is because the behavioural results do not find fear in the ME condition to be recognised more accurately than in the MM condition. However, it is important to note that this result may depend on the nature of occlusion that was used, and may not have been found if the stimuli were different, with information removed rather than concealed behind an occluder (Johnson & Olshausen, 2005).

Alternatively, however, the N170 could simply occur in the absence of feature information to help process occlusion independently of emotion. This is supported in the rN170 of study one, where lower amplitudes in the WF condition, across emotion, are found in comparison to the other PF conditions. This is consistent with past work on the N170 that found amplitude did not vary across expression (Eimer & Holmes, 2002, 2007; Eimer et al., 2003; Neath-Tavares & Itier, 2016; Neath & Itier, 2015; Rossion, 2014). However, this finding may simply be a result of task difficulty with the partial stimuli being harder to recognise. This is supported with ERP research also finding strong amplitudes in response to a harder task, such as the recognition of inverted faces (Bentin et al., 1996) and previous literature showing occlusion to have no effect on the N170 amplitude (Eimer, 1998; Itier et al., 2007; Tang et al., 2014).

In study two, the P100 was also shown to respond maximally to fear in the occluded eyes condition (compared to all other PF conditions). This result, as seen in the N170, could reflect early top-down processing to the eye region that is missing and needed for fear recognition, but it could also reflect task difficulty. The P300

was shown to respond maximally to fear (than happiness) but this effect did not interact with PF condition. This result implies that greater processing is needed for fear recognition or that more activity is generated demonstrating the importance of recognising fear. As there was an interaction in study one, separate analyses were carried out for both tasks. In the expression task, amplitudes were again greatest for fear (than happiness). Additionally, in the gender task, fear (compared to happiness) was associated with the greatest P300 amplitude in the whole face condition; this may be due to the salience of the emotion. Furthermore, disgust was found stronger in the isolated mouth than the minus mouth condition. This finding follows the same argument that features missing for recognition (nose information) have again resulted in a bigger ERP response. Moreover, this is unlikely to be a result of task difficulty as the behavioural results show no accuracy differences between these conditions.

Previous research has shown emotion differences present only in implicit tasks where fear is higher, or an enhancement towards emotional versus neutral expressions (Rossion, 2014). However, the findings of emotion differences are present across task, akin to Turano et al. (2017) who found fear to enhance the early neural coding of faces irrespective of task (categorising expression, identity or both). As no significant task effects were observed in the univariate analysis, this goes against the hypothesis that expression recognition would be stronger in the implicit task. Only a trend for greater amplitudes in the gender task was observed in the N170 and P300. Thus hinting to the importance of implicitly processing expressions due to their biological saliency (Pessoa & Adolphs, 2010). The finding of no task effects corresponds with some previous literature (Schyns et al., 2003; F. W. Smith & Smith, 2016, June, OHBM Abstract; M. L. Smith et al., 2004; Turano et al., 2017). However, it is important to note that explicit and implicit expression recognition was not compared the same in these studies, for example Schyns et al. (2003) and M. L. Smith et al. (2004) asked participants whether a face was expressive or not (happy vs neutral), instead of asking them to discriminate between different emotions. F. W. Smith and Smith (2016, June, OHBM Abstract) asked participants to discriminate between the seven basic emotions in their explicit task, but to firstly perform an identity, as opposed to a gender categorisation task, in their implicit task. Studies that found task effects masked the stimulus (M. L. Smith, 2011) or used the oddball paradigm (Neath-Tavares & Itier, 2016), these implicit tasks differ from those

employed in this chapters experiments. It seems the design of an implicit or explicit task can influence subsequent results.

On visual inspection, the peak for partial stimuli occurs after the whole face stimuli, bilaterally for the N170. This suggests the possibility that the time of decoding may occur later for partial stimuli than whole stimuli. This would be in line with previous literature (Eimer, 1998; Itier et al., 2007; Tang et al., 2014; Tang et al., 2018). However, no latency analyses have been run with the analysed ERP data and the peak timing for partial and whole stimuli can only be hinted at from the ERP plots. An investigation into the latency of the ERP peaks would enable this to be tested, to see whether univariate ERP differences between emotion would occur later for partial than whole face stimuli.

Overall, results from the univariate analysis show that when information needed to process an emotion is missing, amplitudes are stronger. This heightened amplitude, found principally in response to occluded eye stimuli and fear recognition, is interesting. To some extent this higher amplitude may reflect the occurrence of prediction or error signals in predictive coding, however, this study was not set up to directly test this account. Therefore, the heightened amplitudes cannot simply imply feedback; they may instead be due to a number of other factors, such as task difficulty or the nature of occlusion. Testing the predictive coding account directly is an important avenue for future research; this will be discussed further in the general discussion (5.6, Chapter 5).

3.4.3 Comparison of results to fMRI study.

Decoding accuracies were also amplified in the occluded eye conditions of the previous fMRI study. This significance was revealed with the highest decoding accuracy in the ME condition for implicit expression decoding in V1, EVC, FG and IOG; and the highest decoding accuracy in the MO condition for explicit expression decoding in V1, EVC, FG, IOG and the insula. The ME condition was also significant in the FG (at $p < .01$) and insula (at $p < .01$), with the amygdala also showing ME significance (at $p < .05$) for explicit expression decoding. Furthermore in the STS, the ME and MO conditions were significant in explicit expression decoding, with the MO significant in implicit expression decoding. Thus it seems that whilst the occluded eye effects are more prevalent for implicit expression decoding in the fMRI study, there are hints that these effects are present across both tasks. This matches the significance of occluded eye effects present across both tasks

in this EEG study. Furthermore, as aforementioned, the N170 is thought to reflect the FG or STS, but not IOG activation (Pitcher et al., 2011; Wronka & Walentowska, 2011), thus the N170 peak in the occluded eye conditions in this study, corroborates with the high decoding accuracies seen in the ME and MO conditions for these areas of the brain. Therefore, the apparent discrepancy between the fMRI and EEG study in terms of task results can be explained when considering which regions of the brain each study taps into. As aforementioned, the STS results in the fMRI study map onto the more robust decoding found in the explicit compared with the implicit task for the EEG study. Furthermore, no specific task effects were found with the univariate EEG analysis, although it is important to note that this analysis would have lacked sensitivity and cannot be directly compared with the fMRI multivariate analysis, finding task differences in decoding accuracy.

3.5 Conclusion

Following up from the previous study, this chapter explored the neural time-course of expression processing under conditions of occlusion. Given evidence that the brain can predict rich information about the visual environment, it was important to understand the temporal dynamics of processing and compensating for missing feature information. Multivariate pattern analysis (MVPA) showed reliable decoding of facial expression (happy, fear and disgust) in conditions missing feature information, with more robust decoding in the explicit task. Significant expression decoding was possible from 50-700ms, with three decoding phases potentially inferring the presence of feedforward and feedback processes. Furthermore, a supplementary univariate analysis showed enhanced early ERP responses (P100 and N170), independent of task, to stimuli with occluded eye information. This response was heightened if the emotion needed information for recognition from the eye region (thus it mainly affected fear recognition). This amplitude lends to speculate the involvement of feedback, as the brain could be forming a prediction of the occluded facial feature. However, from these results it was not possible to ascertain the amount of feedback taking place and whilst it can elucidate some timing information as to when feedback occurs (post 170ms stimulus onset), information related to where this feedback takes place cannot be established. Furthermore, this result contradicts with previous research showing responses to stimuli missing eye information to have no effect on the N170 (Eimer, 1998; Itier et al., 2007). Moreover, heightened amplitudes cannot simply be taken to imply feedback, as the

result could be due to a number of other factors, such as task difficulty or the nature of occlusion. Overall, results broadly agree with the fMRI experiment, further adding to previous research in understanding how the brain deals with occlusion.

Chapter 4: Shared Representations in the Perception and Production of Facial Expressions; Testing the Embodied Account of Emotion Recognition

4.1 Introduction

There is an accumulation of evidence that visual recognition of emotion may depend on a primitive embodied simulation account, whereby we internally simulate another's expression to aid recognition (Goldman & Sripada, 2005; Niedenthal, 2007). The embodied account can be evidenced by studies showing the importance of somatosensory and motor regions when visually recognising facial expressions (Dalgleish, 2004; Kober et al., 2008; Saarimäki et al., 2015). As expressions are often fleeting, and features can be occluded, expression recognition by visual signal alone can be challenging (Wood, Rychlowska, et al., 2016).

The role of the primary motor cortex in emotion recognition has also been ascertained (Banissy et al., 2010; van der Gaag et al., 2007). Furthermore, secondary motor regions have been implicated in recognition, including the supplementary motor area (SMA), premotor and posterior parietal cortex (van der Gaag et al., 2007). These regions could be involved in embodiment, especially since the ventral premotor and posterior parietal cortex is defined as part of the human mirror neuron system (HMNS), considered to support simulation (see Figure 1.8, Chapter 1) (Iacoboni & Dapretto, 2006; Kircher et al., 2013; Oberman et al., 2007).

To study embodiment in emotion recognition, a number of studies have found overlaps in brain activation across the perception and motor production of an emotional expression (Hennenlotter et al., 2005; Kircher et al., 2013). Whilst finding sensorimotor activation, a number of other interconnected regions relevant to emotion processing were activated, including the FG, amygdala and insula (Hennenlotter et al., 2005; Kircher et al., 2013).

Despite this, research into the embodied simulation account of expression recognition is still in its infancy. The prediction of a strongly embodied account of emotion recognition, predicting representational overlap in brain regions across perception and production, with multivariate analysis, has yet to be tested. Furthermore, studies have been predominately designed to test models that propose the recruitment of shared brain networks in action (Crammond, 1997; Grèzes & Decety, 2001; Hardwick et al., 2017; Jeannerod, 2001). Theories of embodiment, addressed in Chapter 1 (1.2.1), will be summarised. Followed by this, lesion, TMS

and fMRI studies supportive of the embodied account of emotion will be outlined; these strands of research demonstrate the importance of pre-/ primary motor and somatosensory cortices in expression recognition (Wood, Rychlowska, et al., 2016).

4.1.1 Theories of embodiment.

According to simulation based accounts, such as the theory of embodied cognition or embodied simulation, expression recognition is aided by simulation-like processes, see Chapter 1 (1.2.1) (Niedenthal et al., 2006). This is because neural activity overlaps in sensory, motor and affective systems, across the recognition and experience or production of an emotion (Niedenthal, 2007). Embodiment is closely linked to research investigating mimicry (the "chameleon effect") (Chartrand & Bargh, 1999) and the phenomena of emotional contagion (Hatfield & Cacioppo, 1994), as these automatic unconscious social behaviours play an important role in processing a sender's (often subtle) expressions (Niedenthal et al., 2009).

Goldman and Sripada (2005) outlined the reverse simulation models of embodiment, which detail the link between imitation, experience and recognition (see Figure 1.6, Chapter 1). However, the role of imitation is questioned as some research has shown no benefit of mimicry on facilitating expression recognition (Blairy et al., 1999; Hess & Blairy, 2001). This finding can be explained with Goldman and Sripada (2005) "as if" loop model of simulation whereby recognition can occur without facial feedback or mimicry (see Figure 1.6, Chapter 1). Thus, this model suggests that there is a direct link between visual and somatosensory representations of what an expression would feel like (Goldman & Sripada, 2005) and has close parallels with the "as if" body loop postulated in the Somatic Marker hypothesis (Damasio, 1996), detailed further in Chapter 1 (1.2.1). Moreover, Goldman and de Vignemont (2009) further separated imitation from embodiment, proposing that imitation does not meet the criteria for embodiment on its own. They state that imitation does not directly affect an individual's own behaviour and cognitions, but a receiver's own facial musculature can lead to embodiment by influencing their mood or emotion (Goldman & de Vignemont, 2009). Furthermore, Goldman and Sripada (2005)'s unmediated resonance model, corresponding with the mirror neuron system, details how observing an emotive face directly produces sub-threshold brain activation in the correspondent motor substrates for that emotion (see 1.2.1, Chapter 1).

4.1.2 Patient investigations.

In a lesion mapping fMRI study, Adolphs et al. (2000) asked subjects (N = 108 with focal brain lesions, N = 18 normal controls) to rate the six basic emotions on intensity. Mean emotion recognition scores were separated into two groups; analysing subjects in the lowest half (N = 54) or quartile (N = 27), respectively with the upper half or quartile of scores. Patient's scores were correlated with the ratings given by the normal controls. Findings demonstrated that patients with focal brain lesions to their right somatosensory cortex were impaired in emotion recognition (Adolphs et al., 2000). Furthermore, low emotion recognition scores were associated with lesions in the right somatosensory related cortices, including S1 and S2, as well as the anterior supra-marginal gyrus and lesions in the left frontal operculum, see Figure 4.74. As these patients do not have damage to their visual cortices, impairment as a result of somatosensory lesions is consistent with the idea that expression recognition is embodied. It seems that these lesions are preventing somatosensory representations of another's emotion to be internally generated, and thus the patient cannot simulate and recognise an individual's expression.

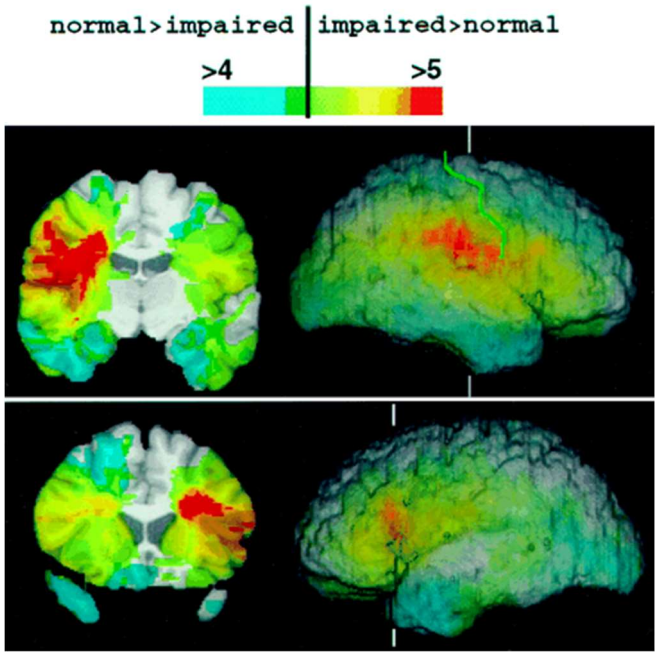

Figure 4.74. Distribution of lesion overlaps (upper quartile of subjects scores subtracted from the lowest quartile); red corresponds to locations where lesions resulted in emotion recognition impairments (RH somatosensory cortices, left frontal operculum), blue corresponds to lesions associated with normal performance, white lines show the position of the sagittal slice, RH top, LH bottom. From Adolphs et al. (2000).

Besides Adolphs et al. (2000), most lesion studies were based on a few single case studies. Whilst Adolphs et al. (2000) is important to the understanding of somatosensory cortex lesions in the recognition of facial expressions, it is not clear whether recognition ability is exclusively related to damage in the somatosensory regions. This is because lesions commonly cause damage to surrounding areas, thus more research restricted to the somatosensory cortices is essential to understand the exact role of the somatosensory cortex (Adolphs et al., 2000).

4.1.3 TMS investigations of shared networks.

Studies have applied TMS to areas of the somatosensory cortex to demonstrate the importance of this area in the recognition of emotional expression (Pitcher et al., 2011), see 1.2.2 in Chapter 1. However, the key studies will be summarised again here. Pitcher et al. (2008) applied TMS to the right somatosensory cortex and r-OFA, this disruption independently compromised the discrimination of facial expression but not identity. Similarly the suppression of somatosensory or premotor cortex activity (TMS to the right somatosensory and right premotor cortex) impaired the discrimination of auditory emotions but not identity performance (Banissy et al., 2010).

Furthermore, studies have applied TMS to the pre-motor cortex (PMC); this research has also demonstrated the role of simulation processes in recognising expressions (Balconi & Bortolotti, 2013). Balconi and Bortolotti (2013) showed PMC disruption to result in increased RTs and false alarms when recognising anger or fear, overall showing the importance of the PMC in detecting emotion. This specific impairment to recognise negative emotions is supported by Pourtois et al. (2004), where TMS applied to the right SC disrupted fear but not happiness recognition. However, Rochas et al. (2013) found TMS applied to the left pre-SMA, to impair the recognition of happiness but not fear or anger; supporting the seemingly robust ability to recognise happiness (F. W. Smith & Schyns, 2009).

Overall, studies inhibiting the somatosensory and premotor cortex areas are indicative of disrupting embodied cognition, as TMS seemingly disrupts the role of these areas in internally simulating an expression and later using this simulation to recognise a sender's facial expression (Pitcher et al., 2011).

4.1.4 fMRI investigations of shared networks for perception, production and imitation.

fMRI studies have investigated the embodiment of emotion by identifying shared networks of regions across perception, production and imitation tasks; these experiments, as aforementioned in Chapter 1 (1.2.2), have found overlaps in the premotor cortex (PMD and PMV) (Carr et al., 2003; Hennenlotter et al., 2005; Kircher et al., 2013; Leslie et al., 2004; Montgomery & Haxby, 2008; van der Gaag et al., 2007), further supporting the role of embodiment in this area for emotion recognition. Experiments have found additional overlaps in secondary motor and somatosensory regions (detailed further in 1.2.2, Chapter 1) including the SMA, pre-SMA, S1 and S2 cortices (Hardwick et al., 2017; Hennenlotter et al., 2005; Kircher et al., 2013; Leslie et al., 2004; van der Gaag et al., 2007), which could result from viewing dynamic displays of emotions in the perception tasks. The role of the somatosensory cortex in subjective emotional experience was also explored in a MVPA study (Kragel & LaBar, 2016); whilst the study of emotional experience differs from emotion recognition, it is important to consider. They found that experienced emotion could be decoded from patterns of activation in the right primary somatosensory cortex (see 1.2.2.1, Chapter 1, for more detail).

Although the above-mentioned studies suggest similar involvement of brain regions, only recently has neuroimaging literature been quantitatively synthesised to compare brain networks across tasks (Hardwick et al., 2017). Thus, a meta-analysis identified a reliable premotor-parietal and somatosensory network across the tasks, with bilateral clusters in the premotor cortices (PMD, PMV) across perception and production, see Figure 4.75; these results were similar when the meta-analysis was separated according to the body part they investigated (face, leg and arm). The face meta-analyses consisted of imagery, observation and execution studies involved in mouth movements, speech and facial expressions, thus it does not solely reflect overlapping networks in facial expression recognition. Furthermore, it is worth noting that these results need to be considered exploratory as the face execution meta-analysis only contained 13 studies ($N > 20$ studies necessary to analyse the results sufficiently) (Eickhoff et al., 2016). Nonetheless, these results are consistent with the previously mentioned research.

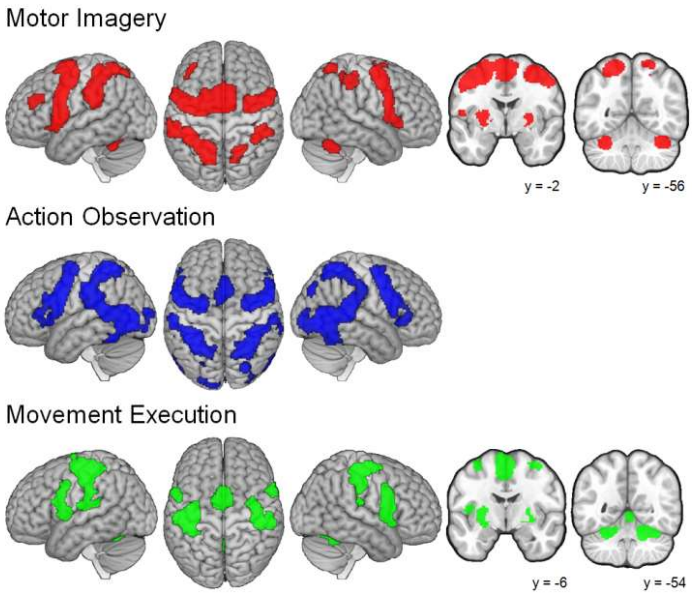

Figure 4.75. Brain activation networks from a meta-analysis investigating motor imagery (N = 4902 participants), action observation (N = 11032 participants) and movement execution (N = 2302 participants); across the three tasks there is similarity evident in premotor-parietal and somatosensory areas, from Hardwick et al. (2017).

Additional frontal and subcortical regions of the brain have also been found to overlap in the perception, production and imitation of facial expression (see 1.2.2, Chapter 1, for more detail): with frontal regions including the IFG and dorsolateral PFC (Carr et al., 2003; Kircher et al., 2013) and subcortical regions including the amygdala, insula, cerebellum and hippocampus (Carr et al., 2003; Hennenlotter et al., 2005; Kircher et al., 2013; Leslie et al., 2004; Montgomery & Haxby, 2008; van der Gaag et al., 2007). However, in Hardwick et al. (2017) subcortical regions were not activated in perception but consistently activated in production tasks; these regions included the thalamus, putamen and cerebellum. Lastly, overlaps were seen in the parietal regions including the posterior parietal cortex, more specifically the IPL (Hardwick et al., 2017; Montgomery & Haxby, 2008; van der Gaag et al., 2007), an area characteristically involved in processing multisensory information (Hardwick et al., 2017). Furthermore, activations of the STS, FG, ventral amygdala and visual cortex were found in perception, validating the role of face-selective regions in emotion recognition (Hardwick et al., 2017; Hennenlotter et al., 2005; Leslie et al., 2004; Montgomery & Haxby, 2008; van der Gaag et al., 2007).

4.1.5 Methodological fMRI considerations.

The fMRI experiments began investigating shared networks in the perception and imitation of expression (Carr et al., 2003; Leslie et al., 2004). Whilst these are important and imitation requires the production of a desired facial expression, the task inherently provides visual or perceptual input. Furthermore, caution needs to be taken with studies that induce emotions with personal scenarios (van der Gaag et al., 2007) as this will cause variation amongst participants and activate additional brain regions associated with cognition. A few recent studies have, however, devised production tasks where motor aspects of producing expressions are studied without any visual or cognitive influences (Hennenlotter et al., 2005; Kircher et al., 2013; Montgomery & Haxby, 2008). Moving forward, it is very important to obtain a true production measure to understand the brain regions involved in producing expressions.

Furthermore, it is important for the perception, imitation or production tasks to run on separate runs or blocks in the scanner to prevent participant's temptation to imitate or produce expressions during the perception trials. In Montgomery and Haxby (2008), the STS was unexpectedly activated in production when shown a static word stimuli, as this region is thought to exclusively have a role in imagined biological motion. This surprising finding may therefore result from combining tasks in the same run. Moreover, it is important that perception tasks are carried out first and participants are naïve to the subsequent production tasks to remove any implicit biases for a motor response during the perception of expression. Notably, van der Gaag et al. (2007) found premotor activation to overlap when participants were naïve to the production tasks ahead. This finding suggests the strong involvement of premotor areas and the role of motor preparation in observation. Again moving forward to the present study it is very important to separate the experimental tasks in order to truly measure the brain regions involved in the embodiment of emotion.

The choice of stimuli is also very important with the use of dynamic stimuli preferable over static displays of expression to increase ecological validity. However, it is important to note that dynamic stimuli are associated with more brain activation (Leslie et al., 2004; van der Gaag et al., 2007), thus careful thought should be given as to why some brain regions are active, such as the greater likelihood of STS activation with moving stimuli. To further this point, studies requiring a participant to move in the scanner are associated with motion artefacts, thus Leslie et

al. (2004) chose to use smiling movies where the mouth was always closed and imitation could subsequently be performed with the mouth closed. However, happy expressions are usually depicted with the mouth open; and this could cause variation in brain activation among other studies using open mouthed happiness expressions. Van der Gaag et al. (2007) tried to reduce motion artefacts in the imitation task by analysing brain activation when stimuli were presented on screen, before simulation had taken place, as they argued that this would reflect when participants would attend to the motor aspects of the expression whilst avoiding any motion artefacts. Although, a truer reflection of the brain activation would have been garnered during movement and this would have partially eradicated the problem of visual input for expression imitation.

Moreover, whilst similar areas have been shown to overlap across studies, this co-activation may reflect different populations of voxels within the regions (Hardwick et al., 2017). Thus, multivariate approaches are needed to fully investigate the overlap in activity of voxels or representations in the brain. To date it is unclear whether the same representations are utilised across perception and motor production. Finding the same representations across these tasks, suggests that we internally simulate another's expression in perception to aid expression recognition (Niedenthal et al., 2006; Niedenthal et al., 2009); as such the visual representation of an expression may activate a motor or somatosensory representation, allowing the experience of that emotion and subsequent recognition (Goldman & de Vignemont, 2009; Goldman & Sripada, 2005).

4.1.6 Rationale and hypothesis.

Overall, the collection of lesion, TMS and fMRI results provide a good basis to understand the neural networks involved in the perception and production of facial expressions. This literature is in support of an embodied simulation account of emotion recognition and shows the perception, imitation and production of an expression to consistently activate pre-/primary motor and somatosensory cortices (Wood, Rychlowska, et al., 2016).

However, as mentioned previously, there is no literature investigating whether there is representational overlap across the sensory perception and motor production of expression, to advocate a strongly embodied account (Crammond, 1997; Grèzes & Decety, 2001; Hardwick et al., 2017; Jeannerod, 2001). Therefore the present study will investigate this using fMRI and multivariate pattern analysis

(MVPA) to further understand the neural mechanisms of embodiment. A number of brain regions will be explored, with a particular emphasis on studying overlap in premotor cortices. This is because previous literature and understanding of the HMNS, suggests that the premotor cortices are strongly involved in embodiment.

H1: The same brain representations will be found in premotor cortices across the perception and production of emotional expressions.

Perceptual and sensorimotor areas will also be defined to confirm a network of face-selective and motor-sensitive brain regions, previously identified in the fMRI literature. However, it is worth noting that a true face and somatosensory localiser was not implemented in the present study.

4.2 Methods

4.2.1 Participants.

A total of seventeen participants (9 females, 8 male) took part in this experiment, aged 18-35 years **(**M = 24.06, SD = 4.78), two additional pilot subjects were tested but not used due to using a different design. Excessive head motion prevented the use of data in two participants and technical problems prevented the use of data from two further participants; thus, the final sample consisted of 13 participants (7 females, 6 males), aged 20-34 (M = 24.08, SD = 4.03). Participants were recruited via Scannexus (the company operating the scanning facilities at Maastricht Brain Imaging Centre) and paid for their participation. All were right-handed with normal or corrected to normal vision. Participants gave written, informed consent in accordance to approved ethics by the Psychology Research Ethics Committee at the University of East Anglia.

4.2.2 Stimuli.

In the perception task (task one) participants were presented with grey-scale STOIC movies from the database of dynamic and static faces expressing highly recognizable emotions (Roy et al., see http://mapageweb.umontreal.ca/gosselif/cv.html and http://www.mapageweb.umontreal.ca/gosselif/sroyetal_sub.pdf). Ten identities (5 males and 5 females) were chosen each posing happiness, disgust and sadness. These dynamic stimuli were presented for 500ms, with their faces cropped into an oval.

The 30 stimuli from 10 identities and 3 emotions were presented at a visual angle height of 6.5° using Psychtoolbox 3 for Matlab (Brainard, 1997; Pelli, 1997). A static noise stimulus was also created from neutral faces by scrambling the phase spectrum through Fourier analysis (F.W. Smith & Rossit, 2018). This gives similar low-level properties to the original without any image structure. Therefore, this provided a control condition.

4.2.3 Design and procedure.

This experiment consisted of two separate tasks. In the first task participants were asked to explicitly recognise facial expression while in the fMRI scanner. Each trial started with a fixation cross so participants maintained their gaze on fixation throughout, the stimuli was then presented for 500ms, followed by an ISI response period. This rapid-event related design required participants to undertake a one-back task and press their response button when they detected an emotion category that repeated across trials (such as two happy, disgust or sad expressions presented one after another). These four perception runs each lasted 424 seconds (212 TR2 volumes) with four second trials and 12 seconds fixation at the start and end of each run (see Figure 4.76). Participants were given 100 trials per run; 60 emotion trials (10 trials per emotion, repeated twice), 20 null events (requiring fixation only) and 20 noise trials (used as a control).

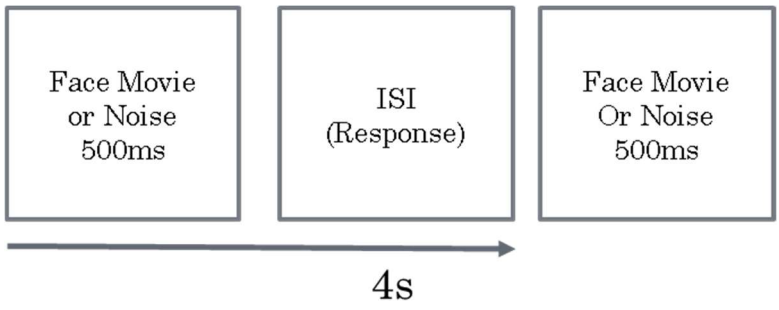

Figure 4.76. Experimental sequence in task one.

In the second task, participants were asked to produce the same basic facial expression categories viewed in the perception task while in the fMRI scanner. Thus, participants were asked to move a specific set of facial muscles (perform happy facial movements by moving the corners of the mouth up, perform sadness by moving the corners of the mouth down and perform disgust by wrinkling their nose). This was a block design protocol, whereby each block preceded with an instruction (cue) to move appropriate facial muscles or make a right index finger movement

(control condition). These movements were to take place at fixed intervals within the block when the fixation marker changed colour to red and green. Participants were to refrain from the movement and simply fixate when the marker was black and white (see Figure 4.77); the fixation marker changed every second allowing participants to make the movement five times. This 'Move' period occurred in the first 10 seconds of a 20 second on/off cycle; after this participants were to 'Rest' for 10 seconds (see Figure 4.77). Birn, Cox, and Bandettini (2004) argued that a block design with 10 seconds on followed by 10 seconds off is a good method for reducing motion artefacts associated with speech-related movements of the face. Overall participants carried out four production runs each lasting 338 seconds, 170 TR2 volumes; there were 16 blocks per run and 4 blocks of each movement.

Participants were naïve to the second task until they had taken part in the perception runs; this was to remove any implicit biases for a motor response in the first part of the experiment. Therefore, before the participants carried out the production task they were given some practice examples to ensure they understood and could perform the task. For these practice trials, stimuli of each expression (happy, sad and disgust) were taken from the Cohn-Kanade database. These practice trials followed the same temporal sequence as task two, where participants were to mimic the facial expression shown on screen every two seconds within the 10 second block, see Figure 4.77. There were multiple blocks for each expression; after this, participants were asked if they understood the procedure before continuing to the main task.

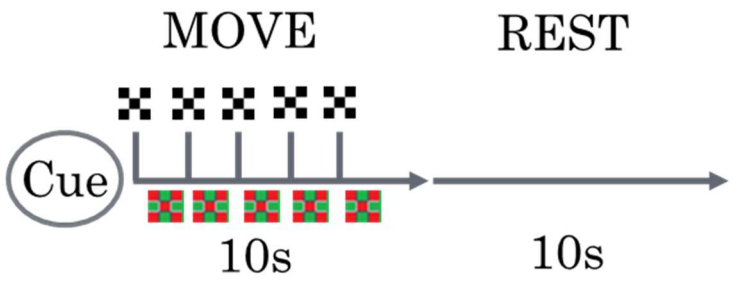

Figure 4.77. Experimental sequence of task two.

The scanning session itself took less than 1 hour 30 minutes, including time for set up (10 minutes), anatomy scans (10 minutes) and the main experiment runs. Additional time was required for participants to complete the MRI-screening forms, ask questions, read the information sheets, sign consent and receive debriefing

information (15 minutes). Participants were also shown the static versions of the stimulus before entering the scanner to familiarise themselves with the stimuli (see Appendix A for stimulus sheets).

4.2.4 MRI data acquisition.

MRI data were collected with a 3T Siemens Prisma fit scanner with a 64 channel head coil and integrated parallel imaging techniques (Scannexus, Brains Unlimited, Maastricht, Netherlands). Participants were positioned head first, supine in the scanner. Blood oxygen level-dependent (BOLD) signals were recorded with a gradient echo-planar imaging sequence (TE = 30ms, TR = 2000ms, FOV = 200mm x 200mm, Flip angle = 77˚, matrix size 80x80 and slice thickness = 2.5mm (no gap) giving 2.5mm isotropic voxels). Data, collected from 35 oblique slices of the brain, was positioned to cover the premotor, somatosensory, parietal and visual cortex. High resolution anatomical scans were recorded in the same session (3DMPRAGE, 1 x 1 x 1mm^3 resolution).

4.2.5 MRI data processing and analysis.

BrainVoyager QX [version 2.8] (BrainInnovation, Maastricht, The Netherlands) was used for fMRI data analysis (Goebel et al., 2006). Firstly, standard pre-processing steps were applied for each subject independently, these included slice scan time correction, 3D motion correction and temporal filtering. No spatial smoothing was carried out to maintain voxel resolution. Anatomical and functional data were transformed into ACPC and then Talairach space.

4.2.5.1 Task 1:

4.2.5.1.1 General Linear Model (GLM) univariate analysis.

A GLM approach was used to estimate blood oxygen level-dependent (BOLD) response amplitude to faces and noise stimuli in four predictors, one for each of the three expressions plus one for phase noise. The data was spatially smoothed with a Gaussian Filter function of 6mm full width half maximum (FWHM). A contrast was subsequently computed between emotion and phase noise. To identify active brain regions, corrected for multiple comparisons, a cluster threshold of 200 voxels (cluster level $p < .05$) was applied at t = 4.318 (corrected to voxel-wise $p = .001$) using the Cluster-level Statistical Threshold Estimator [BrainVoyager Qx Plug-in].

4.2.5.1.2 Multivariate analysis.

A GLM was applied to estimate response amplitudes independently for each voxel in each run on a single trial basis to create the patterns for MVPA (3 emotions X 10 identities, repeated twice, and 20 noise stimuli, giving 80 predictors per run). The resulting beta weights estimate peak activation for each single-trial, based on a standard 2γ model of hemodynamic response function (F. W. Smith & Muckli, 2010). These beta weight voxel estimates formed the input for the pattern classification analyses described below.

4.2.5.2 Task 2:

4.2.5.2.1 General Linear Model (GLM) univariate analysis.

A GLM approach was used to estimate blood oxygen level-dependent (BOLD) response amplitude to face movement and finger movement stimuli in four predictors, one for each of the three facial movements plus one for finger movement. In the first level GLM analysis (run on each subject individually), motion parameters and the movement cues were also included. The data was spatially smoothed with a 6mm FWHM Gaussian Filter, akin to task one. A contrast was subsequently computed between face and finger movement. Furthermore, to identify brain regions, corrected for multiple comparisons, a cluster threshold of 200 voxels (cluster threshold $p < .05$) was applied at t = 4.318 (corrected to voxel-wise $p = .001$) using the Cluster-level Statistical Threshold Estimator [Brain Voyager Qx Plug in].

4.2.5.2.2 Multivariate analysis.

A GLM was applied to estimate response amplitudes independently for each voxel in each run on a single block basis (16 blocks, four for each movement type, giving 16 predictors per run). The resulting beta weights estimate peak activation for each single-trial, based on a standard 2γ model of hemodynamic response function (F. W. Smith & Muckli, 2010). These beta weight voxel estimates formed the input for the pattern classification analyses described below.

4.2.6 ROI selection.

4.2.6.1 Task 1:

Perceptual regions of interest (ROIs) were defined from an orthogonal Face > Noise GLM contrast, appropriate for the main interest of studying expression, to reveal a face network of regions (bilateral STS, FG and early visual cortex or EVC), as well as premotor regions (bilateral PM1 and PM2). This a priori contrast was run to prevent double dipping (Kriegeskorte, Simmons, Bellgowan, & Baker, 2009). The

peak voxels within each ROI were selected using a threshold of t > 2.5; this is a low threshold to account for the weak signal strength caused by the nature of an event-related design. The localisation of each region will be defined in turn; with a posterior STS defined between the superior temporal gyrus (STG) and the medial temporal gyrus (MTG), the FG located medially between the inferior temporal gyrus and the parahippocampal gyrus and a posterior EVC defined around the calcarine sulcus. The identified PM1 and PM2 regions were guided by the univariate GLM analysis (Task 1); with PM1 reflecting a dorsal to ventral premotor region and PM2 reflecting a ventral area of the premotor cortex. These were respectively defined in the superior and inferior pre-central sulcus. It is important to note that not all the regions could be defined in all participants, see Table 4.5. ROIs were subsequently created into 9mm radius spheres using a TalCoord2Voi 2.0m [BrainVoyager Qx Plug-in]. In one analysis, all active voxels within the 9mm sphere were investigated; this radius size was chosen based on previous research (Anzellotti, Fairhall, & Caramazza, 2014; Furl, Henson, Friston, & Calder, 2013) and the results can be found in Appendix O. However, depending on how the voxels are distributed within each ROI, this analysis can produce weak results especially when studying XC effects. These weak effects occur if voxels are too diffused within each ROI. Furthermore, voxel size could vary considerably between the ROIs. Thus, further analyses were carried out to examine the 100 most sensitive voxels within each 9mm sphere. Selecting the top 100 voxels is typical in fMRI research (F. W. Smith & Goodale, 2015), and this analysis selection was used in V1 for Chapter 2.

4.2.6.2 Task 2:

Production ROIs were defined from an orthogonal Face Movement > Finger Movement GLM contrast to reveal the following sensorimotor areas (the SMA proper and bilateral sensorimotor cortices (S1/M1), as well as bilateral premotor regions: PM1, PM2 and bilateral secondary somatosensory cortices, S2). Again this a priori contrast was appropriate for the main interest of studying expression and carried out to prevent double dipping (Kriegeskorte et al., 2009). The peak voxels within each ROI were selected using a threshold (t) of > 3. The localisation of each region will be defined in turn; with the SMA (proper) defined posterior to the vertical commissure anterior line (VCA, coordinates 0, 0, 0) (Mayka, Corcos, Leurgans, & Vaillancourt, 2006; Picard & Strick, 2001) and the S1/M1 region defined in the central sulcus, with S2 in the parietal operculum. The premotor

regions, PM1 and PM2 were defined from the univariate GLM analysis (Task 2). Again, it is important to note that not all regions could be defined in each participant, see Table 4.5. Again, ROIs were subsequently created into 9mm radius spheres using a TalCoord2Voi 2.0m [BrainVoyager Qx Plug-in] and all active voxels within the 9mm sphere were investigated, see results in Appendix O. Again, further analyses were carried out to examine the 100 most sensitive voxels within each 9mm sphere.

Table 4.5.

Peak voxel coordinates (x, y, z) of each ROI averaged across participants, SD in brackets (all to 2d.p.). The final column details the number of participants each ROI was defined in; please note that not all regions could be defined in all participant.

Task	ROI	x	y	z	n of participants ROI defined
Perception	r-STS	47.38 (4.81)	-42.77 (5.55)	8.08 (3.17)	13
	l-STS	-51.08 (5.57)	47.75 (7.47)	9.25 (4.87)	12
	r-FG	36 (4.20)	-54.9 (4.11)	-16.4 (3.75)	10
	l-FG	-39.27 (4.00)	-52.64 (5.10)	-14 (3.33)	11
	EVC	-0.15 (13.64)	-98 (3.57)	-1.54 (6.63)	13
	r-PM1	41.15 (5.78)	-3.15 (4.07)	45.77 (5.58)	13
	l-PM1	-40.23 (8.04)	-3.69 (4.97)	48.69 (6.71)	13
	r-PM2	38.46 (3.32)	5 (4.57)	28.77 (3.83)	13
	l-PM2	-41.42 (4.86)	4.33 (5.76)	28.34 (4.78)	12
Production	SMA	2 (4.80)	-10 (4.99)	56.23 (3.31)	13
	r-S1/M1	46.08 (4.70)	-15.38 (3.03)	39.85 (3.30)	13
	l-S1/M1	-46.77 (5.44)	-14.15 (5.95)	37.54 (3.41)	13
	r-PM1	43.85 (6.07)	-9.23 (3.94)	50.85 (4.20)	13
	l-PM1	-45.82 (6.58)	-9.36 (6.96)	50.27 (6.37)	11
	r-PM2	58.54 (3.61)	-0.92 (4.45)	21.23 (9.04)	13
	l-PM-2	-58.55 (1.88)	-1.64 (3.52)	17.73 (6.35)	11
	r-S2	45.54 (4.16)	-15.38 (4.39)	17 (2.15)	13
	l-S2	-46.17 (3.41)	-14.83 (4.39)	16.83 (2.15)	12

4.2.7 MVPA.

Classifiers were built independently for each ROI (see ROI's in Table 4.5 above); and combined for bilateral ROIs (such that an additional classifier was built for PM1 which encompassed r-PM1 and l-PM1). Pattern classifiers were trained to discriminate between the three expressions, independently for each task (perception and production), using a Linear Support Vector Machine (LIBSVM 3.12 toolbox, Chang & Lin, 2011). Accordingly, these classifiers were trained to learn the mapping between multivariate observations of brain activation and the expression presented or produced, to test for pattern information that discriminates the emotions either in perception or production (in the ROIs defined). The classifiers were trained with beta values from a set of single-trial or single-block brain activity patterns. These were tested on independent single trials or single blocks (beta weights) for each emotion in the independent set of test data. An n-fold leave-one-run-out cross-validation approach was used to estimate performance, whereby the model was built from n – 1 runs and tested on the nth independent run (Greening et al., 2018; F. W. Smith & Goodale, 2015; F. W. Smith & Muckli, 2010).

In further cross-classification analyses, the classifier was trained to discriminate emotion on perception and tested to discriminate emotion on production, and vice versa, see Figure 4.78. Analyses were computed individually for each region of interest (N=13). Again an n-fold leave-one-run-out cross-validation approach was used. Performance for each direction of training and testing the classifier was computed and averaged to test for evidence of similarity across both tasks; the regions analysed were either based on ROIs defined from perception or production. Data was trained on single trials and tested on single blocks to generalise across perception, or trained on single blocks and tested on single trials to generalise across production. For all analyses, decoding accuracy was reported for each ROI using one-tailed one-sample t-test results with chance at 33.3%. Significance levels are presented on graphs to $p < .05$ and $p < .05$ FDR corrected.

The LIBSVM toolbox (version 3.12) was employed (Chang & Lin, 2011). Default parameters were used for the linear SVM with C = 1. Before inputting data into the SVM, the training data was normalised to lie within -1 and 1, with the test data normalised using the relevant parameters from the training data (max, range) (Chang & Lin, 2011; F. W. Smith & Goodale, 2015; F. W. Smith & Muckli, 2010; Vetter et al., 2014).

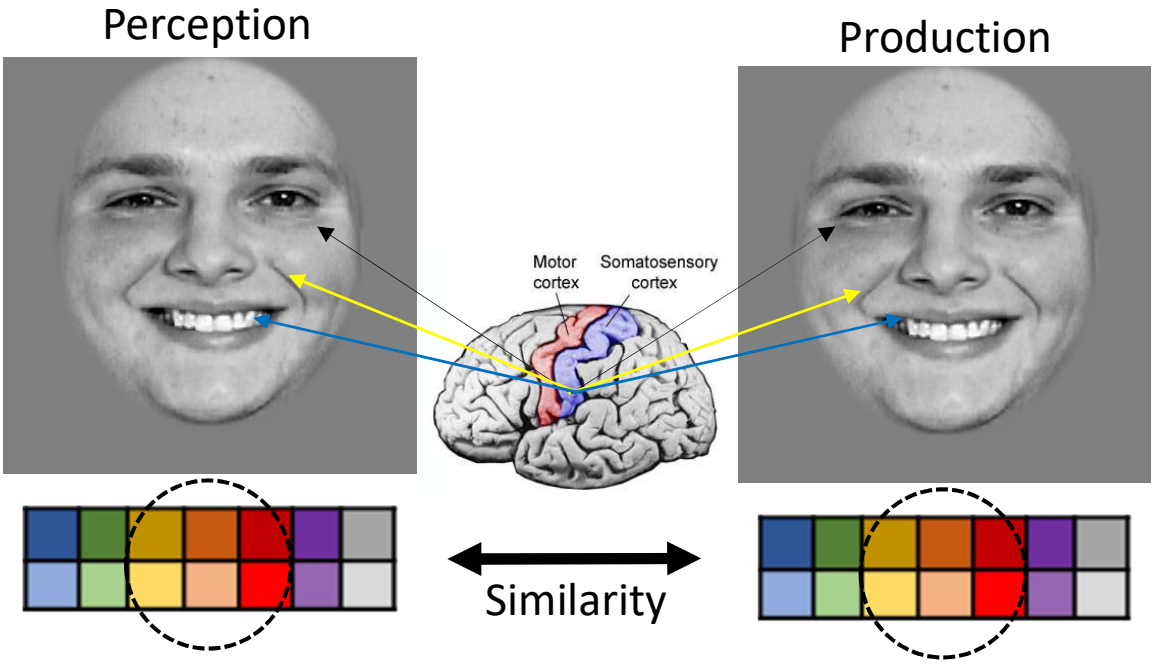

Figure 4.78. Example MVPA analysis; testing for pattern similarity across the perception and production task of expression in ROIs, namely sensorimotor regions.

4.3 Results

Results from the whole brain univariate analysis will be presented first. The univariate analysis from the perception task shows the regions of the brain that are activated when viewing expressions over viewing noise trials. The univariate analysis, from the production task, shows the regions of the brain that are activated when executing expressions over executing finger movements. These results are important for understanding the underlying networks involved in the perception and production of emotional expressions, and further add to the previous univariate literature. The correspondent surface maps, created with the whole brain analysis (WBA), helped guide the regions defined for the multivariate analysis. Therefore the probability maps showing the regions defined across subjects are presented next, followed by the multivariate results.

Subsequently, the MVPA results for the top significant 100 voxels in each ROI are explored, presenting the decoding results within perception and production, before the cross-classification results. The MVPA results are the main focus for this chapter, with a particular emphasis on the cross-classification findings. The cross-classification results are important for exploring potential representational overlap in brain regions across perception and production of expression. MVPA results for 9mm radius ROI's can be found in Appendix O; these results are informative but associated with disadvantages with larger ROI's relating to diffusion and voxel size differences, outlined above in ROI selection.

4.3.1 Univariate Whole Brain Analysis (WBA).

4.3.1.1 Task 1:

Stronger activation for viewing emotional expressions, over noise stimulus, is shown in the following bilateral brain regions: the premotor cortex (PMD and PMV), IOG, SFG and pre-SMA, as well as the rSTS and rMT, see Figure 4.79.

4.3.1.2 Task 2:

Stronger activation for a facial emotion movement, over a finger movement, is shown in the following bilateral brain regions: the premotor cortex (PMD and PMV), S1, M1, SMA and the RCZ, as well as the rSPOC, rVIP and rS2, see Figure 4.80.

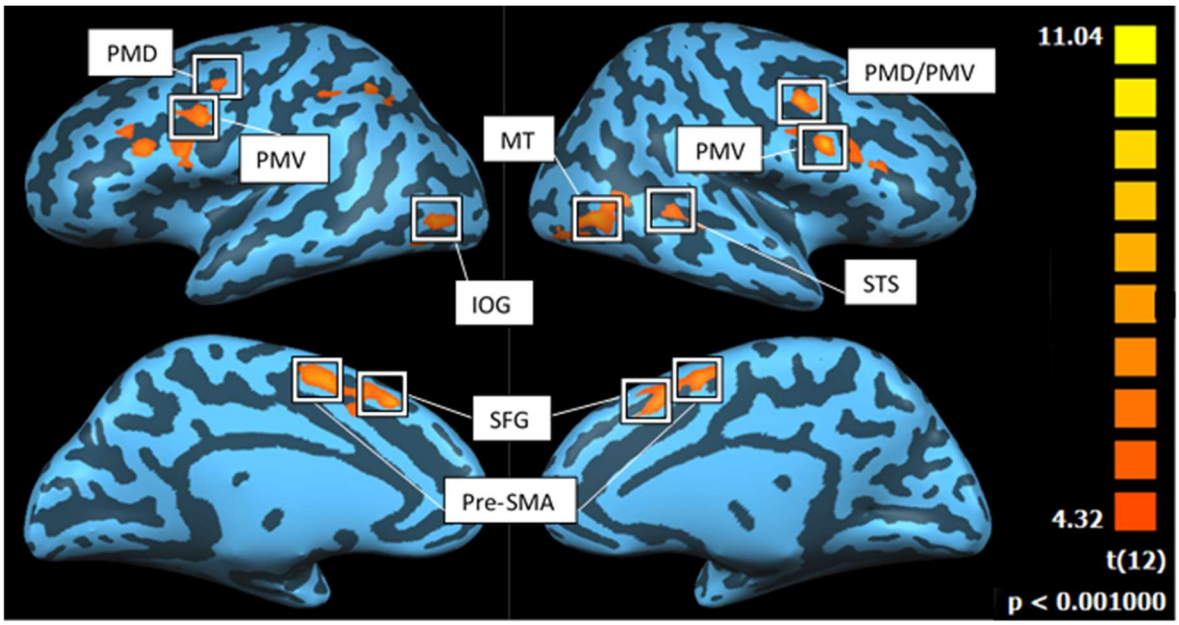

Figure 4.79. Surface maps showing the regions activated for emotion vs phase noise in the perception task; from left to right hemisphere.

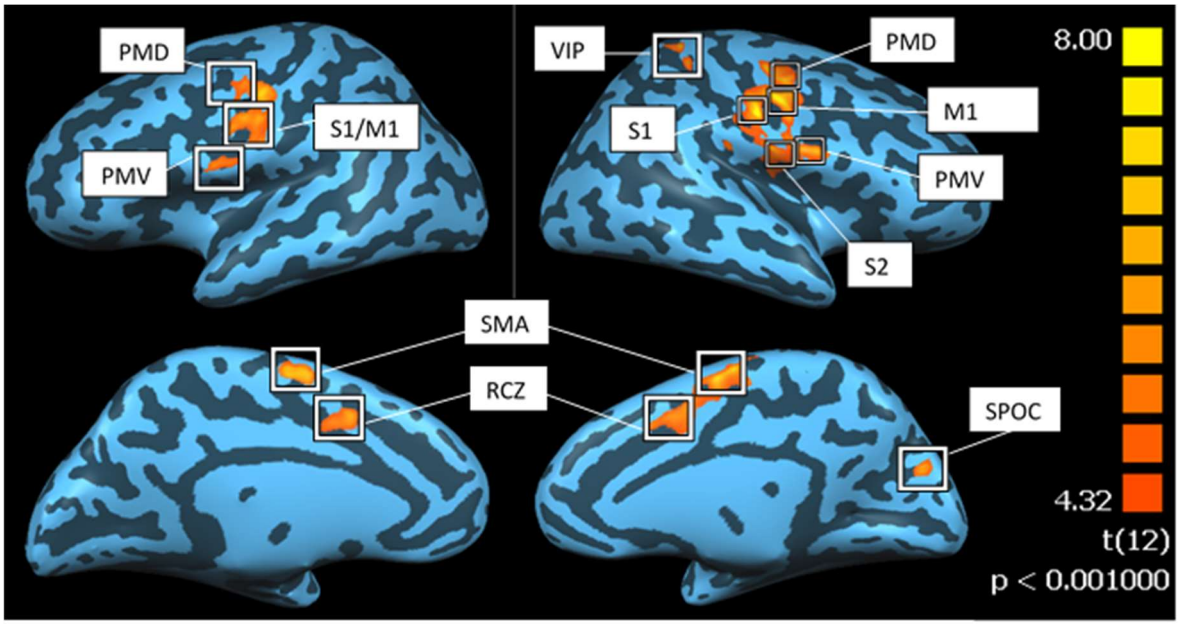

Figure 4.80. Surface maps showing the regions activated for face movement vs finger movement in the production task; from left to right hemisphere.

4.3.2 Regions defined.

The following bilateral brain regions were defined in the perception task in most subjects (see Table 4.5 for participant number): PM1, PM2, STS and FG. Each region was created into a probabilistic map to investigate whether the activation was spatially consistent across subjects, see Figure 4.81. The maps show a focal location for each ROI with little spatial variability. More consistency is found within the

rPM2 and lFG, where there is a higher percentage of subjects ROI's that overlap (nearer to 100%).

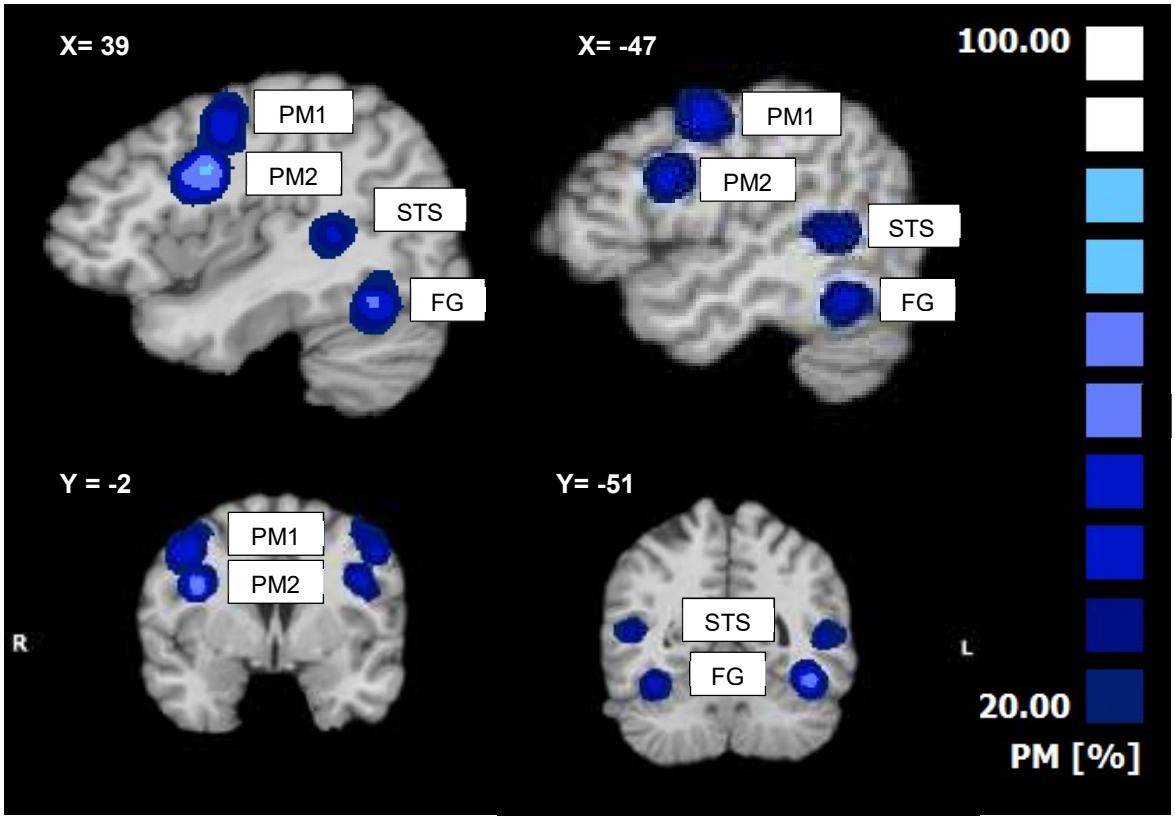

Figure 4.81. Probability map of perceptual ROIs, averaged across all subjects with available ROI's. From Right to Left Hemisphere.

The following bilateral brain regions were identified in the production task for most subjects (see Table 4.5 for participant number): PM1, S1/M1, S2 as well as the SMA. Each region was created into a probabilistic map to investigate whether the activation was spatially consistent across subjects, see Figure 4.82. Again, the maps show a focal location for each ROI with little spatial variability.

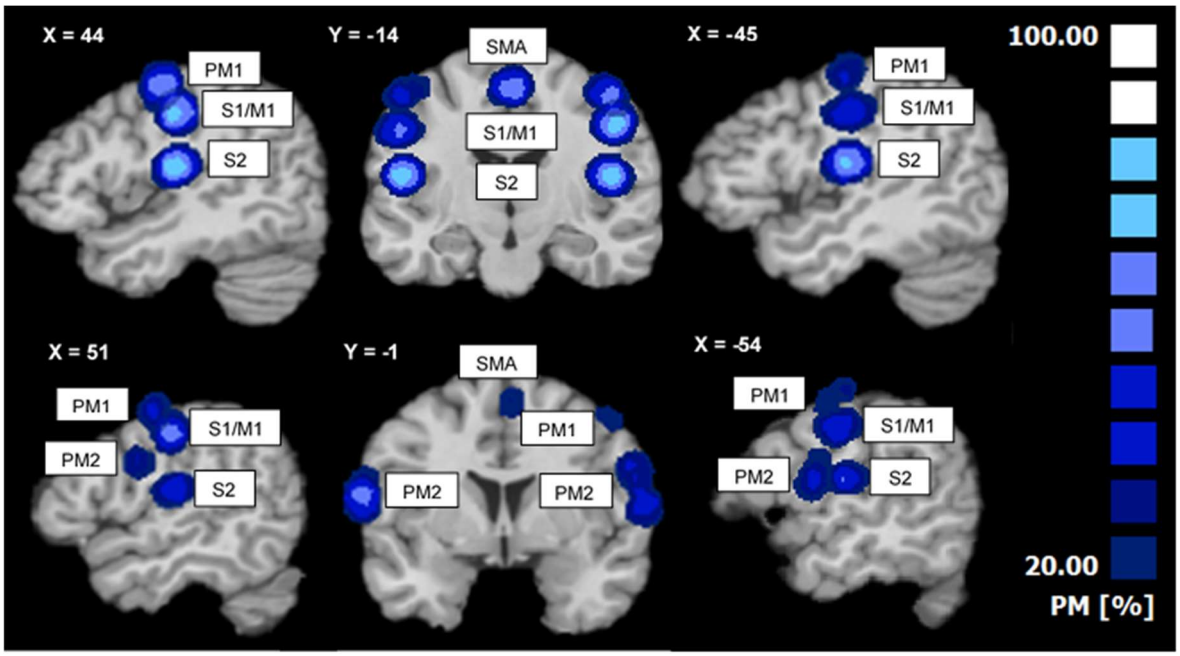

Figure 4.82. Probability maps of production ROIs, averaged across all subjects with available ROI's. From Right to Left Hemisphere.

4.3.3 Decoding results.

4.3.3.1 Decoding within perception and production.

Results for decoding of expression in the perception task are presented first, followed by decoding in the production task. ROI results are given for each hemisphere in turn (right then left), before the result of the combined bilateral ROI is given. The bars on the graph are either displayed in blue or grey: blue bars represent premotor regions of the brain, whereas grey bars represent either the face network or sensorimotor regions of the brain, depending on whether the results are from the perception or production task respectively. Furthermore, the result graph axis begins at 30% in both tasks; however, please note that this scale is set to 40% in the perception task and 80% in the production task, to account for variability in decoding accuracy between the tasks. This 30-40% scaling in the perception task was deemed necessary to clearly portray the differences in accuracy among the ROI's (this difference in scaling is used throughout the decoding results).

One-sample t-tests showed significant decoding (FDR $p < .05$) in the perception task for the r-PM1 ($t(12) = 2.608$, $p = .0115$, $d = .72$ (medium effect-size)), PM2 ($t(11) = 2.547$, $p = .0136$, $d = .74$ (medium effect-size)), l-FG ($t(10) = 2.806$, $p = .009$, $d = .85$ (large effect-size)) and EVC ($t(12) = 2.788$, $p = .008$, $d = .77$ (medium effect-size)) ROIs, see Figure 4.83. There was also a trend towards decoding in the lSTS ($t(11) = 2.280$, $p = .022$, $d = .66$ (medium effect-size)).

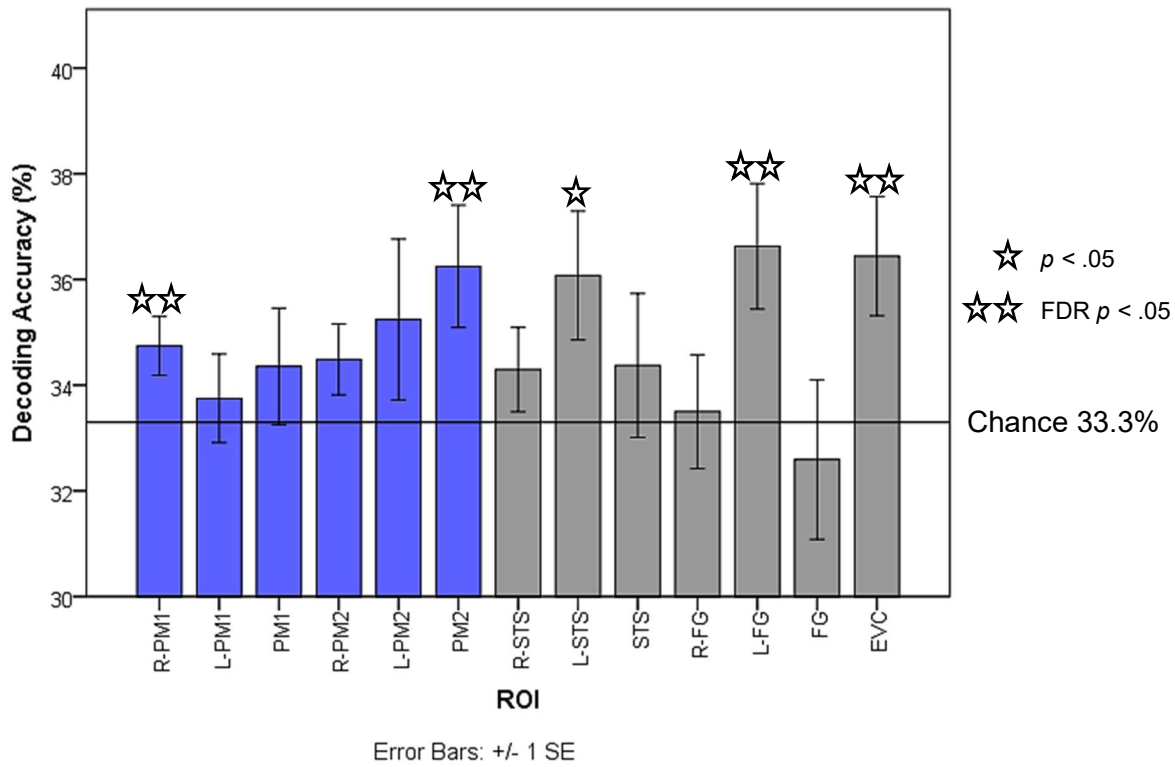

Figure 4.83. Expression decoding accuracy from the significant voxels (100) analysis in the perception task, one-sample t-test results represented with stars. Blue bars represent premotor regions of the brain; grey bars represent the face network of brain regions.

One-sample t-tests showed significant decoding in all ROIs (FDR $p < .05$; large effect sizes, *d's > 1.5*) for the production task, see Figure 4.84.

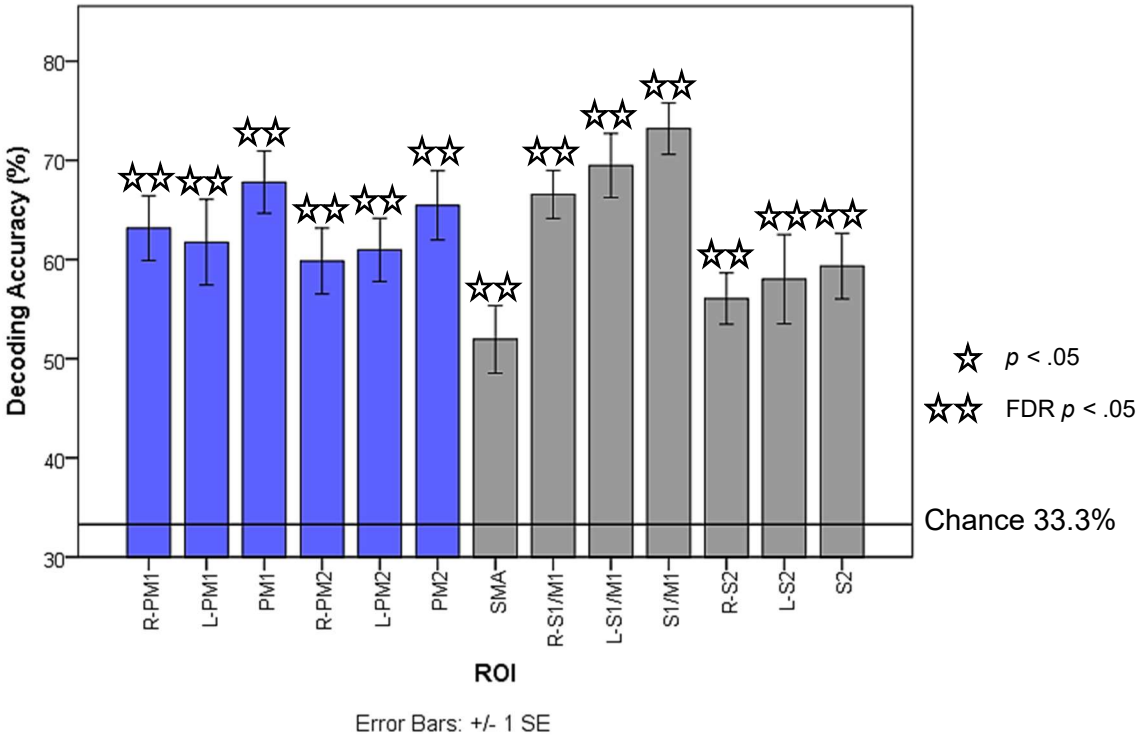

Figure 4.84. Expression decoding accuracy from the significant voxels (100) analysis in the production task, one-sample t-test results represented with stars. Blue bars represent premotor regions of the brain; grey bars represent sensorimotor regions of the brain.

4.3.3.2 Cross-classification.

The cross-classification results based on ROIs defined in the perception task are presented first, followed by ROIs defined in the production task. For these analyses, classifiers were trained on one task and test on another, and vice versa.

Although there were no significant FDR effects in cross-decoding based on the perceptual ROIs, one-sample t-tests showed decoding trends in the l-PM1 ($t(12) = 3.000$, $p = .006$, $d = 0.83$ (large effect-size)) and FG ($t(8) = 2.105$, $p = .034$, $d = 0.70$ (medium effect-size)) ROIs, see Figure 4.85. Furthermore, with the focus on the premotor regions, a Bonferroni correction ($p < .008$) was applied to these regions (six ROIS highlighted in blue within the graph), where the l-PM1 was significant.

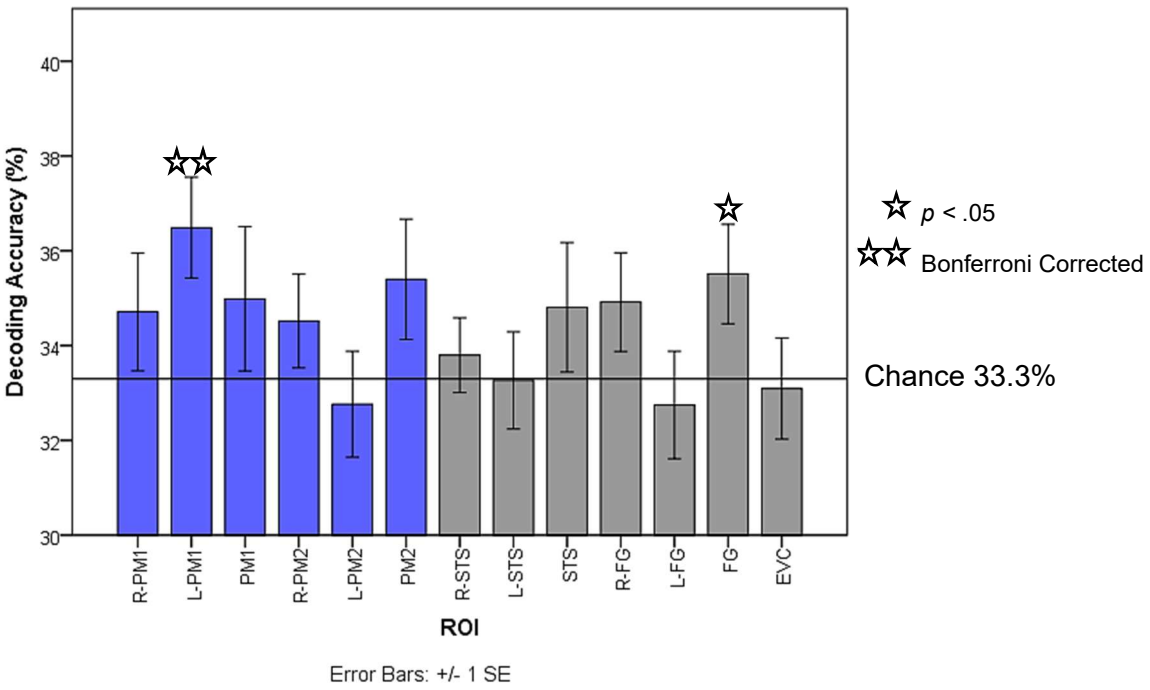

Figure 4.85. Expression decoding accuracy from the significant voxels (100) cross-classification analysis, one-sample t-test results represented with stars. ROIs defined from the perception task. Blue bars represent premotor regions of the brain; grey bars represent the face network of brain regions.

Although there were no significant FDR effects in cross-decoding based on the production ROIs, one-sample t-tests showed decoding trends in the r-PM1 ($t(12) = 1.843$, $p = .045$, $d = 0.51$ (medium effect-size)) and PM1 ($t(10) = 2.634$, $p = .013$, $d = 0.79$ (medium to large effect-size)) ROIs, see Figure 4.86.

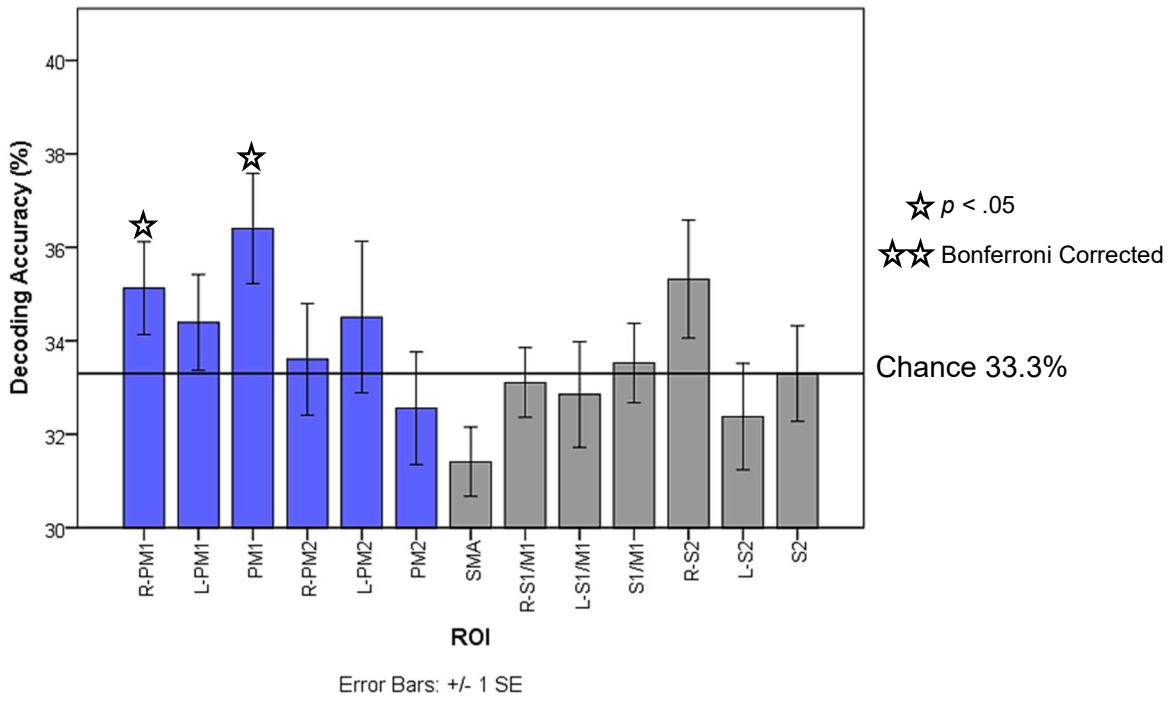

Figure 4.86. Expression decoding accuracy from the significant voxels (100) cross-classification analysis, one-sample t-test results represented with stars. ROIs defined from the production task. Blue bars represent premotor regions of the brain; grey bars represent sensorimotor regions of the brain.

4.3.4 Supplementary Analyses.

The results presented above define ROIs separately in the perception and production tasks; but to corroborate with the previous fMRI investigations, outlined in the introduction that detail the shared networks for perception, production and imitation, a univariate analysis was carried out. This found overlapping networks of brain regions or voxels across the perception and production task, thus providing another way to test the embodied account of emotion recognition, without the use of MVPA. It was apparent that similar regions were identified using this method, including the SMA, premotor cortices and STS, see overlap in Figure 4.87.

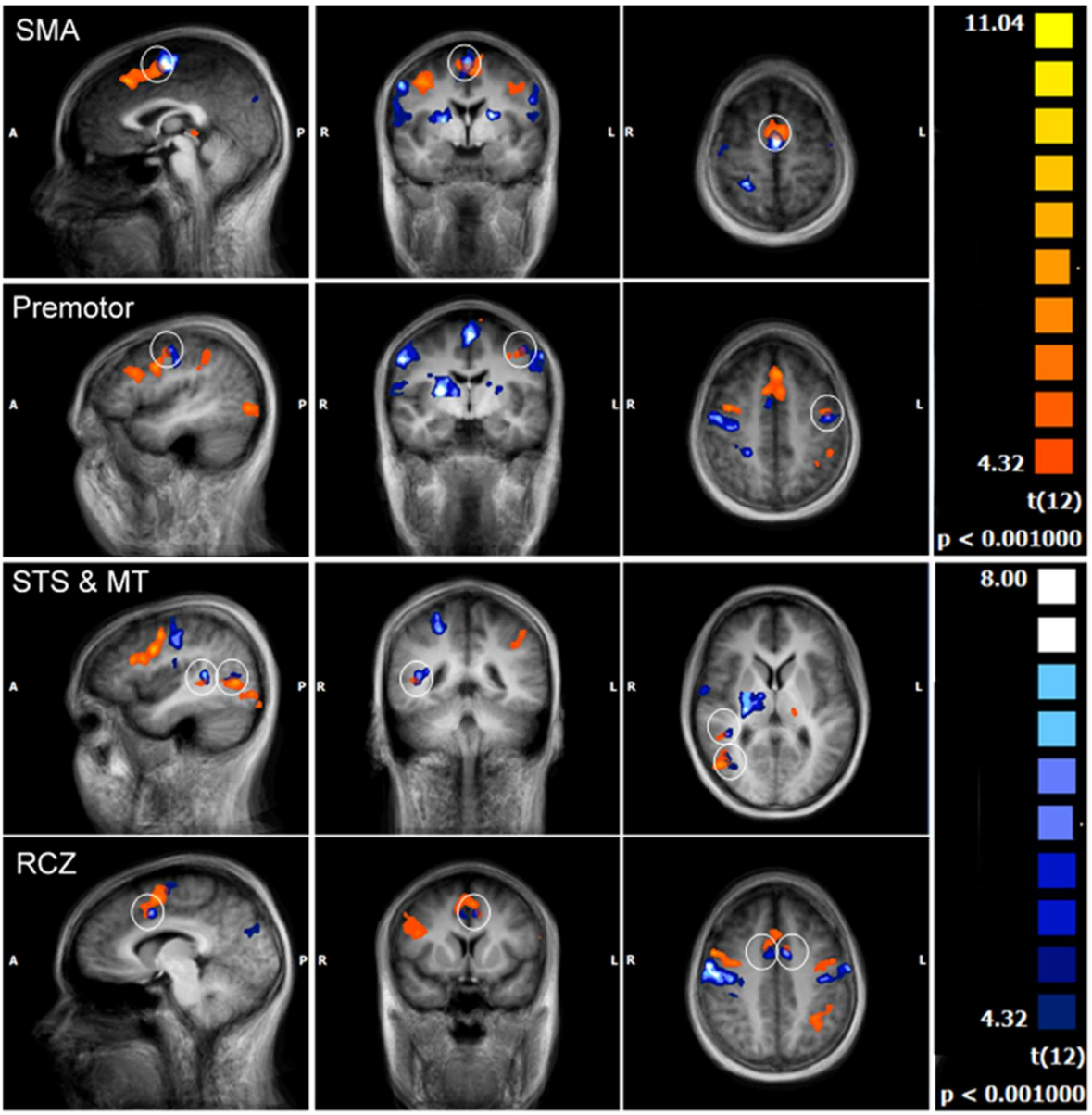

Figure 4.87. The regions activated that overlap between the two tasks (overlapping regions are purple and displayed within a white circle); orange scaling reflecting the activation in the perception task, and blue scaling reflecting the production task.

Furthermore, to confirm that the ROI's from single subjects, created into probability maps, are consistent with the group level RFX analyses, Figures P-1 to P-9 were created to show this, see Appendix P.

Overall the univariate, multivariate and supplementary analyses consistently show the involvement of the premotor cortex in the perception and production of emotional expressions. Importantly, the MVPA results demonstrate that the premotor cortex (dorsal and ventral) can discriminate facial expressions in both perception and production; with a dorsal premotor ROI, defined in the perception task showing a similar representation (Bonferroni corrected) of facial expression across perception

and production and a strong trend towards this similarity within dorsal premotor regions defined in the production task.

4.4 Discussion

Previously, little research had investigated the production of facial expressions in the brain (Hardwick et al., 2017), and whilst studies had found overlapping voxels across the perception and production of expression (Hennenlotter et al., 2005; Kircher et al., 2013), research had not investigated representational overlap. This study primarily set out to investigate representational overlap within the premotor cortices across the sensory perception and motor production of expression (H1). Thus, the cross-classification analyses from the premotor cortices are outlined first, with reference to other decoding and supplementary analyses to help understand the effects. Following this, results from other regions of the brain, including sensorimotor and perceptual areas, are summarised and discussed.

4.4.1 Representations of expression in premotor cortices.

Importantly, the present findings demonstrate the role of the premotor cortices in emotion recognition. This is shown in the cross-decoding results, whereby a perceptually defined premotor ROI (l-PM1) shows a similar representation of facial expression across perception and production (Bonferroni corrected) and a strong trend for a similar effect is present within production defined dorsal to ventral premotor regions (rPM1 and PM1). These premotor results or trends towards representational overlap in perception and production are supportive of the main experimental hypothesis (H1). Besides these premotor regions, representational overlap was not found in other areas of the brain. It is surprising that an effect was not shown in the somatosensory regions; however, it may be that the ROI defined is only tapping into the motor specific sub-region of S1. A face localiser with tactile stimulation could have been implemented to better define this brain region (i.e. area 3a from area 3b); accordingly this will provide a stronger test to investigate the effects in somatosensory cortex. Furthermore, it is important to note that even though this study did not find representational overlap in the somatosensory cortices, it does not mean that effects were not present.

Previous TMS and fMRI research has highlighted the importance of the premotor regions in emotion recognition, showing disruption to the premotor cortex to interfere with the recognition of anger and fear (Balconi & Bortolotti, 2013) and overlap in activity across the perception, imitation and execution of facial

expressions in the premotor cortices (Carr et al., 2003; Hardwick et al., 2017; Hennenlotter et al., 2005; Leslie et al., 2004; Montgomery & Haxby, 2008; van der Gaag et al., 2007). However, this is the first experiment to find representational overlap in premotor regions, across the perception and production of an emotional expression using MVPA.

During this experiment, classifiers are trained on one task (perception or production) and tested on the other (i.e. production or perception) to test for similarity in the ROIs discriminating emotion across the tasks. Therefore, the similarity or overlap found within this neural structure provides support for the simulation or embodied account of emotion recognition, especially the reverse simulation models of embodiment, in the recognition of basic emotions (happiness, sadness, disgust) (Goldman & de Vignemont, 2009; Goldman & Sripada, 2005; Niedenthal, 2007; Wood, Rychlowska, et al., 2016). This reverse simulation model demonstrates the link between experiencing an emotion and then correspondingly being able to recognise the emotion, thus activation in pre-motor brain regions when visually recognising a facial expression is supportive of the embodied simulation account (Goldman & Sripada, 2005; Niedenthal, 2007; Saarimäki et al., 2015).

More importantly, this finding of overlap is present in a dorsal to ventral premotor region, an area considered important in expression recognition (Wood, Rychlowska, et al., 2016), with the ventral premotor cortex considered to be part of the HMNS in supporting simulation (Iacoboni & Dapretto, 2006; Kircher et al., 2013; Oberman et al., 2007). Thus, the unmediated resonance model may be particularly relevant in explaining how this face-based emotion recognition is carried out in the premotor cortices (Goldman & Sripada, 2005). Previous MVPA research investigating action had begun to challenge the involvement of the premotor cortex in the HMNS, suggesting that it was more concerned with observing one's own actions (Oosterhof et al., 2013). However, this study, with the use of MVPA, was able to provide stronger evidence of an embodied simulation account of emotion recognition.

In support of these cross-classification results, the decoding results within both perception and production demonstrate that the premotor cortex can discriminate between facial expression categories; where in the perception task both the ROI spanning dorsal to ventral PMC (r-PM1) and the ventral PMC (PM2) could decode expression above chance, and in the production task, the left, right and

bilateral PM1 and PM2 regions of interest (encompassing dorsal and ventral parts of the premotor cortex) could also decode expression significantly above chance. Furthermore, the univariate WBA demonstrates the activation of the bilateral premotor cortices (PMD and PMV) in both tasks, and in the supplementary overlap analysis it seems that perceiving and producing a facial expression recruit partially overlapping networks of brain regions.

4.4.2 Representations of expression in other regions of the brain.

Given literature showing activation of similar voxels in sensorimotor areas for perception and production (Hardwick et al., 2017; Hennenlotter et al., 2005; Leslie et al., 2004; Montgomery & Haxby, 2008; van der Gaag et al., 2007), somatosensory (or pre-SMA) TMS stimulation interfering with emotion recognition (Banissy et al., 2010; Pitcher et al., 2008; Rochas et al., 2013) and impaired recognition performance among patients with somatosensory lesions (Adolphs et al., 2000), it may seem surprising that this study did not find representational overlap in other primary or secondary motor and somatosensory areas. Effects were only present in the production task whereby the SMA, as well as the left, right and bilateral S1/M1 and S2 regions of interest could decode expression significantly above chance.

As aforementioned a localiser was not used to map out the somatosensory regions and finding no representational overlap in this study does not mean that there were no effects. However, the univariate WBA analysis also demonstrated segregation in results; with the perception task activating the pre-SMA and the production task activating the SMA, bilateral S1/M1 and rS2. In the supplementary overlap analysis both tasks seemed to recruit the SMA, but no overlap was shown in the somatosensory cortices.

Nonetheless, results from the motor sensitive brain regions provide validation that the production task activates the sensorimotor networks within the brain (Kanwisher, 2010; Meier et al., 2008). This network was also shown to activate in production tasks of fMRI studies (Carr et al., 2003; Hardwick et al., 2017; Leslie et al., 2004). It is interesting to note that van der Gaag et al. (2007) found neutral expressions versus emotion (happy, fear and disgust) to generate greater activation in bilateral S1 and S2, with emotion versus neutral to generate greater activation bilaterally in the insula, frontal operculum (IFG), right anterior STS and pre-SMA.

Thus it appears the embodiment of emotion may be more associated with frontal than somatosensory regions (van der Gaag et al., 2007).

Results from the face-selective brain regions validate that the perception task reliably activates the perceptual face network in the brain (Haxby & Gobbini, 2011; Haxby et al., 2000), with the l-FG and EVC significantly decoding expression above chance, with a trend towards decoding in the l-STS. When cross decoding, none of the face regions (bilateral STS, FG and EVC; although there was a trend in the FG) could decode expression; however, this was to be expected as these regions are primarily involved in perceptual face processing. This network was shown to activate in perception tasks of the fMRI studies investigating shared networks for perception, production and imitation (Hardwick et al., 2017; Hennenlotter et al., 2005; Leslie et al., 2004; Montgomery & Haxby, 2008; van der Gaag et al., 2007). Furthermore, perceptual MVPA decoding studies have found similar effects, with decoding of expression possible in perceptual face areas, including the FG (Harry et al., 2013; Wegrzyn et al., 2015), EVC or IOG (Greening et al., 2018; Wegrzyn et al., 2015), STS (Greening et al., 2018; Peelen et al., 2010; Said et al., 2010; Wegrzyn et al., 2015; Zhang et al., 2016) and LO/VT areas of the brain (Greening et al., 2018).

4.4.3 Limitations and future directions.

4.4.3.1 Are the results due to imagery?

There is an argument that the results could be due to imagery, whereby participants imagine moving their facial muscles during the perception task or imagine an expression in the production task without truly executing it. Ideally, without time and practical constraints, the perception and production task would have been carried out on separate days to train the participants outside of the scanner to execute the required facial movements at the appropriate times. Additionally the use of a camera or EMG equipment during the experiment would have enabled monitoring the subject during the experimental tasks. A camera was set up in Kircher et al. (2013)'s study to check that participants were not imitating during their observation runs and if they were correctly executing expressions in the movement conditions; Kircher et al. (2013) vigilantly stopped the run and started it again if they observed any of these problems. Despite these concerns, activation was present within the S1/M1 region of interest (an area encompassing the brains motor structures) in the production task and not in the perception task; therefore it seems likely that the results are driven by participants externally making a motor movement

correctly over imagining a particular expression. Furthermore, the peak of activation appeared to be located anteriorly in the motor rather than the tactile part of S1. The motor part of S1, namely area BA3a, behind the central sulcus, has close connections with the motor cortex receiving proprioceptive information (Keysers, Kaas, & Gazzola, 2010); whereas regions successively posterior to this, BA3b, as well as BA1 and BA2 in the postcentral sulcus are areas involved in tactile processing. Thus, it is important to reiterate the importance of using a face localiser with tactile stimulation to define the areas within somatosensory cortex in future research.

Furthermore, it is important to note that early regions, such as the S1/M1, are not reliably activated during motor imagery (Dechent, Merboldt, & Frahm, 2004; Hétu et al., 2013), and it appears that motor imagery involves higher level regions, such as premotor, prefrontal, parietal and supplementary motor areas (Dechent et al., 2004; Gerardin et al., 2000; Hanakawa et al., 2003; Hétu et al., 2013; Park et al., 2015). Therefore, as activation was found in the S1/M1 ROI in this study, it further contends the idea that results could be a result of imagery. However, it would have been beneficial to implement an imagery task in the present research to control for the potential role of this factor; thus imagery cannot be completely disregarded in the current study. Furthermore, contradictory research has shown M1 to be activated during imagery, with studies showing overlap in motor imagery and execution in primary motor, bilateral premotor and parietal regions of the brain (Case et al., 2015; Gerardin et al., 2000; Hétu et al., 2013; Sugata et al., 2016), with an area in M1, namely area 4a, a sub-region more specifically related to implicit mental simulation processing (Tomasino & Gremese, 2016).

4.4.3.2 Were appropriate stimuli used?

Dynamic displays of expression were used in this study; this choice of stimuli was preferable despite the potential confounds with finding greater brain activation, see methodological fMRI considerations in the chapter introduction (4.1.5). However, it would have also been important to consider the number of emotional expressions and the inclusion of a neutral expression in this study. Studies have varied in the number of expressions tested with Hennenlotter et al. (2005) testing for overlap between happiness and neutral, to Carr et al. (2003) testing all six basic emotions without a neutral expression. This study reliably tested between three basic emotions; however, the inclusion of neutral would have been beneficial as activity between perception and production cannot be tested for affect-specificity

without this. Nonetheless this research addressed all the methodological concerns addressed in the chapter introduction (4.1.5), including the creation of a production task devoid of any face stimuli or cognitive influences, as well as removing any implicit biases to execute a facial expression in the perceptual task.

4.4.3.3 Are results exclusive to the embodiment of facial expressions?

Whilst these results provide evidence that there is similarity across the sensory perception and motor production of expression, it does not address whether these results are specific to the recognition of facial expressions or actions more generally. It may be that as faces are such biologically salient signals (Pessoa & Adolphs, 2010), see Chapter 2, that the overlaps found are specific to this. Hardwick et al. (2017) compared the face meta-analyses with leg and arm meta-analyses of action observation and execution; they found more activation in the face meta-analyses for inferior regions, the left thalamus and bilateral amygdala when observing faces. Although there are some differences, it seems that a general shared brain network in action exists, which encompasses the premotor and parietal cortices as well as the SMA, and is inherently similar to shared face networks (Crammond, 1997; Grèzes & Decety, 2001; Hardwick et al., 2017; Jeannerod, 2001). Leslie et al. (2004) further showed this with the similar shared network for the perception and production of hand actions to facial expressions. This non-exclusivity to faces may mean that the premotor results found in this study, likely reflect generalised representational overlap across the sensory perception and motor production of action. Therefore, in addition to tentatively supporting a strongly embodied account of emotion recognition, results may support the existence of an embodied account of action (Goldman & Sripada, 2005).

4.4.4 Wider implications.

The embodied nature of motor imagery and perception is appealing. There has been considerable interest using action imagery or simulation to improve skill acquisition and development, particularly in sport, as well as in rehabilitation settings for patients who have experienced a stroke, spinal cord injury or suffer from Parkinson's disease (Case et al., 2015; Hardwick et al., 2017; Tamir, Dickstein, & Huberman, 2007; Zimmermann-Schlatter, Schuster, Puhan, Siekierka, & Steurer, 2008). Research has shown that recurrent motor imagery increases premotor and primary motor activation in the brain (Case et al., 2015). Applying this principle, motor imagery could benefit a number of clinical populations that have difficulties

recognising emotions such as autism, anxiety, depression, schizophrenia and PTSD sufferers.

4.5 Conclusion

Given evidence that sensorimotor regions of the brain are active when perceiving and producing a facial expression, it was important to understand whether this activation was representationally similar. In the present study, participants were to perceive and later produce three basic facial expressions (happiness, disgust and sadness) in the scanner. Multivariate pattern analysis (MVPA) showed reliable decoding of expression in a face network of brain regions within the perception task, and sensorimotor regions within the production task. Furthermore, within perception and production, there was reliable expression decoding in premotor brain regions. Trends towards decoding expression in premotor brain regions were also shown within the cross-classification analyses, when the classifier was trained to discriminate emotion on perception and tested to discriminate emotion on production, or vice versa. These cross-classification results demonstrate representational overlap across the sensory perception and motor production of expression; and tentatively support a strongly embodied account of emotion recognition whereby we internally simulate another's expression to aid recognition (Goldman & Sripada, 2005). Thus visual recognition of emotion may depend in part on a primitive embodied account.

SECTION 3
-
General Discussion

Chapter 5: General Discussion

5.1 Chapter Overview

The research presented in this thesis explored the visual recognition of emotion, in particular the decoding of high-level influences on facial expression recognition. Both fMRI and EEG data were collected, and this data was primarily analysed with MVPA to examine the representation of facial expressions of emotion. Chapters 2 and 3 investigated extracted patterns of activation to understand how occluded facial features are represented in different brain regions and different time points, with pattern similarity across non-overlapping face parts implying the role of top-down contextual mechanisms. Furthermore, these chapters explored the effects of task, to further understand how the brain processes missing facial feature information when emotion is perceived in an explicit or implicit context. Chapter 4 investigated representational overlap across the sensory perception and motor production of expression, with pattern similarity testing for an embodied account of expression recognition. The results from chapters' 2 to 4 will be summarised in the present chapter, followed by a discussion of methodological and theoretical implications, with suggestions for future research.

5.2. Summary of Results

5.2.1 Chapters 2 and 3.

5.2.1.1 The high level influence of spatial context on expression processing.

Experiments conducted in Chapters 2 and 3 explore facial feature occlusion in expression recognition, given evidence that the brain can predict rich information about the visual environment. This is because it was important to understand how the brain processes and compensates for missing feature information, and more generally understand how the brain deals with occlusion. The fMRI study of Chapter 2 focuses on the occluded information contained within early visual (V1-V3), face and emotion sensitive areas, whilst the EEG study in Chapter 3 focussed on the temporal dynamics of processing occlusion (in posterior brain regions). MVPA results showed reliable decoding of facial expression (happy, fear and disgust) within conditions missing feature information. Importantly in Chapter 2, there were similar patterns of decoding across non-overlapping samples of face information, suggestive of the involvement of feedback mechanisms beyond low-level processing. These

cross-decoding results suggest the occurrence of a high-level context effect occurring in V1 and EVC (Clark, 2013; Greening et al., 2018; Heeger, 2017; Lee & Mumford, 2003; F. W. Smith & Muckli, 2010; Tang et al., 2014; Tang et al., 2018). Additional support for the potential role of feedback is provided by the presence of a later decoding peak post 300ms in Chapter 3. However, a follow-up univariate analysis with a novel finding of enhanced ERP responses to stimuli with occluded eye information (predominantly in fear recognition) suggests that the brain could be forming a prediction of this occluded facial feature. Nonetheless, this result may be due to an abundance of factors including task difficulty.

5.2.1.2 The high level influence of task goals on expression processing.

The experiments conducted in Chapters 2 and 3 also explore how task context affects the decoding of expression within and across conditions with non-overlapping feature information. Results from Chapter 2 find more robust decoding of expression under implicit processing conditions in early visual areas (V1-V3) and the IOG, but more robust decoding of expression under explicit processing conditions in the STS. More robust decoding of expression was suggested to occur in the explicit task of Chapter 3 (with more significant time points overall; Figure 3.47 for the explicit task compared to Figure 3.48 for the implicit task and Figure 3.64 for the explicit task compared to Figure 3.65 for the implicit task), these results are aligned more to decoding in the STS than early visual areas of the brain and thus correspond to the previous results. Thus it seems that implicit expression decoding, where participants carry out a gender task but the classifier can decode the emotion shown, is more prominent in early visual areas, and explicit expression decoding, where participants carry out an expression task and the classifier is decoding the emotion, more recruits the STS.

It is not clear why implicit expression decoding is generally higher in the early visual regions. The enhancement of processing in conditions where attention is not explicitly directed to an emotion, tentatively suggests that as expressions are such biologically salient signals (Pessoa & Adolphs, 2010), feedback may be enhanced under these conditions. The rapid automatic activation of subcortical pathways, when attention is not explicitly directed to an emotional task (Critchley et al., 2000; Gur et al., 2002; Hariri et al., 2000; Scheuerecker et al., 2007), further supports the biological significance of implicitly processing facial expressions. Finding higher explicit expression decoding in the STS corresponds with previous

research, finding this brain region to activate intentionally in processing faces under explicit conditions (Winston et al., 2002); although other studies have also shown decoding in the STS under implicit conditions (Said et al., 2010; Wegrzyn et al., 2015; Zhang et al., 2016). Furthermore, K. N. Kay and Yeatman (2017) found a categorisation or a one-back task, to affect both high-level and early visual responses through modulation from the intraparietal sulcus (IPS), in comparison to a sensory fixation task. Thus, the task goals of an experiment act as a high-level influence on perception of facial expression.

5.2.2 Chapter 4.

5.2.2.1 The high level influence of embodiment on expression processing.

The experiment conducted in Chapter 4 explores embodiment in emotion recognition, investigating the overlapping representations in the perception and production of facial expressions. Results demonstrated reliable decoding of expression in dorsal and ventral premotor brain regions within perception and production, as well as trends towards representational overlap in the dorsal premotor regions of the brain across the sensory perception and motor production of expression. These findings are partially compatible with previous research showing the ventral premotor cortex to be part of the HMNS in supporting simulation (Iacoboni & Dapretto, 2006; Kircher et al., 2013; Oberman et al., 2007), and generally an area regarded important in expression recognition (Wood, Rychlowska, et al., 2016). The results of this chapter tentatively support a strongly embodied account of emotion recognition, whereby we internally simulate another's expression to aid recognition (Goldman & Sripada, 2005). Furthermore, the embodied nature of emotion recognition is thought to be a high-level influence on the recognition of expression, as it is implied that sensorimotor simulation is fed back to a visual input (see Figure 5.88), continuingly regulating the perception of a stimulus (K. N. Kay & Yeatman, 2017; Wood, Lupyan, et al., 2016; Wood, Rychlowska, et al., 2016).

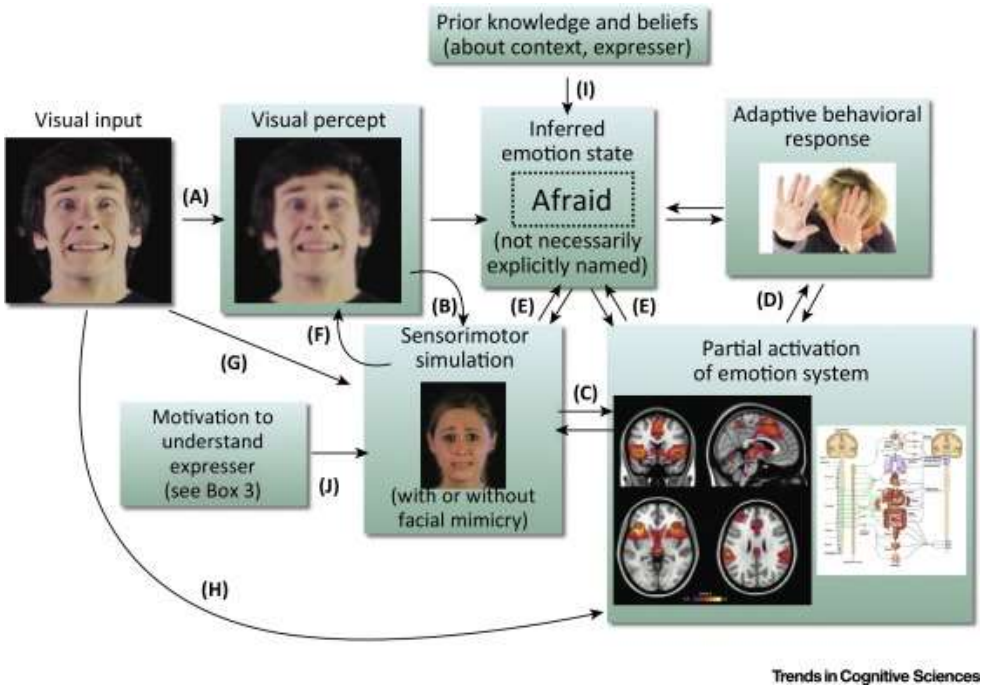

Figure 5.88. Facial expression recognition, importantly demonstrating the iterative loop between visual perception and sensorimotor simulation (B, F), and the engagement of visual, sensorimotor, premotor and subcortical cortices, from Wood, Rychlowska, et al. (2016).

5.3 Theoretical Implications

5.3.1 Mechanisms involved in recognising occluded facial expressions.

The results of Chapters 2 and 3 support the role of the visual processing pathway in expression recognition as this research shows the activation of early visual and temporal areas in the recognition of expression. Finding similar information across conditions missing non-overlapping or complementary feature information is in line with predictive coding and recurrent feedback models of object completion (O'Reilly et al., 2013; F. W. Smith & Muckli, 2010; Tang et al., 2014; Tang et al., 2018; Wyatte et al., 2014), as well as other approaches (addressed in more detail below) to help explain ambiguous information processing. This is apparent in Chapter 2, with sensitivity in early visual areas to occluded face features, suggesting the role of feedback and lateral interactions (F. W. Smith & Muckli, 2010). Whereas in Chapter 3 the increased ERP amplitudes potentially reflect the occurrence of prediction or error signals in predictive coding, or recurrent feedback signals in models of object completion, helping predict and fill in the important

missing feature information needed for recognition (Greening et al., 2018; Hajcak et al., 2010).

Evidently the results of Chapters 2 and 3 demonstrate high-level effects in the processing of occluded facial expressions; however, there are various possible models that could account for and explain these findings. These include predictive coding (Clark, 2013; Friston, 2005, 2008; Rao & Ballard, 1999), recurrent feedback models of object completion (O'Reilly et al., 2013; Tang et al., 2014; Tang et al., 2018; Wyatte et al., 2012), Bayesian (Lee & Mumford, 2003) and coherence infomax (W. A. Phillips et al., 1995) accounts of processing as well as a hierarchical neural network model (Heeger, 2017); these accounts, whilst outlined and addressed in Chapter 2, will be considered in turn for the results of Chapters 2 and 3.

In predictive coding, visual regions may expect certain incoming sensory information, such as whole face stimuli, however, when the observed stimuli is different from expectation, such that these faces have missing features, there may be an overall increased response to the occluded stimuli, and each visual region would have to compute the difference between the expected and observed incoming sensory information (Clark, 2013). Thus, predictions regarding the content of the missing information are likely formed in higher cortical levels and fed back to early visual regions; whilst prediction errors are likely transmitted back to higher-level regions in an attempt to account for the current sensory information (Rao & Ballard, 1999) (see Figure 2.11, Chapter 2). Predictive coding is potentially implicated due to the heightened decoding in the XC results of early visual regions, as well as the strengthened ERP amplitudes to partial face stimuli.

However, neither of these chapters tested the predictive coding account directly and the influences from feedback and lateral interactions cannot strictly be distinguished. Unfortunately existing models of V1 do not account well for the role of such influences (Carandini et al., 2005; Olshausen & Field, 2005; F. W. Smith & Muckli, 2010; Tang et al., 2018). Whilst, standard models on the response properties of neurons, such as grating response, are well established, it is surprising that a substantial amount of information about how V1 works, what it does and its role is still unknown (Olshausen & Field, 2005). This uncertainty accounts for up to 85% of V1's function, and arises because research has not investigated the properties of a representative sample of neurons in V1 when presented with ecologically complex stimuli (Carandini et al., 2005; Olshausen & Field, 2005). Furthermore, it is known

that V1 has considerable feedback connections from a number of brain regions, and thus V1 cannot be studied on its own (Muckli, 2010; Muckli & Petro, 2013; Muckli et al., 2013; Olshausen & Field, 2005).

In recurrent feedback models of object completion, extra-striate visual regions would immediately, following the feedforward process, send recurrent feedback signals to weak or non-activated V1 neurons in an attempt to process occluded face stimuli (Wyatte et al., 2014). This process continues automatically along hierarchically adjacent areas in the visual stream until object completion (Wyatte et al., 2012; Wyatte et al., 2014). Commonly, object completion is fully achieved after recurrent signals in the inferior temporal cortex are fed back to V1 (Wyatte et al., 2012); increased responses from the N170 ERP, located along this region of the brain, in response to partial stimuli, and the XC results for the EO to ME pair in the FG, are supportive of this model.

Results can also be explained with alternative Bayesian accounts of processing; in this account the bottom-up observations of the partial face stimuli would be concurrently assimilated with the top-down contextual priors to create probabilistic inferences regarding the content of the missing facial feature information (Kersten et al., 2004; Lee & Mumford, 2003; Yuille & Kersten, 2006). Thus the occluded face stimuli would initially lead to an overall decrease in response, but over time processing the occlusion amplifies the early visual response signals.

Finally the results could be explained with the hierarchical neural network model, proposed by Heeger (2017). This theory encompasses elements from the preceding models of visual processing, as neural activity in each region of the brain depends on a contribution from a feedforward, a feedback and a prior drive. Thus, in whole face conditions, neural responses are likely to depend on the feedforward bottom-up drive, where stimuli can be recognised in a feedforward computational model. However, in partial face conditions, neural responses are likely to also depend on a contribution from both the feedback and prior drive; whereby sensory representations are partially constructed from top-down contextual knowledge, and expectation is combined with sensory input to predict, for example, ambiguous missing feature stimuli. It is important to note that both of these chapters found interesting effects in the occluded eye conditions, these were demonstrated with high decoding accuracies in occluded eye conditions (ME and MO) within both tasks in

Chapter 2 and early ERP responses (P100 and N170), independent of task, to stimuli with occluded eye information in Chapter 3. This response was heightened if the emotion (e.g. fear) needed information for recognition from the eye region. Together these models help understand the role of bottom-up and top-down processes in early visual areas, advancing beyond the standard model of V1, in an attempt to account for its unknown function and feedback connections (Olshausen & Field, 2005).

Overall various possible models could account for the current findings and it is unclear without future research which model provides the best explanation; suggestions on how to test the predictive coding account directly are given in the future research section. Nonetheless, the current research is able to ascertain the role of contextual mechanisms (feedback and lateral interactions); highlighting the important role context has in shaping the activity of neurons in early sensory areas and the potential influence of top-down computations in expression recognition. The XC results found in Chapter 2 demonstrate the contextual mechanisms at work, as when there is no shared visual information given between two distinct partial face conditions, successful XC cannot just be a result of low-level processing in V1. This is further emphasised in the computational low-level modelling analysis where the XC results were at chance. Therefore these results together show that decoding performance is likely driven by top-down feedback processes or possibly lateral interactions in V1, providing contextual information regarding the occluded portion of a faces expression. Furthermore, the MVPA results in Chapter 3 (3.2.2.2 and 3.3.2.2) showed reliable decoding of facial expression from 50ms, in conditions missing feature information. In addition to this, the significant decoding in the neural time-course of occluded expression processing, appeared to resemble three decoding phases, potentially inferring the presence of feedforward and feedback processes (Cauchoix et al., 2014; Kaneshiro et al., 2015; Li et al., 2018).

5.3.2 The role of simulation in recognising facial expressions.

The results of Chapter 4 are generally supportive of simulation based theories of embodiment, where it seems that expression recognition is aided by simulation-like processes and potentially facial feedback (Niedenthal et al., 2006). This is evidenced by the overlapping neural representation trends in pre-motor brain regions when perceiving and producing specific facial expressions (Goldman & Sripada, 2005; Niedenthal, 2007; Saarimäki et al., 2015).

This account assumes the involvement of motor, premotor and somatosensory cortices in expression recognition. The ventral premotor cortex is considered to be part of the HMNS in supporting simulation, thus the reliable decoding found in dorsal and ventral premotor regions, within perception and production, supports the important role of the ventral premotor cortex in expression recognition (Iacoboni & Dapretto, 2006; Kircher et al., 2013; Oberman et al., 2007; Wood, Rychlowska, et al., 2016). The MN system is in line with Goldman and Sripada (2005)'s unmediated resonance model of expression recognition, which suggests that sub-threshold activation occurs in response to viewing an emotive face in the motor substrate for that emotion. Whilst this research shows the potential involvement of the premotor regions in the recognition of expression, it did not reveal overlap in S1/M1 activity. As aforementioned in Chapter 4, this could be a fault in the localisation of S1, to fully understand this, a face localiser with tactile stimulation, should have been employed to define regions involved in tactile somatosensory processing rather than movement. Despite this, results demonstrate some support for representational overlap across the sensory perception and motor production of expression, and tentatively support a strongly embodied account of emotion recognition, whereby we internally simulate another's expression to aid recognition (Goldman & Sripada, 2005). It is important to note that the embodied account of emotion recognition also extends to other actions, such as social hand gestures (Montgomery & Haxby, 2008). These results support a different approach to Chapters 2 and 3; focussed instead on simulation-like processes and not visual routes of expression recognition (Goldman & Sripada, 2005).

5.3.3 Uniting the visual mechanisms and the role of simulation in recognising facial expressions.

The results from Chapters 2 and 3 are disparate from Chapter 4, addressing different important questions related to how we recognise facial expressions. It may be that the accounts cannot individually provide a full understanding of expression recognition, as both the visual and sensorimotor pathways create sources of information in constructing a prediction of another's emotion (Wood, Rychlowska, et al., 2016). Therefore, it is important to understand how these two routes are combined and interact to work together.

The only study to link simulation based accounts of embodiment with the visual route of recognition, was carried out by Kragel and LaBar (2016), as they

investigated the role of the somatosensory cortex and asked participants to self-report their own emotional experience to visually presented stimuli. The behavioural results on how the participants experienced an emotion, were found to mirror the emotional content of the presented expression and were further decodable from fMRI activity in the right somatosensory cortex (Kragel & LaBar, 2016). This study therefore shows that the somatosensory cortices can link the visual perception of an emotion with one's own sensory experience (Kragel & LaBar, 2016). This element was missing in the embodiment study of Chapter 4, but could have been easily achieved with the implementation of a somatosensory localiser for the face; this localiser defines tactile simulation and these regions of somatosensory cortex may be those that are important in emotional experience. The S1/M1 region defined in Chapter 4 mainly corresponded to proprioception (or area BA3a), as opposed to most of the somatosensory cortex involved in tactile processing (BA3b, BA1 and BA2).

Wood, Rychlowska, et al. (2016) detailed the importance of the visual route to recognition, whereby an individual relies on diagnostic facial features as well as contextual knowledge of an expression for recognition, as emotions likely occur in response to specific contexts or events. These regularities develop an individual's conceptual knowledge of each emotion and in turn may be used to assist subsequent emotion recognition (Wood, Rychlowska, et al., 2016). However, they also detail how an individual may additionally make use of sensorimotor simulation for recognition. As aforementioned, this may be particularly apparent in the recognition of ambiguous or subtle expressions or during a particularly demanding task, especially in judging the genuineness of a smile (Niedenthal et al., 2010; Wood, Rychlowska, et al., 2016). Thus, it may be that the visual system is more important for recognition of the basic emotions, until a more complex task is introduced, where individuals cannot rely on visual diagnostic information or their contextual knowledge of an expression pertaining to a particular situation for recognition.

Furthermore, Wood, Lupyan, et al. (2016) incorporate both accounts as being involved in the recognition of emotion, showing how sensorimotor simulation is fed back to shape a current visual percept or input (see Figure 5.88). Whilst Goldman and Sripada (2005) outlined several models of embodiment, suggesting that these accounts provide a rapid, evolutionally adaptive cue for recognition, they further note that the visual route of recognition may be an invaluable compensatory method. Thus, these studies further support the importance of both visual and non-visual

routes to expression recognition, and how information is likely fed back to the visual system. Overall, it is not clear how these different routes are combined to work together because there is no single strategy employed in expression recognition, highlighting the overarching complexity of processing emotions.

5.4 Wider Implications

The paradigms developed in this thesis could reveal novel insights into how expression perception fails in particular conditions. Previous research has shown impairments in the recognition of expressions from the upper portion of the face (in particular the eyes) in individuals with Autism (Baron-Cohen, Wheelwright, Jolliffe, & Therese, 1997; Gross, 2004), but the paradigms employed in Chapters 2 and 3 could have investigated the involvement of early visual, face and emotion sensitive brain areas associated with this impairment. Furthermore, these individuals are suggested to compensate their impairments with greater expertise processing emotions from the mouth (Gross, 2004), thus it would be interesting to see these compensatory methods for expression perception in the brain, using the current research's PF stimuli. Based on the literature this expertise is believed to be a result of a highly developed secondary emotion system, a lower face expression recognition system that can be learned later in life (Gross, 2004). This contrasts with the primary system that focuses on the importance of upper face recognition, whilst this is normally present at birth, this system is deficient in autistic individuals (Gross, 2004). Furthermore, accuracy and speed of expression recognition has been shown to be affected when motor imagery, to stimulate and recognise expressions, has not been performed (Neal & Chartrand, 2011; Niedenthal et al., 2001); thus training individuals (especially clinical populations who have difficulties recognising emotions, such as autism, anxiety, depression, schizophrenia and PTSD sufferers) to simulate these expressions may be beneficial. Thus the paradigm employed in Chapter 4 could have included an aspect of motor imagery training (Tamir et al., 2007; Zimmermann-Schlatter et al., 2008), to see if post training results are associated with greater expression perception. However, research has shown some clinical populations to be able to recognise emotions without the use of simulation. These populations include autistic (McIntosh, Reichmann-Decker, Winkielman, & Wilbarger, 2006) and Moebius Syndrome (bilateral facial paralysis) sufferers (Rives Bogart & Matsumoto, 2010) who potentially rely on pattern matching or alternative

methods of recognition. Thus, it appears that difficulties in expression perception in the current thesis may indicate a number of individual differences.

5.4.1 Affective computing.

The results from these chapters are also relevant for the study of affective computing or emotion artificial intelligence (AI). This novel field of research is developing intelligent machines that can recognise expressions, through face images, vocal intonations and body language. Currently, these systems are being developed by a number of companies including Affectiva, CrowdEmotion and eyeris. The AI systems that recognise facial expression from face images are based on Action Units (AUs) or the FACS (Facial Action Coding System) to classify facial expressions (see 1.1.4 in Chapter 1 for more detail on these systems for categorising facial units). These software development kits (SDK) are based on an abundance of face images around the world and the technology can classify numerous spontaneous facial expressions with a high level of speed and accuracy. Furthermore, these systems are used in an abundance of settings, investigating driver state data to improve road safety and aiding market research by investigating consumer emotional engagement with advertisements (Affectiva, 2018). However, these deep-learning trained expression recognition models are only based on whole face bottom-up models of visual processing. Therefore, the models do not account for the role of high-level effects when processing partial face stimuli or simulation type mechanisms of expression recognition. Thus, these models are missing how occluded feature information would be processed, as the absence of FACs or AUs would prevent this bottom-up model from recognising an expression. Furthermore, simulation processes appear to be more adept at recognising subtle ambiguous expressions, such as the genuineness of a smile (Niedenthal et al., 2010; Wood, Rychlowska, et al., 2016); thus bottom-up models would likely miss the recognition of these subtleties in emotion. Overall, whilst the study of affective computing is especially relevant to this thesis, the alternative routes of processing emotional expressions are not accounted for but are vitally important in gaining a full understanding of expression recognition.

5.5 Limitations

Each chapter has demonstrated considerable evidence of high-level influences on facial expression recognition, showing the visual areas carrying information about hidden parts of a face stimulus, as well as the high-level

influences of task and embodiment. However, the decoding of these influences and full understanding into the visual recognition of emotion is challenging and fundamentally influenced by many factors. It is important to carefully consider the statistical power of the studies, as well as the localisation of brain regions and choice of stimuli. It is also important to note that eye movements could play a role in these studies. Nonetheless participants were explicitly told to fixate on a central cross in each of the experiments, which should reduce the effects of eye movements on results. Future work would benefit from the use of eye-tracking equipment to make sure participants eyes remain on fixation.

5.5.1 Power.

Whilst neuroscientific studies of brain activation and the use of subsequent analytical techniques have advanced the understanding into the brains basis of expression recognition, there are concerns over the generalisability and statistical power of neuroimaging research (Button et al., 2013; Poldrack et al., 2017). These problems are generally a result of small sample sizes in MRI research; ideally a minimum of 20 participants in one experimental group are needed, but research power would benefit from nearer to 30 or more participants (Poldrack et al., 2017). Unfortunately the present fMRI research studies were not able to scan more participants due to funding and time constraints, with 12 participants in Chapter 2 and 13 participants in Chapter 4. As also aforementioned, the EEG study in Chapter 3 would benefit from more participants, in order to run the cross-classification analyses.

However, many existing fMRI decoding studies have tested below 20 participants (Greening et al., 2018; Harry et al., 2013; Liang et al., 2017; Oosterhof et al., 2010; Peelen et al., 2010; Petro et al., 2013; F. W. Smith & Muckli, 2010; Wegrzyn et al., 2015) and have found significant results. Thus, the sample sizes in this thesis may have been sufficient. Overall, it is important to note that the findings in each of these chapters are promising, with strong effect-sizes.

In Chapter 2, ANOVAs to investigate task and PF condition, or cross-classified pair on decoding accuracy were reported with partial eta-squared (η_p^2) as a measure of effect-size. In Cohen (1988), a large effect-size is demonstrated with a value greater than 0.14; a medium effect-size greater than 0.06 and a low effect-size greater than 0.01. The basic decoding results in V1 and EVC demonstrated

considerably high effect-sizes for PF condition and task, with effect-sizes for the PF and task interactions greater than $\eta_p^2 = 0.32$. Furthermore, the cross-classification decoding results in V1 and EVC demonstrated considerably high effect-sizes for cross-classification pair and task, with effect-sizes for the cross-decoding interactions between cross-classification pair and task greater than $\eta_p^2 = 0.69$. The cross-decoding effect-sizes strengthen results, showing the high-level contextual influences on the processing of occluded facial expressions, as well as the high-level task effects on expression recognition. The findings of high-level effects within the expression decoding analyses of V1 are also bolstered with the large effect-sizes shown in the V1 univariate analysis. Weaker results were found in the additional ROIs with more varied effect-sizes, however, medium to large effect-sizes were shown for some of these ROIs, including the STS and IOG, in the basic and cross-classification decoding results.

In Chapter 3, ANOVAs to investigate task, emotion and PF condition on mean amplitude were carried out in the univariate ERP analysis, which also reported partial eta-squared. Results in this chapter was also associated with large effect-sizes; with the effect of PF condition high (> .14) in both studies for all ROIs (rN170, lN170, P100 and P300), with high amplitudes in the MO, for instance, further supporting the importance of mouth information and features diagnostic for task completion. Furthermore, there are large effect-sizes associated with emotion in both studies, particularly in the P300 where amplitudes were greatest for fear and weakest for happiness. There was also medium to large effect-sizes associated with task even though there was no significance, these are shown in the P300 of study one and rN170, lN170 and P100 of study two whereby the amplitudes are greater in the gender than the emotion task. These results display some novel supporting effects for the task hypothesis as amplitudes were stronger in the implicit task, even though these are absent as a result of power. Lastly the significant interactions between emotion and PF condition in the N170 (rN170 in study one, lN170 study two) and P100 (study two) showed large effect-sizes, as well as an interaction between task, emotion and PF condition in the P300 of study one; these further support the observed amplitude increases to occluded eye information in fear recognition.

In Chapter 3, the t-test results for each time point's decoding accuracy was reported with Cohen's *d* as a measure of effect-size, whereby $d > 0.80$ is thought to

be a large effect-size, $d > .050$ a medium effect-size, and $d > .020$ a small effect-size. In study one, the effect-sizes were greatest for explicit expression decoding in the WF condition between 100ms and 700ms (*d*'s = 0.58 to 1.09). Medium to large effect-sizes were also found in the ME, MO and MM condition. In study two, the effect-sizes were greatest in the ME condition between 50ms and 250ms (*d*'s = 0.58 to 0.74), with small to medium effect-sizes in the WF, ME and MO conditions. These results bolster the findings of early decoding accuracy for expression and the importance of the eyes and mouth in early expression recognition. For implicit expression decoding, study one showed medium effect-sizes for trends in the WF condition, but a medium effect-size for the EO significance in study two. Overall, both in terms of the number of significant time points and larger effect-sizes, explicit decoding of expression is greater than implicit decoding of expression in the EEG analyses.

In Chapter 4, the t-test results for each ROI's decoding accuracy were again reported with Cohen's *d*. In the basic decoding results, effect-sizes were $d = 0.70$ or above in both ventral and dorsal premotor regions. There was a large effect-size in the cross-classification results for a perceptually defined dorsal premotor region ($d = 0.83$); whilst cross-classification results were weaker in the production task, there where trends in the dorsal premotor regions, defined from production, associated with medium to large effect-sizes (0.51 and 0.79). Overall, all significant effects, including those that did not survive FDR correction produced medium to large effect-sizes. Therefore, the effect-sizes bolster the representational overlap findings, further tentatively supporting a strongly embodied account of emotion recognition.

5.5.2 Localisation of brain regions.

In the present research, the fMRI study of Chapter 2 used retinotopic mapping to localise early visual cortex (EVC). This is an invaluable localisation method to ascertain the boundaries of V1-V3 and subsequently investigate activation and representation occurring in a mapped position of visual space. This localisation led to the conclusion that information about facial expression can be read out from early visual brain regions, and demonstrated the strong involvement of contextual influences in early visual processing when devoid of overlapping feedforward information. This retinotopic mapping was based on each individual subject. This strengthened the results from Greening et al. (2018) who also found neural information in EVC to generalise across independent face parts, but through

mapping the cortex less effectively with a cytoarchitectonic map (Eickhoff et al., 2005). As aforementioned in Chapter 2 (2.1.1.2.1), this method is sub-optimal because it applies the same map to all participants and consequently does not account for individual differences.

Although, the localisation of EVC was well-defined and the main focus was to understand the contextual effects in this area for the present research; traditional face localiser scans (using a faces > objects contrast) to define the STS and FG, would have been beneficial to understand the potential role of these higher-level areas to effects observed within the retinotopically defined V1. Instead these regions were selected with key words in the meta-analysis from the NeuroSynth database, again this method does not account well for individual differences. Nonetheless, there were significant results in the STS and FG, with effects corresponding to previous research of decoding expression (Harry et al., 2013; Liang et al., 2017; Said et al., 2010; Wegrzyn et al., 2015; Zhang et al., 2016), including a recent study by Li et al. (2018) which also elucidated two distinct stages of face processing in a clearly defined FG. These stages included a rapid feedforward face-selective decoding around 180ms in posterior FG, and later decoding of expression between 230ms-460ms in mid-fusiform regions. This later decoding phase may resemble an integration of information, and consequently a possible backwards projection of top-down information. Furthermore the results correspond with research finding high-level representations in the STS (Peelen et al., 2010; Skerry & Saxe, 2014). However, decoding accuracy was generally lower in the FG and STS of the current research and their definition could reflect this. It is also important to mention that the complementary EEG study of Chapter 3 cannot supply further information on this problem, as ERP's are only loosely tied to specific brain regions, and in general, the neuroscientific technique is associated with low spatial resolution.

Adding to this, the fMRI study of Chapter 4 could have also benefitted from the application of these face localiser scans, but as aforementioned, this study most importantly would have benefitted from a tactile somatosensory face localiser. This is because in the present research the sensorimotor cortex was broadly defined as S1/M1, which only resembles a specific sub-region of S1 (likely area 3a, the area involved in movement) and completely misses the other parts of S1 (e.g. area 3b) that deal with tactile simulation. Thus, representational overlap between the sensory

perception and motor production of expression may have been present if the somatosensory cortex was better defined.

5.5.3 Choice of stimuli.

An abundance of studies are based on the assumption of basic emotions and the experimental chapters in the present research are no exception, investigating happiness and disgust, with the addition of fear in Chapters 2 and 3, and sadness in Chapter 4. These basic emotions are normally depicted as static displays, portrayed with full intensity and associated with an easy recognition task. Whilst this somewhat enables greater comparison among studies, it is important to remember that facial expressions in the real world may be difficult to recognise, as faces are often seen for fleeting moments of time, in peripheral vision with constrained viewing conditions, whereby subtle expression judgements are required (e.g. smile authenticity) (Bayle et al., 2011; Bould, Morris, & Wink, 2008; Calvo, Fernández-Martín, et al., 2014; Calvo & Nummenmaa, 2015; Korb, With, Niedenthal, Kaiser, & Grandjean, 2014; Niedenthal et al., 2010; F. W. Smith & Rossit, 2018). More complex tasks or emotions, including the recognition of compound and dynamic emotions (Du, Tao, & Martinez, 2014; Gold et al., 2013), will enable the tasks to be more akin to real life, increasing their ecological validity. As previously mentioned, however, dynamic stimuli are associated with more brain regions activated, such as the STS (see 4.1.5 in Chapter 4), and thus the reason for a brain regions activation (in response to recognition of expression or movement) needs to be understood. Despite this possible difference, Duchaine and Yovel (2015) stated that face areas of the brain (FFA and OFA) extract comparable information from both static and dynamic faces, and other research has suggested that differences between these stimuli, in a participant's overall ability to recognise an expression, plays a surprisingly minor role (Gold et al., 2013).

The use of more complex emotions and increasing a tasks difficulty may have yielded different results in the present research. It is possible that the EVC decoding results may be more significant if subtle or ambiguous expressions are used. This is because the decoding of complex emotions could require more activation of higher visual areas, to process the stimuli and consequently feed information back to EVC (Alink et al., 2010). Furthermore, some basic emotions could be associated with increased feedback, as they are expected to be the most salient. Thus, the brain would need to process potentially threatening expressions

(such as fear and anger) (Pessoa & Adolphs, 2010) that are absent of large easily-identifiable facial shape deformations from the mouth (Du & Martinez, 2011).

Furthermore, research has shown that sensorimotor simulation may be particularly important for the recognition of subtle or ambiguous expressions, when a task is harder (Hess & Blairy, 2001; Niedenthal et al., 2010; Rychlowska, Cañadas, et al., 2014; Wood, Rychlowska, et al., 2016). This is particularly prominent in the processing of a smile, considered to be the most complex facial expression (Korb et al., 2014; Niedenthal et al., 2010; Rychlowska, Cañadas, et al., 2014). The judgement of a genuine, or a Duchenne smile, relies on the recognition of subtle structural and temporal information, and disrupting mimicry (and presumably embodied simulation) impairs the differentiation of a false from a Duchenne smile (Rychlowska, Cañadas, et al., 2014; Wood, Rychlowska, et al., 2016). Furthermore, Neal and Chartrand (2011) showed mimicry to enhance subsequent expression recognition in the 'Reading the Mind in the Eyes' task (RMET), testing secondary subtle non-prototypical emotions. Moreover, Wood, Rychlowska, et al. (2016) stated that embodied simulation would be more likely to occur in ambiguous situations, when an individual does not know what an expresser is feeling. Thus, if more subtle or ambiguous emotions were used in this chapter, it is possible that being asked to produce these expressions may lead to greater activation in sensorimotor brain regions as greater simulation is likely needed for recognition.

It is not only important to consider expression choice but also how the partial stimuli were created in Chapters 2 and 3. As aforementioned, the recognition of a partially occluded object is affected by its nature of occlusion (Johnson & Olshausen, 2005), in this thesis an occluder with a different background colour was used. With this black occluder on a grey background, the hidden region looked occluded rather than simply missing, thus it was possible that amodal completion was used to complete the continuation of a face (Johnson & Olshausen, 2005). Features would appear to be missing or removed if grey occluders to match the background colour were used, as this would prevent amodal completion. Thus, this type of occlusion may affect results, whereby missing feature information may not have been read out from the early visual brain. It would be interesting to compare the current method of occlusion with deletion (e.g. using grey occluders), to see if the neural mechanisms underlying expression recognition of partial faces is affected by the nature of occlusion and subsequent amodal completion. Whilst deletion would be

a good method to investigate, it would be of additional interest to investigate natural occlusion; such as having a pair of sunglasses, as opposed to a block shape, occluding facial information for expression recognition. However, these stimulus changes would present a problem or a trade-off with object processing. Nonetheless, the occlusion used in the present research provides interesting results regarding the processing of incomplete stimuli.

5.6 Future Directions

To reiterate, results of Chapters 2 and 3 are compatible with accounts of predictive coding. This is because unpredictable sensory inputs (missing facial features) are thought to require more activation of early (V1) and higher visual areas; and the present results show increased decoding in early visual areas for the ME compared to the WF condition (Chapter 2), or strengthened amplitudes in higher-level brain regions to faces missing feature information (Chapter 3) (Alink et al., 2010; Rao & Ballard, 1999). Importantly, the XC results of Chapter 2 also show compatibility with accounts of predictive coding, with the suggestion of feedback mechanisms beyond low-level processing; finding similar representation-specific decoding in the absence of V1 input across non-overlapping samples of face information. However, neither Chapters 2 nor 3 differentiate between prediction and prediction error activity as they were not set up to directly test the account of predictive coding (Kok & de Lange, 2015). As such, the activity found can only potentially reflect the occurrence of prediction or prediction error signals. Thus, to directly test this account, the experimental design would need to be amended to measure prediction and prediction error signals occurring in the occluded face areas.

Studies that have directly tested predictive coding have taken advantage of paired associative learning, by pairing a high or low frequency auditory cue with a visual stimulus (den Ouden, Daunizeau, Roiser, Friston, & Stephan, 2010; den Ouden, Friston, Daw, McIntosh, & Stephan, 2009; Kok & de Lange, 2015). These studies find a greater V1 response to a violation in the pairing; when a target is not preceded by its cue or there was no visual stimulus presented (Kok & de Lange, 2015). This suggests a prediction error indicative of predictive coding, as representation-specific activity begins before visual input to make a prediction, and any violation leads to an increased response (Kok & de Lange, 2015). It is important to note that stimuli with any attentional effects (related to interest and/or surprise) are removed as these effects will also lead to an enhanced V1 response (Kok & de

Lange, 2015); this is a challenge in research and may be more problematic with the use of facial images as attention could be drawn to the eyes and/or mouth (F. W. Smith et al., 2008; M. L. Smith et al., 2005). However, this problem can be overcome by introducing an irrelevant task where attention to the paired associations between stimuli are not focussed on (den Ouden et al., 2010; den Ouden et al., 2009).

Apparent motion illusion studies have also been used to directly test the predictive coding account (Alink et al., 2010; Muckli et al., 2005). These paradigms ask participants to fixate at a set point, whilst other bars appear on screen to create a predictable or unpredictable illusion of motion (Alink et al., 2010; Muckli et al., 2005). The predictable illusions of motion are associated with less activity in V1, compared to unpredictable stimuli (Alink et al., 2010). However, these studies need to consider how predictive coding works in ecologically valid environments, particularly in the perception of expressions.

Paired association and apparent motion illusion studies are hard to implement to directly test predictive coding in respect to the current research. Alternatively, research has shown that predictive coding can be investigated by looking closer into the neural architecture of V1, separating this brain region into its different cortical layers (Muckli et al., 2015). This is because each layer differentially contains feedforward and feedback connections, and looking at the layers involved in feedback can help isolate and investigate these effects. Contextual feedback has been found in superficial outer layers of V1, this feedback is likely projecting from extra-striate visual, cortical and subcortical brain regions (Muckli et al., 2015). However, top-down feedback has also been found to activate deep layers of V1 (Kok, Bains, van Mourik, Norris, & de Lange, 2016). Therefore, carrying out the same paradigm using a 7T fMRI scanner will enable the cortical layers to be mapped, to subsequently investigate feedback effects that could be expected in either deep or superficial layers of V1.

Furthermore, research has investigated the influence of task dependent feedback on specific sub-regions of V1, conceptualising the role of predictive coding in this process (Petro et al., 2013). They did this by mapping the feedforward cortical representation of two non-overlapping facial feature locations (the eyes and mouth) in V1, presenting contrast-reversing checkerboards where these features would appear on face stimuli (Petro et al., 2013). Participants carried out facial expression and gender classification tasks, and a classifier was trained to decode expression or

gender in the two feature locations, as well as a rest-of-V1 region (Petro et al., 2013). Petro et al. (2013) investigated decoding within these V1 regions as a function of task, subsequently they found implicit task effects, which may be a result of prediction error responses; for example, expression changes occurring when participants are asked to judge gender, may be surprising and lead to a prediction error. Furthermore, the observed task influences cannot be explained by feedforward visual feature processing, as the same images were presented in both tasks. Petro et al. (2013) also found V1 to process facial expression and gender in the two feedforward feature locations, as well as in the outside rest-of-V1 region, indicative of distributed feedback to V1. As this study used whole face images, the effects that occur when facial features are occluded cannot be investigated. If the cortical representation of the eyes and mouth were localised in the current research, the predictive coding account could be tested to further understand how the brain processes missing facial feature information, when emotion is perceived in an explicit or implicit context. This is because if stimuli with occluded eye or mouth information can be respectively decoded in their mapped cortical regions, it is suggestive of prediction or prediction error responses, whereby information is being transmitted to higher-level regions to account for the current sensory information devoid of overlapping feedforward input. Furthermore, akin to Petro et al. (2013), the regions of V1 can be tested as a function of task, as the same feedforward information is presented in the expression and gender recognition tasks.

In addition to this, more research needs to be undertaken uniting the two routes to the study of visual recognition; visual and non-visual (simulation-based) routes to expression recognition. This can be achieved by testing whether representation in the sensorimotor cortices is linked to emotion recognition accuracy, or by comparing correlations in visual, somatosensory or premotor cortex with recognition performance in simple and more complex emotion tasks. Furthermore, the relative contribution of visual compared to somatosensory and premotor brain regions can be tested by measuring decoding in each of these regions. It would be interesting to see how the two routes are combined for recognition of basic and more complex expressions.

Overall, however, a continuation of MVPA research is needed, as investigating representational overlap is more insightful than past univariate fMRI research. This is because it is more sensitive in recognising cognitive states, as well

as distinguishing how these cognitive states are represented or organised within the brain (Coutanche et al., 2016; Norman et al., 2006). MVPA allows an investigation beyond brain activation, at spatial information contained in fine-grained patterns of activity, in order to investigate specific representational content within an individual region (Haynes, 2015; Mur et al., 2009). This approach also allows a consideration into patterns of response for content based brain processing, which can be combined with patterns in computational models (Haynes, 2015). Unfortunately, data from the past univariate research lacks sensitivity, as it is spatially smoothed and activation is averaged across voxels in ROIs (Haynes & Rees, 2006; Mur et al., 2009; Norman et al., 2006). Consequently, this analysis restricts the understanding of cognitive states, while MVPA can potentially discriminate patterns of activation in separate conditions, even if at a univariate level, activation is the same among the conditions (Norman et al., 2006; Tong & Pratte, 2012). Todd, Nystrom and Cohen (2013) highlight that reaction time could be a potential factor confounding MVPA, but a follow-up comment and controversies paper by Woolgar, Golland and Bode (2014), propose that the value and sensitivity of MVPA outweighs the reduced specificity of these analyses, that discard the direction of neural effects. They further state that whilst alternative univariate analyses specify the direction of underlying neural effects, these analyses are also susceptible to confounds (Woolgar, Golland & Bode, 2014). It is also important to further use a combination of fMRI and EEG brain imaging techniques, as this provides a comprehensive picture at both a high spatial and a high temporal brain resolution (Fusar-Poli et al., 2009).

5.7 General Conclusion

In conclusion, this thesis demonstrates several high-level influences on facial expression perception that can be decoded in the brain: contextual information arising from occluded faces, task goals and embodiment. Many effective strategies are seemingly adopted to aid the visual recognition of emotion, including top-down contextual mechanisms to the visual system and sensorimotor simulations in sensory and motor regions of the brain. This follows on the two main strands outlined in Chapter 1, as it is evident that both visual and non-visual (simulation-based) routes are involved in expression recognition. As such, results are in keeping with models such as predictive coding (and other approaches such as recurrent feedback models of object completion, Bayesian and coherent infomax accounts of processing and Heeger (2017)'s hierarchical neural network model) emphasising the use of top-

down information to aid current visual processing, as well as embodied theories of emotion recognition, including the unmediated resonance model and the role of the premotor cortices. It appears that the two routes of visual information can be combined to work together but there is no single strategy employed in expression recognition, showing the complexity of processing emotions. It may be that the visual route is more important until a task is harder and embodied simulation is needed. Overall the results of the present experiments extend understanding and knowledge of how the brain visually recognises emotion, and enables further research directions in this field.

References

Adolphs, R. (2002). Neural systems for recognizing emotion. *Current Opinion in neurobiology, 12*(2), 169-177. https://doi.org/10.1016/S0959-4388(02)00301-X

Adolphs, R. (2002). Recognizing Emotion from Facial Expressions: Psychological and Neurological Mechanisms. *Behavioral and Cognitive Neuroscience Reviews, 1*(1), 21-62. https://doi.org/10.1177/1534582302001001003

Adolphs, R. (2010). Social cognition: feeling voices to recognize emotions. *Current Biology, 20*(24), R1071-1072. https://doi.org/10.1016/j.cub.2010.11.019

Adolphs, R., Damasio, H., Tranel, D., Cooper, G., & Damasio, A. R. (2000). A Role for Somatosensory Cortices in the Visual Recognition of Emotion as Revealed by Three-Dimensional Lesion Mapping. *The Journal of Neuroscience, 20*(7), 2683-2690. https://doi.org/10.1523/JNEUROSCI.20-07-02683.2000

Affectiva. (2018, September 23). Retrieved from www.affectiva.com

Alink, A., Schwiedrzik, C. M., Kohler, A., Singer, W., & Muckli, L. (2010). Stimulus Predictability Reduces Responses in Primary Visual Cortex. *The Journal of Neuroscience, 30*(8), 2960-2966. https://doi.org/10.1523/JNEUROSCI.3730-10.2010

Allen-Walker, L., & Beaton, A. A. (2015). Empathy and perception of emotion in eyes from the FEEST/Ekman and Friesen faces. *Personality and Individual Differences 72*, 150-154. https://doi.org/10.1016/j.paid.2014.08.037

Anzellotti, S., & Caramazza, A. (2016). From Parts to Identity: Invariance and Sensitivity of Face Representations to Different Face Halves. *Cerebral Cortex, 26*(5), 1900-1909. https://doi.org/10.1093/cercor/bhu337

Anzellotti, S., Fairhall, S. L., & Caramazza, A. (2014). Decoding Representations of Face Identity That are Tolerant to Rotation. *Cerebral Cortex, 24*(8), 1988-1995. https://doi.org/10.1093/cercor/bht046

Apicella, F., Sicca, F., Federico, R. R., Campatelli, G., & Muratori, F. (2013). Fusiform Gyrus responses to neutral and emotional faces in children with Autism Spectrum Disorders: a High Density ERP study. *Behavioural Brain Research, 251*, 155-162. http://doi.org/10.1016/j.bbr.2012.10.040

Aziz-Zadeh, L., Sheng, T., & Gheytanchi, A. (2010). Common premotor regions for the perception and production of prosody and correlations with empathy and

prosodic ability. *PLoS One, 5*(1), e8759. https://doi.org/10.1371/journal.pone.0008759

Bagby, R. M., Parker, J. D. A., & Taylor, G. J. (1994). The twenty-item Toronto Alexithymia scale—I. Item selection and cross-validation of the factor structure. *Journal of Psychosomatic Research,38*(1), 23-32. https://doi.org/10.1016/0022-3999(94)90005-1

Balconi, M., & Bortolotti, A. (2013). The "simulation" of the facial expression of emotions in case of short and long stimulus duration. The effect of pre-motor cortex inhibition by rTMS. *Brain Cognition, 83*(1), 114-120. https://doi.org/10.1016/j.bandc.2013.07.003

Balconi, M., & Canavesio, Y. (2016). Is empathy necessary to comprehend the emotional faces? The empathic effect on attentional mechanisms (eye movements), cortical correlates (N200 event-related potentials) and facial behaviour (electromyography) in face processing. *Cognition and Emotion 30*(2), 210-224. https://doi.org/10.1080/02699931.2014.993306

Banissy, M. J., Sauter, D. A., Ward, J., Warren, J. E., Walsh, V., & Scott, S. K. (2010). Suppressing sensorimotor activity modulates the discrimination of auditory emotions but not speaker identity. *The Journal of Neuroscience, 30*(41), 13552-13557. https://doi.org/10.1523/JNEUROSCI.0786-10.2010

Bannert, M. M., & Bartels, A. (2013). Decoding the yellow of a gray banana. *Current Biology, 23*(22), 2268-2272. https://doi.org/10.1523/JNEUROSCI.0786-10.2010

Baron-Cohen, S. (2004). *The essential difference.* UK: Penguin.

Baron-Cohen, S., & Wheelwright, S. (2004). The Empathy Quotient: An Investigation of Adults with Asperger Syndrome or High Functioning Autism, and Normal Sex Differences. *Journal of Autism and Developmental Disorders, 34*(2), 163-175. https://doi.org/10.1023/B:JADD.0000022607.19833.00

Baron-Cohen, S., Wheelwright, S., & Jolliffe, A. T. (1997). Is there a" language of the eyes"? Evidence from normal adults, and adults with autism or Asperger syndrome. *Visual Cognition, 4*(3), 311-331. https://doi.org/10.1080/713756761

Bastiaansen, J. A., Thioux, M., & Keysers, C. (2009). Evidence for mirror systems in emotions. *Philosophical Transactions of the Royal Society of London B:*

Biological Sciences, 364(1528), 2391-2404. https://doi.org/10.1098/rstb.2009.0058

Batty, M., & Taylor, M. J. (2003). Early processing of the six basic facial emotional expressions. *Cognitive Brain Research, 17*(3), 613-620. http://doi.org/10.1016/S0926-6410(03)00174-5

Bayle, D. J., Schoendorff, B., Hénaff, M.-A., & Krolak-Salmon, P. (2011). Emotional Facial Expression Detection in the Peripheral Visual Field. *PLoS One, 6*(6), e21584. https://doi.org/10.1371/journal.pone.0021584

Bentin, S., Allison, T., Puce, A., Perez, E., & McCarthy, G. (1996). Electrophysiological Studies of Face Perception in Humans. *Journal of Cognitive Neuroscience, 8*(6), 551-565. https://doi.org/10.1162/jocn.1996.8.6.551

Bettadapura, V. (2012). Face Expression Recognition and Analysis: The State of the Art. *arXiv preprint arXiv:1203.6722*.

Birn, R. M., Cox, R. W., & Bandettini, P. A. (2004). Experimental designs and processing strategies for fMRI studies involving overt verbal responses. *Neuroimage, 23*(3), 1046-1058. https://doi.org/10.1016/j.neuroimage.2004.07.039

Blairy, S., Herrera, P., & Hess, U. (1999). Mimicry and the Judgment of Emotional Facial Expressions. *Journal of Nonverbal Behavior, 23*(1), 5-41. https://doi.org/10.1023/A:1021370825283

Blau, V. C., Maurer, U., Tottenham, N., & McCandliss, B. D. (2007). The face-specific N170 component is modulated by emotional facial expression. *Behavioral and Brain Functions, 3*(1), 7. https://doi.org/10.1186/1744-9081-3-7

Bombari, D., Schmid, P. C., Schmid Mast, M., Birri, S., Mast, F. W., & Lobmaier, J. S. (2013). Emotion recognition: The role of featural and configural face information. *The Quarterly Journal of Experimental Psychology, 66*(12), 2426-2442. https://doi.org/10.1080/17470218.2013.789065

Bould, E., Morris, N., & Wink, B. (2008). Recognising subtle emotional expressions: The role of facial movements. *Cognition and Emotion, 22*(8), 1569-1587. https://doi.org/10.1080/02699930801921156

Brainard, D. H. (1997). The psychophysics toolbox. *Spatial vision, 10*, 433-436. https://doi.org/10.1163/156856897X00357

Bruce, V., & Young, A. (1986). Understanding face recognition. *British Journal of Psychology, 77*(3), 305-327. https://doi.org/10.1111/j.2044-8295.1986.tb02199.x

Button, K. S., Ioannidis, J. P. A., Mokrysz, C., Nosek, B. A., Flint, J., Robinson, E. S. J., & Munafò, M. R. (2013). Power failure: why small sample size undermines the reliability of neuroscience. *Nature Reviews Neuroscience, 14 (5)*, 365. https://doi.org/10.1038/nrn3475

Calder, A. J., & Young, A. W. (2005). Understanding the recognition of facial identity and facial expression. *Nature Reviews Neuroscience, 6*(8), 641-651. https://doi.org/10.1038/nrn1724

Calvo, M. G., Fernández-Martín, A., & Nummenmaa, L. (2014). Facial expression recognition in peripheral versus central vision: role of the eyes and the mouth. *Psychological research, 78*(2), 180-195. https://doi.org/10.1007/s00426-013-0492-x

Calvo, M. G., Gutiérrez-García, A., Fernández-Martín, A., & Nummenmaa, L. (2014). Recognition of Facial Expressions of Emotion is Related to their Frequency in Everyday Life. *Journal of Nonverbal Behavior, 38*(4), 549-567. https://doi.org/10.1007/s10919-014-0191-3

Calvo, M. G., & Nummenmaa, L. (2015). Perceptual and affective mechanisms in facial expression recognition: An integrative review. *Cognition and Emotion, 30 (6)*, 1081-1106. https://doi.org/10.1080/02699931.2015.1049124

Carandini, M., Demb, J. B., Mante, V., Tolhurst, D. J., Dan, Y., Olshausen, B. A., . . . Rust, N. C. (2005). Do We Know What the Early Visual System Does? *The Journal of Neuroscience, 25*(46), 10577-10597. https://doi.org/10.1523/jneurosci.3726-05.2005

Carlson, T., Tovar, D. A., Alink, A., & Kriegeskorte, N. (2013). Representational dynamics of object vision: The first 1000 ms. *Journal of Vision, 13*(10), 1-1. https://doi.org/10.1167/13.10.1

Carr, L., Iacoboni, M., Dubeau, M. C., Mazziotta, J. C., & Lenzi, G. L. (2003). Neural mechanisms of empathy in humans: a relay from neural systems for imitation to limbic areas. *Proceedings of the National Academy of Sciences, 100*(9), 5497-5502. https://doi.org/10.1073/pnas.0935845100

Case, L. K., Pineda, J., & Ramachandran, V. S. (2015). Common coding and dynamic interactions between observed, imagined, and experienced motor

and somatosensory activity. *Neuropsychologia, 79*, 233-245. https://doi.org/10.1016/j.neuropsychologia.2015.04.005

Cauchoix, M., Barragan-Jason, G., Serre, T., & Barbeau, E. J. (2014). The neural dynamics of face detection in the wild revealed by MVPA. *The Journal of Neuroscience, 34*(3), 846-854. https://doi.org/10.1523/JNEUROSCI.3030-13.2014

Chang, C.-C., & Lin, C.-J. (2011). LIBSVM: A library for support vector machines. *ACM Transactions on Intelligent Systems and Technology, 2*(3), 1-27. https://doi.org/10.1145/1961189.1961199

Chartrand, T. L., & Bargh, J. A. (1999). The chameleon effect: The perception–behavior link and social interaction. *Journal of Personality and Social Psychology, 76*(6), 893-910. https://doi.org/10.1037/0022-3514.76.6.893

Cichy, R. M., Pantazis, D., & Oliva, A. (2014). Resolving human object recognition in space and time. *Nature Neuroscience, 17*(3), 455-462. https://doi.org/10.1038/nn.3635

Clark, A. (2013). Whatever next? Predictive brains, situated agents, and the future of cognitive science. *Behavioral and Brain Sciences, 36*(3), 181-204. https://doi.org/10.1017/S0140525X12000477

Cohen, J. (1988). *Statistical power analysis for the behavioral sciences* (2nd ed.). Hillsdale, NJ: Lawrence Erlbaum Associates

Cosmides, L., & Tooby, J. (1994). Origins of domain-specificity: The evolution of functional organization. In L. Hirschfeld & S. Gelman (Eds.), *Mapping the Mind: Domain- specificity in Cognition and Culture* (pp. 85-118). New York: Cambridge University Press.

Coutanche, M. N., Solomon, S. H., & Thompson-Schill, S. L. (2016). A meta-analysis of fMRI decoding: Quantifying influences on human visual population codes. *Neuropsychologia, 82*, 134-141. https://doi.org/10.1016/j.neuropsychologia.2016.01.018

Crammond, D. J. (1997). Motor imagery: never in your wildest dream. *Trends in Neurosciences, 20*(2), 54-57. https://doi.org/10.1016/S0166-2236(96)30019-2

Critchley, H., Daly, E., Phillips, M., Brammer, M., Bullmore, E., Williams, S., . . . Murphy, D. (2000). Explicit and implicit neural mechanisms for processing of social information from facial expressions: A functional magnetic

resonance imaging study. *Human Brain Mapping, 9*(2), 93-105. https://doi.org/10.1002/(SICI)1097-0193(200002)9:2<93::AID-HBM4>3.0.CO;2-Z

Dailey, M. N., Cottrell, G. W., Padgett, C., & Adolphs, R. (2002). EMPATH: A Neural Network that Categorizes Facial Expressions. *Journal of Cognitive Neuroscience, 14*(8), 1158-1173. https://doi.org/10.1162/089892902760807177

Dailey, M. N., Joyce, C., Lyons, M. J., Kamachi, M., Ishi, H., Gyoba, J., & Cottrell, G. W. (2010). Evidence and a computational explanation of cultural differences in facial expression recognition. *Emotion*, *10*(6), 874-893. https://doi.org/10.1037/a0020019

Dalgleish, T. (2004). The emotional brain. *Nature Reviews Neuroscience, 5*(7), 583-589. https://doi.org/10.1038/nrn1432

Damasio, A. R. (1996). The somatic marker hypothesis and the possible functions of the prefrontal cortex. *Philosophical Transactions of the Royal Societyof London B: Biological Sciences, 351*(1346), 1413-1420. https://doi.org/10.1098/rstb.1996.0125

Das, K., Giesbrecht, B., & Eckstein, M. P. (2010). Predicting variations of perceptual performance across individuals from neural activity using pattern classifiers. *Neuroimage, 51*(4), 1425-1437. https://doi.org/10.1016/j.neuroimage.2010.03.030

de Lange, F. P., Heilbron, M., & Kok, P. (2018). How do expectations shape perception? Trends in cognitive sciences, *22*(9), 764-779. https://doi.org/10.1016/j.tics.2018.06.002

De Vos, M., Thorne, J. D., Yovel, G., & Debener, S. (2012). Let's face it, from trial to trial: Comparing procedures for N170 single-trial estimation. *Neuroimage, 63*(3), 1196-1202. https://doi.org/10.1016/j.neuroimage.2012.07.055

Dechent, P., Merboldt, K.-D., & Frahm, J. (2004). Is the human primary motor cortex involved in motor imagery? *Cognitive Brain Research, 19*(2), 138-144. https://doi.org/10.1016/j.cogbrainres.2003.11.012

den Ouden, H. E. M., Daunizeau, J., Roiser, J., Friston, K. J., & Stephan, K. E. (2010). Striatal Prediction Error Modulates Cortical Coupling. *The Journal of Neuroscience, 30*(9), 3210-3219. https://doi.org/10.1523/JNEUROSCI.4458-09.2010

den Ouden, H. E. M., Friston, K. J., Daw, N. D., McIntosh, A. R., & Stephan, K. E. (2009). A Dual Role for Prediction Error in Associative Learning. *Cerebral Cortex, 19*(5), 1175-1185. https://doi.org/10.1093/cercor/bhn161

di Pellegrino, G., Fadiga, L., Fogassi, L., Gallese, V., & Rizzolatti, G. (1992). Understanding motor events: a neurophysiological study. *Experimental Brain Research, 91*(1), 176-180. https://doi.org/10.1007/BF00230027

Dima, D., Stephan, K. E., Roiser, J. P., Friston, K. J., & Frangou, S. (2011). Effective connectivity during processing of facial affect: evidence for multiple parallel pathways. *The Journal of Neuroscience, 31*(40), 14378-14385. https://doi.org/10.1523/JNEUROSCI.2400-11.2011

Du, S., & Martinez, A. M. (2011). The resolution of facial expressions of emotion. *Journal of Vision, 11*(13), 24-24. https://doi.org/10.1167/11.13.24

Du, S., Tao, Y., & Martinez, A. M. (2014). Compound facial expressions of emotion. *Proceedings of the National Academy of Sciences, 111*(15), E1454-1462. https://doi.org/10.1073/pnas.1322355111

Duchaine, B., & Yovel, G. (2015). A revised neural framework for face processing. Annual Review of Vision Science, *1*, 393-416. https://doi.org/10.1146/annurev-vision-082114-035518

Eickhoff, S. B., Nichols, T. E., Laird, A. R., Hoffstaedter, F., Amunts, K., Fox, P. T., . . . Eickhoff, C. R. (2016). Behavior, sensitivity, and power of activation likelihood estimation characterized by massive empirical simulation. *Neuroimage, 137*, 70-85. https://doi.org/10.1016/j.neuroimage.2016.04.072

Eickhoff, S. B., Stephan, K. E., Mohlberg, H., Grefkes, C., Fink, G. R., Amunts, K., & Zilles, K. (2005). A new SPM toolbox for combining probabilistic cytoarchitectonic maps and functional imaging data. *Neuroimage, 25*(4), 1325-1335. https://doi.org/10.1016/j.neuroimage.2004.12.034

Eimer, M. (1998). Does the face-specific N170 component reflect the activity of a specialized eye processor? *NeuroReport, 9*(13), 2945-2948. https://doi.org/10.1097/00001756-199809140-00005

Eimer, M., & Holmes, A. (2002). An ERP study on the time course of emotional face processing. *NeuroReport, 13*(4), 427-431. https://doi.org/10.1097/00001756-200203250-00013

Eimer, M., & Holmes, A. (2007). Event-related brain potential correlates of emotional face processing. *Neuropsychologia, 45*(1), 15-31. https://doi.org/10.1016/j.neuropsychologia.2006.04.022

Eimer, M., Holmes, A., & McGlone, F. P. (2003). The role of spatial attention in the processing of facial expression: An ERP study of rapid brain responses to six basic emotions. *Cognitive, Affective, & Behavioral Neuroscience, 3*(2), 97-110. https://doi.org/10.3758/cabn.3.2.97

Ekman, P. (Ed.) (1982). *Emotion in the human face* (2nd ed.) Cambridge: Cambridge University Press.

Ekman, P. (1994). Strong evidence for universals in facial expressions: A reply to Russell's mistaken critique. *Psychological Bulletin, 115*(2), 268-287. https://doi.org/10.1037/0033-2909.115.2.268

Ekman, P., & Friesen, W. V. (1971). Constants across cultures in the face and emotion. *Journal of personality and social psychology*, *17*(2), 124-129. https://doi.org/10.1037/h0030377

Ekman, P., & Friesen, W. V. (1975). *Unmasking the face: A guide to recognizing emotions from facial cues*. Englewood Cliffs, NJ: Prentice Hall.

Elfenbein, H. A., & Ambady, N. (2002). Is there an in-group advantage in emotion recognition? *Psychological Bulletin, 128*(2), 243-249. https://doi.org/10.1037//0033-2909.128.2.243

Engell, A. D., & Haxby, J. V. (2007). Facial expression and gaze-direction in human superior temporal sulcus. *Neuropsychologia, 45*(14), 3234-3241. https://doi.org/10.1016/j.neuropsychologia.2007.06.022

Field, A. (2009). *Discovering Statistics Using SPSS* (3rd ed.). London: SAGE Publications.

Finzi, E., & Rosenthal, N. E. (2014). Treatment of depression with onabotulinumtoxinA: A randomized, double-blind, placebo controlled trial. *Journal of Psychiatric Research, 52*, 1-6. https://doi.org/10.1016/j.jpsychires.2013.11.006

Fodor, J. A. (1983). *The modularity of the mind: An essay on faculty psychology*. Cambridge, Massachusetts: The MIT Press.

Fox, C. J., Moon, S. Y., Iaria, G., & Barton, J. J. S. (2009). The correlates of subjective perception of identity and expression in the face network: An

fMRI adaptation study. *Neuroimage, 44*(2), 569-580. https://doi.org/10.1016/j.neuroimage.2008.09.011

Fox, E. (2008). *Emotion science: cognitive and neuroscientific approaches to understanding human emotions*. Basingstoke, UK: Palgrave Macmillan.

Friston, K. (2005). A theory of cortical responses. *Philosophical Transactions of the Royal Society of London B: Biological Sciences, 360*(1456), 815-836. https://doi.org/10.1098/rstb.2005.1622

Friston, K. (2008). Hierarchical Models in the Brain. *PLOS Computational Biology, 4*(11), e1000211. https://doi.org/10.1371/journal.pcbi.1000211

Furl, N., Henson, R. N., Friston, K. J., & Calder, A. J. (2013). Top-Down Control of Visual Responses to Fear by the Amygdala. *The Journal of Neuroscience, 33*(44), 17435-17443. https://doi.org/10.1523/jneurosci.2992-13.2013

Fusar-Poli, P., Placentino, A., Carletti, F., Landi, P., Allen, P., Surguladze, S., … Politi, P. (2009). Functional atlas of emotional faces processing: a voxel-based meta-analysis of 105 functional magnetic resonance imaging studies. *Journal of psychiatry & neuroscience: JPN, 34*(6), 418-432. Retrieved from: https://europepmc.org/articles/pmc2783433

Ganel, T., Valyear, K. F., Goshen-Gottshein, Y., & Goodale, M. A. (2005). The involvement of the "fusiform face area" in processing facial expression. *Neuropsychologia 43*(11)*,* 1645-1654. https://doi.org/10.1016/j.neuropsychologia.2005.01.012

Gazzola, V., Spezio, M. L., Etzel, J. A., Castelli, F., Adolphs, R., & Keysers, C. (2012). Primary somatosensory cortex discriminates affective significance in social touch. *Proceedings of the National Academy of Sciences, 109*(25), E1657-1666. https://doi.org/10.1073/pnas.1113211109

Gendron, M., & Feldman Barrett, L. (2009). Reconstructing the past: A century of ideas about emotion in psychology. *Emotion review*, *1*(4), 316-339. https://doi.org/10.1177/1754073909338877

Gerardin, E., Sirigu, A., Lehericy, S., Poline, J. B., Gaymard, B., Marsault, C., . . . Le Bihan, D. (2000). Partially overlapping neural networks for real and imagined hand movements. *Cerebral Cortex, 10 (11),* 1093-1104. https://doi.org/10.1093/cercor/10.11.1093

Ghuman, A. S., Brunet, N. M., Li, Y., Konecky, R. O., Pyles, J. A., Walls, S. A., . . . Richardson, R. M. (2014). Dynamic encoding of face information in the

human fusiform gyrus. *Nature communications, 5*, 5672. https://doi.org/10.1038/ncomms6672

Goebel, R., Esposito, F., & Formisano, E. (2006). Analysis of functional image analysis contest (FIAC) data with brainvoyager QX: From single-subject to cortically aligned group general linear model analysis and self-organizing group independent component analysis. *Human Brain Mapping, 27*(5), 392-401. https://doi.org/10.1002/hbm.20249

Goebel, R., Khorram-Sefat, D., Muckli, L., Hacker, H., & Singer, W. (1998). The constructive nature of vision: direct evidence from functional magnetic resonance imaging studies of apparent motion and motion imagery. *European Journal of Neuroscience, 10*(5), 1563-1573. https://doi.org/10.1046/j.1460-9568.1998.00181.x

Gold, J. M., Barker, J. D., Barr, S., Bittner, J. L., Bromfield, W. D., Chu, N., . . . Srinath, A. (2013). The efficiency of dynamic and static facial expression recognition. *Journal of Vision, 13*(5), 23-23. https://doi.org/10.1167/13.5.23

Goldman, A. I., & de Vignemont, F. (2009). Is social cognition embodied? *Trends in Cognitive Sciences, 13*(4), 154-159. https://doi.org/10.1016/j.tics.2009.01.007

Goldman, A. I., & Sripada, C. S. (2005). Simulationist models of face-based emotion recognition. *Cognition, 94*(3), 193-213. https://doi.org/10.1016/j.cognition.2004.01.005

Gosselin, F., & Schyns, P. G. (2001). Bubbles: a technique to reveal the use of information in recognition tasks. *Vision Research, 41*(17), 2261-2271. https://doi.org/10.1016/S0042-6989(01)00097-9

Greening, S. G., Mitchell, D. G. V., & Smith, F. W. (2018). Spatially generalizable representations of facial expressions: Decoding across partial face samples. *Cortex, 101*, 31-43. https://doi.org/10.1016/j.cortex.2017.11.016

Grèzes, J., & Decety, J. (2001). Functional anatomy of execution, mental simulation, observation, and verb generation of actions: A meta-analysis. *Human Brain Mapping,* 12(1), 1-19. https://doi.org/10.1002/1097-0193(200101)12:1<1::AID-HBM10>3.0.CO;2-V

Grootswagers, T., Wardle, S. G., & Carlson, T. A. (2017). Decoding Dynamic Brain Patterns from Evoked Responses: A Tutorial on Multivariate Pattern

Analysis Applied to Time Series Neuroimaging Data. *Journal of Cognitive Neuroscience, 29*(4), 677-697. https://doi.org/10.1162/jocn_a_01068

Gross, T. F. (2004). The Perception of Four Basic Emotions in Human and Nonhuman Faces by Children With Autism and Other Developmental Disabilities. *Journal of Abnormal Child Psychology, 32*(5), 469-480. https://doi.org/10.1023/b:jacp.0000037777.17698.01

Gur, R. C., Schroeder, L., Turner, T., McGrath, C., Chan, R. M., Turetsky, B. I., . . . Gur, R. E. (2002). Brain Activation during Facial Emotion Processing. *Neuroimage, 16*(3, Part A), 651-662. https://doi.org/10.1006/nimg.2002.1097

Habel, U., Windischberger, C., Derntl, B., Robinson, S., Kryspin-Exner, I., Gur, R., & Moser, E. (2007). Amygdala activation and facial expressions: Explicit emotion discrimination versus implicit emotion processing. *Neuropsychologia, 45*(10), 2369-2377. https://doi.org/10.1016/j.neuropsychologia.2007.01.023

Hajcak, G., MacNamara, A., & Olvet, D. M. (2010). Event-Related Potentials, Emotion, and Emotion Regulation: An Integrative Review. *Developmental Neuropsychology, 35*(2), 129-155. https://doi.org/10.1080/87565640903526504

Hanakawa, T., Immisch, I., Toma, K., Dimyan, M. A., Van Gelderen, P., & Hallett, M. (2003). Functional properties of brain areas associated with motor execution and imagery. *Journal of Neurophysiology, 89*(2), 989-1002. https://doi.org/10.1152/jn.00132.2002

Hardwick, R. M., Caspers, S., Eickhoff, S. B., & Swinnen, S. P. (2017). Neural Correlates of Motor Imagery, Action Observation, and Movement Execution: A Comparison Across Quantitative Meta-Analyses. *bioRxiv,* 198432. https://doi.org/10.1101/198432

Hariri, A. R., Bookheimer, S. Y., & Mazziotta, J. C. (2000). Modulating emotional responses: effects of a neocortical network on the limbic system. *NeuroReport, 11*(1), 43-48. https://doi.org/10.1097/00001756-200001170-00009

Harry, B. B., Williams, M. A., Davis, C., & Kim, J. (2013). Emotional expressions evoke a differential response in the fusiform face area. *Frontiers in human neuroscience, 7,* 692. https://doi.org/10.3389/fnhum.2013.00692

Hatfield, E., & Cacioppo, J. T. (1994). *Emotional contagion*. Cambridge: Cambridge University Press.

Hausfeld, L., De Martino, F., Bonte, M., & Formisano, E. (2012). Pattern analysis of EEG responses to speech and voice: Influence of feature grouping. *Neuroimage, 59*(4), 3641-3651. https://doi.org/10.1016/j.neuroimage.2011.11.056

Haxby, J. V., & Gobbini, M. I. (2011). Distributed Neural Systems for Face Perception. In A. J. Calder, G. Rhodes, M. H. Johnson, & J. V. Haxby (Eds.), *The Oxford Handbook of Face Perception* (pp. 93-110). Oxford, USA: Oxford Universerity Press.

Haxby, J. V., Gobbini, M. I., Furey, M. L., Ishai, A., Schouten, J. L., & Pietrini, P. (2001). Distributed and overlapping representations of faces and objects in ventral temporal cortex. *Science, 293*(5539), 2425-2430. https://doi.org/10.1126/science.1063736

Haxby, J. V., Hoffman, E. A., & Gobbini, M. I. (2000). The distributed human neural system for face perception. *Trends in Cognitive Sciences, 4*(6), 223-233. https://doi.org/10.1016/S1364-6613(00)01482-0

Haynes, J.-D. (2015). A Primer on Pattern-Based Approaches to fMRI: Principles, Pitfalls, and Perspectives. *Neuron, 87*(2), 257-270. https://doi.org/10.1016/j.neuron.2015.05.025

Haynes, J.-D., & Rees, G. (2006). Decoding mental states from brain activity in humans. *Nature Reviews Neuroscience, 7*(7), 523-534. https://doi.org/10.1038/nrn1931

Heberlein, A. S., & Atkinson, A. P. (2009). Neuroscientific Evidence for Simulation and Shared Substrates in Emotion Recognition: Beyond Faces. *Emotion Review, 1*(2), 162-177. https://doi.org/10.1177/1754073908100441

Heeger, D. J. (2017). Theory of cortical function. *Proceedings of the National Academy of Sciences, 114*(8), 1773-1782. https://doi.org/10.1073/pnas.1619788114

Hennenlotter, A., Schroeder, U., Erhard, P., Castrop, F., Haslinger, B., Stoecker, D., . . . Ceballos-Baumann, A. O. (2005). A common neural basis for receptive and expressive communication of pleasant facial affect. *Neuroimage, 26*(2), 581-591. https://doi.org/10.1016/j.neuroimage.2005.01.057

Herrmann, M. J., Aranda, D., Ellgring, H., Mueller, T. J., Strik, W. K., Heidrich, A., & Fallgatter, A. J. (2002). Face-specific event-related potential in humans is independent from facial expression. *International Journal of Psychophysiology, 45*(3), 241-244. https://doi.org/10.1016/S0167-8760(02)00033-8

Hess, U., & Blairy, S. (2001). Facial mimicry and emotional contagion to dynamic emotional facial expressions and their influence on decoding accuracy. *International Journal of Psychophysiology, 40*(2), 129-141. https://doi.org/10.1016/S0167-8760(00)00161-6

Hétu, S., Grégoire, M., Saimpont, A., Coll, M.-P., Eugène, F., Michon, P.-E., & Jackson, P. L. (2013). The neural network of motor imagery: An ALE meta-analysis. *Neuroscience & Biobehavioral Reviews, 37*(5), 930-949. https://doi.org/10.1016/j.neubiorev.2013.03.017

Hinojosa, J. A., Mercado, F., & Carretié, L. (2015). N170 sensitivity to facial expression: A meta-analysis. *Neuroscience & Biobehavioral Reviews, 55*, 498-509. https://doi.org/10.1016/j.neubiorev.2015.06.002

Horley, K., Williams, L. M., Gonsalvez, C., & Gordon, E. (2003). Social phobics do not see eye to eye: A Visual scanpath study of emotional expression processing. *Journal of Anxiety Disorders, 17*(1), 33-44. https://doi.org/10.1016/S0887-6185(02)00180-9

Iacoboni, M., & Dapretto, M. (2006). The mirror neuron system and the consequences of its dysfunction. *Nature Reviews Neuroscience, 7*(12), 942-951. https://doi.org/10.1038/nrn2024

Ibric, M. D., & Dragomirescu, L. (2009). Neurofeedback in pain management. In T. H. Budzynski, H. Kogan-Budzynski, J. R. Evans, & A. Abarbanel (Eds.), *Introduction to QEEG and Neurofeedback* (2nd ed., pp. 417-451). USA: Academic Press.

Igor, S. P., & Robert, F. (2003). *MPEG-4 Facial Animation: The Standard, Implementation and Applications*. New York, NY, USA: John Wiley & Sons, Inc.

Itier, R. J., Alain, C., Sedore, K., & McIntosh, A. R. (2007). Early Face Processing Specificity: It's in the Eyes! *Journal of Cognitive Neuroscience, 19*(11), 1815-1826. https://doi.org/10.1162/jocn.2007.19.11.1815

Itier, R. J., & Batty, M. (2009). Neural bases of eye and gaze processing: The core of social cognition. *Neuroscience & Biobehavioral Reviews, 33*(6), 843-863. https://doi.org/10.1016/j.neubiorev.2009.02.004

Jack, R. E., Blais, C., Scheepers, C., Schyns, P. G., & Caldara, R. (2009). Cultural confusions show that facial expressions are not universal. *Current Biology, 19*(18), 1543-1548. https://doi.org/10.1016/j.cub.2009.07.051

Jacques, C., & Rossion, B. (2006). The time course of visual competition to the presentation of centrally fixated faces. *Journal of Vision, 6*(2), 6-6. https://doi.org/10.1167/6.2.6

Jeannerod, M. (2001). Neural Simulation of Action: A Unifying Mechanism for Motor Cognition. *Neuroimage, 14*(1), S103-S109. https://doi.org/10.1006/nimg.2001.0832

Johnson, J. S., & Olshausen, B. A. (2005). The recognition of partially visible natural objects in the presence and absence of their occluders. *Vision Research, 45*(25-26), 3262-3276. https://doi.org/10.1016/j.visres.2005.06.007

Kaneshiro, B., Perreau Guimaraes, M., Kim, H.-S., Norcia, A. M., & Suppes, P. (2015). A Representational Similarity Analysis of the Dynamics of Object Processing Using Single-Trial EEG Classification. *PLoS One, 10*(8), e0135697. https://doi.org/10.1371/journal.pone.0135697

Kanwisher, N. (2006). Neuroscience. What's in a face? *Science, 311*(5761), 617-618. https://doi.org/10.1126/science.1123983

Kanwisher, N. (2010). Functional specificity in the human brain: A window into the functional architecture of the mind. *Proceedings of the National Academy of Sciences, 107*(25), 11163-11170. https://doi.org/10.1073/pnas.1005062107

Kanwisher, N., & Yovel, G. (2009). Face Perception. In G. G. Berntson & J.T. Cacioppo (Eds.), *Handbook of Neuroscience for the Behavioral Sciences* (volume 2, pp. 841-858. NJ, USA: John Wiley & Sons, Inc.

Kawasaki, H., Tsuchiya, N., Kovach, C. K., Nourski, K. V., Oya, H., Howard, M. A., & Adolphs, R. (2011). Processing of Facial Emotion in the Human Fusiform Gyrus. *Journal of Cognitive Neuroscience, 24*(6), 1358-1370. https://doi.org/10.1162/jocn_a_00175

Kay, J. W., & Phillips, W. A. (2011). Coherent Infomax as a Computational Goal for Neural Systems. *Bulletin of Mathematical Biology, 73*(2), 344-372. https://doi.org/10.1007/s11538-010-9564-x

Kay, K. N., & Yeatman, J. D. (2017). Bottom-up and top-down computations in word- and face-selective cortex. *eLife, 6*, e22341. https://doi.org/10.7554/eLife.22341

Kersten, D., Mamassian, P., & Yuille, A. (2004). Object Perception as Bayesian Inference. *Annual Review of Psychology, 55*(1), 271-304. https://doi.org/10.1146/annurev.psych.55.090902.142005

Keysers, C., Kaas, J. H., & Gazzola, V. (2010). Somatosensation in social perception. *Nature Reviews Neuroscience, 11*, 417-428. https://doi.org/10.1038/nrn2833

Kircher, T., Pohl, A., Krach, S., Thimm, M., Schulte-Rüther, M., Anders, S., & Mathiak, K. (2013). Affect-specific activation of shared networks for perception and execution of facial expressions. *Social Cognitive and Affective Neuroscience, 8*(4), 370-377. https://doi.org/10.1093/scan/nss008

Kober, H., Barrett, L. F., Joseph, J., Bliss-Moreau, E., Lindquist, K., & Wager, T. D. (2008). Functional grouping and cortical–subcortical interactions in emotion: A meta-analysis of neuroimaging studies. *Neuroimage, 42*(2), 998-1031. https://doi.org/10.1016/j.neuroimage.2008.03.059

Kok, P., Bains, L. J., van Mourik, T., Norris, D. G., & de Lange, F. P. (2016). Selective Activation of the Deep Layers of the Human Primary Visual Cortex by Top-Down Feedback. *Current Biology, 26*(3), 371-376. https://doi.org/10.1016/j.cub.2015.12.038

Kok, P., & de Lange, F. P. (2015). Predictive coding in sensory cortex. In Forstmann B. & Wagenmakers E. J. (eds), *An introduction to model-based cognitive neuroscience* (pp. 221-244). New York, USA: Springer.

Kok, P., Failing, M. F., & de Lange, F. P. (2014). Prior Expectations Evoke Stimulus Templates in the Primary Visual Cortex. *Journal of Cognitive Neuroscience, 26*(7), 1546-1554. https://doi.org/10.1162/jocn_a_00562

Korb, S., With, S., Niedenthal, P., Kaiser, S., & Grandjean, D. (2014). The Perception and Mimicry of Facial Movements Predict Judgments of Smile Authenticity. *PLoS One, 9*(6), e99194. https://doi.org/10.1371/journal.pone.0099194

Kosonogov, V., Titova, A., & Vorobyeva, E., (2015). Empathy, but not mimicry restriction, influences the recognition of change in emotional facial

expressions. *The Quarterly Journal of Experimental Psychology 68*(10), 2106-2115. https://doi.org/10.1080/17470218.2015.1009476

Kotsia, I., Buciu, I., & Pitas, I. (2008). An analysis of facial expression recognition under partial facial image occlusion. *Image and Vision Computing, 26*(7), 1052-1067. https://doi.org/10.1016/j.imavis.2007.11.004

Kragel, P. A., & LaBar, K. S. (2016). Somatosensory Representations Link the Perception of Emotional Expressions and Sensory Experience. *eNeuro, 3*(2). https://doi.org/10.1523/ENEURO.0090-15.2016

Kriegeskorte, N., Simmons, W. K., Bellgowan, P. S. F., & Baker, C. I. (2009). Circular analysis in systems neuroscience: the dangers of double dipping. *Nature Neuroscience, 12*, 535-540. https://doi.org/10.1038/nn.2303

Krolak-Salmon, P., Fischer, C., Vighetto, A., & Mauguière, F. (2001). Processing of facial emotional expression: spatio-temporal data as assessed by scalp event-related potentials. *European Journal of Neuroscience, 13*(5), 987-994. https://doi.org/10.1046/j.0953-816x.2001.01454.x

Kunecke, J., Hildebrandt, A., Recio, G., Sommer, W., & Wilhelm, O. (2014). Facial EMG responses to emotional expressions are related to emotion perception ability. *PLoS One, 9*(1), e84053. https://doi.org/10.1371/journal.pone.0084053

Lamme, V. A. F., & Roelfsema, P. R. (2000). The distinct modes of vision offered by feedforward and recurrent processing. *Trends in Neurosciences, 23*(11), 571-579. https://doi.org/10.1016/S0166-2236(00)01657-X

Larsen, R. J., Kasimatis, M., & Frey, K. (2008). Facilitating the Furrowed Brow: An Unobtrusive Test of the Facial Feedback Hypothesis Applied to Unpleasant Affect. *Cognition and Emotion, 6*(5), 321-338. https://doi.org/10.1080/02699939208409689

Lee, T. S., & Mumford, D. (2003). Hierarchical Bayesian inference in the visual cortex. *Journal of the Optical Society of America A, 20*(7), 1434-1448. https://doi.org/10.1364/JOSAA.20.001434

Leppänen, J. M., Hietanen, J. K., & Koskinen, K. (2008). Differential early ERPs to fearful versus neutral facial expressions: A response to the salience of the eyes? *Biological Psychology, 78*(2), 150-158. https://doi.org/10.1016/j.biopsycho.2008.02.002

Leslie, K. R., Johnson-Frey, S. H., & Grafton, S. T. (2004). Functional imaging of face and hand imitation: towards a motor theory of empathy. *Neuroimage, 21*(2), 601-607. https://doi.org/10.1016/j.neuroimage.2003.09.038

Li, S., & Deng, W. (2018). Deep Facial Expression Recognition: A Survey. *Computing Research Repository.* Retrieved from http://arxiv.org/abs/1804.08348

Li, Y., Richardson, R. M., & Ghuman, A. S. (2018). Posterior Fusiform and Midfusiform Contribute to Distinct Stages of Facial Expression Processing. *Cerebral Cortex,* 1-11. https://doi.org/10.1093/cercor/bhy186

Liang, Y., Liu, B., Xu, J., Zhang, G., Li, X., Wang, P., & Wang, B. (2017). Decoding facial expressions based on face-selective and motion-sensitive areas. *Human Brain Mapping, 38*(6), 3113-3125. https://doi.org/10.1002/hbm.23578

Lindquist, K. A., Wager, T. D., Kober, H., Bliss-Moreau, E., & Barrett, L. F. (2012). The brain basis of emotion: a meta-analytic review. *Behavioural and Brain Sciences, 35*(3), 121-143. https://doi.org/10.1017/S0140525X11000446

Luck, S. J. (2014). *An introduction to the event-related potential technique* (2nd ed.). MA, USA: MIT Press.

Maloret, J., & Smith, F. W. (2017). [Top-down Modulation of Expression Recognition in the Primary Visual Cortex; computational modelling]. *Unpublished Raw Data*.

Mayka, M. A., Corcos, D. M., Leurgans, S. E., & Vaillancourt, D. E. (2006). Three-dimensional locations and boundaries of motor and premotor cortices as defined by functional brain imaging: A meta-analysis. *Neuroimage, 31*(4), 1453-1474. https://doi.org/10.1016/j.neuroimage.2006.02.004

McIntosh, D. N., Reichmann-Decker, A., Winkielman, P., & Wilbarger, J. L. (2006). When the social mirror breaks: deficits in automatic, but not voluntary, mimicry of emotional facial expressions in autism. *Developmental Science, 9*(3), 295-302. https://doi.org/10.1111/j.1467-7687.2006.00492.x

Meier, J. D., Aflalo, T. N., Kastner, S., & Graziano, M. S. (2008). Complex organization of human primary motor cortex: a high-resolution fMRI study. *Journal of Neurophysiology, 100*(4), 1800-1812. https://doi.org/10.1152/jn.90531.2008

Meltzoff, A. N., & Moore, M. K. (1977). Imitation of facial and manual gestures by human neonates. *Science, 198*(4312), 75-78. https://doi.org/10.1126/science.198.4312.75

Montgomery, K. J., & Haxby, J. V. (2008). Mirror Neuron System Differentially Activated by Facial Expressions and Social Hand Gestures: A Functional Magnetic Resonance Imaging Study. *Journal of Cognitive Neuroscience, 20*(10), 1866-1877. https://doi.org/10.1162/jocn.2008.20127

Morgan, A. T., Petro, L. S., & Muckli, L. (2016). Cortical feedback to V1 and V2 contains unique information about high-level scene structure. *bioRxiv*. https://doi.org/10.1101/041186

Muckli, L. (2010). What are we missing here? Brain imaging evidence for higher cognitive functions in primary visual cortex V1. *International Journal of Imaging Systems and Technology, 20*(2), 131-139. https://doi.org/10.1002/ima.20236

Muckli, L., De Martino, F., Vizioli, L., Petro, L. S., Smith, F. W., Ugurbil, K., . . . Yacoub, E. (2015). Contextual Feedback to Superficial Layers of V1. *Current Biology, 25*(20), 2690-2695. https://doi.org/10.1016/j.cub.2015.08.057

Muckli, L., Kohler, A., Kriegeskorte, N., & Singer, W. (2005). Primary Visual Cortex Activity along the Apparent-Motion Trace Reflects Illusory Perception. *PLOS Biology, 3*(8), e265. https://doi.org/10.1371/journal.pbio.0030265

Muckli, L., Naumer, M. J., & Singer, W. (2009). Bilateral visual field maps in a patient with only one hemisphere. *Proceedings of the National Academy of Sciences, 106*(31), 13034-13039. https://doi.org/10.1073/pnas.0809688106

Muckli, L., & Petro, L. S. (2013). Network interactions: non-geniculate input to V1. *Current Opinion in Neurobiology, 23*(2), 195-201. https://doi.org/10.1016/j.conb.2013.01.020

Muckli, L., Petro, L. S., & Smith, F. W. (2013). Backwards is the way forward: Feedback in the cortical hierarchy predicts the expected future. *Behavioral and Brain Sciences, 36*(03), 221-221. https://doi.org/10.1017/S0140525X12002361

Mur, M., Bandettini, P. A., & Kriegeskorte, N. (2009). Revealing representational content with pattern-information fMRI—an introductory guide. *Social*

Cognitive and Affective Neuroscience, 4(1), 101-109. https://doi.org/10.1093/scan/nsn044

Murphy, F., Nimmo-Smith, I., & Lawrence, A. (2003). Functional neuroanatomy of emotions: A meta-analysis. *Cognitive, Affective, & Behavioral Neuroscience, 3*(3), 207-233. https://doi.org/10.3758/CABN.3.3.207

Neal, D. T., & Chartrand, T. L. (2011). Embodied Emotion Perception: Amplifying and Dampening Facial Feedback Modulates Emotion Perception Accuracy. *Social Psychological and Personality Science, 2*(6), 673-678. https://doi.org/10.1177/1948550611406138

Neath-Tavares, K. N., & Itier, R. J. (2016). Neural processing of fearful and happy facial expressions during emotion-relevant and emotion-irrelevant tasks: A fixation-to-feature approach. *Biological Psychology, 119*(Supplement C), 122-140. https://doi.org/10.1016/j.biopsycho.2016.07.013

Neath, K. N., & Itier, R. J. (2015). Fixation to features and neural processing of facial expressions in a gender discrimination task. *Brain and Cognition, 99*, 97-111. https://doi.org/10.1016/j.bandc.2015.05.007

Nemrodov, D., Anderson, T., Preston, F. F., & Itier, R. J. (2014). Early sensitivity for eyes within faces: A new neuronal account of holistic and featural processing. *Neuroimage, 97*, 81-94. https://doi.org/10.1016/j.neuroimage.2014.04.042

Nemrodov, D., Niemeier, M., Mok, J. N. Y., & Nestor, A. (2016). The time course of individual face recognition: A pattern analysis of ERP signals. *Neuroimage, 132*, 469-476. https://doi.org/10.1016/j.neuroimage.2016.03.006

Niedenthal, P. M. (2007). Embodying emotion. *Science, 316*(5827), 1002-1005. https://doi.org/10.1126/science.1136930

Niedenthal, P. M., Augustinova, M., Rychlowska, M., Droit-Volet, S., Zinner, L., Knafo, A., & Brauer, M. (2012). Negative Relations Between Pacifier Use and Emotional Competence. *Basic and Applied Social Psychology, 34*(5), 387-394. https://doi.org/10.1080/01973533.2012.712019

Niedenthal, P. M., Brauer, M., Halberstadt, J. B., & Innes-Ker, Å. H. (2001). When did her smile drop? Facial mimicry and the influences of emotional state on the detection of change in emotional expression. *Cognition and Emotion, 15*(6), 853-864. https://doi.org/10.1080/02699930143000194

Niedenthal, P. M., Krauth-Gruber, S., & Ric, F. (2006). *Psychology of emotion: interpersonal, experiential & cognitive approaches.* New York, USA: Psychology Press.

Niedenthal, P. M., Mermillod, M., Maringer, M., & Hess, U. (2010). The Simulation of Smiles (SIMS) model: Embodied simulation and the meaning of facial expression. *Behavioural and Brain Sciences, 33*(6), 417-433; discussion 433-480. https://doi.org/10.1017/S0140525X10000865

Niedenthal, P. M., Winkielman, P., Mondillon, L., & Vermeulen, N. (2009). Embodiment of emotion concepts. *Journal of Personality and Social Psychology, 96*(6), 1120-1136. https://doi.org/10.1037/a0015574

Norman, K. A., Polyn, S. M., Detre, G. J., & Haxby, J. V. (2006). Beyond mind-reading: multi-voxel pattern analysis of fMRI data. *Trends in Cognitive Sciences, 10*(9), 424-430. https://doi.org/10.1016/j.tics.2006.07.005

O'Reilly, R. C., Wyatte, D., Herd, S., Mingus, B., & Jilk, D. J. (2013). Recurrent processing during object recognition. *Frontiers in Psychology, 4*, 124. https://doi.org/10.3389/fpsyg.2013.00124

Oberman, L. M., Winkielman, P., & Ramachandran, V. S. (2007). Face to face: Blocking facial mimicry can selectively impair recognition of emotional expressions. *Social Neuroscience, 2*(3-4), 167-178. https://doi.org/10.1080/17470910701391943

Olshausen, B. A., & Field, D. J. (2005). How Close Are We to Understanding V1? *Neural Computation, 17*(8), 1665-1699. https://doi.org/10.1162/0899766054026639

Oosterhof, N. N., Tipper, S. P., & Downing, P. E. (2012). Viewpoint (In)dependence of Action Representations: An MVPA Study. *Journal of Cognitive Neuroscience, 24*(4), 975-989. https://doi.org/10.1162/jocn_a_00195

Oosterhof, N. N., Tipper, S. P., & Downing, P. E. (2013). Crossmodal and action-specific: neuroimaging the human mirror neuron system. *Trends in Cognitive Science, 17*(7), 311-318. https://doi.org/10.1016/j.tics.2013.04.012

Oosterhof, N. N., Wiggett, A. J., Diedrichsen, J., Tipper, S. P., & Downing, P. E. (2010). Surface-based information mapping reveals crossmodal vision-action representations in human parietal and occipitotemporal cortex. *Journal of Neurophysiology, 104*(2), 1077-1089. https://doi.org/10.1152/jn.00326.2010

Pardàs, M., & Bonafonte, A. (2002). Facial animation parameters extraction and expression recognition using Hidden Markov Models. *Signal Processing: Image Communication, 17*(9), 675-688. https://doi.org/10.1016/S0923-5965(02)00078-4

Park, C.-h., Chang, W. H., Lee, M., Kwon, G. H., Kim, L., Kim, S. T., & Kim, Y.-H. (2015). Which motor cortical region best predicts imagined movement? *Neuroimage, 113*, 101-110. https://doi.org/10.1016/j.neuroimage.2015.03.033

Peelen, M. V., Atkinson, A. P., & Vuilleumier, P. (2010). Supramodal representations of perceived emotions in the human brain. *The Journal of Neuroscience, 30*(30), 10127-10134. https://doi.org/10.1523/JNEUROSCI.2161-10.2010

Pelli, D. G. (1997). The VideoToolbox software for visual psychophysics: Transforming numbers into movies. *Spatial vision, 10*(4), 437-442. https://doi.org/10.1163/156856897X00366

Pepik, B., Benenson, R., Ritschel, T., & Schiele, B. (2015). What is holding back convnets for dections? *In German Conference on Pattern Recognition*, 517-528, Springer, Cham. https://doi.org/10.1007/978-3-319-24947-6_43

Pessoa, L., & Adolphs, R. (2010). Emotion processing and the amygdala: from a 'low road' to 'many roads' of evaluating biological significance. *Nature Reviews Neuroscience, 11*(11), 773-783. https://doi.org/10.1038/nrn2920

Petro, L. S., Smith, F. W., Schyns, P. G., & Muckli, L. (2013). Decoding face categories in diagnostic subregions of primary visual cortex. *European Journal of Neuroscience, 37*(7), 1130-1139. https://doi.org/10.1111/ejn.12129

Phan, K. L., Wager, T., Taylor, S. F., & Liberzon, I. (2002). Functional Neuroanatomy of Emotion: A Meta-Analysis of Emotion Activation Studies in PET and fMRI. *Neuroimage, 16*(2), 331-348. https://doi.org/10.1006/nimg.2002.1087

Phillips, M. L., Drevets, W. C., Rauch, S. L., & Lane, R. (2003). Neurobiology of emotion perception I: the neural basis of normal emotion perception. *Biological Psychiatry, 54*(5), 504-514. https://doi.org/10.1016/S0006-3223(03)00168-9

Phillips, W. A., Clark, A., & Silverstein, S. M. (2015). On the functions, mechanisms, and malfunctions of intracortical contextual modulation. *Neuroscience & Biobehavioral Reviews, 52*, 1-20. https://doi.org/10.1016/j.neubiorev.2015.02.010

Phillips, W. A., Kay, J., & Smyth, D. (1995). The discovery of structure by multi-stream networks of local processors with contextual guidance. *Network: Computation in Neural Systems, 6*(2), 225-246. https://doi.org/10.1088/0954-898X_6_2_005

Picard, N., & Strick, P. L. (2001). Imaging the premotor areas. *Current Opinion in Neurobiology, 11*(6), 663-672. https://doi.org/10.1016/S0959-4388(01)00266-5

Picton, T. W. (1992). The P300 wave of the human event-related potential. *Journal of clinical neurophysiology, 9*(4), 456-479. Retrieved from: https://www.researchgate.net/publication/21690394

Pitcher, D., Garrido, L., Walsh, V., & Duchaine, B. C. (2008). Transcranial magnetic stimulation disrupts the perception and embodiment of facial expressions. *The Journal of Neuroscience, 28*(36), 8929-8933. https://doi.org/10.1523/JNEUROSCI.1450-08.2008

Pitcher, D., Walsh, V., & Duchaine, B. C. (2011). Transcranial magnetic stimulation studies of face processing. In A. J. Calder, G. Rhodes, M. H. Johnson, & J. V. Haxby (Eds.), *The Oxford Handbook of Face Perception*. (pp. 367-386). Oxford, USA: Oxford Universerity Press.

Poldrack, R. A., Baker, C. I., Durnez, J., Gorgolewski, K. J., Matthews, P. M., Munafò, M. R., . . . Yarkoni, T. (2017). Scanning the horizon: towards transparent and reproducible neuroimaging research. *Nature Reviews Neuroscience, 18*, 115-126. https://doi.org/10.1038/nrn.2016.167

Pourtois, G., Sander, D., Andres, M., Grandjean, D., Reveret, L., Olivier, E., & Vuilleumier, P. (2004). Dissociable roles of the human somatosensory and superior temporal cortices for processing social face signals. *European Journal of Neuroscience, 20*(12), 3507-3515. https://doi.org/10.1111/j.1460-9568.2004.03794.x

Provine, R. R. (1986). Yawning as a stereotyped action pattern and releasing stimulus. *Ethology, 72*(2), 109-122. https://doi.org/10.1111/j.1439-0310.1986.tb00611.x

Puce, A., Latinus, M., Rossi, A., Parada, F., Love, S., Ashourvan, A., & Jayaraman, S. (2015). Neural Bases for Social Attention in Healthy Humans. In: Puce A., Bertenthal B. (eds), *The Many Faces of Social Attention* (pp. 93-127). Cham, Switzerland: Springer International Publishing.

Rao, R. P. N., & Ballard, D. H. (1999). Predictive coding in the visual cortex: a functional interpretation of some extra-classical receptive-field effects. *Nature Neuroscience, 2*(1), 79-87. https://doi.org/10.1038/4580

Rives Bogart, K., & Matsumoto, D. (2010). Facial mimicry is not necessary to recognize emotion: Facial expression recognition by people with Moebius syndrome. *Social Neuroscience, 5*(2), 241-251. https://doi.org/10.1080/17470910903395692

Rizzolatti, G., Camarda, R., Fogassi, L., Gentilucci, M., Luppino, G., & Matelli, M. (1988). Functional organization of inferior area 6 in the macaque monkey. *Experimental Brain Research, 71*(3), 491-507. https://doi.org/10.1007/BF00248742

Rochas, V., Gelmini, L., Krolak-Salmon, P., Poulet, E., Saoud, M., Brunelin, J., & Bediou, B. (2013). Disrupting pre-SMA activity impairs facial happiness recognition: an event-related TMS study. *Cerebral Cortex, 23*(7), 1517-1525. https://doi.org/10.1093/cercor/bhs133

Rossion, B. (2014). Understanding face perception by means of human electrophysiology. *Trends in Cognitive Science, 18*(6), 310-318. https://doi.org/10.1016/j.tics.2014.02.013

Rousselet, G. A., Ince, R. A. A., van Rijsbergen, N. J., & Schyns, P. G. (2014). Eye coding mechanisms in early human face event-related potentials. *Journal of Vision, 14*(13), 7-7. https://doi.org/10.1167/14.13.7

Rousselet, G. A., Mace, M. J., & Fabre-Thorpe, M. (2004). Animal and human faces in natural scenes: How specific to human faces is the N170 ERP component? *Journal of Vision, 4*(1), 13-21. https://doi.org/10.1167/4.1.2

Rychlowska, M., Cañadas, E., Wood, A., Krumhuber, E. G., Fischer, A., & Niedenthal, P. M. (2014). Blocking Mimicry Makes True and False Smiles Look the Same. *PLoS One, 9*(3), e90876. https://doi.org/10.1371/journal.pone.0090876

Rychlowska, M., Korb, S., Brauer, M., Droit-Volet, S., Augustinova, M., Zinner, L., & Niedenthal, P. M. (2014). Pacifiers Disrupt Adults' Responses to Infants'

Emotions. *Basic and Applied Social Psychology, 36*(4), 299-308. https://doi.org/10.1080/01973533.2014.915217

Rychlowska, M., Zinner, L., Musca, S. C., & Niedenthal, P. M. (2012). From the eye to the heart: eye contact triggers emotion simulation. In *Proceedings of the 4th Workshop on Eye Gaze in Intelligent Human Machine Interaction* (p. 5). ACM.

Saarimäki, H., Gotsopoulos, A., Jääskeläinen, I. P., Lampinen, J., Vuilleumier, P., Hari, R., . . . Nummenmaa, L. (2015). Discrete Neural Signatures of Basic Emotions. *Cerebral cortex 26*(1), 2563-2573 https://doi.org/10.1093/cercor/bhv086

Sadeh, B., Podlipsky, I., Zhdanov, A., & Yovel, G. (2010). Event-related potential and functional MRI measures of face-selectivity are highly correlated: A simultaneous ERP-fMRI investigation. *Human Brain Mapping, 31*(10), 1490-1501. https://doi.org/10.1002/hbm.20952

Said, C. P., Moore, C. D., Engell, A. D., Todorov, A., & Haxby, J. V. (2010). Distributed representations of dynamic facial expressions in the superior temporal sulcus. *Journal of Vision, 10*(5), 11-11. https://doi.org/10.1167/10.5.11

Saxe, R. (2006). Uniquely human social cognition. *Current Opinion in Neurobiology, 16*(2), 235-239. https://doi.org/10.1016/j.conb.2006.03.001

Scheuerecker, J., Frodl, T., Koutsouleris, N., Zetzsche, T., Wiesmann, M., Kleemann, A. M., . . . Meisenzahl, E. M. (2007). Cerebral differences in explicit and implicit emotional processing--an fMRI study. *Neuropsychobiology, 56*(1), 32-39. https://doi.org/10.1159/000110726

Schmidt, K.L. & Cohn, J.F. (2001). Human Facial Expressions as adaptations: evolutionary questions in facial expression research. *Yearbook of physical anthropology*. 44, 3-24. https://doi.org/10.1002/ajpa.20001

Schyns, P. G., Jentzsch, I., Johnson, M., Schweinberger, S. R., & Gosselin, F. (2003). A principled method for determining the functionality of brain responses. *NeuroReport, 14*(13), 1665-1669. https://doi.org/10.1097/00001756-200309150-00002

Schyns, P. G., Petro, L. S., & Smith, M. L. (2007). Dynamics of Visual Information Integration in the Brain for Categorizing Facial Expressions. *Current Biology, 17*(18), 1580-1585. https://doi.org/10.1016/j.cub.2007.08.048

Schyns, P. G., Petro, L. S., & Smith, M. L. (2009). Transmission of Facial Expressions of Emotion Co-Evolved with Their Efficient Decoding in the Brain: Behavioral and Brain Evidence. *PLoS One, 4*(5), e5625. https://doi.org/10.1371/journal.pone.0005625

Sel, A., Forster, B., & Calvo-Merino, B. (2014). The emotional homunculus: ERP evidence for independent somatosensory responses during facial emotional processing. *The Journal of Neuroscience, 34*(9), 3263-3267. https://doi.org/10.1523/JNEUROSCI.0106-13.2014

Simpson, D. (2005). Phrenology and the neurosciences: Contributions of FJ Gall and JG Spurzheim. *ANZ journal of surgery, 75*(6), 475-482. https://doi.org/10.1111/j.1445-2197.2005.03426.x

Skerry, A. E., & Saxe, R. (2014). A Common Neural Code for Perceived and Inferred Emotion. *The Journal of Neuroscience, 34*(48), 15997-16008. https://doi.org/10.1523/jneurosci.1676-14.2014

Smith, A. T., Singh, K. D., Williams, A. L., & Greenlee, M. W. (2001). Estimating Receptive Field Size from fMRI Data in Human Striate and Extrastriate Visual Cortex. *Cerebral Cortex, 11*(12), 1182-1190. https://doi.org/10.1093/cercor/11.12.1182

Smith, F. W., & Goodale, M. A. (2015). Decoding Visual Object Categories in Early Somatosensory Cortex. *Cerebral Cortex, 25*(4), 1020-1031. https://doi.org/10.1093/cercor/bht292

Smith, F. W., & Muckli, L. (2010). Nonstimulated early visual areas carry information about surrounding context. *Proceedings of the National Academy of Sciences, 107*(46), 20099-20103. https://doi.org/10.1073/pnas.1000233107

Smith, F. W., Muckli, L., Brennan, D., Pernet, C., Smith, M. L., Belin, P., . . . Schyns, P. G. (2008). Classification images reveal the information sensitivity of brain voxels in fMRI. *Neuroimage, 40*(4), 1643-1654. https://doi.org/10.1016/j.neuroimage.2008.01.029

Smith, F. W., & Rossit, S. (2018). Identifying and detecting facial expressions of emotion in peripheral vision. *PLoS One, 13*(5), e0197160. https://doi.org/10.1371/journal.pone.0197160

Smith, F. W., & Schyns, P. G. (2009). Smile through your fear and sadness: transmitting and identifying facial expression signals over a range of viewing

distances. *Psychological Science, 20*(10), 1202-1208. https://doi.org/10.1111/j.1467-9280.2009.02427.x

Smith, F. W., & Smith, M. L. (2016, June). *Explicit and Implicit Representations of Facial Expressions revealed by EEG Decoding.* Poster session presented at the meeting of the Organization for Human Brain Mapping (OHBM), Geneva, Switzerland.

Smith, M. L. (2011). Rapid Processing of Emotional Expressions without Conscious Awareness. *Cerebral Cortex, 22*(8), 1748-1760. https://doi.org/10.1093/cercor/bhr250

Smith, M. L., Cottrell, G. W., Gosselin, F., & Schyns, P. G. (2005). Transmitting and Decoding Facial Expressions. *Psychological Science, 16*(3), 184-189. https://doi.org/10.1111/j.0956-7976.2005.00801.x

Smith, M. L., Gosselin, F., & Schyns, P. G. (2004). Receptive Fields for Flexible Face Categorizations. *Psychological Science, 15*(11), 753-761. https://doi.org/10.1111/j.0956-7976.2004.00752.x

Smith, M. L., & Merlusca, C. (2014). How task shapes the use of information during facial expression categorizations. *Emotion, 14*(3), 478-487. https://doi.org/10.1037/a0035588

Spezio, M. L., Adolphs, R., Hurley, R. S. E., & Piven, J. (2007). Analysis of face gaze in autism using "Bubbles". *Neuropsychologia 45*(1), 144-151. https://doi.org/10.1016/j.neuropsychologia.2006.04.027

Stefanics, G., Kremláček, J., & Czigler, I. (2014). Visual mismatch negativity: A predictive coding view. *Frontiers in Human Neuroscience, 8*, 666. https://doi.org/10.3389/fnhum.2014.00666

Strack, F., Martin, L. L., & Stepper, S. (1988). Inhibiting and facilitating conditions of the human smile: A nonobtrusive test of the facial feedback hypothesis. *Journal of Personality and Social Psychology, 54*(5), 768-777. https://doi.org/10.1037/0022-3514.54.5.768

Sugata, H., Hirata, M., Yanagisawa, T., Matsushita, K., Yorifuji, S., & Yoshimine, T. (2016). Common neural correlates of real and imagined movements contributing to the performance of brain–machine interfaces. *Scientific Reports, 6*, 24663. https://doi.org/10.1038/srep24663

Tamir, R., Dickstein, R., & Huberman, M. (2007). Integration of Motor Imagery and Physical Practice in Group Treatment Applied to Subjects With Parkinson's

Disease. *Neurorehabilitation and Neural Repair, 21*(1), 68-75. https://doi.org/10.1177/1545968306292608

Tang, H., Buia, C., Madhavan, R., Crone, Nathan E., Madsen, Joseph R., Anderson, William S., & Kreiman, G. (2014). Spatiotemporal Dynamics Underlying Object Completion in Human Ventral Visual Cortex. *Neuron, 83*(3), 736-748. https://doi.org/10.1016/j.neuron.2014.06.017

Tang, H., Schrimpf, M., Lotter, W., Moerman, C., Paredes, A., Ortega Caro, J., . . . Kreiman, G. (2018). Recurrent computations for visual pattern completion. *Proceedings of the National Academy of Sciences*, 201719397. https://doi.org/10.1073/pnas.1719397115

Tarr, M. J., & Gauthier, I. (2000). FFA: a flexible fusiform area for subordinate-level visual processing automatized by expertise. *Nature Neuroscience, 3*(8), 764-769. https://doi.org/10.1038/77666

Tell, D., Davidson, D., & Camras, L.A. (2014). Recognition of Emotion from Facial Expressions with Direct or Averted Eye Gaze and Varying Expression Intensities in Children with Autism Disorder and Typically Developing Children. *Autism research and treatment*, 816137. http://dx.doi.org/10.1155/2014/816137

Tian, Y., Kanade, T., & Cohn, J. (2011). Facial Expression Recognition. In S. Z. Li & A. K. Jain (Eds.), *Handbook of Face Recognition* (pp. 487-519). London: Springer-Verlag.

Todd, M. T., Nystrom, L.E., & Cohen, J.D. (2013). Confounds in multivariate pattern analysis: theory and rule representation case study. *Neuroimage 77,* 157-165. https://doi.org/10.1016/j.neuroimage.2013.03.039

Tomasino, B., & Gremese, M. (2016). The Cognitive Side of M1. *Frontiers in Human Neuroscience, 10*, 298. https://doi.org/10.3389/fnhum.2016.00298

Tong, F., & Pratte, M. S. (2012). Decoding Patterns of Human Brain Activity. *Annual Review of Psychology, 63*(1), 483-509. https://doi.org/10.1146/annurev-psych-120710-100412

Turano, M. T., Lao, J., Richoz, A.-R., Lissa, P. d., Degosciu, S. B. A., Viggiano, M. P., & Caldara, R. (2017). Fear boosts the early neural coding of faces. *Social Cognitive and Affective Neuroscience, 12*(12), 1959-1971. https://doi.org/10.1093/scan/nsx110

van der Gaag, C., Minderaa, R. B., & Keysers, C. (2007). Facial expressions: what the mirror neuron system can and cannot tell us. *Social Neuroscience, 2*(3-4), 179-222. https://doi.org/10.1080/17470910701376878

Vetter, P., Smith, F. W., & Muckli, L. (2014). Decoding sound and imagery content in early visual cortex. *Currrent Biology, 24*(11), 1256-1262. https://doi.org/10.1016/j.cub.2014.04.020

Vuillemier, P., Armony, J. L, Driver, J. & Dolan, R. J. (2001). Effects of attention and emotion on face processing in the human brain: an event-related fMRI study. *Neuron, 30*(3)*,* 829-841. https://doi.org/10.1016/S0896-6273(01)00328-2

Wegrzyn, M., Riehle, M., Labudda, K., Woermann, F., Baumgartner, F., Pollmann, S., . . . Kissler, J. (2015). Investigating the brain basis of facial expression perception using multi-voxel pattern analysis. *Cortex, 69*, 131-140. https://doi.org/10.1016/j.cortex.2015.05.003

Whalen, P. J., Kagan, J., Cook, R. G., Davis, F. C., Kim, H., Polis, S., . . . Johnstone, T. (2004). Human Amygdala Responsivity to Masked Fearful Eye Whites. *Science, 306*(5704), 2061. https://doi.org/10.1126/science.1103617

Wicker, B., Keysers, C., Plailly, J., Royet, J. P., Gallese, V., & Rizzolatti, G. (2003). Both of Us Disgusted in My Insula: The Common Neural Basis of Seeing and Feeling Disgust. *Neuron, 40*(3), 655-664. https://doi.org/10.1016/S0896-6273(03)00679-2

Wild, B., Erb, M., Eyb, M., Bartels, M., & Grodd, W. (2003). Why are smiles contagious? An fMRI study of the interaction between perception of facial affect and facial movements. *Psychiatry Research: Neuroimaging, 123*(1), 17-36. https://doi.org/10.1016/s0925-4927(03)00006-4

Wilson-Mendenhall, C. D., Barrett, L. F., & Barsalou, L. W. (2013). Neural evidence that human emotions share core affective properties. *Psychological science*, *24*(6), 947-956. https://doi.org/10.1177/0956797612464242

Winston, J. S., Strange, B. A., O'Doherty, J., & Dolan, R. J. (2002). Automatic and intentional brain responses during evaluation of trustworthiness of faces. *Nature Neuroscience, 5*(3), 277-283. https://doi.org/10.1038/nn816

Wollmer, M. A., de Boer, C., Kalak, N., Beck, J., Götz, T., Schmidt, T., . . . Kruger, T. H. C. (2012). Facing depression with botulinum toxin: A randomized

controlled trial. *Journal of Psychiatric Research, 46*(5), 574-581. https://doi.org/10.1016/j.jpsychires.2012.01.027

Wood, A., Lupyan, G., Sherrin, S., & Niedenthal, P. (2016). Altering sensorimotor feedback disrupts visual discrimination of facial expressions. *Psychonomic Bulletin & Review, 23*(4), 1150-1156. https://doi.org/10.3758/s13423-015-0974-5

Wood, A., Rychlowska, M., Korb, S., & Niedenthal, P. (2016). Fashioning the Face: Sensorimotor Simulation Contributes to Facial Expression Recognition. *Trends in Cognitive Sciences, 20*(3), 227-240. https://doi.org/10.1016/j.tics.2015.12.010

Woolgar, A., Golland, P., & Bode, S. (2014). Coping with confounds in multivoxel pattern analysis: what should we do about reaction time differences? A comment on Todd, Nystron & Cohen 2013. *Neuroimage, 98,* 506-512. https://doi.org/10.1016/j.neuroimage.2014.04.059

Wronka, E., & Walentowska, W. (2011). Attention modulates emotional expression processing. *Psychophysiology, 48*(8), 1047-1056. https://doi.org/10.1111/j.1469-8986.2011.01180.x

Wyatte, D., Curran, T., & O'Reilly, R. (2012). The limits of feedforward vision: Recurrent processing promotes robust object recognition when objects are degraded. *Journal of Cognitive Neuroscience, 24*(11), 2248-2261. https://doi.org/10.1162/jocn_a_00282

Wyatte, D., Jilk, D. J., & O'Reilly, R. C. (2014). Early recurrent feedback facilitates visual object recognition under challenging conditions. *Frontiers in Psychology, 5*, 674. https://doi.org/10.3389/fpsyg.2014.00674

Xu, M., Lauwereyns, J., & Iramina, K. (2012). Dissociation of category versus item priming in face processing: an event-related potential study. *Cognitive Neurodynamics, 6*(2), 155-167. https://doi.org/10.1007/s11571-011-9185-6

Xu, X., & Biederman, I. (2010). Loci of the release from fMRI adaptation for changes in facial expression, identity, and viewpoint. *Journal of Vision, 10*(14), 36-36. https://doi.org/10.1167/10.14.36

Yarkoni, T., Poldrack, R. A., Nichols, T. E., Van Essen, D. C., & Wager, T. D. (2011). Large-scale automated synthesis of human functional neuroimaging data. *Nature methods, 8*(8), 665-670. https://doi.org/10.1038/nmeth.1635

Yovel, G. (2016). Neural and cognitive face-selective markers: An integrative review. *Neuropsychologia, 83*(Supplement C), 5-13. https://doi.org/10.1016/j.neuropsychologia.2015.09.026

Yuille, A., & Kersten, D. (2006). Vision as Bayesian inference: analysis by synthesis? *Trends in Cognitive Sciences, 10*(7), 301-308. https://doi.org/10.1016/j.tics.2006.05.002

Zhang, H., Japee, S., Nolan, R., Chu, C., Liu, N., & Ungerleider, L. G. (2016). Face-selective regions differ in their ability to classify facial expressions. *Neuroimage, 130*, 77-90. https://doi.org/10.1016/j.neuroimage.2016.01.045

Zimmermann-Schlatter, A., Schuster, C., Puhan, M. A., Siekierka, E., & Steurer, J. (2008). Efficacy of motor imagery in post-stroke rehabilitation: a systematic review. *Journal of NeuroEngineering and Rehabilitation, 5*(1), 8. https://doi.org/10.1186/1743-0003-5-8

Appendices

Appendix A. Stimulus Sheets

Chapter 2 and Chapter 3 (Study 1):

Chapter 3 (Study 2):

Chapter 4:

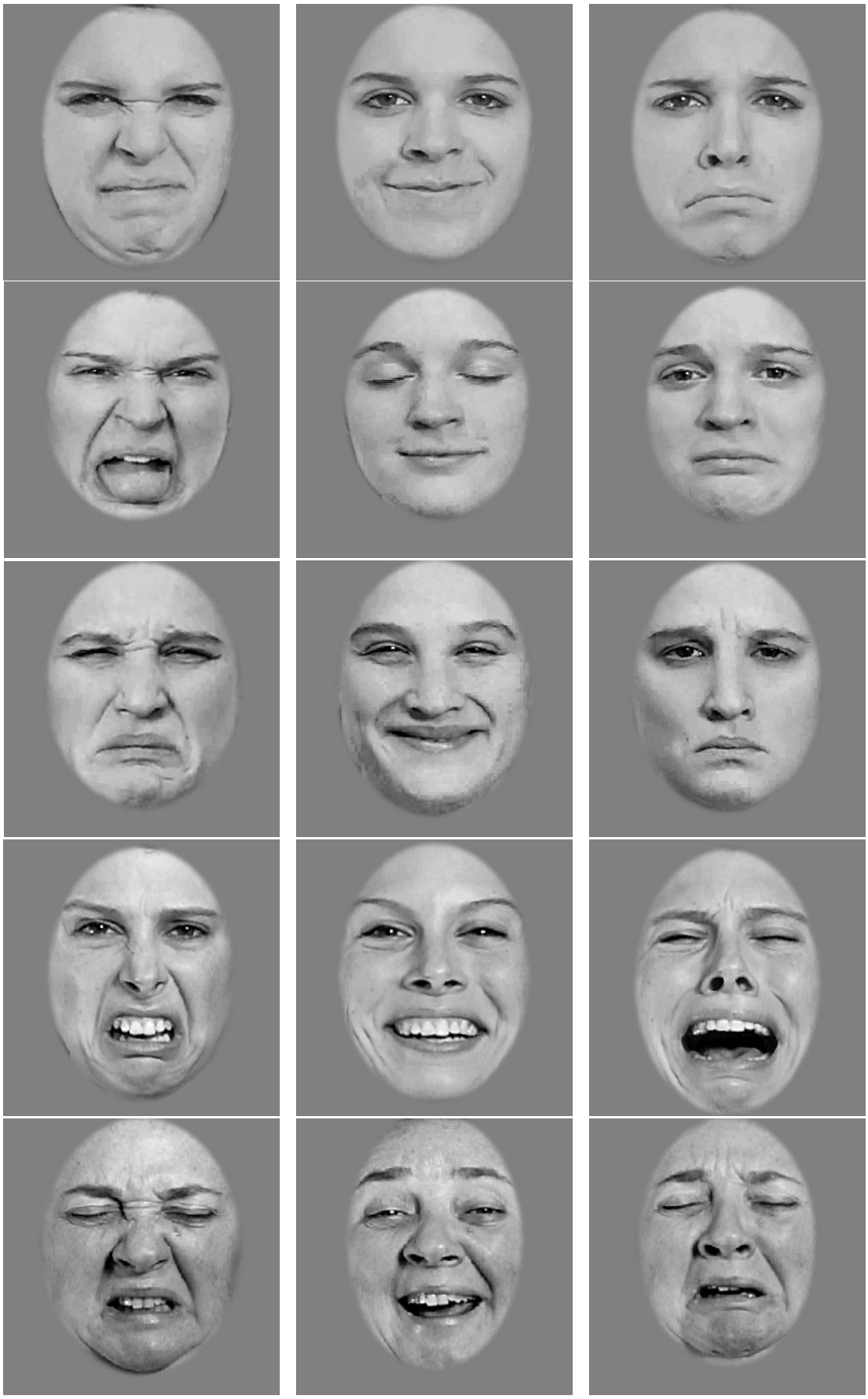

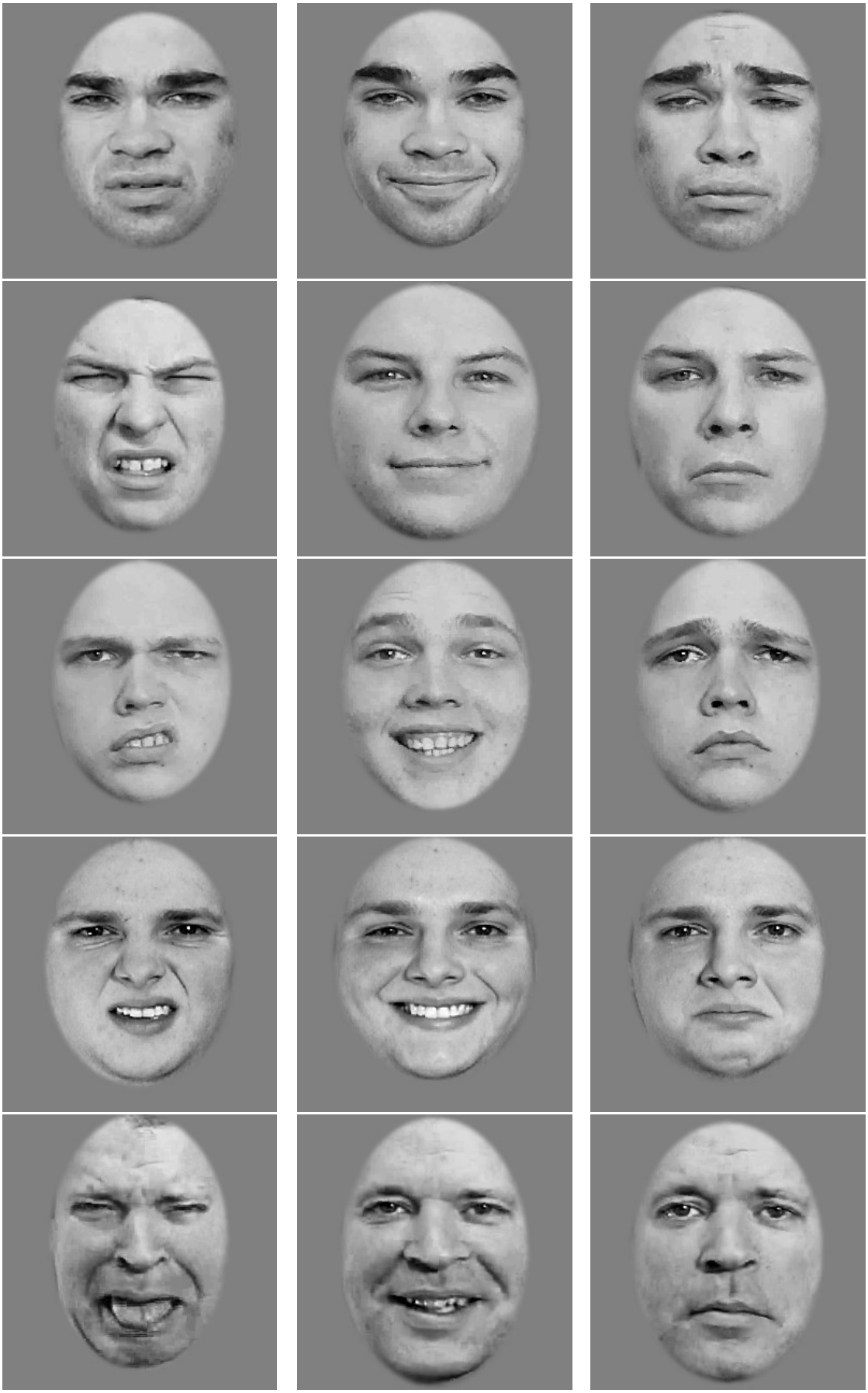

Appendix B. Univariate Whole Brain Analysis (WBA)

Chapter 2:

Firstly a univariate analysis was run to contrast between explicit and implicit expression recognition. This analysis was run to study the involvement of task, providing a complement to the MVPA results and hypothesis (H3) investigating the decoding effects in task context for emotion processing. Here, explicit expression recognition refers to when a participant is performing an emotion perception task, whereas implicit expression recognition refers to when a participant is performing a gender perception task. An explicit vs implicit contrast reveals the following activated brain regions in recognition: rIFG, rIOG, SFG, anterior cingulate, precuneus, lMFG, lIPL, lS2. The rIFG is the only region that has stronger activation in the explicit case, all other regions are more active during the implicit case, see Figure B-1. This is potentially an interesting finding for the involvement of implicit perception in expression recognition, but it is important to note that these results could be due to the explicit task being more difficult than the implicit task (see behavioural results in Table 2.2).

A further univariate analysis was run to contrast between brain regions activated for WF against the ME and MM partial face conditions across both tasks. This analysis was carried out to investigate the differences in brain activation between viewing a whole face, devoid of occlusion, to viewing a face with an important facial feature for recognition occluded, such as the eyes or mouth. The contrast is related to the central premise of this study, investigating how the brain deals with occlusion in expression recognition. This contrast reveals the following peak activated brain regions for WF against ME and MM: bilateral FG, SPOC, middle occipital gyrus, superior parietal lobule (SPL), left insula, lIFG, lpSTS, left post central sulcus and the rIOG. Most regions were higher for the ME and MM conditions, with the left precuneus being the only region higher for WF. This analysis shows there to be stronger activation in the brain to missing feature conditions, see Figure B-2.

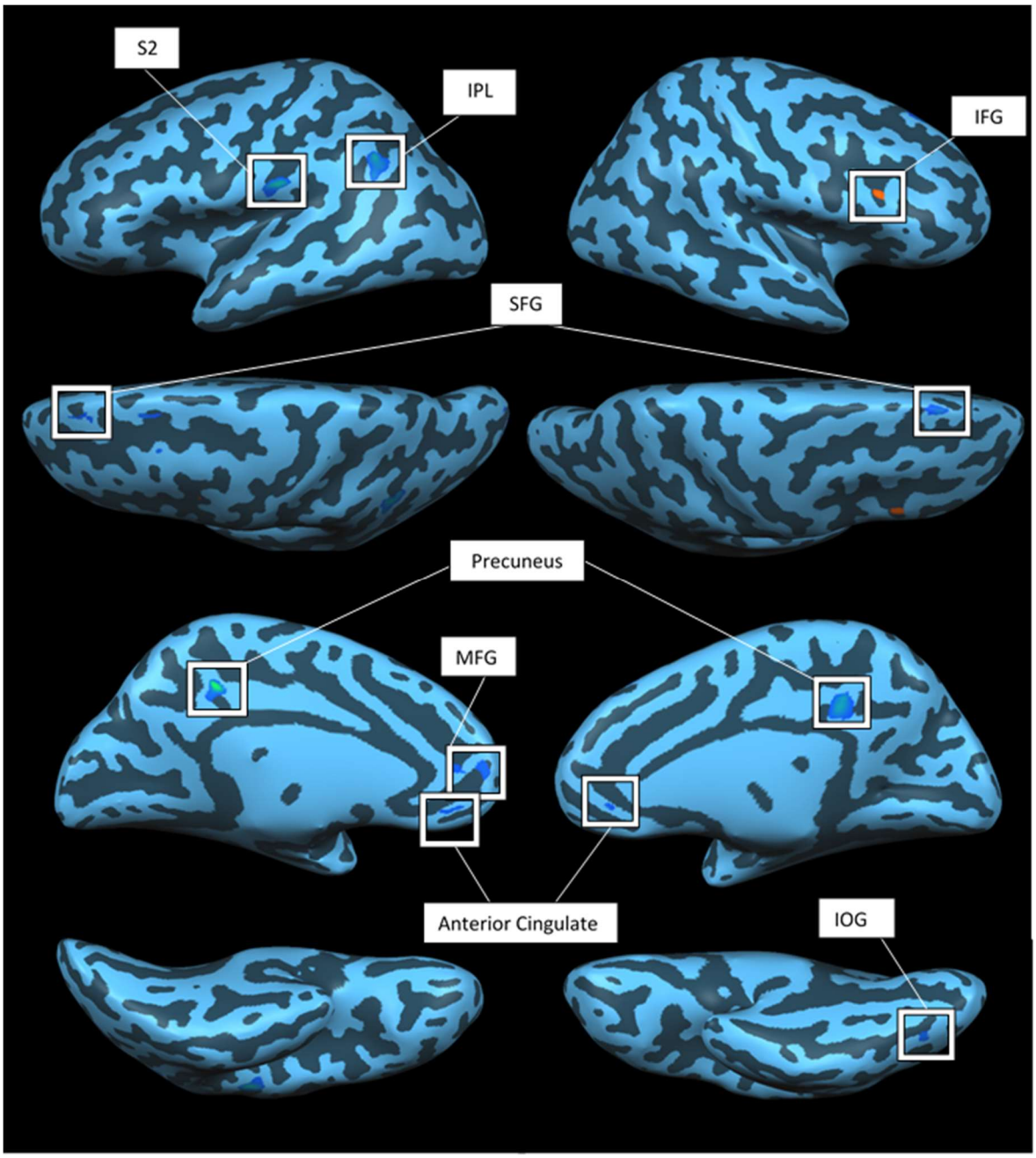

Figure B-1. Surface maps showing the regions activated for explicit vs implicit. Red clusters: more active during the implicit task; Blue clusters: more active for explicit; from left to right hemisphere.

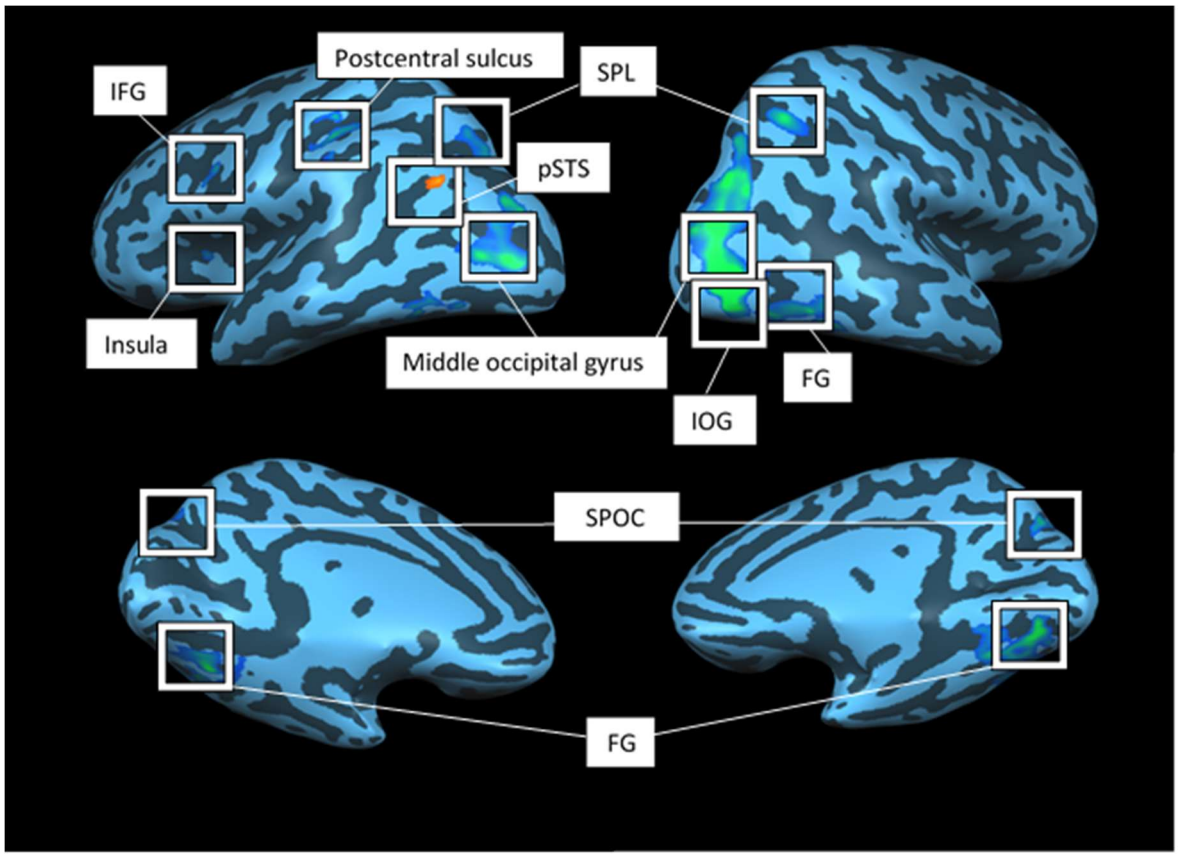

Figure B-2. Surface maps showing the regions activated for WF vs ME/MM. Red clusters: more activation for WF condition; Blue clusters: more active for ME/MM conditions; from left to right hemisphere.

Appendix C. Other Visual Regions

Chapter 2:

Basic decoding.

One-tailed one-sample t-tests were also carried out for decoding expression in V2, V3 and 1000 voxels in V1; akin to V1, these regions showed higher significance in all PF conditions for implicit decoding. However, in the explicit expression condition, where V1 showed significance in the WF, ME and MO conditions; V2 only showed significance in the WF and MO condition, and V3 showed no significance for these conditions but significance in the MM condition. Nonetheless for 1000 voxels in V1 we get the same results as 100 voxels in V1, with significance in the WF, ME and MO explicit decoding conditions. A repeated measures ANOVA showed a highly significant main effect of PF condition on decoding accuracy ($p < .001$), as well as main effect of task ($p < .001$) and a significant interaction ($p < .001$) in each of these regions. These results are the same, albeit more significant, than the results from V1 100 voxels.

For decoding of gender, one-sample t-test results between the visual regions differ. In V2 and for 1000 voxels in V1, implicit decoding in the MM condition was significant; there was also additional significance for 1000 voxels in V1 for the implicit WF condition. For V3, there was significant implicit decoding in the EO, but unlike all other regions there was significance in explicit decoding, namely the MO condition. A repeated measures ANOVA showed results to differ in each of the visual regions tested. Similar to V1 (100 voxels) (Appendix G), no main effect of PF condition was found for V2 and 1000 voxels in V1, however, unlike V1, there was no main effect of task on decoding accuracy in these regions. For V3, there was a main effect of PF condition and task on decoding accuracy, as well as a significant interaction ($p = .049$).

Cross classification.

One-sample t-tests were also carried out for decoding expression in 1000 voxels in V1; akin to V1 and EVC, there was significance in implicit conditions (for EO vs ME and the MO vs MM cross classification pairs). For explicit decoding there was additional significance in the EO vs ME pair. A repeated measures ANOVA was also conducted on 1000 voxels in V1, similar to 100 voxels in V1 and 1000 voxels in EVC, this showed a significant main effect of task and cross-classification comparison on decoding accuracy, as well as a significant interaction.

Appendix D: Statistics (ANOVA and t-test results)

Chapter 2:

Table D1.

Simple effects ANOVA for the emotion accuracy behavioural results; significance shows main effect of emotion (Chapter 2).

PF	*Result, significance shows main effect of emotion*
WF	$F(2,22) = 22.719$, $p < .001$, $\eta_p^2 = .674$
EO	$F(1.376, 15.134) = 9.869$, $p = .004$, $\eta_p^2 =$ .473 (greenhouse-geisser corrected)
ME	$F(1.289, 14.178) = 23.194$, $p < .001$, $\eta_p^2 =$ .678 (greenhouse-geisser corrected)
MO	$F(1.185, 13.038) = 31.590$, $p < .001$, $\eta_p^2 =$ .742 (greenhouse-geisser corrected)
MM	$F(2, 22) = 3.737$, $p = .040$, $\eta_p^2 = .254$

Table D2.

Simple-effects ANOVA for the emotion accuracy behavioural results; significance shows main effect of PF condition (Chapter 2).

Emotion	*Result, significance shows main effect of PF*
Disgust	$F(4,44) = 13.635$, $p < .001$, $\eta_p^2 = .553$
Fear	$F(4,44) = 10.030$, $p < .001$, $\eta_p^2 = .477$
Happy	$F(1.851, 20.359) = 3.847$, $p = .041$, $\eta_p^2 = .259$ (greenhouse-geisser corrected)

Table D3.

Paired sample t-tests comparing the differences between the emotions for each PF condition (Chapter 2).

PF	Comparison	t	df	*p*
WF	D vs F	3.618	11	.004
	D vs H	-2.419	11	.034
	F vs H	-7.864	11	>.001
EO	D vs F	-2.104	11	.059
	D vs H	-4.190	11	.002
	F vs H	-3.011	11	.012
ME	D vs F	3.548	11	.005
	D vs H	-3.622	11	.004
	F vs H	-6.603	11	>.001
MO	D vs F	4.062	11	.002
	D vs H	-4.581	11	.001
	F vs H	-7.793	11	>.001
MM	D vs F	.857	11	.410
	D vs H	-1.735	11	.111
	F vs H	-3.347	11	.007

Table D4.

Paired sample t-tests comparing the differences between the PF conditions for each emotion (Chapter 2).

Emotion	Comparison	t	df	*p*
Disgust	WF_D - EO_D	4.612	11	0.001
	WF_D - ME_D	0.567	11	0.582
	WF_D - MO_D	2.188	11	0.051
	WF_D - MM_D	1.452	11	0.175
	EO_D - ME_D	-7.924	11	<0.001
	EO_D - MO_D	-4.802	11	0.001
	EO_D - MM_D	-4.173	11	0.002
	ME_D - MO_D	1.326	11	0.212
	ME_D - MM_D	1.174	11	0.265
	MO_D - MM_D	0.136	11	0.895
Fear	WF_F - EO_F	-2.369	11	0.037
	WF_F - ME_F	1.337	11	0.208
	WF_F - MO_F	3.080	11	0.010
	WF_F - MM_F	-2.545	11	0.027
	EO_F - ME_F	3.938	11	0.002
	EO_F - MO_F	4.466	11	0.001
	EO_F - MM_F	0.527	11	0.609
	ME_F - MO_F	2.964	11	0.013
	ME_F - MM_F	-2.973	11	0.013
	MO_F - MM_F	-3.960	11	0.002
Happy	WF_H - EO_H	2.373	11	0.037
	WF_H - ME_H	-0.093	11	0.928
	WF_H - MO_H	0.857	11	0.410
	WF_H - MM_H	1.765	11	0.105
	EO_H - ME_H	-2.933	11	0.014
	EO_H - MO_H	-2.170	11	0.053
	EO_H - MM_H	0.089	11	0.931
	ME_H - MO_H	1.773	11	0.104
	ME_H - MM_H	2.356	11	0.038
	MO_H - MM_H	1.772	11	0.104

Table D5.

Simple-effects ANOVA for the gender accuracy behavioural results; significance shows main effect of gender (Chapter 2).

PF	*Result, significance shows main effect of gender*
WF	$F(1,11) = .186$, $p = .674$, $\eta_p^2 = .017$
EO	$F(1,11) = 19.809$, $p = .001$, $\eta_p^2 = .643$
ME	$F(1,11) = 1.941$, $p = .191$, $\eta_p^2 = .150$
MO	$F(1,11) = 1.443$, $p = .255$, $\eta_p^2 = .116$
MM	$F(1,11) = .560$, $p = .470$, $\eta_p^2 = .048$

Table D6.

Simple-effects ANOVA for the gender accuracy behavioural results; significance shows main effect of PF condition (Chapter 2).

Gender	*Result, significance shows main effect of PF*
Male	$F(4,44) = 4.183$, $p = .006$, $\eta_p^2 = .275$
Female	$F(1.650, 18.145) = 17.471$, $p < .001$, $\eta_p^2 = .614$ (greenhouse geisser corrected)

Table D7.

Paired sample t-tests comparing the differences between the PF conditions for male and female faces (Chapter 2).

Gender	Comparison	t	df	*p*
Male	WF_M - EO_M	2.017	11	0.069
	WF_M - ME_M	2.419	11	0.034
	WF_M - MO_M	3.317	11	0.007
	WF_M - MM_M	1.449	11	0.175
	EO_M - ME_M	0.185	11	0.857
	EO_M - MO_M	2.017	11	0.069
	EO_M - MM_M	-0.804	11	0.438
	ME_M - MO_M	1.685	11	0.120
	ME_M - MM_M	-1.239	11	0.241
	MO_M - MM_M	-2.862	11	0.015
Female	WF_F - EO_F	5.842	11	<0.001
	WF_F - ME_F	1.393	11	0.191
	WF_F - MO_F	1.170	11	0.267
	WF_F - MM_F	2.462	11	0.032
	EO_F - ME_F	-5.167	11	<0.001
	EO_F - MO_F	-3.694	11	0.004
	EO_F - MM_F	-5.062	11	<0.001
	ME_F - MO_F	0.944	11	0.365
	ME_F - MM_F	1.198	11	0.256
	MO_F - MM_F	0.000	11	1.000

Table D8.

One-tailed one sample t-test results for basic decoding in primary visual cortex (V1).

Task	PF	Result
Explicit expression decoding	WF	*t*(11)= 1.823, *p* = .048, *d* = 0.526 (medium effect-size)
	EO	*t*(11)= 0.752, *p* = .234, *d* = 0.217 (small effect-size)
	ME	*t*(11)= 1.847, *p* = .046, *d* = 0.533 (medium effect-size)
	MO	*t*(11)= 6.111, *p* <.001, *d* = 1.764 (large effect-size)
	MM	*t*(11)= 1.060, *p* = .156, d = 0.3059 (small effect-size)
Implicit expression decoding	WF	*t*(11)= 8.726, *p* <.001, *d* = 2.519 (large effect-size)
	EO	*t*(11)= 3.776, *p* = .002, *d* = 1.090 (large effect-size)
	ME	*t*(11)= 9.680, *p* <.001, *d* = 2.794 (large effect-size)
	MO	*t*(11)= 3.918, *p* = .001, *d* = 1.131 (large effect-size)
	MM	*t*(11)= 7.215, *p* <.001, *d* = 2.083 (large effect-size)

Table D9.

Paired sample t-tests to explore the effect of task for each PF condition (V1).

	t	df	*p*
WF Explicit - WF Implicit	-3.306	11	.007
EO Explicit - EO Implicit	-2.905	11	.014
ME Explicit - ME Implicit	-6.130	11	<.001
MO Explicit - MO Implicit	-1.717	11	.114
MM Explicit - MM Implicit	-5.377	11	<.001

Table D10.

One-tailed one sample t-test results for basic decoding in early visual cortex (EVC).

Task	PF	Result
Explicit expression decoding	WF	$t(11)= 4.154$, $p <.001$, $d = 1.199$ (large effect-size)
	EO	$t(11)= 0.987$, $p =.172$, $d = 0.285$ (small effect-size)
	ME	$t(11)= 1.787$, $p =.051$, $d = 0.516$ (medium effect-size)
	MO	$t(11)= 6.351$, $p <.001$, $d = 1.833$ (large effect-size)
	MM	$t(11)= 2.449$, $p =.016$, $d = 0.707$ (medium effect-size)
Implicit expression decoding	WF	$t(11)= 12.964$, $p <.001$, $d = 3.742$ (large effect-size)
	EO	$t(11)= 8.605$, $p <.001$, $d = 2.484$ (large effect-size)
	ME	$t(11)= 17.908$, $p <.001$, $d = 5.169$ (large effect-size)
	MO	$t(11)= 11.524$, $p <.001$, $d = 3.327$ (large effect-size)
	MM	$t(11)= 15.236$, $p <.001$, $d = 4.398$ (large effect-size)

Table D11.

Paired sample t-tests to explore the effect of task for each PF condition (EVC).

	t	df	*p*
WF Explicit - WF Implicit	-11.827	11	<.001
EO Explicit - EO Implicit	-5.278	11	<.001
ME Explicit - ME Implicit	-11.222	11	<.001
MO Explicit - MO Implicit	-5.734	11	<.001
MM Explicit - MM Implicit	-8.493	11	<.001

Table D12.

One-tailed one sample t-test results for cross-classification analyses in primary visual cortex (V1).

Task	XC	Result
Explicit expression decoding	EO - ME	$t(11)= 0.322$, $p =.377$, $d = 0.093$
	MO - MM	$t(11)= 0.047$, $p =.482$, $d = 0.014$
	EO - MO	$t(11)= 2.107$, $p =.029$, $d = 0.608$ (medium effect-size)
Implicit expression decoding	EO - ME	$t(11)= 5.033$, $p <.001$, $d =1.453$ (large effect-size)
	MO - MM	$t(11)= 6.031$, $p <.001$, $d = 1.741$ (large effect-size)
	EO - MO	$t(11)= -3.226$, $p =.996$, $d = -0.931$

Table D13.

Paired sample t-tests to explore the effect of task for each condition pair (V1).

	t	df	*p*
EO-ME Explicit – EO-ME Implicit	-4.531	11	.001
MO-MM Explicit – MO-MM Implicit	-3.749	11	.003
EO-MO Explicit – EO-MO Implicit	3.419	11	.006

Table D14.

One-tailed one sample t-test results for cross-classification analyses in early visual cortex (EVC).

Task	XC	Result
Explicit expression decoding	EO - ME	$t(11)= 1.346$, $p =.103$, $d = 0.389$ (small effect-size)
	MO - MM	$t(11)= 2.964$, $p =.006$, $d = 0.856$ (large effect-size)
	EO - MO	$t(11)= 5.065$, $p <.001$, $d = 1.462$ (large effect-size)
Implicit expression decoding	EO - ME	$t(11)= 12.718$, $p <.001$, $d = 3.671$ (large effect-size)
	MO - MM	$t(11)= 4.918$, $p <.001$, $d = 1.420$ (large effect-size)
	EO - MO	$t(11)= -5.145$, $p =.999$, $d = -1.485$

Table D15.

Paired sample t-tests to explore the effect of task for each condition pair (EVC).

	t	df	*p*
EO-ME Explicit – EO-ME Implicit	-13.452	11	<.001
MO-MM Explicit – MO-MM Implicit	-1.762	11	.106
EO-MO Explicit – EO-MO Implicit	6.598	11	<.001

Table D16.

One-tailed one sample t-test results for basic decoding in the fusiform gyrus (FG).

Task	PF	Result
Explicit expression decoding	WF	$t(59)= 3.802$, $p <.001$, $d = 0.491$ (small effect-size)
	EO	$t(59)= 2.279$, $p =.013$, $d = 0.294$ (small effect-size)
	ME	$t(59)= 2.407$, $p =.001$, $d = 0.311$ (small effect-size)
	MO	$t(59)= 6.253$, $p <.001$, $d = 0.807$ (large effect-size)
	MM	$t(59)= 0.745$, $p =.230$, $d = 0.096$
Implicit expression decoding	WF	$t(59)= 2.584$, $p =.006$, $d = 0.334$ (small effect-size)
	EO	$t(59)= 1.161$, $p =.125$, $d = 0.150$
	ME	$t(59)= 7.080$, $p <.001$, $d = 0.914$ (large effect-size)
	MO	$t(59)= 3.125$, $p =.001$, $d = 0.403$ (small effect-size)
	MM	$t(59)= 4.225$, $p <.001$, $d = 0.545$ (medium effect-size)

Table D17.

Paired sample t-tests to explore the effect of task for each PF condition (FG).

	t	df	*p*
WF Explicit - WF Implicit	.080	59	.937
EO Explicit - EO Implicit	.817	59	.417
ME Explicit - ME Implicit	-3.350	59	.001
MO Explicit - MO Implicit	1.336	59	.187
MM Explicit - MM Implicit	-3.185	59	.002

Table D18.

One-tailed one sample t-test results for basic decoding in the superior temporal sulcus (STS).

Task	PF	Result
Explicit expression decoding	WF	$t(59)= 4.039$, $p <.001$, $d = 0.521$ (medium effect-size)
	EO	$t(59)= 3.676$, $p <.001$, $d = 0.475$ (small effect-size)
	ME	$t(59)= 5.598$, $p <.001$, $d = 0.723$ (medium effect-size)
	MO	$t(59)= 5.792$, $p <.001$, $d = 0.748$ (medium effect-size)
	MM	$t(59)= 1.652$, $p =.052$, $d = 0.213$ (small effect-size)
Implicit expression decoding	WF	$t(59)= -0.470$, $p =.680$, $d = -0.061$
	EO	$t(59)= -0.619$, $p =.731$, $d = -0.080$
	ME	$t(59)= 0.061$, $p =.476$, $d =0.008$
	MO	$t(59)= 2.872$, $p =.003$, $d = 0.371$ (small effect-size)
	MM	$t(59)= 0.700$, $p =.244$, $d = 0.090$

Table D19.

Paired sample t-tests to explore the effect of task for each PF condition (STS).

	t	df	*p*
WF Explicit - WF Implicit	3.536	59	.001
EO Explicit - EO Implicit	3.253	59	.002
ME Explicit - ME Implicit	4.402	59	<.001
MO Explicit - MO Implicit	2.847	59	.006
MM Explicit - MM Implicit	.711	59	.480

Table D20.

One-tailed one sample t-test results for basic decoding in the inferior occipital gyrus (IOG).

Task	PF	Result
Explicit expression decoding	WF	$t(59)= 0.740$, $p =.231$, $d = 0.096$
	EO	$t(59)= 0.198$, $p =.422$, $d = 0.026$
	ME	$t(59)= -1.34$, $p =.907$, $d = -0.173$
	MO	$t(59)= 2.905$, $p =.003$, $d = 0.375$ (small effect-size)
	MM	$t(59)= 2.106$, $p =.020$, $d = 0.272$ (small effect-size)
Implicit expression decoding	WF	$t(59)= 4.777$, $p <.001$, $d = 0.617$ (medium effect-size)
	EO	$t(59)= 2.950$, $p =.002$, $d = 0.381$ (small effect-size)
	ME	$t(59)= 8.582$, $p <.001$, $d = 1.108$ (large effect-size)
	MO	$t(59)= 2.530$, $p =.007$, $d = 0.327$ (small effect-size)
	MM	$t(59)= 7.448$, $p <.001$, $d = 0.962$ (large effect-size)

Table D21.

Paired sample t-tests to explore the effect of task for each PF condition (IOG).

	t	df	*p*
WF Explicit - WF Implicit	-3.040	59	.004
EO Explicit - EO Implicit	-2.112	59	.039
ME Explicit - ME Implicit	-8.474	59	<.001
MO Explicit - MO Implicit	.185	59	.854
MM Explicit - MM Implicit	-4.590	59	<.001

Table D22.

One-tailed one sample t-test results for basic decoding in the amygdala (AMY).

Task	PF	Result
Explicit expression decoding	WF	$t(59)= 0.100$, $p =.460$, $d = 0.013$
	EO	$t(59)= -0.804$, $p =.788$, $d = -0.104$
	ME	$t(59)= 2.356$, $p =.011$, $d = 0.304$ (small effect-size)
	MO	$t(59)= 0.269$, $p =.394$, $d = 0.035$
	MM	$t(59)= -1.159$, $p =.874$, $d = -0.150$
Implicit expression decoding	WF	$t(59)= -1.025$, $p =.845$, $d = -0.132$
	EO	$t(59)= 3.808$, $p <.001$, $d = 0.492$ (small effect-size)
	ME	$t(59)= -1.136$, $p =.870$, $d = -0.147$
	MO	$t(59)= 1.474$, $p =.073$, $d = 0.190$
	MM	$t(59)= -2.449$, $p =.991$, $d = -0.316$

Table D23.

Paired sample t-tests to explore the effect of task for each PF condition (AMY).

	t	df	*p*
WF Explicit - WF Implicit	.838	59	.406
EO Explicit - EO Implicit	-2.886	59	.005
ME Explicit - ME Implicit	2.383	59	.020
MO Explicit - MO Implicit	-1.035	59	.305
MM Explicit - MM Implicit	1.055	59	.296

Table D24.

One-tailed one sample t-test results for basic decoding in the insula (INS).

Task	PF	Result
Explicit expression decoding	WF	$t(59)= 0.761$, $p =.225$, $d = 0.098$
	EO	$t(59)= -1.041$, $p =.849$, $d = -0.134$
	ME	$t(59)= 3.163$, $p =.001$, $d = 0.408$ (small effect-size)
	MO	$t(59)= 3.706$, $p <.001$, $d = 0.478$ (small effect-size)
	MM	$t(59)= -2.229$, $p =.985$, $d = -0.288$
Implicit expression decoding	WF	$t(59)= -0.442$, $p =.670$, $d = -0.057$
	EO	$t(59)= -0.497$, $p =.689$, $d = -0.064$
	ME	$t(59)= -0.954$, $p =.828$, $d = -0.123$
	MO	$t(59)= -1.570$, $p =.939$, $d = -0.203$
	MM	$t(59)= 0.091$, $p =.464$, $d = 0.012$

Table D25.

Paired sample t-tests to explore the effect of task for each PF condition (INS).

	t	df	*p*
WF Explicit - WF Implicit	.826	59	.412
EO Explicit - EO Implicit	-.451	59	.653
ME Explicit - ME Implicit	2.583	59	.012
MO Explicit - MO Implicit	3.744	59	<.001
MM Explicit - MM Implicit	-2.085	59	.041

Table D26.

One-tailed one sample t-test results for cross-classification analyses in the fusiform gyrus (FG).

Task	XC	Result
Explicit expression decoding	EO - ME	$t(59)= 2.435$, $p =.009$, $d = 0.314$ (small effect-size)
	MO - MM	$t(59)= 0.563$, $p =.288$, $d = 0.073$
	EO - MO	$t(59)= 1.378$, $p =.087$, $d = 0.178$
Implicit expression decoding	EO - ME	$t(59)=2.731$, $p =.004$, $d = 0.353$ (small effect-size)
	MO - MM	$t(59)= 2.456$, $p =.009$, $d = 0.317$ (small effect-size)
	EO - MO	$t(59)= -0.003$, $p =.501$, $d = -0.0004$

Table D27.

One-tailed one sample t-test results for cross-classification analyses in the superior temporal sulcus (STS).

Task	XC	Result
Explicit expression decoding	EO - ME	$t(59)= 3.050$, $p =.002$, $d = 0.394$ (small effect-size)
	MO - MM	$t(59)= 1.256$, $p =.107$, $d = 0.162$
	EO - MO	$t(59)= 4.837$, $p <.001$, $d = 0.625$ (medium effect-size)
Implicit expression decoding	EO - ME	$t(59)= 2.234$, $p =.015$, $d = 0.288$ (small effect-size)
	MO - MM	$t(59)= 0.423$, $p =.337$, $d = 0.055$
	EO - MO	$t(59)= 2.210$, $p =.016$, $d = 0.285$ (small effect-size)

Table D28.

One-tailed one sample t-test results for cross-classification analyses in the inferior occipital gyrus (IOG).

Task	XC	Result
Explicit expression decoding	EO - ME	$t(59)= -2.998$, $p =.998$, $d = -0.387$
	MO - MM	$t(59)= 0.773$, $p =.221$, $d = 0.100$
	EO - MO	$t(59)= 2.432$, $p =.009$, $d = 0.314$ (small effect-size)
Implicit expression decoding	EO - ME	$t(59)= 5.789$, $p <.001$, $d = 0.747$ (medium effect-size)
	MO - MM	$t(59)= 5.650$, $p <.001$, $d = 0.729$ (medium effect-size)
	EO - MO	$t(59)= -0.149$, $p =.559$, $d = -0.019$

Table D29.

Paired sample t-tests to explore the effect of task for each condition pair (IOG).

	t	df	*p*
EO-ME Explicit – EO-ME Implicit	-6.598	59	<.001
MO-MM Explicit – MO-MM Implicit	-3.666	59	.001
EO-MO Explicit – EO-MO Implicit	1.495	59	.140

Table D30.

One-tailed one sample t-test results for cross-classification analyses in the amygdala (AMY).

Task	XC	Result
Explicit expression decoding	EO - ME	*t*(59)= 0.633, *p* =.265, *d* = 0.0817
	MO - MM	*t*(59)= -0.297, *p* =.616, *d* = -0.038
	EO - MO	*t*(59)= 1.842, *p* =.035, *d* = 0.238 (small effect-size)
Implicit expression decoding	EO - ME	*t*(59)= 0.210, *p* =.417, *d* = 0.027
	MO - MM	*t*(59)= 1.029, *p* =.154, *d* = 0.133
	EO - MO	*t*(59)= -1.391, *p* =.915, *d* = -0.180

Table D31.

One-tailed one sample t-test results for cross-classification analyses in the insula (INS).

Task	XC	Result
Explicit expression decoding	EO - ME	*t*(59)= 0.497, *p* =.311, *d* = 0.064
	MO - MM	*t*(59)= 1.539, *p* =.065, *d* = 0.199
	EO - MO	*t*(59)= 1.952, *p* =.028, *d* = 0.252 (small effect-size)
Implicit expression decoding	EO - ME	*t*(59)= -1.407, *p* =.918, *d* = -0.182
	MO - MM	*t*(59)= 0.935, *p* =.177, *d* = 0.121
	EO - MO	*t*(59)= 0.914, *p* =.182, *d* = 0.118

Table D32.

Univariate analysis in V1: Paired sample t-tests to explore the effect of task for each PF condition.

PF	Result
WF	$t(11) = .861$, $p = .408$
EO	$t(11) = 1.184$, $p = .261$
ME	$t(11) = 1.947$, $p = .077$
MO	$t(11) = .313$, $p = .760$
MM	$t(11) = 2.972$, $p = .013$

Chapter 3:

Table D33.

Simple-effects ANOVA for the emotion accuracy behavioural results (Chapter 3, Study 1); significance shows main effect of emotion.

PF	*Result, significance shows main effect of emotion*
WF	$F(2, 26) = 15.801$, $p < .001$, $\eta_p^2 = .549$
EO	$F(2, 26) = 12.126$, $p < .001$, $\eta_p^2 = .483$
ME	$F(1.234, 16.045) = 15.857$, $p = .001$, $\eta_p^2 = .550$ (greenhouse-geisser corrected)
MO	$F(2, 26) = 29.897$, $p < .001$, $\eta_p^2 = .697$
MM	$F(2, 26) = 3.398$, $p = .049$, $\eta_p^2 = .207$

Table D34.

Simple-effects ANOVA for the emotion accuracy behavioural results (Chapter 3. Study 1); significance shows main effect of PF condition.

Emotion	*Result, significance shows main effect of PF*
Disgust	$F(1.961, 25.490) = 6.541$, $p = .005$, $\eta_p^2 = .335$ (greenhouse-geisser corrected)
Fear	$F(2.024, 26.306) = 22.122$, $p < .001$, $\eta_p^2 = .630$ (greenhouse-geisser corrected)
Happy	$F(4, 52) = 6.230$, $p < .001$, $\eta_p^2 = .324$

Table D35.

Paired sample t-tests comparing the differences between the emotions for each PF condition (Chapter 3, Study 1).

PF	Comparison	t	df	*p*
WF	D vs F	2.075	13	.058
	D vs H	-3.718	13	.003
	F vs H	-5.980	13	<.001
EO	D vs F	-3.211	13	.007
	D vs H	-4.319	13	.001
	F vs H	-1.619	13	.129
ME	D vs F	2.577	13	.023
	D vs H	-2.727	13	.017
	F vs H	-7.208	13	<.001
MO	D vs F	3.545	13	.004
	D vs H	-4.607	13	<.001
	F vs H	-7.926	13	<.001
MM	D vs F	-.856	13	.407
	D vs H	-2.233	13	.044
	F vs H	-2.414	13	.031

Table D36.

Paired sample t-tests comparing the differences between the PF conditions for each emotion (Chapter 3, Study 1).

Emotion	Comparison	t	df	*p*
Disgust	WF_D - EO_D	4.225	13	.001
	WF_D - ME_D	1.135	13	.277
	WF_D - MO_D	2.745	13	.017
	WF_D - MM_D	1.395	13	.186
	EO_D - ME_D	-3.344	13	.005
	EO_D - MO_D	-3.836	13	.002
	EO_D - MM_D	-3.733	13	.003
	ME_D - MO_D	1.000	13	.336
	ME_D - MM_D	.580	13	.572
	MO_D - MM_D	.132	13	.897
Fear	WF_F - EO_F	-2.270	13	.041
	WF_F - ME_F	4.258	13	.001
	WF_F - MO_F	4.988	13	<.001
	WF_F - MM_F	-2.349	13	.035
	EO_F - ME_F	4.639	13	<.001
	EO_F - MO_F	5.986	13	<.001
	EO_F - MM_F	-.105	13	.918
	ME_F - MO_F	2.963	13	.011
	ME_F - MM_F	-4.556	13	.001
	MO_F - MM_F	-5.453	13	<.001
Happy	WF_H - EO_H	4.020	13	.001
	WF_H - ME_H	1.108	13	.288
	WF_H - MO_H	-.586	13	.568
	WF_H - MM_H	2.914	13	.012
	EO_H - ME_H	-2.539	13	.025
	EO_H - MO_H	-3.294	13	.006
	EO_H - MM_H	-.790	13	.444
	ME_H - MO_H	-1.125	13	.281
	ME_H - MM_H	2.232	13	.044
	MO_H - MM_H	2.754	13	.016

Table D37.

Simple-effects ANOVA for the gender accuracy behavioural results (Chapter 3, Study 1); significance shows main effect of gender.

PF	*Result, significance shows main effect of gender*
WF	$F(1, 13) = .650$, $p = .435$, $\eta_p^2 = .048$
EO	$F(1, 13) = 18.539$, $p = .001$, $\eta_p^2 = .588$
ME	$F(1, 13) = 6.707$, $p = .022$, $\eta_p^2 = .340$
MO	$F(1, 13) = .068$, $p = .799$, $\eta_p^2 = .005$
MM	$F(1, 13) = .650$, $p = .435$, $\eta_p^2 = .048$

Table D38.

Simple-effects ANOVA for the gender accuracy behavioural results (Chapter 3, Study 1); significance shows main effect of PF condition.

Gender	*Result, significance shows main effect of PF*
Male	$F(1.926, 25.036) = 24.182$, $p < .001$, $\eta_p^2 = .650$ (greenhouse-geisser corrected)
Female	$F(4, 52) = 3.069$, $p = .024$, $\eta_p^2 = .191$

Table D39.

Paired sample t-tests comparing the differences between the PF conditions for male and female faces (Chapter 3, Study 1).

Gender	Comparison	t	df	*p*
Male	WF_M - EO_M	2.687	13	.019
	WF_M - ME_M	4.048	13	.001
	WF_M - MO_M	2.806	13	.015
	WF_M - MM_M	2.820	13	.014
	EO_M - ME_M	-.283	13	.782
	EO_M - MO_M	.091	13	.928
	EO_M - MM_M	-.520	13	.612
	ME_M - MO_M	.563	13	.583
	ME_M - MM_M	-.120	13	.907
	MO_M - MM_M	-.583	13	.583
Female	WF_F - EO_F	5.593	13	<.001
	WF_F - ME_F	.000	13	1.000
	WF_F - MO_F	2.290	13	.039
	WF_F - MM_F	1.461	13	.168
	EO_F - ME_F	-6.183	13	<.001
	EO_F - MO_F	-5.096	13	<.001
	EO_F - MM_F	-5.751	13	<.001
	ME_F - MO_F	2.309	13	.038
	ME_F - MM_F	1.091	13	.295
	MO_F - MM_F	-1.446	13	.172

Table D40.

Simple-effects ANOVA for the rN170 (Chapter 3, Study 1); significance shows main effect of emotion.

PF	*Result, significance shows main effect of emotion*
WF	$F(2, 26) = 4.278$, $p = .025$, $\eta_p^2 = .248$
EO	$F(2, 26) = 4.219$, $p = .026$, $\eta_p^2 = .245$
ME	$F(2, 26) = .760$, $p = .478$, $\eta_p^2 = .055$
MO	$F(2, 26) = 6.844$, $p = .004$, $\eta_p^2 = .345$
MM	$F(2, 26) = .793$, $p = .463$, $\eta_p^2 = .058$

Table D41.

Simple-effects ANOVA for the rN170 (Chapter 3, Study 1); significance shows main effect of PF condition.

Emotion	*Result, significance shows main effect of PF*
Disgust	$F(4, 52) = 4.767$, $p = .002$, $\eta_p^2 = .268$
Fear	$F(4, 52) = 11.950$, $p < .001$, $\eta_p^2 = .479$
Happy	$F(4, 52) = 21.022$, $p < .001$, $\eta_p^2 = .618$

Table D42.

Paired sample t-tests comparing the differences between the emotions for the significant PF conditions in the rN170 (Chapter 3, Study 1).

PF	Comparison	t	df	*p*
WF	D vs F	-1.561	13	.143
	D vs H	-2.890	13	.013
	F vs H	-1.366	13	.195
EO	D vs F	.355	13	.728
	D vs H	2.491	13	.027
	F vs H	2.053	13	.061
MO	D vs F	-1.071	13	.303
	D vs H	2.624	13	.021
	F vs H	3.256	13	.006

Table D43.

Paired sample t-tests comparing the differences between the PF conditions for each emotion in the rN170 (Chapter 3, Study 1).

Emotion	Comparison	t	df	*p*
Disgust	WF_D - EO_D	1.937	13	.075
	WF_D - ME_D	3.353	13	.005
	WF_D - MO_D	2.701	13	.018
	WF_D - MM_D	1.625	13	.128
	EO_D - ME_D	1.348	13	.201
	EO_D - MO_D	.600	13	.559
	EO_D - MM_D	-1.022	13	.325
	ME_D - MO_D	-1.157	13	.268
	ME_D - MM_D	-2.719	13	.018
	MO_D - MM_D	-2.466	13	.028
Fear	WF_F - EO_F	3.416	13	.005
	WF_F - ME_F	8.513	13	<.001
	WF_F - MO_F	4.000	13	.002
	WF_F - MM_F	2.416	13	.031
	EO_F - ME_F	1.772	13	.100
	EO_F - MO_F	-.212	13	.835
	EO_F - MM_F	-2.054	13	.061
	ME_F - MO_F	-2.670	13	.019
	ME_F - MM_F	-4.415	13	.001
	MO_F - MM_F	-2.038	13	.062
Happy	WF_H - EO_H	4.932	13	<.001
	WF_H - ME_H	7.045	13	<.001
	WF_H - MO_H	6.473	13	<.001
	WF_H - MM_H	4.326	13	.001
	EO_H - ME_H	.169	13	.868
	EO_H - MO_H	.588	13	.567
	EO_H - MM_H	-3.259	13	.006
	ME_H - MO_H	.486	13	.635
	ME_H - MM_H	-3.995	13	.002
	MO_H - MM_H	-4.633	13	<.001

Table D44.

Simple-effects ANOVA for the P300 gender task (Chapter 3, Study 1); significance shows main effect of emotion.

PF	*Result, significance shows main effect of emotion*
WF	$F(2, 26) = 5.503$, $p = .010$, $\eta_p^2 = .297$
EO	$F(2, 26) = .234$, $p = .793$, $\eta_p^2 = .018$
ME	$F(2, 26) = 1.161$, $p = .329$, $\eta_p^2 = .082$
MO	$F(2, 26) = 2.104$, $p = .142$, $\eta_p^2 = .139$
MM	$F(2, 26) = 2.356$, $p = .115$, $\eta_p^2 = .153$

Table D45.

Simple-effects ANOVA for the P300 gender task (Chapter 3, Study 1); significance shows main effect of PF condition.

Emotion	*Result, significance shows main effect of PF*
Disgust	$F(4, 52) = 2.708$, $p = .040$, $\eta_p^2 = .172$
Fear	$F(4, 52) = 2.712$, $p = .040$, $\eta_p^2 = .173$
Happy	$F(4, 52) = 1.824$, $p = .138$, $\eta_p^2 = .123$

Table D46.

Paired sample t-tests comparing the differences between the emotions for the significant WF condition in the P300 (Chapter 3, Study 1).

PF	Comparison	t	df	*p*
WF	D vs F	-2.548	13	.024
	D vs H	.283	13	.781
	F vs H	2.998	13	.010

Table D47.

Paired sample t-tests comparing the differences between the PF conditions for the significant emotions in the P300 (Chapter 3, Study 1).

Emotion	Comparison	t	df	*p*
	WF_D - EO_D	1.607	13	.132
	WF_D - ME_D	.391	13	.702
	WF_D - MO_D	-1.080	13	.300
	WF_D - MM_D	2.650	13	.020
Disgust	EO_D - ME_D	-.493	13	.630
	EO_D - MO_D	-2.715	13	.018
	EO_D - MM_D	1.260	13	.230
	ME_D - MO_D	-1.737	13	.106
	ME_D - MM_D	1.222	13	.244
	MO_D - MM_D	3.372	13	.005
	WF_F - EO_F	3.786	13	.002
	WF_F - ME_F	1.230	13	.241
	WF_F - MO_F	1.442	13	.173
	WF_F - MM_F	3.518	13	.004
Fear	EO_F - ME_F	-1.608	13	.132
	EO_F - MO_F	-1.388	13	.189
	EO_F - MM_F	-.746	13	.469
	ME_F - MO_F	.158	13	.877
	ME_F - MM_F	.938	13	.365
	MO_F - MM_F	.825	13	.424

Table D48.

Simple-effects ANOVA for the emotion accuracy behavioural results (Chapter 3, Study 2); significance shows main effect of gender.

PF	*Result, significance shows main effect of emotion*
WF	$F(1, 19) = 2.416$, $p = .137$, $\eta_p^2 = .113$
EO	$F(1, 19) = .060$, $p = .809$, $\eta_p^2 = .003$
ME	$F(1, 19) = .083$, $p = .777$, $\eta_p^2 = .004$
MO	$F(1, 19) = .315$, $p = .581$, $\eta_p^2 = .016$
MM	$F(1, 19) = 8.855$, $p = .008$, $\eta_p^2 = .318$

Table D49.

Simple-effects ANOVA for the emotion accuracy behavioural results (Chapter 3, Study 2); significance shows main effect of PF condition.

Emotion	*Result, significance shows main effect of PF*
Fear	$F(2.600, 49.393) = 12.003$, $p < .001$, $\eta_p^2 = .387$ (greenhouse-geisser corrected)
Happy	$F(4, 76) = 10.611$, $p < .001$, $\eta_p^2 = .358$

Table D50.

Paired sample t-tests comparing the differences between the PF conditions for the significant emotions (Chapter 3, Study 2).

Emotion	Comparison	t	df	*p*
Fear	WF_F - EO_F	3.359	19	.003
	WF_F - ME_F	-2.128	19	.047
	WF_F - MO_F	-2.703	19	.014
	WF_F - MM_F	-.463	19	.649
	EO_F - ME_F	-4.712	19	<.001
	EO_F - MO_F	-5.409	19	<.001
	EO_F - MM_F	-3.922	19	.001
	ME_F - MO_F	.089	19	.930
	ME_F - MM_F	2.305	19	.033
	MO_F - MM_F	1.608	19	.124
Happy	WF_H - EO_H	3.737	19	.001
	WF_H - ME_H	-.167	19	.869
	WF_H - MO_H	.137	19	.892
	WF_H - MM_H	4.607	19	<.001
	EO_H - ME_H	-3.344	19	.003
	EO_H - MO_H	-3.520	19	.002
	EO_H - MM_H	-.542	19	.594
	ME_H - MO_H	.231	19	.820
	ME_H - MM_H	4.222	19	<.001
	MO_H - MM_H	4.614	19	<.001

Table D51.

Simple-effects ANOVA for the gender accuracy behavioural results (Chapter 3, Study 2); significance shows main effect of gender.

PF	*Result, significance shows main effect of gender*
WF	$F(1, 19) = .140$, $p = .712$, $\eta_p^2 = .007$
EO	$F(1, 19) = 19.919$, $p < .001$, $\eta_p^2 = .512$
ME	$F(1, 19) = 1.638$, $p = .216$, $\eta_p^2 = .079$
MO	$F(1, 19) = 2.531$, $p = .128$, $\eta_p^2 = .118$
MM	$F(1, 19) = .205$, $p = .656$, $\eta_p^2 = .011$

Table D52.

Simple-effects ANOVA for the gender accuracy behavioural results (Chapter 3, Study 2); significance shows main effect PF condition.

Gender	*Result, significance shows main effect of PF*
Male	$F(4, 76) = .872$, $p = .485$, $\eta_p^2 = .044$
Female	$F(2.047, 38.893) = 17.034$, $p < .001$, $\eta_p^2 = .473$ (greenhouse-geisser corrected)

Table D53.

Paired sample t-tests for PF condition in female stimuli (Chapter 3, Study 2).

Gender	Comparison	t	df	*p*
Female	WF_F - EO_F	4.916	19	<.001
	WF_F - ME_F	-.170	19	.867
	WF_F - MO_F	1.914	19	.071
	WF_F - MM_F	1.921	19	.070
	EO_F - ME_F	-5.708	19	<.001
	EO_F - MO_F	.3.860	19	.001
	EO_F - MM_F	-4.449	19	.001
	ME_F - MO_F	3.120	19	.006
	ME_F - MM_F	2.123	19	.047
	MO_F - MM_F	-.622	19	.542

Table D54.

Simple-effects ANOVA for the lN170 (Chapter 3, Study 2); significance shows main effect of emotion.

PF	*Result, significance shows main effect of emotion*
WF	$F(1, 19) = 1.564$, $p = .226$, $\eta_p^2 = .076$
EO	$F(1, 19) = 2.771$, $p = .112$, $\eta_p^2 = .127$
ME	$F(1, 19) = 1.883$, $p = .186$, $\eta_p^2 = .090$
MO	$F(1, 19) = 1.157$, $p = .296$, $\eta_p^2 = .057$
MM	$F(1, 19) = 13.435$, $p = .002$, $\eta_p^2 = .414$

Table D55.

Simple-effects ANOVA for the lN170 (Chapter 3, Study 2); significance shows main effect of PF condition.

Emotion	*Result, significance shows main effect of PF*
Fear	$F(2.502, 47.547) = 6.295$, $p = .002$, $\eta_p^2 = .249$ (greenhouse-geisser corrected)
Happy	$F(2.673, 50.780) = 2.807$, $p = .055$, $\eta_p^2 = .129$ (greenhouse-geisser corrected)

Table D56.

Paired sample t-tests comparing the differences between the PF conditions for each emotion in the lN170 (Chapter 3, Study 2).

Emotion	Comparison	t	df	*p*
Fear	WF_F - EO_F	-.296	19	.770
	WF_F - ME_F	.497	19	.625
	WF_F - MO_F	1.062	19	.302
	WF_F - MM_F	-2.444	19	.024
	EO_F - ME_F	1.021	19	.320
	EO_F - MO_F	1.610	19	.124
	EO_F - MM_F	-4.434	19	<.001
	ME_F - MO_F	.543	19	.593
	ME_F - MM_F	-3.961	19	.001
	MO_F - MM_F	-4.486	19	<.001
Happy	WF_H - EO_H	-.375	19	.712
	WF_H - ME_H	1.399	19	.178
	WF_H - MO_H	1.401	19	.177
	WF_H - MM_H	-.981	19	.339
	EO_H - ME_H	1.909	19	.071
	EO_H - MO_H	1.917	19	.070
	EO_H - MM_H	-1.201	19	.245
	ME_H - MO_H	-.457	19	.653
	ME_H - MM_H	-3.366	19	.003
	MO_H - MM_H	-2.912	19	.009

Table D57.

Simple-effects ANOVA for the P100 (Chapter 3, Study 2); significance shows main effect of emotion.

PF	*Result, significance shows main effect of emotion*
WF	$F(1, 19) = 1.313$, $p = .266$, $\eta_p^2 = .065$
EO	$F(1, 19) = 4.367$, $p = .050$, $\eta_p^2 = .187$
ME	$F(1, 19) = 2.825$, $p = .109$, $\eta_p^2 = .129$
MO	$F(1, 19) = 4.532$, $p = .047$, $\eta_p^2 = .193$
MM	$F(1, 19) = 1.886$, $p = .186$, $\eta_p^2 = .090$

Table D58.

Simple-effects ANOVA for the P100 (Chapter 3, Study 2); significance shows main effect of PF condition.

Emotion	*Result, significance shows main effect of PF*
Fear	$F(2.539, 48.237) = 5.781$, $p = .003$, $\eta_p^2 = .233$ (greenhouse-geisser corrected)
Happy	$F(2.765, 52.527) = 1.826$, $p = .158$, $\eta_p^2 = .088$ (greenhouse-geisser corrected)

Table D59.

Paired sample t-tests comparing the differences between the PF conditions for fear in the P100 (Chapter 3, Study 2).

Emotion	Comparison	t	df	*p*
	WF_F - EO_F	.181	19	.858
	WF_F - ME_F	-3.919	19	.001
	WF_F - MO_F	-.583	19	.567
	WF_F - MM_F	-1.787	19	.090
Fear	EO_F - ME_F	-3.499	19	.002
	EO_F - MO_F	-.984	19	.338
	EO_F - MM_F	-2.475	19	.023
	ME_F - MO_F	3.668	19	.002
	ME_F - MM_F	2.473	19	.023
	MO_F - MM_F	-1.655	19	.114

Appendix E. Confusion Matrices

Chapter 2:

a.

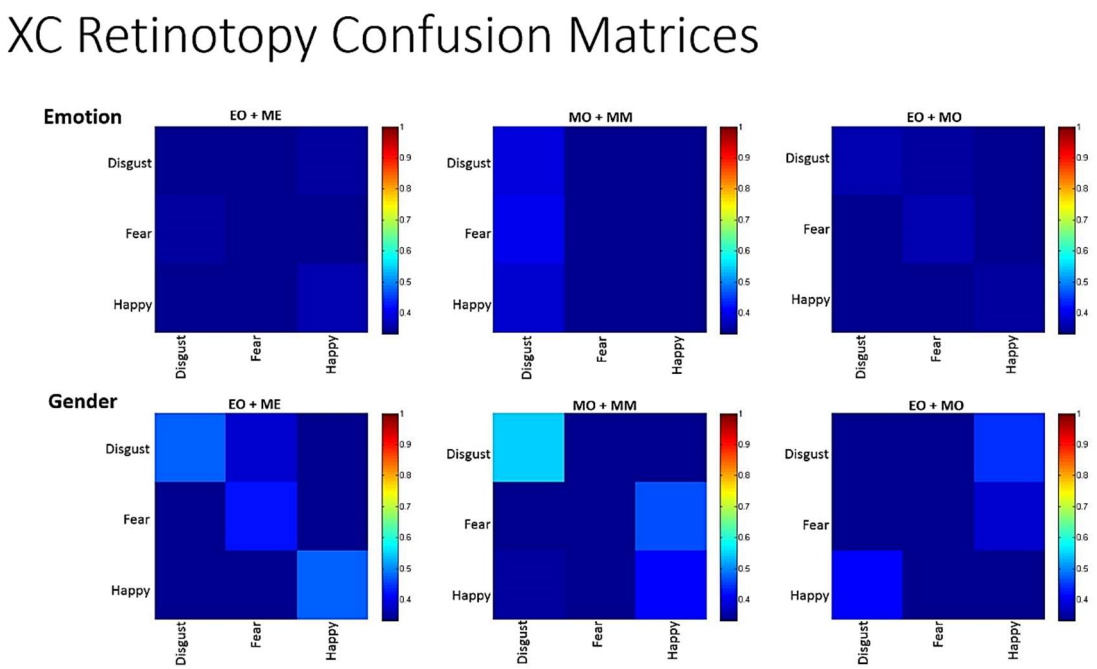

b.

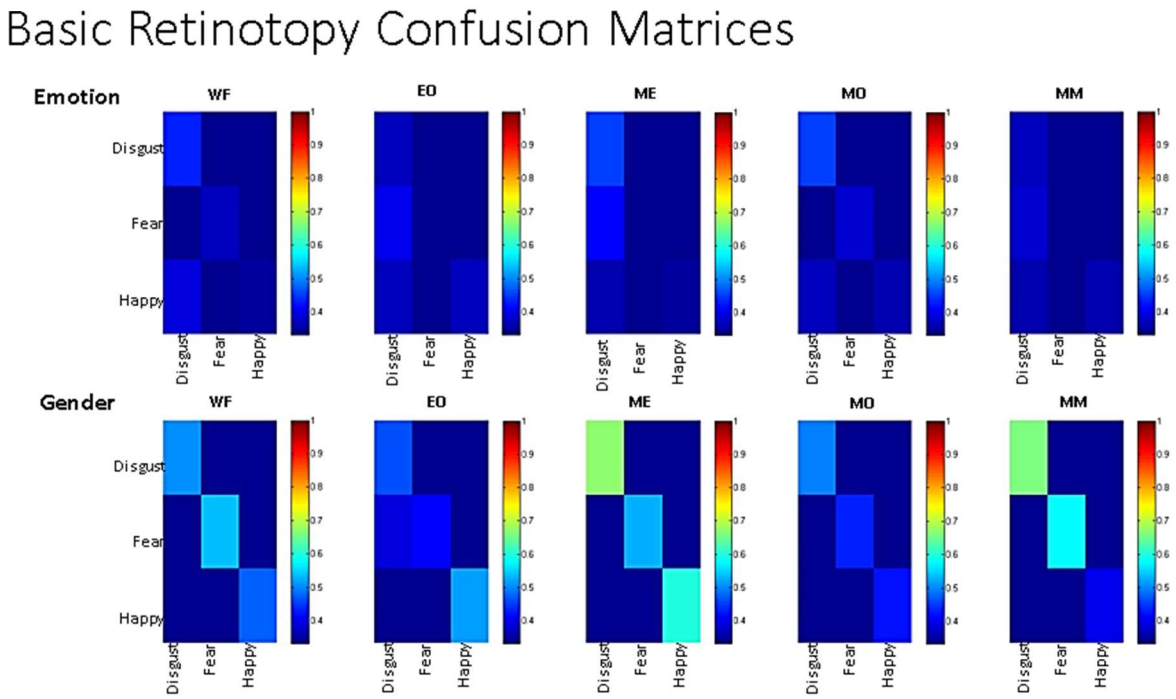

Figure E-1. Confusion matrices for V1 and EVC. a. Cross-classification confusion matrices between emotion for each cross-classification pair (EO and ME; MO and MM; EO and MO) in the emotion and gender task. b. Basic decoding confusion matrices between emotion for each PF condition in the emotion and gender task.

Appendix F. Full results from Task x ROI x Voxel Size Repeated Measures ANOVA

Chapter 2:

Basic decoding.

A 2 (task) x 5 (ROI) x 5 (voxel size) x 5 (PF) repeated measures ANOVA was carried out. ROI and voxel size were included in the analysis for comparability to Wegrzyn et al. (2015). Wegrzyn et al. (2015) found no interaction of ROI by voxel size and subsequently averaged across the voxel sizes. This method will also be applied in this study if no interactions are found. The ANOVA showed no main effect of task, $F(1, 11) = .121$, $p = .735$ or PF condition, $F(4, 44) = 2.313$, $p = .072$, but a significant main effect of ROI, $F(4, 44) = 6.171$, $p < .001$, $\eta_p^2 = .359$ and voxel size on decoding accuracy, $F(4, 44) = 3.542$, $p = .014$, $\eta_p^2 = .244$. Further investigation into the ROI main effect shows the greatest decoding accuracy in the FG and the IOG, followed by the STS, and the lowest decoding accuracies in the AMY and INS. Pairwise comparisons reveal significant differences between the AMY and FG, AMY and IOG, as well as the INS and IOG. In respect to voxel size, there appears to be a trend between higher amounts of voxels and greater decoding (see Figure 2.27), however, there was no significance within pairwise comparisons. Furthermore this ANOVA showed significant interactions between task and ROI, $F(4, 44) = 7.058$, $p < .001$, $\eta_p^2 = .391$, as well as a three-way interaction between task, ROI and PF condition, $F(16, 176) = 2.302$, $p = .004$, $\eta_p^2 = .173$. However, there were no significant interactions with voxel size; further analyses will thus average across this variable akin to Wegrzyn et al. (2015).

Appendix G. Gender Decoding Results

Chapter 2:

Basic decoding.

Explicit gender decoding refers to when a participant is performing the gender recognition task and the classifier is decoding gender in their brain, whereas implicit gender decoding refers to when a participant is asked to judge emotion but the classifier is again decoding gender in their brain.

Primary visual cortex (V1).

For decoding of gender, one sample t-tests showed implicit decoding only significantly above chance in the WF condition (p = .003), see Figure G-1. A repeated measures ANOVA did not show a main effect of PF condition on decoding accuracy, $F(4, 44) = 1.844$, $p = .138$, $\eta_p^2 = .144$, but a significant main effect of task, $F(1, 11) = 6.692$, $p = .025$, $\eta_p^2 = .378$ with decoding accuracy significantly higher in the implicit task (M = 52.1%) compared to the explicit task (M = 48.8%). There was no significant interaction, $F(4, 44) = 1.017$, $p = .409$, $\eta_p^2 = .085$.

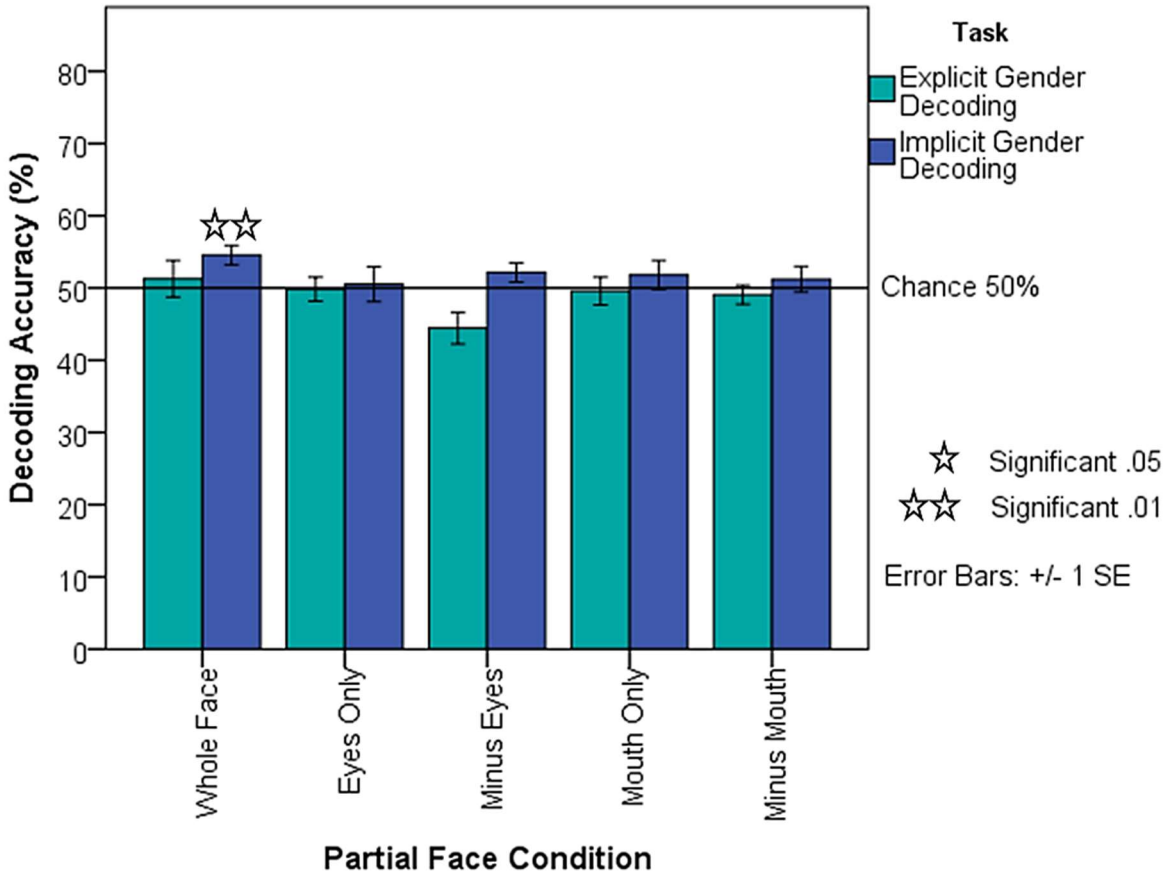

Figure G-1. Explicit and implicit gender decoding accuracy of the PF conditions. Results from one-sample t-tests included with stars representing significance above chance.

Early visual cortex.

For decoding of gender, one sample t-tests show implicit decoding significantly above chance in the WF (p = .005), ME (p = .039) and MM condition (p = .023) of EVC, see Figure G-2. A repeated measures ANOVA showed no main effect of PF condition $F(4, 44) = .517$, $p = .724$, $\eta_p^2 = .045$ but an effect of task $F(1, 11) = 6.924$, $p = .023$, $\eta_p^2 = .386$ on decoding accuracy, with higher decoding accuracy in the implicit task (53%) compared to the explicit task (50.8%). There was no significant interaction, $F(4, 44) = 1.376$, $p = .258$, $\eta_p^2 = .111$.

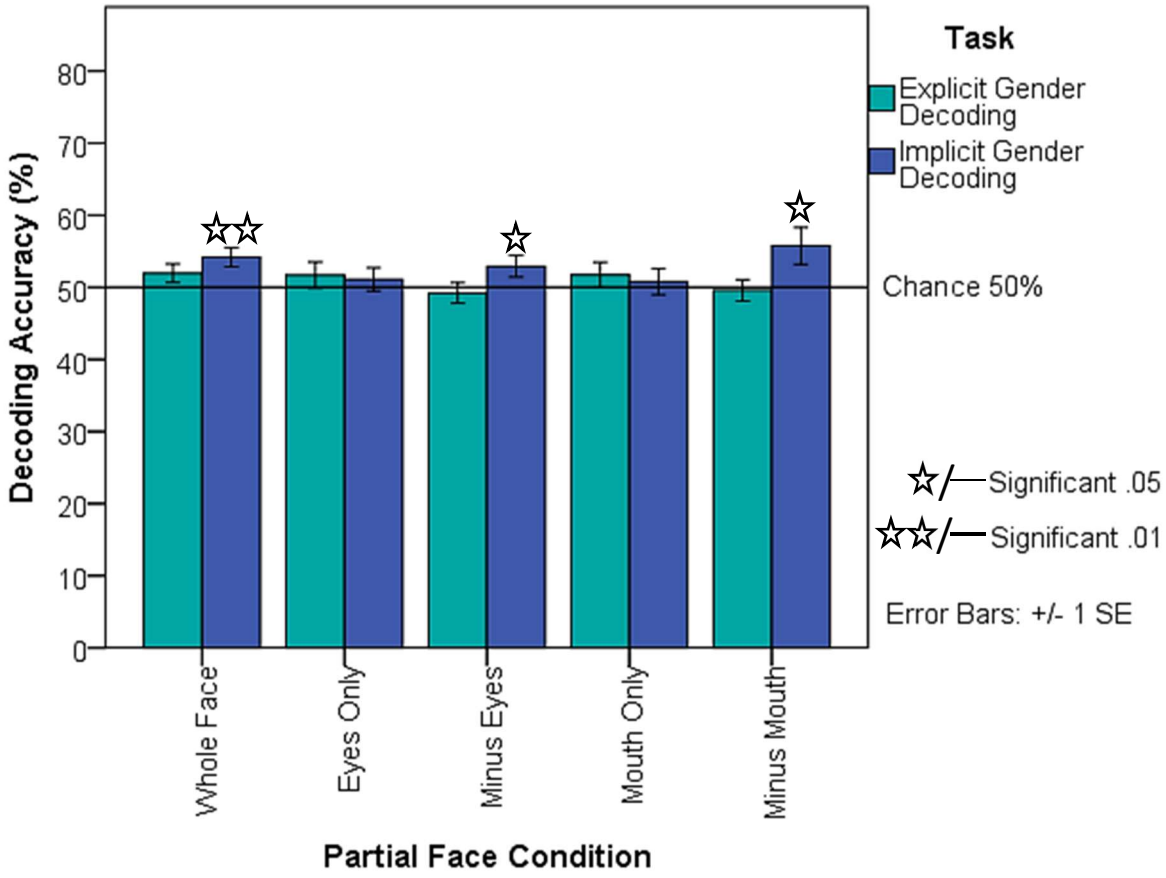

Figure G-2. Explicit and implicit gender decoding accuracy of the PF conditions for 1000 voxels in EVC, significant results from one-sample t-tests represented with stars.

Due to the low decoding accuracies in the gender task, only the expression decoding data was cross classified.

Appendix H. Computational Modelling

Chapter 2:

Whilst the strong cross decoding results imply that they are not a result of low-level confounds in V1, further research using computational modelling was conducted within the laboratory (Maloret & Smith, 2017, Unpublished Raw Data). This aimed to investigate the extent to which expression recognition across the PF conditions relied on higher or lower level processes. A linear SVM was trained to learn the mapping between each image as a set of pixels and expression label, to test whether information within different pixels was able to discriminate emotions for each PF condition. One-sample t-tests show decoding in all PF conditions significantly above chance ($p < .05$). A repeated measures ANOVA was conducted to investigate PF condition on decoding accuracy, these basic decoding results demonstrate no significant main effect of PF condition (see Figure H-1). There were no significant differences between the PF conditions and WF condition in the standard model of V1, but significant differences between the PF conditions in the MVPA analysis (with better decoding in the ME and MM conditions than the WF condition).

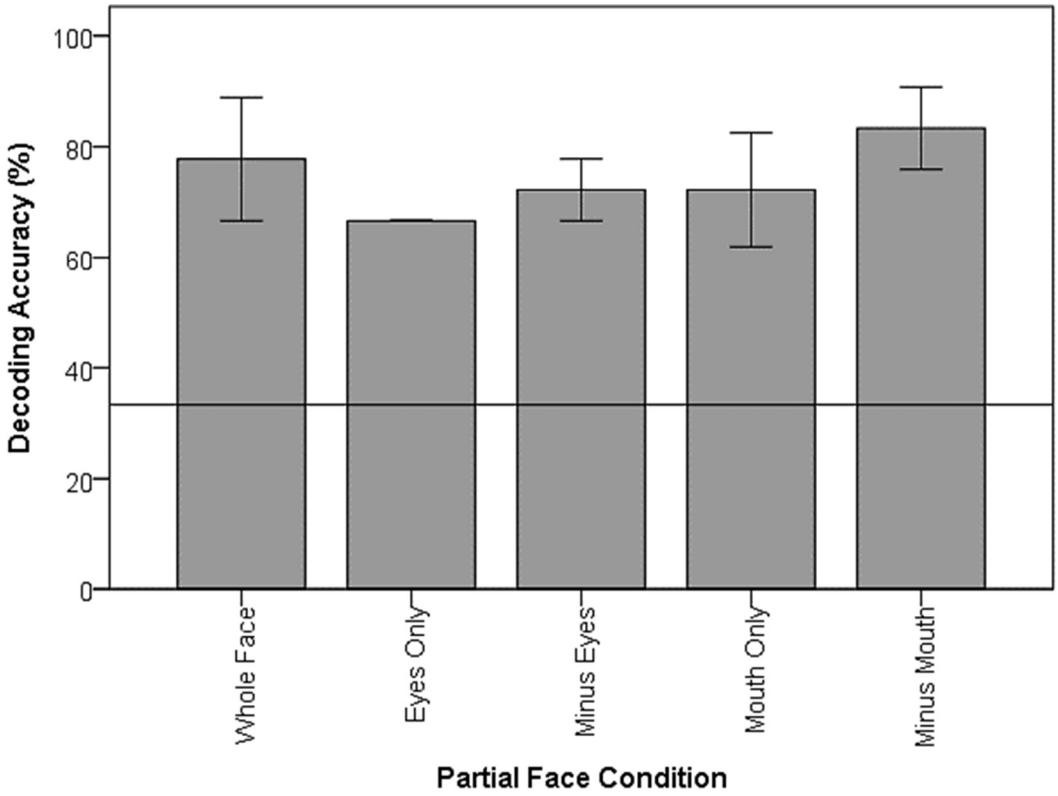

Figure H-1. Expression decoding accuracy from the computational pixel value model of the PF conditions for V1.

Cross-classification results reveal decoding accuracy at chance level for each condition pair of PF conditions, see Figure H-2. Thus significance observed in the MVPA analysis support the idea that decoding performance in this study may be driven by top-down feedback processes in V1.

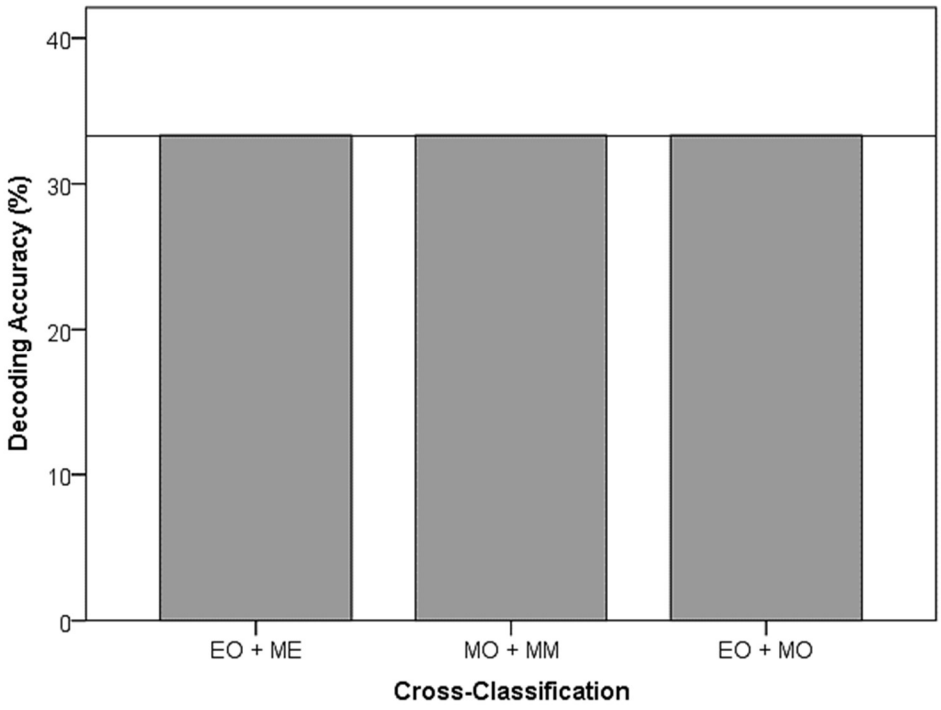

Figure H-2. Expression decoding accuracy from the computational pixel value model of the condition pairs of PF conditions for V1.

Appendix I. Correlates with Empathy

Chapter 3:

It is also important to consider interplay between expression recognition and individual differences, in particular ones level of empathy and ability to describe their own emotions. This is because high levels of empathy have been associated with an increase in ratings of emotional intensity (Allen-Walker & Beaton, 2015), as well as face detection, increased mimicry and ERP amplitudes among individuals (Balconi & Canavesio, 2016). It is thus suggested that greater levels of empathy will facilitate greater emotion recognition (Balconi & Canavesio, 2016).

One particular study found individuals with high empathy to recognise a change in facial expression, from a series of 100 images morphing into a new emotion, earlier than those with low empathy; thus they were better able to detect subtle expressions (Kosonogov, Titova, & Vorobyeva, 2015). Empathy was measured with The Empathy Quotient (EQ), results from this also tend to find males score lower than females, and a low score associated with Asperger's syndrome (AS) or high-functioning autism (HFA) (Baron-Cohen & Wheelwright, 2004). Whilst empathy has not been directly tested with partial face stimuli, an abundance of research has tested the effects of partial face recognition in the Autistic population; because of the association between the EQ and the Autism Quotient (AQ), these results can inform how occlusion and one's level of empathy affects recognition.

Results have found individuals with Autism to be significantly impaired at recognising expressions in the upper face (Gross, 2004), in particular complex expressions from the eyes only (Baron-Cohen, Wheelwright, Jolliffe, & Therese, 1997) and the recognition of fear and sadness (Tell, Davidson, & Camras, 2014). Moreover, literature occluding face parts has found Autistic populations to perform reliably better in recognising expressions from another's mouth (Spezio, Adolphs, Hurley, & Piven, 2007). Therefore those with low levels of empathy may have greater difficulty recognising partial eyes only stimuli. In addition, the personality trait, Alexithymia, has been shown to contribute to impaired emotion recognition (Bagby et al., 1994). With evidence that empathy is related to recognition, it was hypothesised that individuals higher in empathy (& lower in Alexithymia) will be more accurate at recognising expressions.

Materials.

The Empathy Quotient (EQ).

The 60-item Empathy quotient (EQ) (Baron-Cohen & Wheelwright, 2004) was used; this provides a self-reported measure of empathy in adults that is both high in test-retest reliability (r = .97) and internal consistency (Cronbach's a = .92). This questionnaire consists of 40 Likert scale questions designed to measure empathy and 20 control questions; participants select the most relevant response on a four point scale from 'strongly agree' to 'strongly disagree' (Baron-Cohen, 2004; Baron-Cohen & Wheelwright, 2004). Participant's responses to the empathy questions are scored out of 80, with each item scoring zero, one or two points. The test identifies variations in empathy among the general population and also provides a form of assessment into disorders associated with social impairment such as Autism. Accordingly participants with scores less than or equal to 30 points are classed low in empathy, and more likely to have Asperger Syndrome (AS) or high-functioning autism (HFA) than participants who score greater than 30 points.

In study one, the EQ score ranged from 15 to 60 points (M score = 39.07, SD = 13.3), with four participants (M age = 27, SD = 6.16; all male) categorised low in empathy (M score = 20.5, SD = 4.15) and 12 participants (age M = 24.75, SD = 2.77; 8 females, 4 males) categorised high in empathy (M score = 45.25, SD = 8.78). Whereas in study two, the EQ score ranged from 23 to 66 points (M score = 46.3, SD = 10.81), with only one participant (male, aged 28) classified as low in empathy, with a score of 23. A total of 19 participants (M age 23.58, SD = 4.25; 10 females, 9 males) were classified high in empathy (M score = 47.53, SD = 9.64).

Toronto Alexithymia Scale (TAS).

The Toronto Alexithymia Scale (TAS) (Bagby et al., 1994) was also used. This 20-item scale provides a measure of Alexithymia, a personality trait associated with difficulties identifying and describing one's own emotion, as well as subsequent difficulties in recognising others emotions and being empathetic (Bird & Cook, 2013; Jongen et al., 2014; Sifneos, 1973). This self-report measure is also high in both test-retest reliability (r = .77) and internal consistency (Cronbach's a = .81) (Bagby et al., 1994). Each item requires participants to select the most relevant response on a five point likert scale from 'I strongly disagree' to 'I strongly agree'; participants responses are scored out of 100, with each item scoring one to five points (Bagby et al., 1994). Accordingly participants with scores greater than

or equal to 61 were classed high in alexithymia, scores between 52-60 with possible-alexithymia and less than or equal to 51 as non-alexithymia (Bagby et al., 1994).

In study one, the TAS score ranged from 31 to 59 points (M score = 43.44, SD = 8.06), with no participants categorised as high alexithymia, three participants (M age = 26, *SD* = 1.73; one female, two males) categorised as having possible-alexithymia (M score = 57, *SD* = 1.41) and 13 participants (M age = 25.15, *SD* = 4.14; seven females, six males) with no alexithymia (M score = 40.31, *SD* = 5.22). The two questionnaires correlate significantly, $r(14) = -.719$, $p = .004$ (two-tailed). In study two, the TAS score ranged from 29 to 69 points (M score = 45.25, SD = 9.93), with one male participant (aged 28) placed in the high alexithymia group scoring 69 points, three participants (M age = 21.33, SD = 2.52; one female, two males) having possible-alexithymia (M score = 55.67, SD = 3.3) and 16 participants (M age = 24, SD = 4.43; 9 females, 7 males) with no alexithymia (M score = 41.81, SD = 7.34). Interestingly, the participant who scored highest in alexithymia was the same participant who scored lowest in empathy. Furthermore, there is a significantly strong correlation between these two measures, $r(20) = -.703$, $p = .001$ (two-tailed).

Empathy Results.

In study one, both the EQ $r(14) = -.004$, $p = .989$ (two-tailed), and the TAS $r(14) = .141$, $p = .630$ (two-tailed), showed no significant correlations with accuracy on the emotion task. Furthermore, both the EQ $r(14) = .180$, $p = .538$ (two-tailed), and the TAS $r(14) = -.133$, $p = .649$ (two-tailed), showed no significant correlations with accuracy on the gender task. In addition to this, in study two, both the EQ $r(20) = -.260$, $p = .268$ (two-tailed), and the TAS $r(20) = .116$, $p = .627$ (two-tailed), showed no significant correlations with accuracy on the emotion task. Lastly, in study two, both the $r(20) = -.245$, $p = .298$ (two-tailed), and the TAS $r(20) = -.023$, $p = .922$, showed no significant correlations with accuracy on the gender task.

Overall, in both studies no effects of empathy (from the EQ and alexithymia scale) on emotion recognition were revealed. These results were against expectations, individuals higher in empathy (& lower in Alexithymia) were not more accurate at recognising expressions. This is surprising given evidence that empathy is related to recognition (Allen-Walker & Beaton, 2015; Balconi & Canavesio, 2016; Kosonogov et al., 2015). These results may be a result of the small samples used in these two studies, and the subsequent distribution of scores (with only four

participants showing low in empathy in study one and only one participant showing low in empathy and high in alexithymia in study two). Ideally future research should gather a greater distribution of scores and also use the AQ. It would be interesting to see if the previous partial stimuli effects within the autistic population, including greater expression recognition ability with mouth only stimuli, and impairments in recognising expression, particularly fear and sadness, in eyes only or upper face stimuli, are replicated with this stimulus set (Baron-Cohen et al., 1997; Gross, 2004; Spezio et al., 2007; Tell et al., 2014).

Appendix J. Study 1: Artefact Correction Results

Chapter 3:

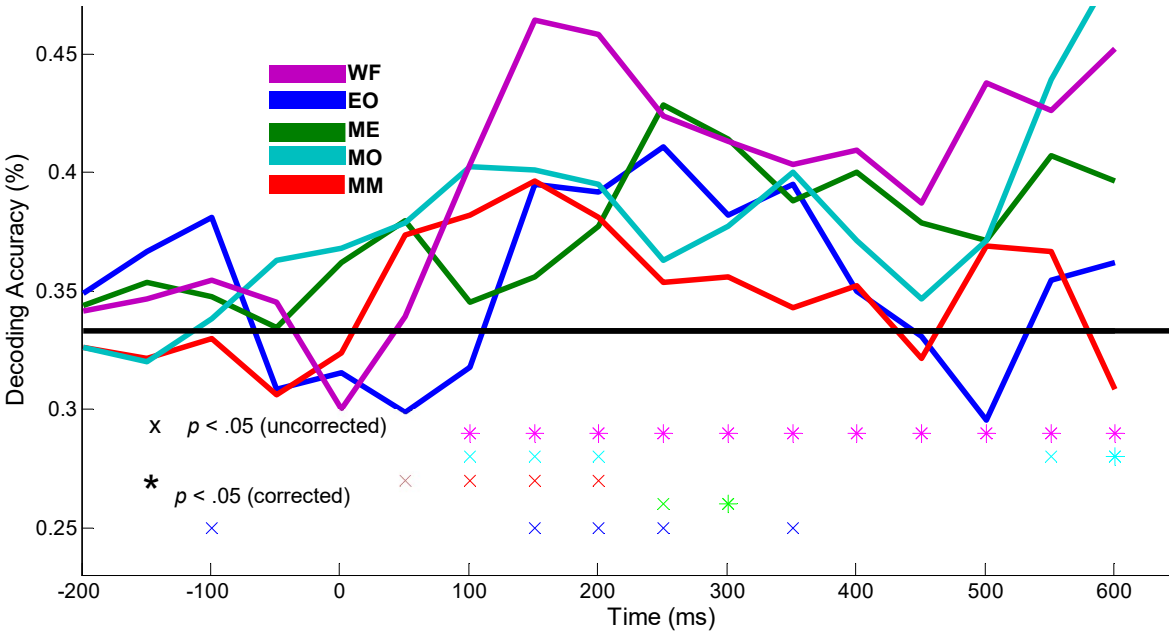

Figure J-1. Decoding Expression, Expression Task.

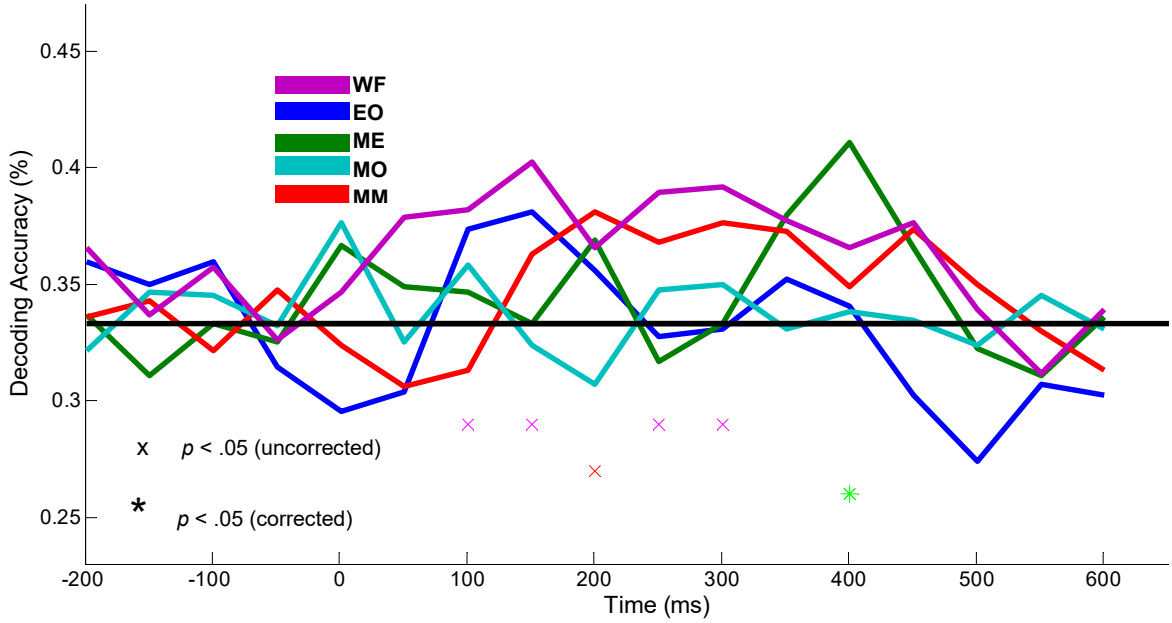

Figure J-2. Decoding Expression, Gender Task.

Appendix K. Study 1: Expression Analysis of Gender Data

Chapter 3:

An ANOVA (akin to the emotion task) exploring the effects of PF and emotion was conducted. There was a significant main effect of PF condition, $F(2.141, 27.831) = 24.396$, $p < .001$, $\eta_p^2 = .652$ (greenhouse-geisser corrected) and emotion on accuracy, $F(2, 26) = 5.440$, $p = .011$, $\eta_p^2 = .295$, whereby gender was better recognised when happiness was shown (M = 95.99%), than disgust (M = 94.56%) or fear (M = 94.25%) (Figure K-1). Furthermore there was a significant interaction between PF and emotion, $F(3.517, 45.721) = 2.966$, $p = .035$, $\eta_p^2 = .186$ (greenhouse-geisser corrected).

Again a simple effects analysis was undertaken: EO and MM were the only significant ANOVAs testing the effect of emotion ($p < .05$) where happiness was the most accurately recognised expression in these PF conditions. All three ANOVAs testing the effect of PF condition for each emotion were significant ($p < .05$), with gender most accurately recognised when shown WF stimuli and least accurately recognised when shown EO stimuli. Additional post-hoc tests were carried out, see Figure K-2. These tests revealed differences in the EO condition between disgust and happiness as well as fear and happiness (p's = .037); showing that gender could be recognised better when happiness was shown (see Figure K-1). There were no significant post-hoc tests in the MM condition.

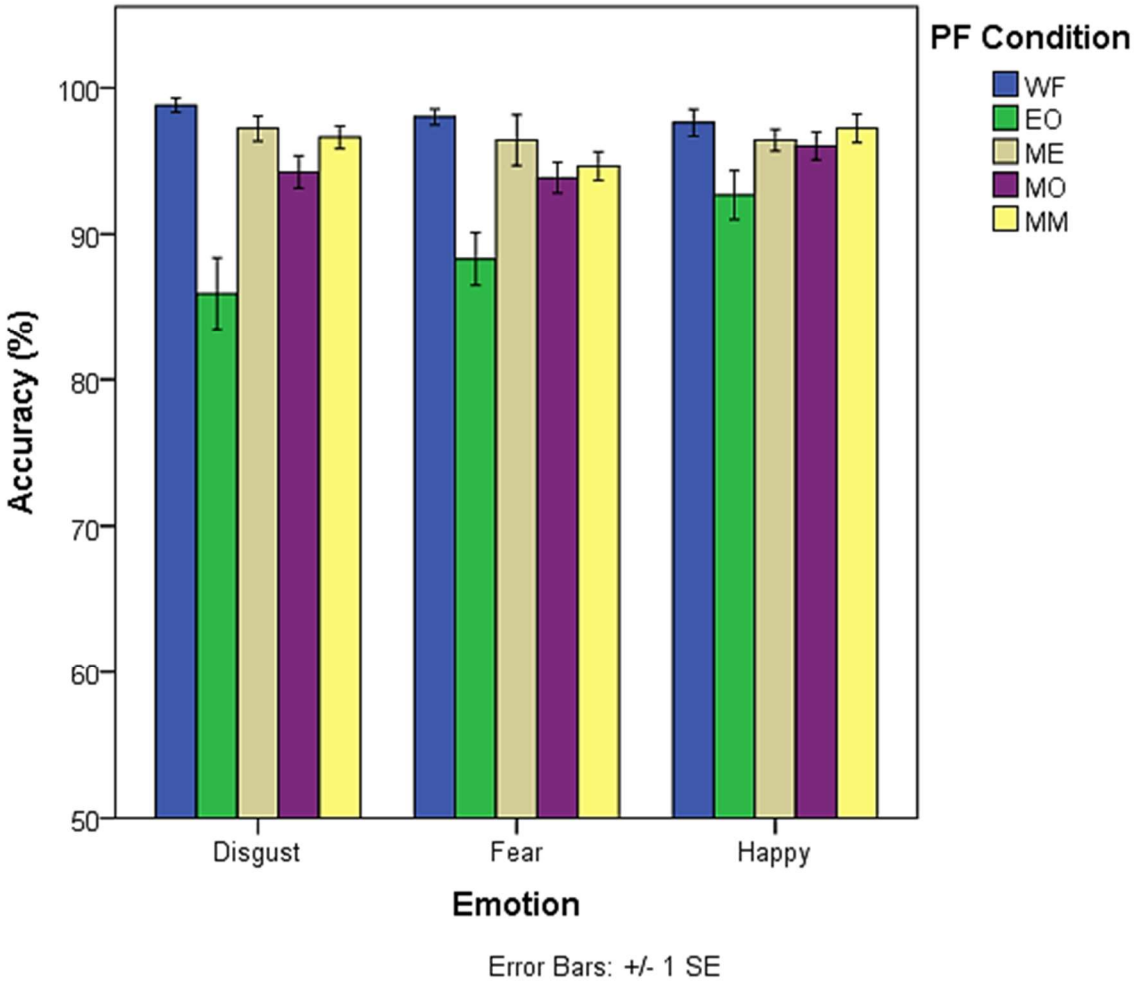

Figure K-1. Overall recognition accuracy (%) in each PF condition for each emotion.

A. Disgust

	Whole Face	Eyes Only	Minus Eyes	Mouth Only	Minus Mouth
Whole Face					
Eyes Only					
Minus Eyes					
Mouth Only					
Minus Mouth					

B. Fear

	Whole Face	Eyes Only	Minus Eyes	Mouth Only	Minus Mouth
Whole Face					
Eyes Only					
Minus Eyes					
Mouth Only					
Minus Mouth					

C. Happy

	Whole Face	Eyes Only	Minus Eyes	Mouth Only	Minus Mouth
Whole Face					
Eyes Only					
Minus Eyes					
Mouth Only					
Minus Mouth					

$p < .05$ corrected (bonferroni)
$p < .05$ uncorrected
$p > .05$

Figure K-2. Paired sample t-test results comparing the differences between the PF conditions for each emotion.

Overall, in disgust, fear and happiness there were differences between the EO and other PF conditions, where performance was worse in the EO condition (Figure K-1 & K-2). Even for gender recognition, results support the importance of the nose and mouth when participants are shown a disgust expression, and the importance of the mouth when participants are shown a happy expression, however, the importance of the eyes when shown fear was less pronounced in gender recognition (F. W. Smith & Schyns, 2009; M. L. Smith et al., 2005).

Appendix L. Study 1: Reaction Time Data

Chapter 3:

Emotion RT.

A two-way repeated measures ANOVA was employed to explore the effects of PF condition and emotion on RT in the expression task. There was a significant main effect of PF condition, $F(2.217, 28.816) = 15.521$, $p < .001$, $\eta_p^2 = .544$ (greenhouse-geisser corrected) and emotion on RT, $F(2, 26) = 52.721$, $p < .001$, $\eta_p^2 = .802$, whereby happiness was recognised quickest (M = 719.77ms) followed by disgust (M = 813.58ms) and fear (M = 854.65ms) (Figure L-1). Furthermore there was a significant interaction between PF and emotion, $F(3.646, 47.404) = 11.284$, $p < .001$, $\eta_p^2 = .465$ (greenhouse-geisser corrected).

Again a simple effects analysis was undertaken, all five ANOVAs testing the effect of emotion at each PF condition were significant ($p < .05$, with happiness fastest RT, disgust slowest when eyes present, fear slowest when mouth information present), as well as all three of those testing the effect of PF condition on disgust and happiness at $p < .001$ as the EO and MM conditions had slower RTs (fear was not significant at $p = .165$). Additional post-hoc tests were carried out, see Figures L-2 and L-3.

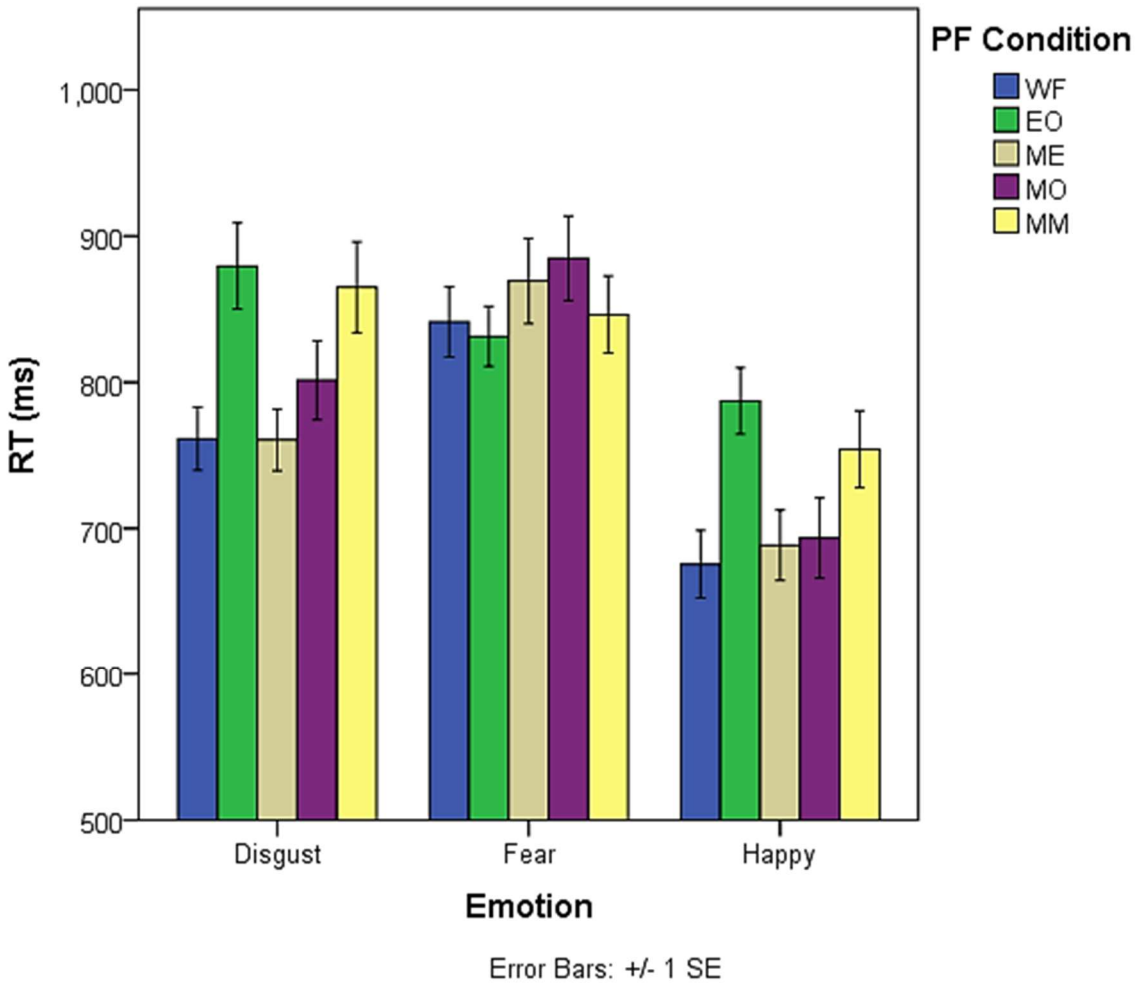

Figure L-1. Overall RT (ms) in each PF condition for each emotion.

Overall, participants showed greater RT differences between all the emotions when there was mouth information present (Figure L-2). In disgust there were no significant differences between EO and MM, as well as WF and ME, respectively reflecting the slowest and quickest RTs, whereas in happiness, significance between the EO and MM to the other PF conditions reflect the slowest RTs in happiness (Figure L-3 & L-1). These results correspond to the accuracy results, with high accuracy associated with faster RTs, and low accuracy with slower RTs. Again, this supports the importance of the nose and mouth in disgust and the mouth in happiness recognition (F. W. Smith & Schyns, 2009; M. L. Smith et al., 2005).

A. WF

	Disgust	Fear	Happy
Disgust			
Fear			
Happy			

D. MO

	Disgust	Fear	Happy
Disgust			
Fear			
Happy			

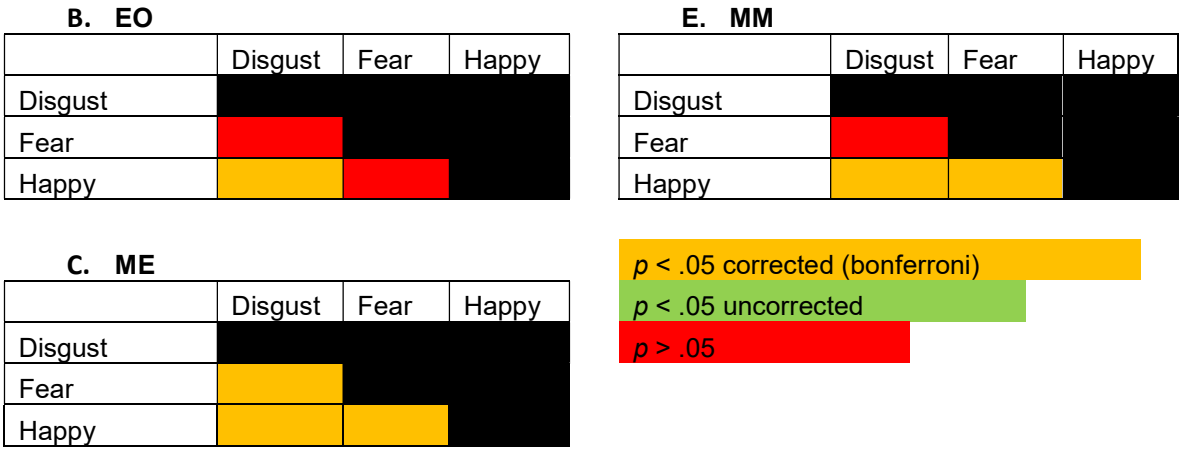

Figure L-2. Paired sample t-test results comparing the differences between the emotions for each PF condition.

Figure L-3. Paired sample t-test results comparing the differences between the PF conditions for each emotion.

Gender RT.

A two-way repeated measures ANOVA was employed to explore the effects of PF condition and gender on RT (Figure L-4). There was no significant main effect of gender $F(1, 13) = 1.132$, $p = .307$, $\eta_p^2 = .080$, but a significant main effect of PF, $F(2.395, 31.140) = 28.220$, $p < .001$, $\eta_p^2 = .685$ (greenhouse-geisser corrected), as

well as a significant interaction, $F(1.898, 24.677) = 3.489$, $p = .048$, $\eta_p^2 = 212$ (greenhouse-geisser corrected).

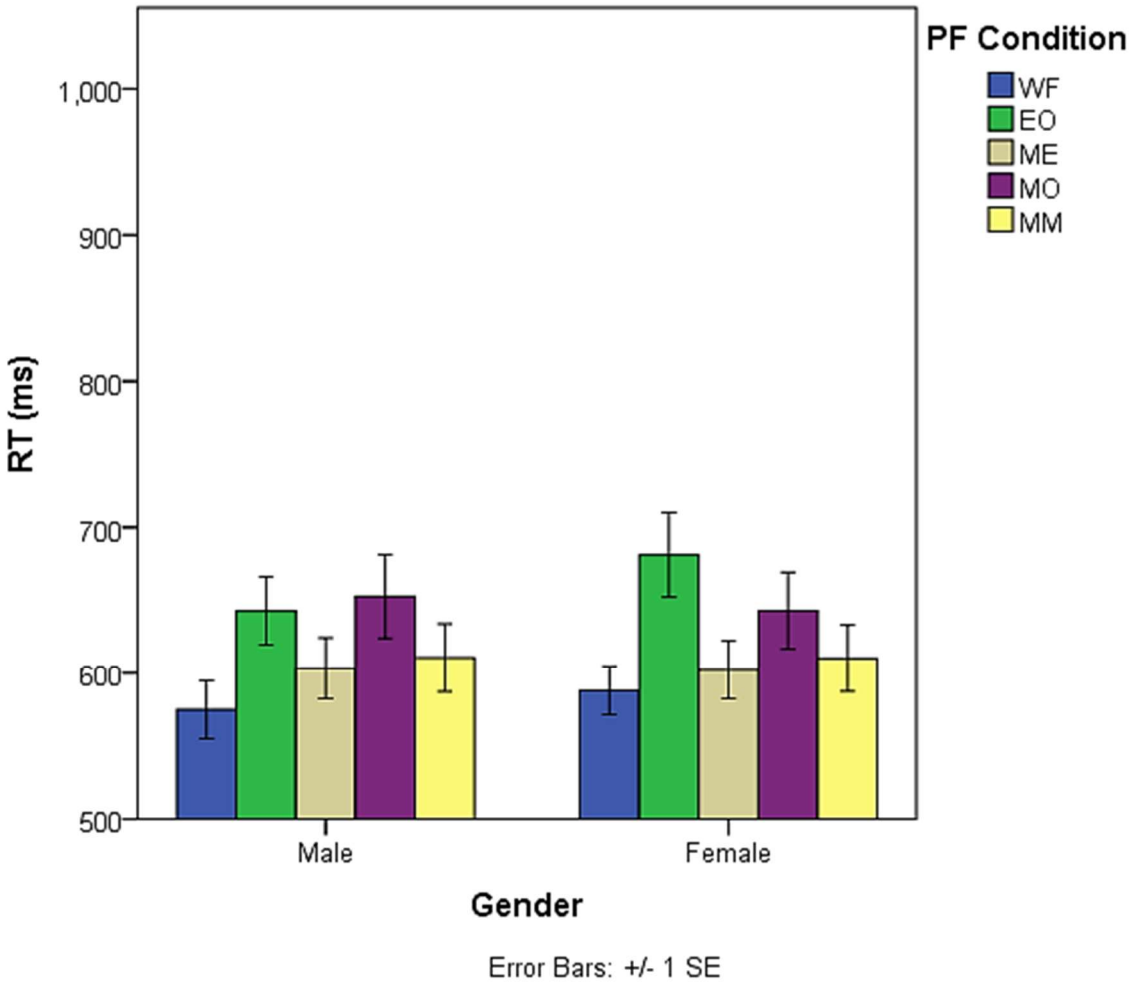

Figure L-4. Overall RT (ms) in each PF condition between male and female stimuli.

As a result of the significant interaction, a simple effects analysis was undertaken. ANOVAs testing the effect of gender at each PF condition only found significance in the EO condition ($p = .032$). Testing the effect of PF condition on gender found significance for both male and female faces ($p < .001$). The significant differences seen in the male faces between the WF and PF conditions, show WF male stimuli to be recognised quicker (see also Figure L-5). Nonetheless, reaction times for male faces are similar across all PF conditions. However, the differences seen in the female faces between the EO and other PF conditions show EO female stimuli to be recognised slower. It is unclear why it this is. Again, these results

correspond to the accuracy results, with high accuracy associated with faster RTs, and low accuracy with slower RTs.

A. Male

	Whole Face	Eyes Only	Minus Eyes	Mouth Only	Minus Mouth
Whole Face					
Eyes Only					
Minus Eyes					
Mouth Only					
Minus Mouth					

B. Female

	Whole Face	Eyes Only	Minus Eyes	Mouth Only	Minus Mouth
Whole Face					
Eyes Only					
Minus Eyes	p = .058				
Mouth Only					
Minus Mouth					

p < .05 corrected (bonferroni)
p < .05 uncorrected
p > .05

Figure L-5. Paired sample t-test results comparing the differences between the PF conditions for male and female faces.

An ANOVA (akin to the emotion task) exploring the effect of PF condition and emotion was conducted (Figure L-6). There was a significant main effect of PF condition, $F(2.448, 31.827) = 26.903$, $p < .001$, $\eta_p^2 = .674$ (greenhouse-geisser corrected) but no significant main effect of emotion on RT, $F(2, 26) = 1.891$, $p = .171$, $\eta_p^2 = .127$ or significant interaction, $F(3.808, 49.502) = .627$, $p = .638$, $\eta_p^2 = .046$ (greenhouse-geisser corrected).

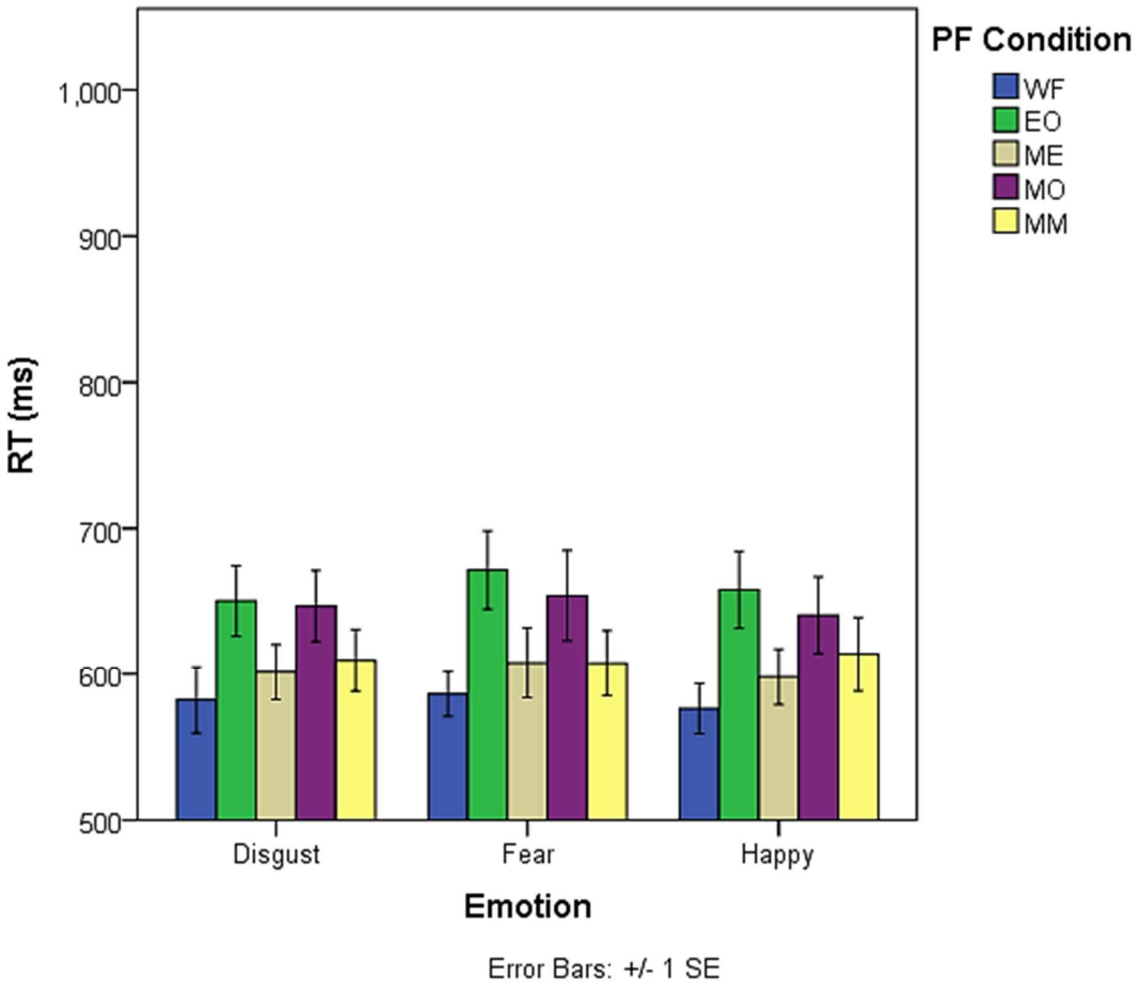

Figure L-6. Overall RT (ms) in each PF condition for each emotion.

Appendix M. Study 2: Expression Analysis of Gender Data

Chapter 3:

A two-way repeated measures ANOVA was also employed to explore the effects of PF condition and emotion on accuracy in the gender task. There was a significant main effect of PF condition, $F(2, 76) = 11.233$, $p < .001$, $\eta_p^2 = .372$ and emotion on accuracy, $F(1, 19) = 8.305$, $p = .010$, $\eta_p^2 = .304$, whereby gender was better recognised when happiness (M = 88.39%), rather than fear was shown (M = 86.80%) (Figure M-1). There was no significant interaction between PF and emotion on accuracy, $F(2, 76) = 1.979$, $p = .106$, $\eta_p^2 = .094$.

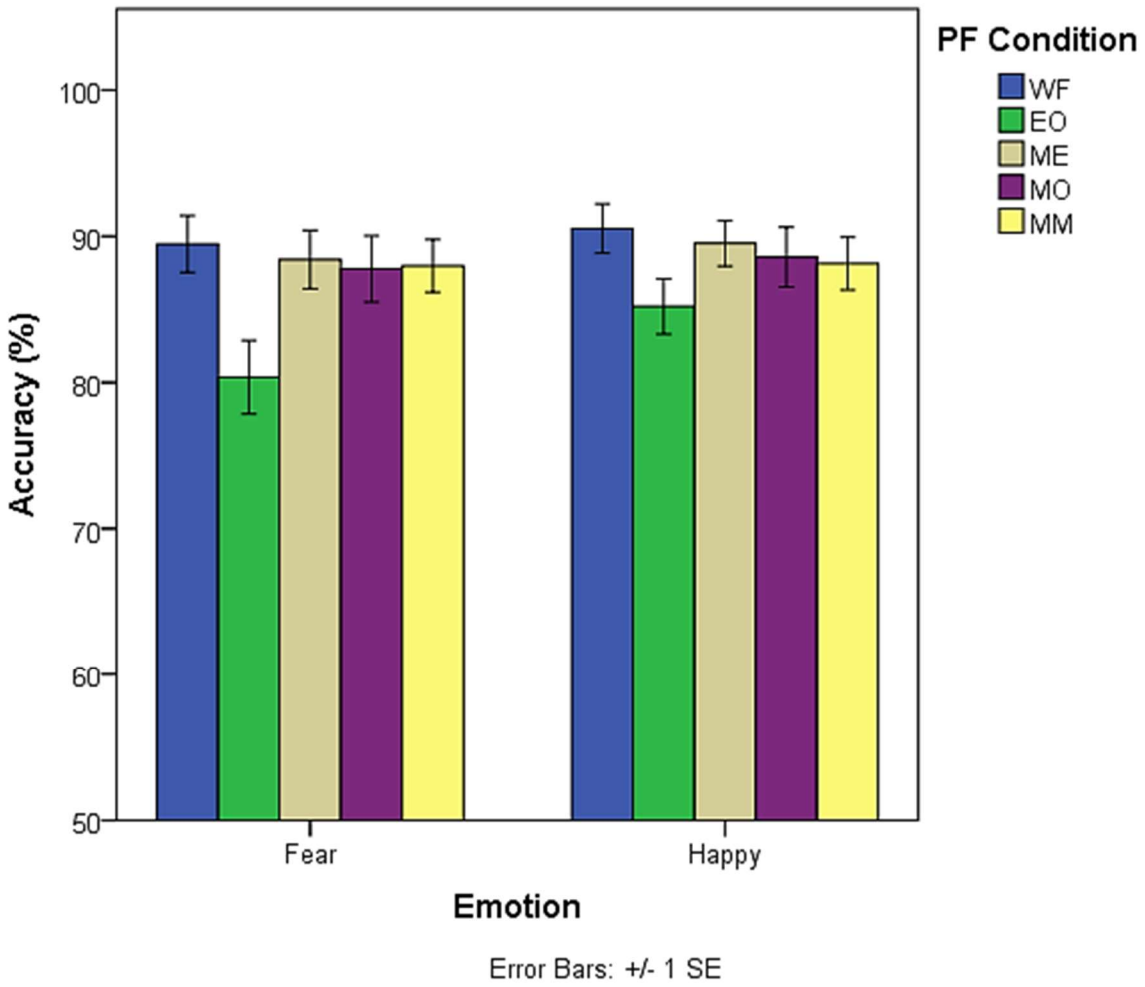

Figure M-1. Overall recognition accuracy (%) in each PF condition between the emotions.

Appendix N. Study 2: Reaction Time Data

Chapter 3:

Emotion RT.

A two-way repeated measures ANOVA was employed to explore the effects of PF condition and emotion on RT in the expression task. There was a significant main effect of PF condition, $F(2.701, 51.328) = 46.718$, $p < .001$, $\eta_p^2 = .711$ (greenhouse-geisser corrected), and emotion on RT, $F(1, 19) = 6.370$, $p = .021$, $\eta_p^2 = .251$ with RT faster for happiness (M = 755.66ms) than fear (M = 775.96ms) (Figure N-1). Furthermore there was a significant interaction between PF and emotion, $F(4, 76) = 4.697$, $p = .002$, $\eta_p^2 = .198$, showing the importance of different face regions in this task.

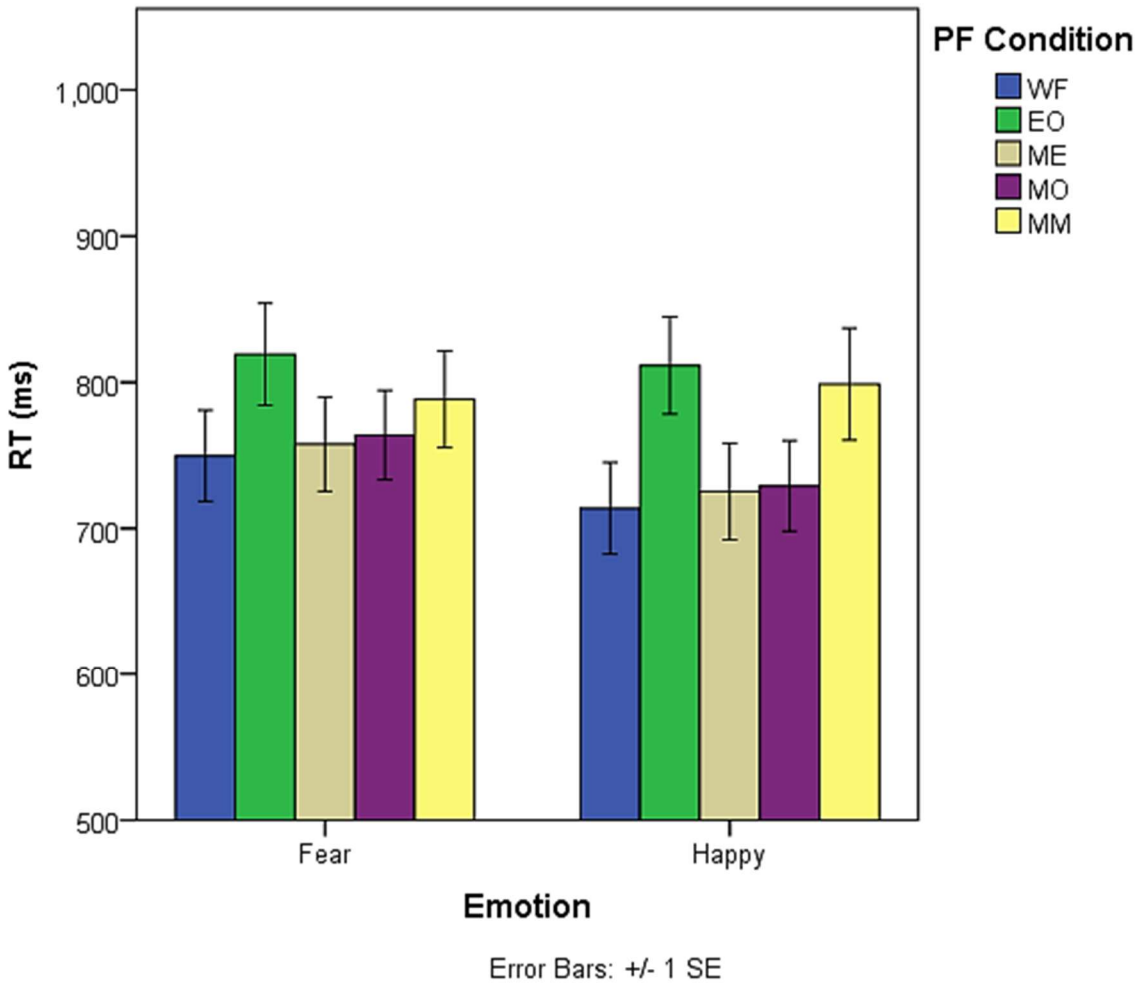

Figure N-1. Overall RT (ms) in each PF condition for each emotion.

Again a simple effects analysis was undertaken. ANOVAs testing the effect of emotion found significance in WF, ME and MO ($p < .05$), with quicker RTs for happiness than fear in all three conditions. Testing the effect of PF condition on emotion found significance for both fear and happy ($p < .001$). Further post-hoc tests were carried out (see Figure N-2). In fear and happiness there are more differences between the EO and MM conditions in relation to all other conditions (Figure N-2), this is because RTs are longer in these conditions (Figure N-1). This is against the importance of the eyes in fear but corroborates the importance of the mouth in happiness; it could be that the mouth is important for fear when only two emotions are investigated (Neath-Tavares & Itier, 2016).

A. Fear

Figure N-2. Paired sample t-test results comparing the differences between the PF conditions for each emotion.

Gender RT.

A two-way repeated measures ANOVA was employed to explore the effects of PF condition and gender on RT in the gender task (Figure N-3). There was a significant main effect of PF condition, $F(2.086, 39.641) = 27.828$, $p < .001$, $\eta_p^2 = .594$ (greenhouse-geisser corrected) but no significant main effect of gender on RT, $F(1, 19) = .222$, $p = .643$, $\eta_p^2 = .012$. There was no significant interaction between PF and gender, $F(2.106, 40.012) = 2.599$, $p = .084$, $\eta_p^2 = .120$ (greenhouse-geisser corrected).

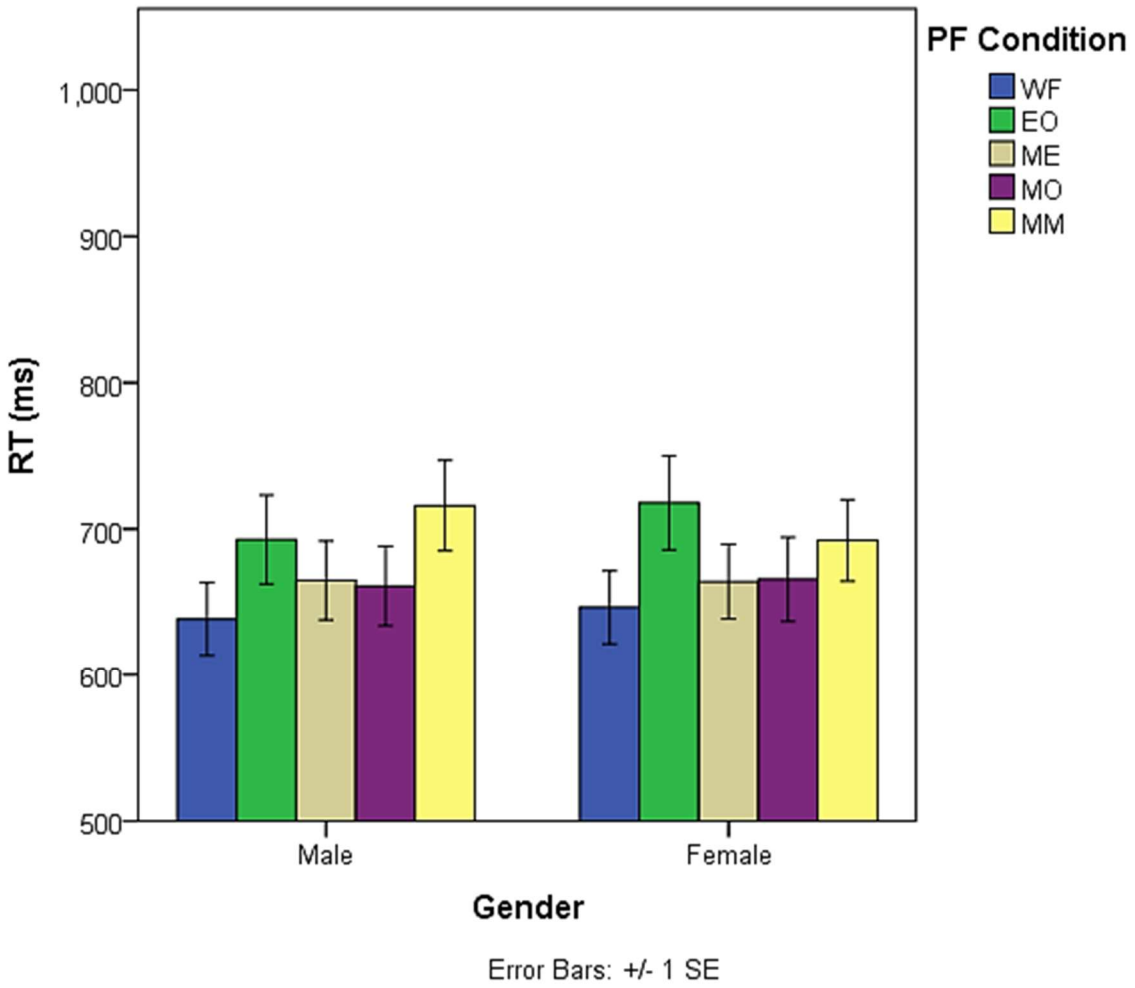

Figure N-3. Overall RT (ms) in each PF condition for each gender.

A two-way repeated measures ANOVA was also employed to explore the effects of PF condition and emotion on RT. In the gender task, there was a significant main effect of PF condition, $F(2.033, 38.626) = 26.465$, $p < .001$, $\eta_p^2 = .582$ (greenhouse-geisser corrected), and emotion on RT, $F(1, 19) = 9.526$, $p = .006$, $\eta_p^2 = 334$, with RT faster for happiness (M = 670.84ms) than fear (M = 680.36ms) (Figure N-4). There was no significant interaction between PF and emotion, $F(4, 76) = .596$, $p = .666$, $\eta_p^2 = .030$.

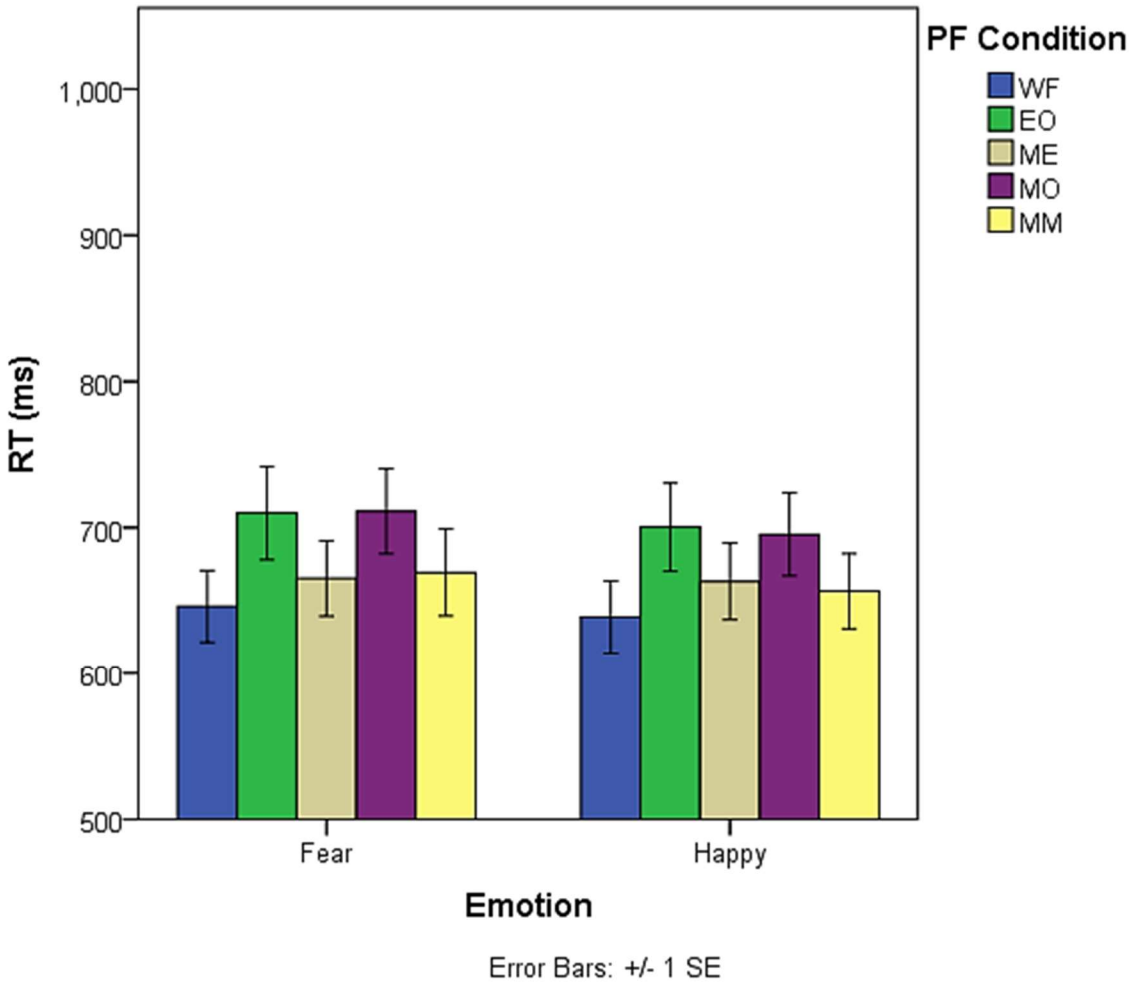

Figure N-4. Overall RT (ms) in each PF condition for each emotion.

Appendix O. Decoding Results for 9mm Radius Spheres

Chapter 4:

Decoding within Perception and Production.

Results for decoding of expression in the perception task are presented first, followed by decoding in the production task. ROI results are given for each hemisphere in turn (right then left), before the result of the combined bilateral ROI is given. The bars on the graph are either displayed in blue or grey: blue bars represent premotor regions of the brain, whereas grey bars represent either the face network or sensorimotor regions of the brain, depending on whether the results are from the perception or production task respectively. Furthermore, the result graph axis begins at 30% in both tasks; however, please note that this scale is set to 40% in the perception task and 80% in the production task, to account for variability in decoding accuracy between the tasks. This 30-40% scaling in the perception task was deemed necessary to clearly portray the differences in accuracy among the ROI's (this difference in scaling is used throughout the decoding results).

Although there were no significant FDR effects in the perception task, one-sample t-tests showed decoding trends in the r-PM1 ($t(12) = 1.837$, $p = .046$, $d = 0.51$ (medium effect-size)), PM1 ($t(12) = 3.021$, $p = .005$, $d = 0.84$ (large effect-size)), FG ($t(8) = 2.706$, $p = .013$, $d = 0.90$ (large effect-size)) and EVC ($t(12) = 2.208$, $p = .024$, $d = 0.61$ (medium effect-size)) ROIs, see Figure O-1.

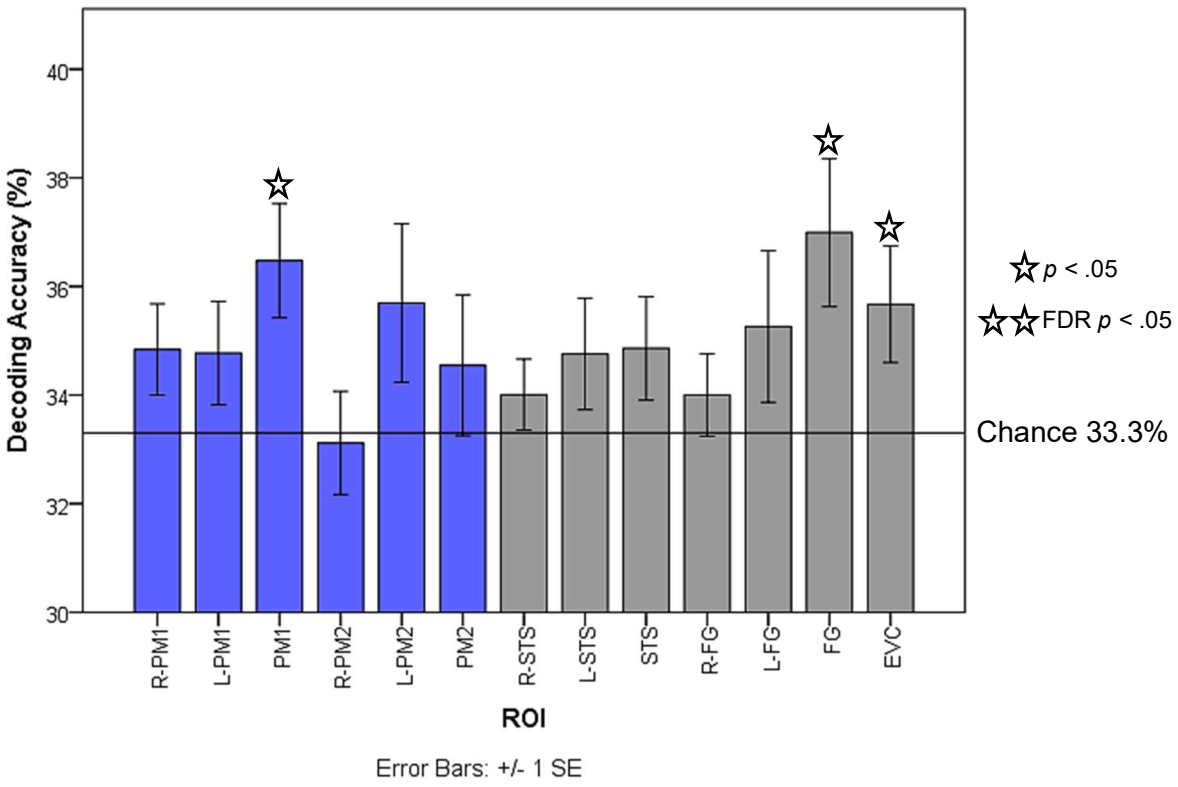

Figure O-1. Expression decoding accuracy of 9mm radius spheres in the perception task, one-sample t-test results represented with stars. Blue bars represent premotor regions of the brain; grey bars represent the face network of brain regions.

One-sample t-tests showed significant decoding in all ROIs (FDR $p < .05$; large effect sizes, *d's > 1.6*) for the production task, see Figure O-2.

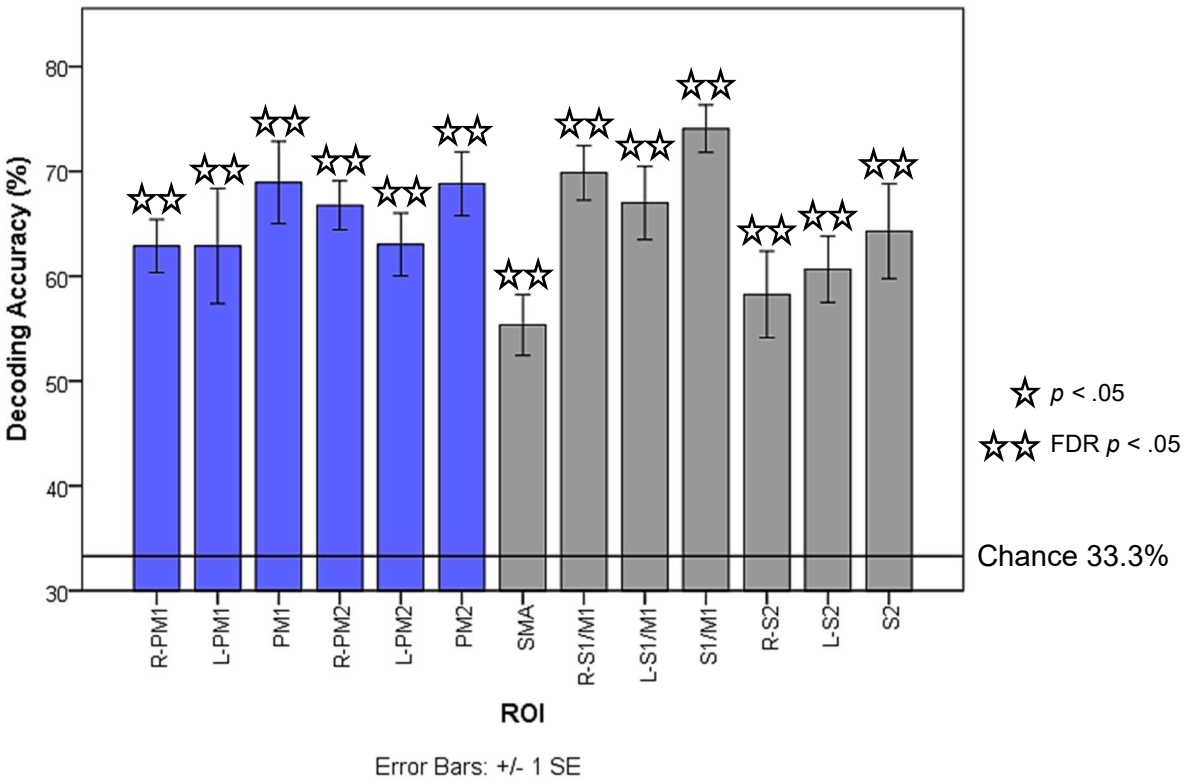

Figure O-2. Expression decoding accuracy of 9mm radius spheres in the production task, one-sample t-test results represented with stars. Blue bars represent premotor regions of the brain; grey bars represent sensorimotor regions of the brain.

Cross classification.

The cross-classification results, based on ROIs defined in the perception task, are presented first; followed by cross classification results based on ROIs defined in the production task.

Although there were no significant FDR effects in cross-decoding based on the perceptual ROIs, one-sample t-tests showed decoding trends in the l-PM1 ($t(12) = 2.491$, $p = .014$, $d = 0.69$ (medium effect-size)), PM1 ($t(12) = 2.095$, $p = .029$, $d = 0.58$ (medium effect-size)), l-PM2 ($t(11) = 2.271$, $p = .022$, $d = 0.66$ (medium effect-size)) and STS ($t(11) = 1.816$, $p = .048$, $d = 0.52$ (medium effect-size)) ROIs, see Figure O-3.

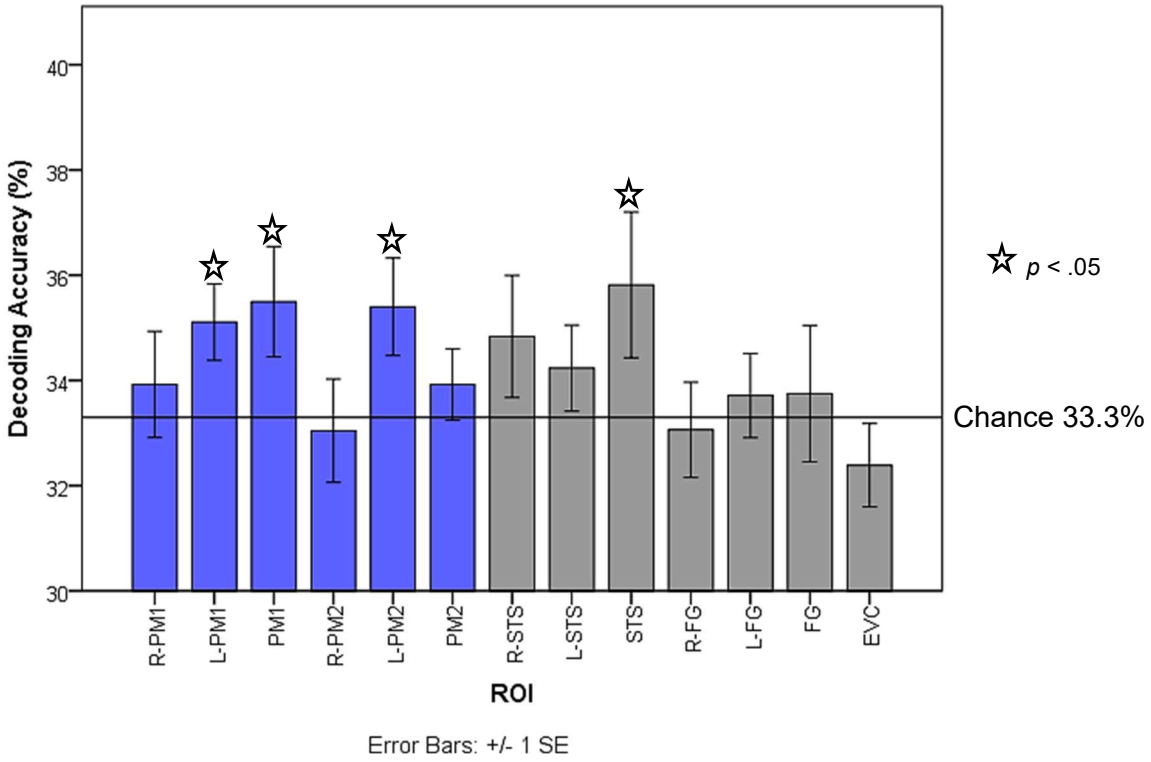

Figure O-3. Cross-classification: expression decoding accuracy of 9mm radius spheres defined in the perception task, one-sample t-test results represented with stars. Blue bars represent premotor regions of the brain; grey bars represent the face network of brain regions.

Although there were no significant FDR effects in cross-decoding based on the production ROIs, one-sample t-tests showed decoding trends in PM1, $t(10) = 1.876$, $p = .045$, $d = 0.57$ (medium effect-size) see Figure O-4.

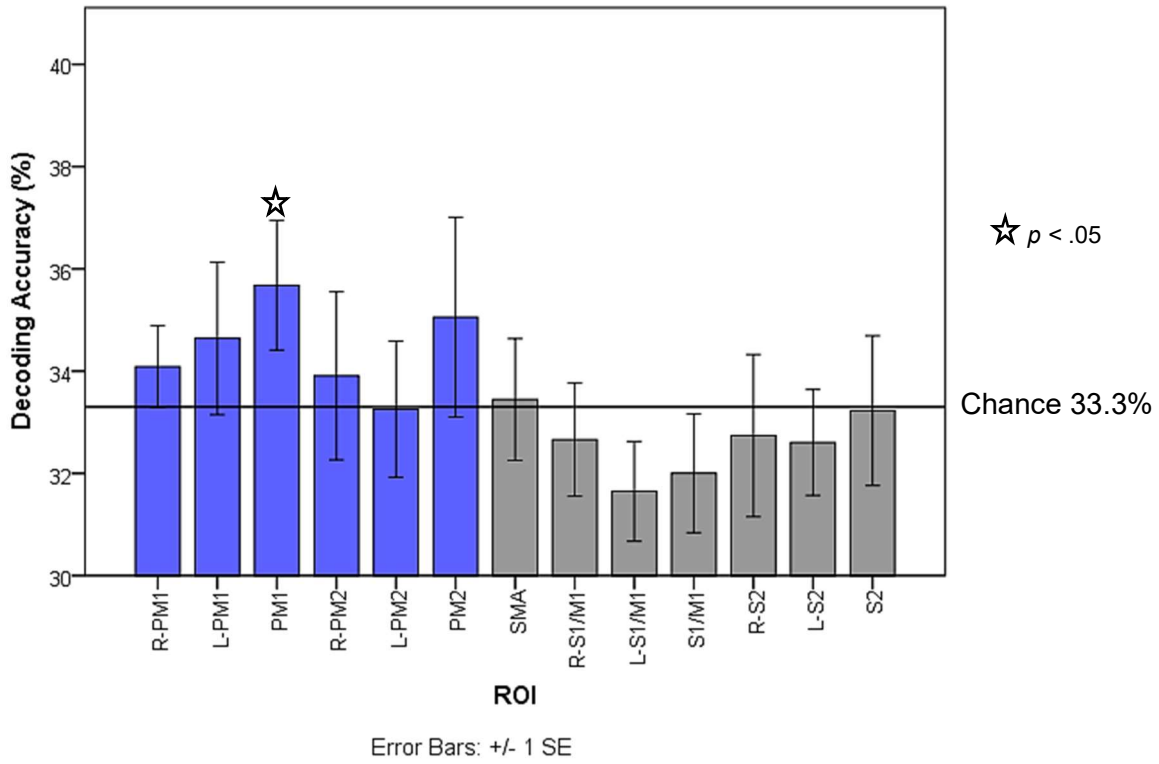

Figure O-4. Cross-classification: expression decoding accuracy of 9mm radius spheres defined in the production task, one-sample t-test results represented with stars. Blue bars represent premotor regions of the brain; grey bars represent sensorimotor regions of the brain.

Appendix P. Consistency between ROIs from single subjects and group level analysis.

Perception (ROI probability map with RFX emotion vs phase noise)

Chapter 4:

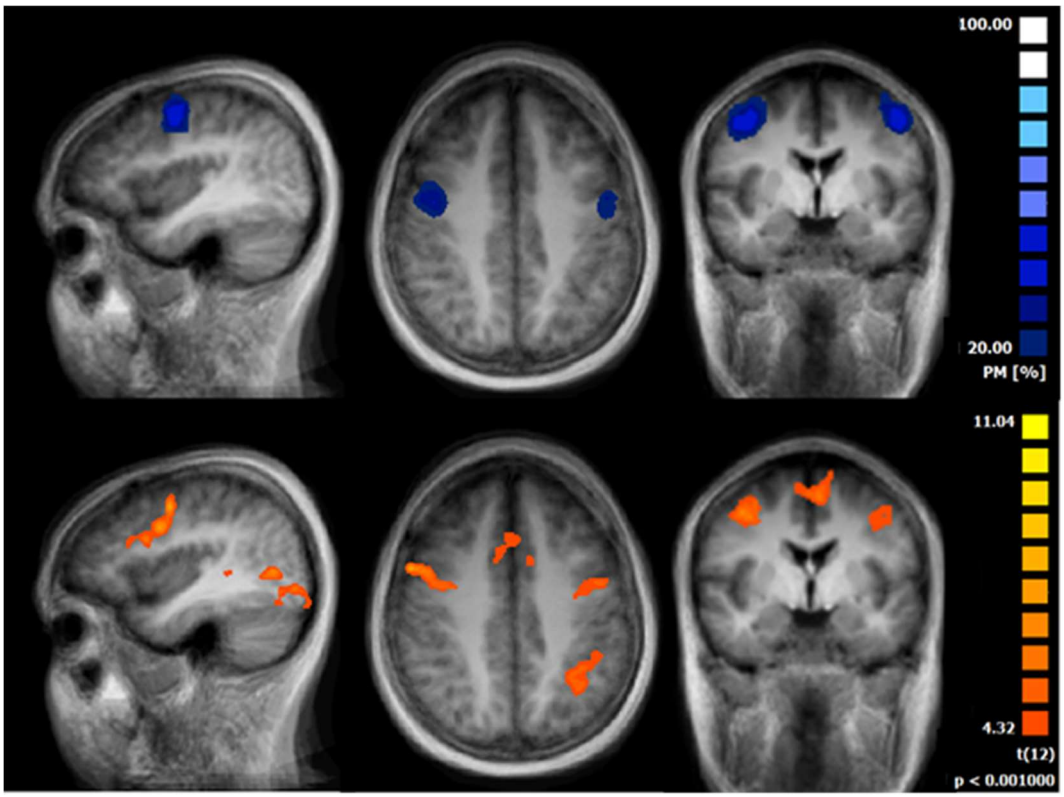

Figure P-1. PM1: probability map (displayed in blue), RFX analysis (in orange).

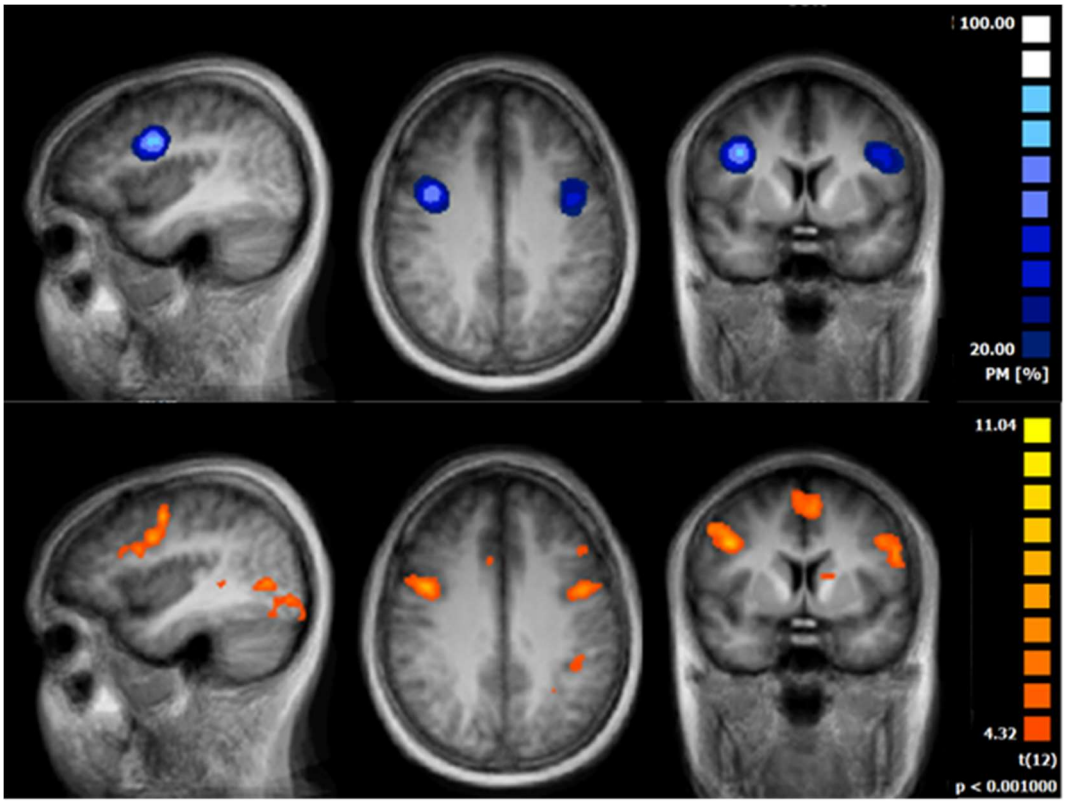

Figure P-2. PM2: probability map (displayed in blue), RFX analysis (in orange).

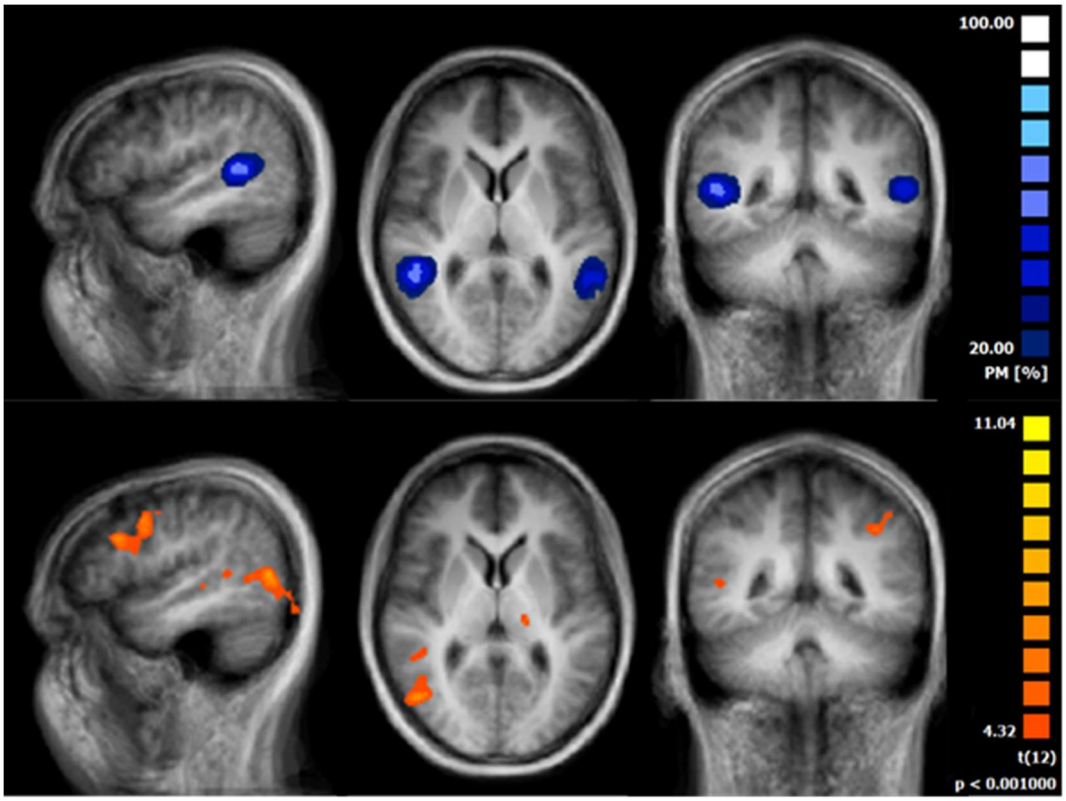

Figure P-3. STS: probability map (displayed in blue), RFX analysis (in orange).

Production (ROI probability map ROI with RFX face movement vs finger movement)

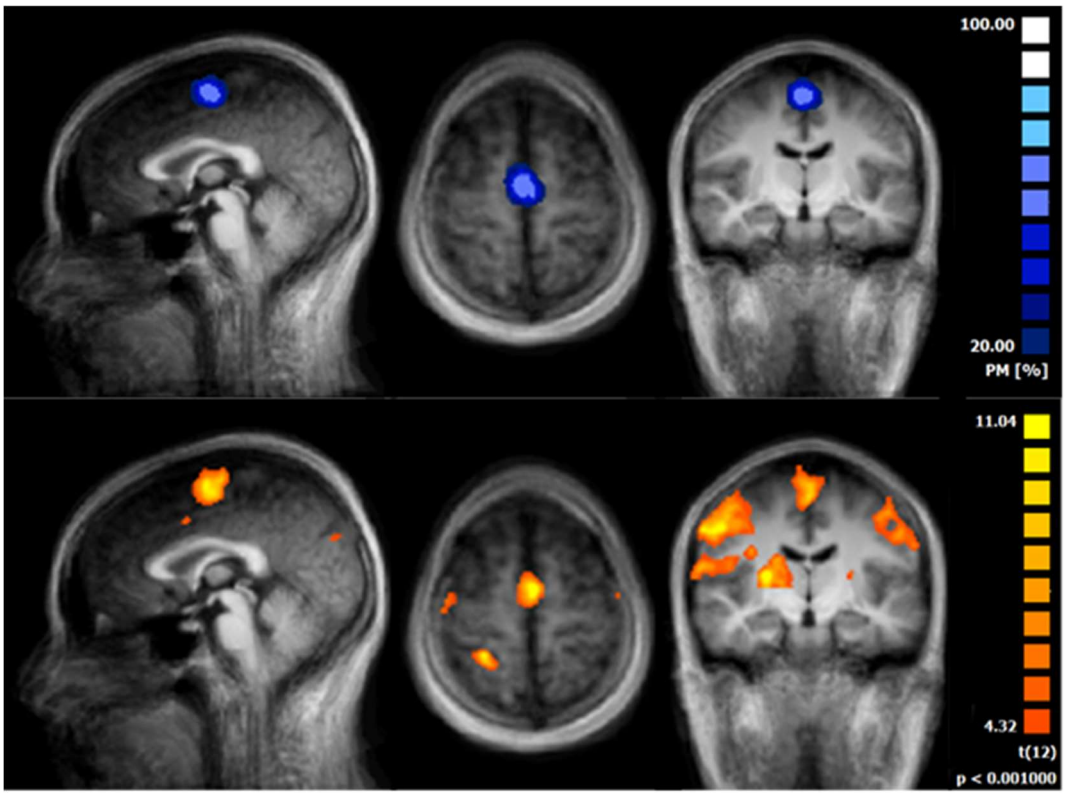

Figure P-4. SMA: probability map (displayed in blue), RFX analysis (in orange).

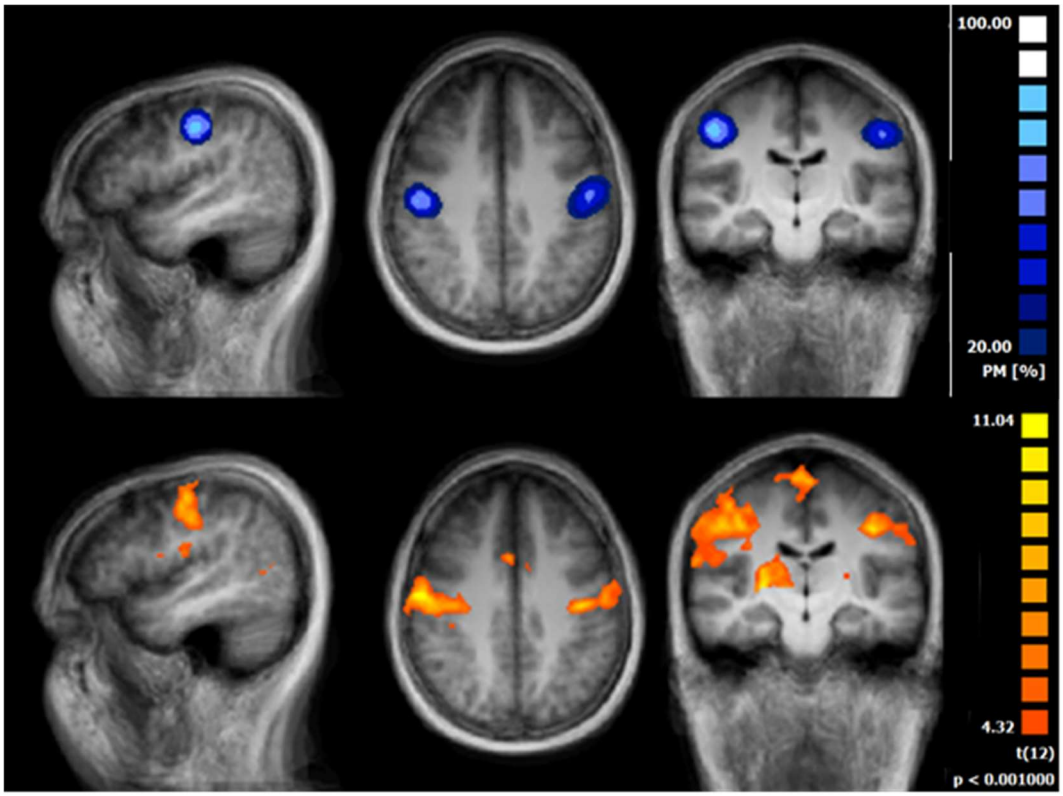

Figure P-5. S1/M1: probability map (displayed in blue), RFX analysis (in orange).

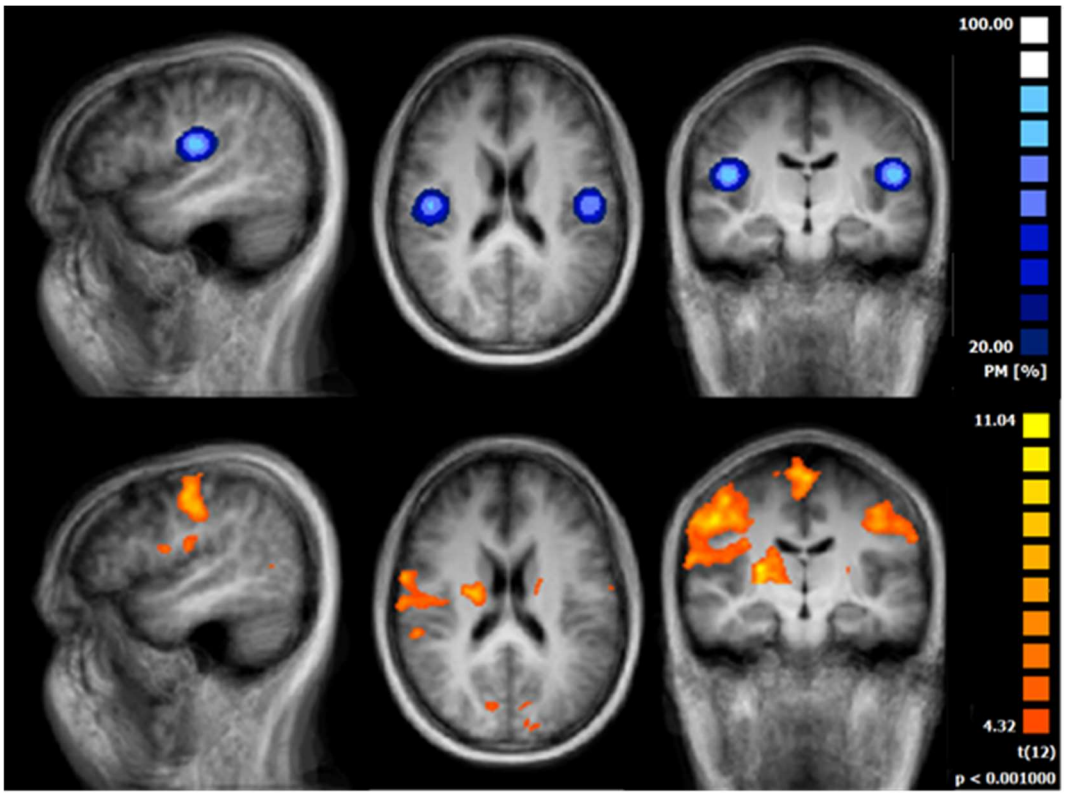

Figure P-6. S2: probability map (displayed in blue), RFX analysis (in orange).

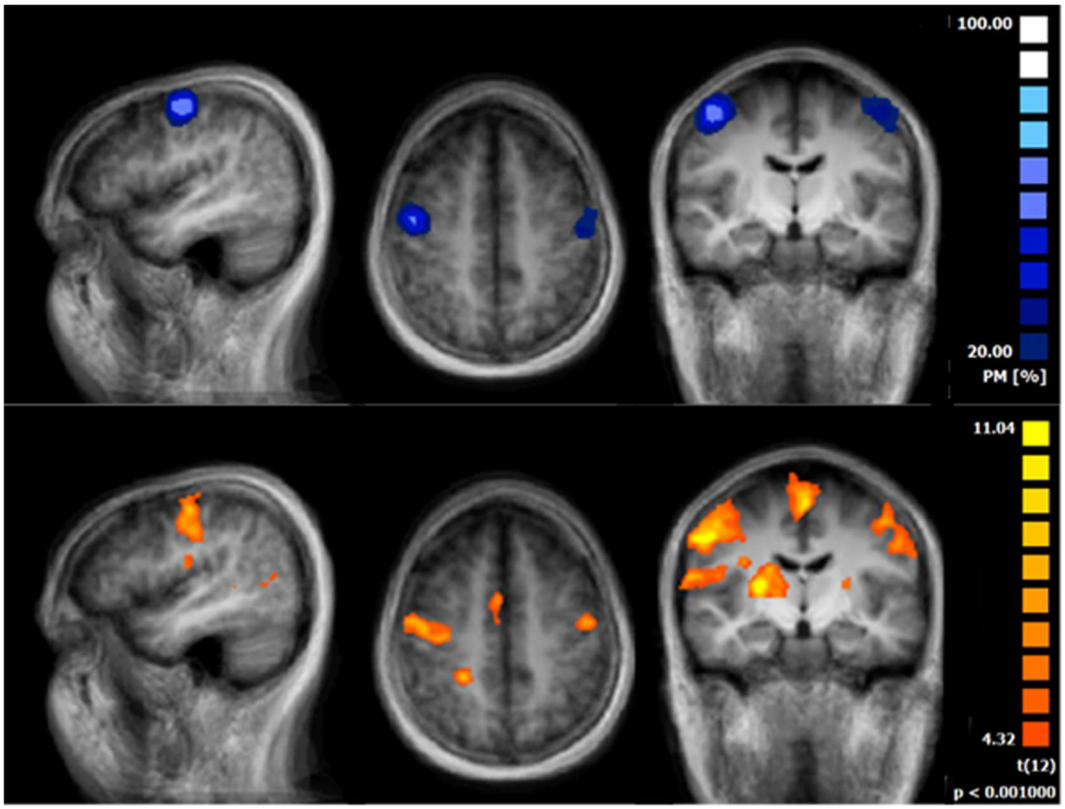

Figure P-7. PM1: probability map (displayed in blue), RFX analysis (in orange).

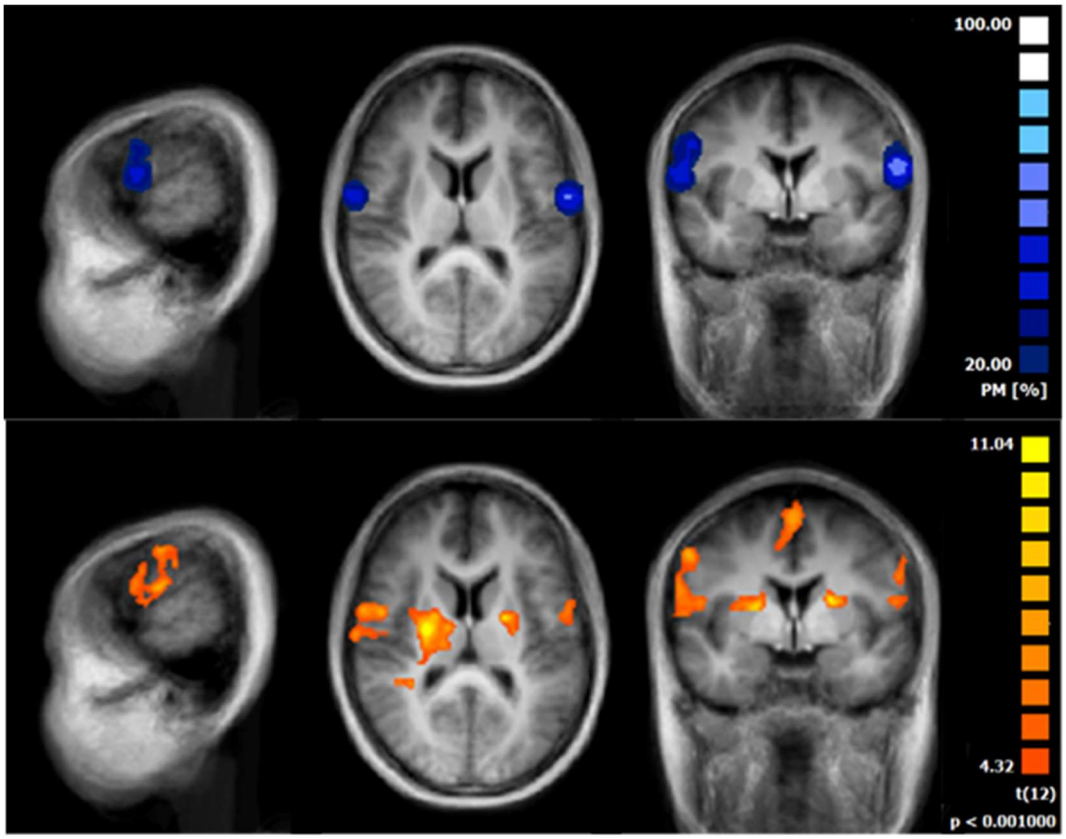

Figure P-8. r-PM2: probability map (displayed in blue), RFX analysis (in orange).

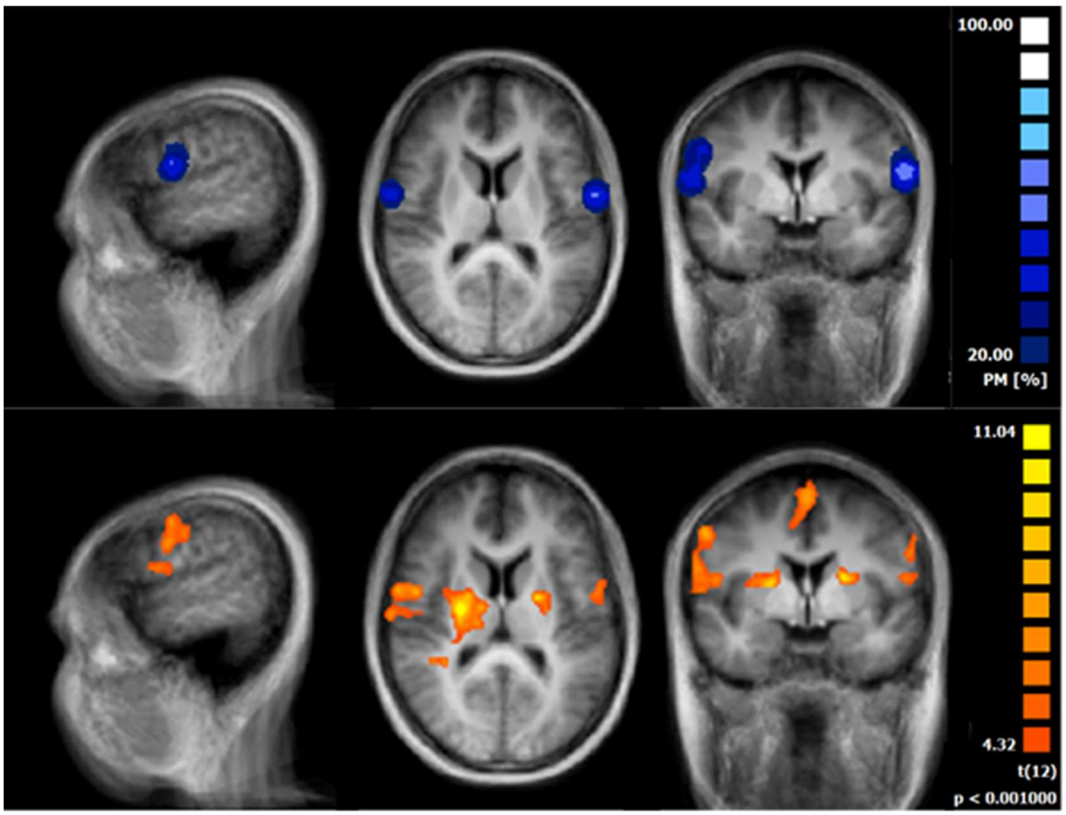

Figure P-9. l-PM2: probability map (displayed in blue), RFX analysis (in orange).